Spring 5-2014

Biogeochemistry of Trace Elements in the Mixing Zone of the Mississippi and Atchafalaya Rivers and Chemical Distributions as Affected by the Deepwater Horizon Blowout

DongJoo Joung
University of Southern Mississippi

The University of Southern Mississippi

BIOGEOCHEMISTRY OF TRACE ELEMENTS IN THE MIXING ZONE OF THE MISSISSIPPI AND ATCHAFALAYA RIVERS AND CHEMICAL DISTRIBUTIONS AS AFFECTED BY THE DEEPWATER HORIZON BLOWOUT

by

DongJoo Joung

Abstract of a Dissertation
Submitted to the Graduate School
of The University of Southern Mississippi
in Partial Fulfillment of the Requirements
for the Degree of Doctor of Philosophy

May 2014

ABSTRACT

BIOGEOCHEMISTRY OF TRACE ELEMENTS IN THE MIXING ZONE OF THE MISSISSIPPI AND ATCHAFALAYA RIVERS AND CHEMICAL DISTRIBUTIONS AS AFFECTED BY THE DEEPWATER HORIZON BLOWOUT

by DongJoo Joung

May 2014

Selected trace elements (TEs), dissolved organic carbon, and nutrients were studied in Louisiana Shelf waters including the Mississippi (MR) and Atchafalaya (AR) River plumes during periods of high, intermediate, and low river discharges. Seasonal variations in TEs were observed at low salinity, reflecting seasonal changes in the river water endmembers. Shelf surface water dissolved Mo, Cs, U, Ni, and Cu showed conservative behavior with minor scattering in some high salinity waters. Based on associated mixing experiments, nutrient and chlorophyll distributions, as well as surface-bottom concentration contrasts, the non-conservative behavior of TEs was variously related to colloidal flocculation (Fe, Cr), biological activity (Fe, Mn), desorption (Ba, Co, Mn), photochemical reaction (Cr) and benthic mobilization (Ba, Co, Cu, Ni, Mn). These processes resulted in seasonal variation of the Ba-salinity relationship in the shelf surface waters, which may lead to considerable uncertainty in paleo-freshwater input estimations. In bottom waters, TEs were either negatively or positively correlated with dissolved oxygen, suggestive of sedimentary diffusion, particle dissolution, or adsorptive removal onto particles under reducing conditions. During bottom water hypoxia, the eberincreases of dissolved Co, Fe and Mn in some high salinity surface waters were observed and were

due to episodic vertical mixing. Different distributions of the studied TEs were observed in the mixing zones of the MR and AR plumes, probably due to the different biogeochemical characteristics of the two river plumes. Additional inputs from the Red River and wetland waters in the AR Basin resulted in different river concentrations and consequently led to a considerable AR contribution for some TEs to the shelf, exceeding the AR hydrological contribution of the shelf. The AR plays a critical role in TE distributions of the Louisiana Shelf waters because it can be the dominant freshwater source to the shelf during summertime.

In addition to the Louisiana Shelf work, the impact of the Deepwater Horizon oil spill on trace element distributions was investigated. An examination of profiles, ancillary data, and oil/dispersant leaching experiments suggests that subsurface concentration changes were related to inputs from crude oil (Co), drilling mud (Ba), and bottom sediment resuspension (Fe). Biological removal of Fe during oil/gas degradation may have been a factor, as well.

The University of Southern Mississippi

BIOGEOCHEMISTRY OF TRACE ELEMENTS IN THE MIXING ZONE OF THE MISSISSIPPI AND ATCHAFALAYA RIVERS AND CHEMICAL DISTRIBUTIONS AS AFFECTED BY THE DEEPWATER HORIZON BLOWOUT

by
DongJoo Joung

A Dissertation
Submitted to the Graduate School
of The University of Southern Mississippi
in Partial Fulfilment of the Requirements
for the Degree of Doctor of Philosophy

Approved:

Alan M. Shiller _____
Director

Laodong Guo _____

Karen Johannesson _____

Jerry Wiggert _____

Scott Milroy _____

Maureen A. Ryan _____
Dean of the Graduate School

May 2014

ACKNOWLEDGMENTS

It would have been impossible to complete this dissertation without the guidance of my committee members and colleagues.

I would like to express my sincerest appreciation to my advisor, Dr. Alan M. Shiller, who always asks me “where is the evidence?” Here is a piece of evidence that could prove his guidance, support, and patience during all my research were excellent. I am sure that more evidence will come during my future research. I would like especially thank to Dr. Laodong Guo, who provided much insight. I also would like to thank Dr. Karen Johannesson, Dr. Jerry Wiggert, and Dr. Scott Milroy, who patiently corrected my dissertation writing.

I would like to thank Dr. Monty Graham, Dr. Stephan Howden, Dr. Vernon Asper, Dr. Charlotte Brunner, and the DMS faculty and staff for their financial support and advice. Many thanks to Kevin Martin, Allison Mojzis, Curtis Caruthers, and Ricky Slaughter for their help with sampling. I would also like to thank former and present lab members as well as DMS colleagues for their support.

Of course, I would like to thank my parents, sisters, and brother, who are always supporting me and encouraging me with their best wishes.

TABLE OF CONTENTS

LIST OF TABLES

Table

LIST OF ILLUSTRATIONS

Figure

CHAPTER I

INTRODUCTION

The study of trace elements, nutrients, and dissolved organic matter in natural waters is important because of their bioavailability and toxicity (Wen et al., 1999; Morel and Price, 2003, Ho et al., 2003; Wang and Guo, 2000; Wand and Dei, 2001) as well as their utilization as proxies for key biogeochemical processes such as paleoproductivity, water column redox reactions, dust input, and fresh/groundwater input (Dymond et al., 1992; Guay and Falkner, 1998; Tribovillard et al., 2006; Shaw et al., 1998; Wang and Sanudo-Wilhelmy, 2009).

Estuaries are partially enclosed water bodies along the coast which are the interface between rivers and the ocean. They are important in various human activities such as fisheries, tourism, and recreation. Estuaries also play an important role in controlling the flux of nutrients, trace elements, organic matter, and pollutants to the ocean via intense chemical, physical, biological, and geological processes. However, biogeochemical characteristics and distributions of trace metals in estuaries are complicated due to temporal and spatial variability of sources and sinks including river and groundwater input, biological activity, flocculation/desorption, atmospheric deposition (both wet and dry), and input from the bottom (Breuer et al., 1999; Tovar-Sanchez et al., 2004; Norisuye et al., 2007; Scholkovitz, 1978). Thus, in order to fully understand the biogeochemistry of chemical constituents in estuarine environments, researche needs to cover wide ranges of spatial and environmental conditions such as river discharge, water column stratification, and water column redox reactions.

Wetlands are another important place that can affect the biogeochemistry of trace elements, nutrients, and dissolved organic matter. Freshwater wetlands including marshes, floodplains and swamps are an interface between the land and river water and play an important role in regulating water quality in rivers and ultimately the estuaries and coastal zones fed by those rivers. Within wetland systems, the nutrients, dissolved organic matter (DOM), and major and trace element distributions can be affected by biological uptake, microbial activity, adsorption onto particles, redox processes, and sedimentation (Bayley, 1995; Fisher and Acreman, 2004; Weis and Weis, 2004; Mullholland, 1981; Chow et al., 2012; Baldwin and Mitchel, 2000; Vymazal, 2007; Olivie-Lauquet et al., 2001). Wetlands are regarded as sinks for DOC, nutrients, and trace elements (Emmett et al., 1994; Fisher and Aceman, 2004; Khan and Brush, 1994). However, other evidence indicates that some floodplains can act as a source of the chemical constituents depending on hydrologic conditions (e.g., flooding and precipitation) (Rucker and Schrautzer, 2010; Kerr et al., 2008; Christopher et al., 2006; Seyler and Boaventura, 2003). Thus, the Atchafalaya River, which passes through the wetlands in the Atchafalaya River Basin, can be contrasted to the highly channelized Mississippi River system and may play a significant role in the distribution of the chemical constituents in Louisiana Shelf waters.

The distribution of trace elements and nutrients in natural waters can also be affected by anthropogenic inputs such as sewage and oil spills. Particularly, the recent Deepwater Horizon oil spill in the Gulf of Mexico was reported to have released an estimated 4.4 ± 0.8 million barrels ($\sim 5.0 \pm 1.0 \times 10^8$ L) of crude oil into the water column (Crone and Tolstoy, 2010). Along with other toxic oil components (e.g.,

polycyclic aromatic hydrocarbons), trace elements in the water column could also be potentially affected by the oil spill due to the fact that some trace metals can be highly enriched in crude oil, though the metal composition may vary with source (Ball et al., 1960; Bieber et al., 1960). However, there are few studies on trace element distributions in marine aquatic environments that have been affected by spills. These include studies of the Prestige fuel oil tanker wreckage off of Spain (Santos-Echeandia, 2008) and the Persian Gulf after the Gulf War (Fowler et al., 1993; Massoud et al., 1998; Al-Abdali et al., 1996). Despite these contamination reports, some laboratory experiments indicate that the contamination of water by metals released from crude oil may be small because of the strong complexation of metals with ligands in crude oil (Portella et al., 2006; Cantu et al., 2000). Thus, it is still unclear what the consequences of the large scale of an oil spill in the Gulf of Mexico would be in aquatic environments.

The ultimate goals of this study are to address the factors regulating temporal and spatial variations of trace elements, nutrients, and dissolved organic matter in the Louisiana Shelf waters including the Mississippi and Atchafalaya River plumes and to address the role of Atchafalaya River Basin in the chemical constituents' fluxes to the Louisiana Shelf. A secondary goal is to address the consequences of the Deepwater Horizon oil spill in terms of trace elements and nutrients.

Background

Site description

The Mississippi River (MR) is one of the largest rivers in terms of amount of outflow (Milliman and Meade, 1983). Agricultural activities along the river lead to an increase in nutrients (Turner and Rabalais, 1991). The lower Mississippi River (MR)

carries about 70% of the total flow of the MR and Red Rivers (RR) to the Gulf of Mexico through the Birdfoot delta, with the remaining 30% flowing through the Atchafalaya River Basin (ARB). The Lower MR has been highly channelized, reducing the interaction of the river with its flood plains. The MR plume initially flows west and is turned anticyclonic toward the coast (to the northwest) into the Louisiana Bight (Hitchcock et al., 1997). The Atchafalaya River (AR) flows from the place where waters of the RR and MR are combined, near Simmesport, Louisiana. Floodplains surrounding the AR are predominantly swamp as it is the largest contiguous fresh water swamp in the United States, with some freshwater marshes in the lower ARB (Xu, 2006). The Atchafalaya Bay (~2 m depth) has a large capacity to trap sediment and is a highly productive ecosystem where interaction of riverine and estuarine waters occur (Lane et al., 2002).

Trace element, nutrients, dissolved organic carbon in the Louisiana Shelf waters (CHAPTER II)

Previously, many trace element studies have been conducted in the Louisiana Shelf waters, including the MR and AR plumes (e.g., Hanor and Chan, 1977; Shiller and Boyle, 1991; Shiller, 1993; Shiller and Mao, 1999; Shim et al., 2012). For example, Shiller and Boyle (1991) observed the largely conservative behavior of dissolved Cu, Fe, Mo, Ni, and Zn in the MR plume during high river discharge, whereas they noted that Cd, Cr, and V showed non-conservative behavior. Similarly, Shim et al. (2012) also reported the conservative behavior of Cu. Rapid removal of Ni has also been observed at low salinity and was suggested to result from biological uptake (Shiller, 1993) as well as adsorption onto suspended particles (Shim et al., 2012). Shim et al. (2012) reported the conservative behavior of Re and Cs and desorption of Co in the MR delta outflow region. For Fe, Shim et al. (2012) observed rapid removal at low salinity in the MR plume,

whereas Shiller and Boyle (1991) reported less intensive Fe removal at a low salinity due to the alkaline nature of MR water (Shiller, 1997). This discrepancy may have resulted from the different filtration procedures between the two studies (Shim et al., 2012). Powell and Wilson-Finelli (2003) observed that a substantial fraction of the Fe in the MR plume was organically complex. The observed non-conservative behavior of Cr in the MR outflow region suggested a temporal variability of the river endmember concentration (Shiller and Boyle, 1991) or photo-reduction of Cr(IV) to the more particle-reactive Cr(III) (Shim et al., 2012).

Non-conservative V behavior was observed in the surface waters in the MR plume area and has been suggested to result from biological uptake (Shiller and Boyle, 1991) as well as mixing with V-depleted bottom water (Shiller and Mao, 1999). In contrast, a nearly conservative dissolved V distribution was observed in the MR plume area following the passage of a hurricane (Shim et al., 2012). Desorption of Ba from fluvial suspended particles has been commonly observed at low salinity during the mixing of Mississippi plume waters (Hanor and Chan, 1977; Shim et al., 2012). For Mn, a rapid increase was found at low salinity on the shelf near the delta and was suggested to result from desorption from the fluvial suspended matter (Shim et al., 2012). Mallini (1992) reported that surface and bottom water enrichment of dissolved Mn in Louisiana Shelf waters were related to reductive dissolution and vertical mixing in summer duringstratification and hypoxia. In general, U has been found to behave conservatively (Swarzenski and McKee, 1998; Shim et al., 2012), though removal was observed during unusually high river flow (Swarzenski and McKee, 1998). In addition, Shiller (1993) reported the contrasting behavior of Cd between the MR delta plume and the extended

mixing zone of the Louisiana Shelf and suggested that the Cd behavior likely resulted from Cd desorption from suspended particles in the MR delta plume and biological uptake in the shelf water. Overall, these previous studies indicate a complex picture of potential seasonal and spatial variability of trace element behavior in this system.

The upward flux of bottom water is an important mechanism for returning nutrients and metals from the shelf bottom to surface water. However, there has been no study to quantify the importance of this upward flux as a mechanism for supplying nutrients to Louisiana Shelf surface waters. Generally, during much of the year, the current in the Louisiana Shelf flows westward along the shore from the Mississippi River to Texas (downcoast), and during the summer, there is a reversal of the current flow (upcoast) (Cochrane and Kelly, 1986; Walker, 2005; Jarosz and Murray, 2005; Nowlin et al., 2005). These current flows are very well correlated with wind stress (Cochrane and Kelly, 1986; Walker, 2005; Jarosz and Murray, 2005; Nowlin et al. 2005). The upcoast wind and current during the summer time causes a freshening of the shelf water because the current entrains the river discharge, causing it to pool over the shelf (Nowlin et al., 2005). This process can intensify the stratification of the water column on the shelf. Thus, the upward flux of nutrients and metals is commonly ignored in studies that examine biogeochemical models of hypoxia on the shelf (see Scavia et al., 2003).

There is, however, some evidence that the flux could be important. For example, Walker (2005) found that the direction of wind changed often from north to south even during the summertime (see Figure 10 in Walker, 2005). Wiseman et al. (1997) reported that the stratification can be broken down when there is intense wind mixing. They also found upwelling favorable wind stress in July and August and strong atmospheric frontal

activity that stimulates vertical mixing and weakens stratification in October and November. Dagg et al. (1988) observed the mixing of bottom waters into the surface layer when winter fronts pass. Shiller and Mao (1999) reported low V in the surface water in the Louisiana Shelf and suggested that it was derived from the mixing between V-depleted bottom water and surface water. All these findings suggest that the water column mixing commonly occurs on the Louisiana Shelf, and thus the vertical flux of materials needs to be addressed.

Implication of Ba distribution in the Louisiana Shelf waters as for paleo-freshwater input (CHAPTER III)

Many studies have used the planktonic foraminiferal Ba/Ca ratio as an indicator of paleo-freshwater input because other proxies (e.g., oxygen isotopes) are affected by additional factors such as temperature (e.g., Hill et al., 2006; Flower et al., 2004; Hall and Chan, 2004). However, the foraminiferal Ba/Ca ratio appears to be affected dominantly by the Ba/Ca ratio of seawater (Lea and Spero, 1994; Honisch et al., 2011); thus, it should reflect the salinity of the water at the time of the foraminifers' calcite formation. Using a contemporary Ba-salinity relationship from a given coastal region, thus provides a means for inferring past salinities or freshwater inputs from planktonic foraminiferal Ba/Ca. However, seasonal freshwater Ba endmember changes, bottom water inputs, submarine groundwater discharge, and anthropogenic inputs (e.g., drilling fluids) may yield changes in Ba-salinity relationships. The seasonal change of the Ba-salinity relationships regardless of the processes could eventually lead to a considerable uncertainty in predicted salinity. Therefore, it is important to understand Ba behavior with different seasons and environmental conditions.

Role of Atchafalaya River Basin in dissolved organic carbon, nutrients and trace elements distributions in the Louisiana Shelf waters. (CHAPTER IV)

Differing estuarine chemical distributions are usually explained by focusing on different characteristics within estuaries. For example, previous studies have reported different distributions of trace elements and nutrients between the Mississippi River and Atchafalaya River estuaries due to physiographic differences (Pakulski et al., 2000; Shiller, 1993). However, the influences of the swamps and the floodplains on the distributions are commonly ignored. Previous studies have pointed out the role of swamps and floodplains on trace element and nutrient distributions (Xu, 2006; Viers et al., 2005).

The different distribution of trace elements (TE) in the AR relative to the MR might be derived from the biogeochemistry in the AR. First, Red River water might have relatively high (or low) concentrations of TE and nutrients. Turner and Rabalais (1991) reported different nutrient distributions at St. Francisville and Morgan City, which represent the MR and AR pathways. They found relatively lower nitrate and silicate (31 and 6%, respectively) and higher total phosphate (30%) in the AR than in the MR and suggested that these differences were probably due to differences in the composition of the Red River, which is an additional contribution to the AR. Second, the Atchafalaya River Swamp, the largest freshwater swamp in North America, could play a role in the distribution of nutrients and trace elements. Indeed, this factor was not considered by Turner and Rabalais (1991). Xu (2006) reported a 27% removal rate of organic nitrogen by biological processes based on the annual average of input-output difference of total Kjeldahl nitrogen (TKN). Xu (2006) showed a higher removal of TKN during high river flow season due to the more inundated area. Viers et al. (2005) reported that plants along

the Solimoes River in the Amazon accumulate metals (Al, Mn, Cu, Fe, Rb) at a rate of up to 20% of the dissolved flux of the river. Third, physiochemical characteristics of Atchafalaya Bay could also be an important factor for the distributions of nutrients and trace elements. Shiller (1993) and Pakulski et al. (2000) revealed the different nutrient distributions in outflow regions of the MR and AR and suggested that the differences were probably due to differences in suspended loads, mixing rates, and marsh interactions. Pakulski et al. (2000) suggested these differences originated from differences in turbidity which affects biomass and phytoplankton species distributions by controlling light availability. Thus, all three factors should be considered together for the T.E. distribution in the AR estuary.

Consequences of the Deepwater Horizon well blowout on trace elements (CHAPTER V)

The Deepwater Horizon (DWH) oil spill occurred April 20, 2010 in the Gulf of Mexico, and the spill lasted until July 15, 2010. As a result, an estimated 4.4 ± 0.8 million barrels (~ $5.0 \pm 1.0 \times 10^8$ L) of crude oil were released into the Gulf of Mexico (Crone and Tolstoy, 2010). Such a large oil release has the potential to seriously impact marine and coastal environments of the northern Gulf (Fowler et al., 1993; Bu-Olayan et al., 1998; Massoud et al., 1998). In addition to the crude oil, up to 1.25×10^{10} moles of methane were released into the deep water (Valentine et al., 2010), and nearly all the methane released was consumed by methanotrophic bacteria (Valentine et al., 2010; Kessler et al., 2011). The consumption of these hydrocarbons caused an estimated respiration of 2-4 $\times 10^{10}$ moles of oxygen at the same time (Kessler et al., 2011; Du and Kessler, 2012). About 6.8×10^6 liters of dispersant, the composition of which is

unknown, were used, 3.8×10^6 L for the surface and 3.0×10^6 L for the deep plume (Kujawinski et al., 2011).

Previously, significant increases of dissolved trace elements were reported after an oil spill near the coast of Spain. Santos-Echeandia et al. (2008) reported an increased dissolved phase concentrations of Cu and Ni in the overlying water column and estimated about 80% (135 kg) and 35% (1700 kg) of Cu and Ni, respectively, were released into the water column (including surface water) as result of the event. Prego and Cobelo-Garcia (2003) investigated the Zn distribution in the same area and found that the concentration was about two orders of magnitude higher than was typical in those waters. Santos-Echeandia et al. (2008) found that the relatively high release rate of Cu relative to Ni and V was derived from the different stability of their complexes with porphyrins in the oil.

From lab experiment, Portella et al. (2006) also revealed the complexation of the metals Ni(II), V(IV), Fe(II), Cd(II) and Pb(II) with ligands of hexanoic acid and 1-propanethiol, that are representative of carboxylic acids and mercaptans, respectively, present in the oil, is the most stable species among all the metals at pH 8. From an oil spill simulation of seawater, Portella et al. (2006) concluded that the metal ions were not released to the water column due to the strong complexation with the ligands. Cantu et al. (2000) also reported that the partitioning of Ni complexed with deoxophyllorythroetioporphyrin (DPEP) from crude oil into aqueous phase is very low due to the strong complexation, so the contamination of drinking water by released metal from crude oil is small. Therefore, different release rates among metals are probably due to the different stability of metal complexes with oil ligands.

The application of dispersants needs to be considered because dispersants can increase the solubility of materials in the oil. For example, Yamada et al. (2003) reported the increased dissolution of PAHs (especially higher molecular weight) was up to six times after the addition of the chemical dispersant. This increased dissolution of the PAHs resulted in higher PAH concentrations in the water column than in the waters where dispersants were not used. Thus, the dispersant has the potential to contribute to the increase of metal concentration in the water column.

Microbial effects on oil degradation are also considerable. Hazen et al. (2010) reported microbial cell densities were about 2 times higher in the subsurface oil plume than the non-plume area, and that γ-Proteobacteria was enriched in the plume. Therefore, it is possible that the metals can be remineralized from the oil. If the role of microbial activity is significant to metal partitioning between the seawater and the floating oil, all the metal concentrations could be increased.

Drilling mud usage is potentially very important for the Ba distribution. It is reported that about 15% of drilling mud solids were barite and contained very high concentrations of particulate Ba (Trocine and Trefy, 1983). Although it has been reported that the solubility of Ba in the mud is very low (Neff, 2007), the enormous use of the mud could have actually increased Ba concentrations. For example, evidence from fluctuating the Ba/Ca ratio in the corals in the Gulf of Mexico, Carriquiry and Horta-Puga (2010) and Deslarzes et al. (1995) suggested that Ba from drilling mud increased the dissolved Ba concentration in the water, and thus in the corals. Drilling mud often contains high concentrations of other elements such as Co, Cu, Fe and Mn. Thus, drilling mud could also potentially affect the trace element distribution in the water column.

Hypotheses and Objectives

Based on the background, there are several hypotheses:

H1. Trace elements, nutrients, and dissolved organic carbon distributions in Louisiana Shelf waters should have significant seasonal variations in relation to river discharge, vertical mixing, and water column redox state (e.g., bottom water hypoxia). During even strong water column stratification, upward mixing could be important for the chemical constituent distributions. (Chapter II)

Objectives for Hypotheses 1:

1. To quantify the sources and sinks of trace elements in the Mississippi/Atchafalaya mixing zones.
2. To compare trace element distributions in different distributary mixing zones during different seasons.
3. To determine the origin of the different distribution of material in the mixing zones.

H2. Barium distribution should vary significantly with seasons due to seasonal changes of river Ba endmembers and benthic remobilization. The seasonal changes of Ba-salinity relationship will lead to uncertainty in paleo-salinity prediction. (Chapter III)

Objectives for Hypotheses 2:

1. To determine the factors for the seasonal changes of Ba-salinity relationships.

H3. Trace elements, nutrients, and dissolved organic carbon in the Mississippi River will be altered by additional inputs from the Red River and wetlands as water passes through the Atchafalaya River Basin, and thus, the Atchafalaya River contribution

of the chemical constituents to the Louisiana Shelf water will be exceeded the AR hydrological contribution. (Chapter IV)

Objectives for Hypotheses 3:

1. To quantify the Red River and wetlands contribution of chemical constituents to the Atchafalaya River water.
2. To determine the fluxes of the chemical constituents into Louisiana Shelf.

H4. In crude oil-contaminated waters Ba, Co and Fe will be affected by leaching from the crude oil, biological uptake, and water column redox state (e.g., dissolved oxygen condition). (Chapter V)

Objectives for Hypotheses 4:

1. To quantify the direct leaching from the crude oil.
2. To understand the consequences of oil spills on trace element distributions in the water column.

REFERENCES

Al-Abdali, F.; Massoud, M. S., Al-Ghadban, A. N. Bottom sediments of the Arabian Gulf-III. Trace metal contents as indicators of pollution and implications for the effect and fate of the Kuwait oil slick. *Environ. Pollut.* **1996**, 93(3), 285-301.

Baldwin, D.S., Mitchell, A.M. The effects of drying and re-flooding on the sediment and soil nutrient dynamics of lowland river-floodplain systems: A synthesis. *Regul. Rivers: Res. Mgmt.* **2000**, 16, 457-467.

Ball, J.S., Wenger, W.J., Hyden, H.J.; Horr, C.A., Myers, A.T. Metal content of twenty-four petroleums. *J. Chem. Eng. Data*, **1960**, 5(4), 553-557.

Bayley, P.B. Understanding large river-floodplain ecosystems. *BioScience.* **1995**, 45(3), 153-158.

Bieber, H., Hartzband, H.M., Kruse, E.C. Volatility of metal-porphyrin complexes in petroleum. *J. Chem. Eng. Data*, **1960**, 5 (4), 540-546.

Breuer, E., Sanudo-Wilhelmy, S.A., Aller, R.C. Trace metals and dissolved organic carbon in an estuary with restricted river flow and a brown tide bloom. *Estuaries* **1999**, 22, 603-615.

Bu-Olayan, A.H.; Subrahmanyam, M.N.V.; Al-Sarawi, M. and Thomas, B.V. Effects of the Gulf War oil spill in relation to trace metals in water, particulate matter, and PAHs from the Kuwait coast. *Environ. Int.* **1998**, 24 (7), 789-797.

Cantu, R., Stencel, J.R., Czernuszewicz, R.S., Jaffe, P.R., Lash, T.D. Surfactant-Enhanced partitioning of nickel and vanadyl deoxophylloerythroetioporphyrins from crude oil into water and their analysis using surface-enhanced Resonance Raman spectroscopy. *Environ. Sci. Technol.* **2000**, 34, 192-198.

Carriquiry, J.D., Horta-Puga, G. The Ba/Ca record of corals from the Southern Gulf of Mexico: Contributions from land-use changes, fluvial discharge and oil-drilling muds. *Mar. Pollut. Bull.* **2010**, 60, 1625-1630.

Chow, A.T., Dai, J., Conner, W.H., Hitchcock, D.R. and Wang, J.-J. Dissolved organic matter and nutrients dynamics of a coastal freshwater forested wetland in Winyah Bay, South Carolina. *Biogeochemistry*, **2012**, DOI 10.1007/s10533-012-9750-z.

Christopher, S.F., Page, B.D., Campbell, J.L., Mitchell, M.J. Contrasting stream water NO_3^- and Ca^{2+} in two nearly adjacent catchments: the role of soil Ca and forest vegetation. *Global Change Biology*, **2006**, 12, 364-381.

Cochrane, J.D., Kelly, F.J. Low-frequency circulation on the Texas-Louisiana continental shelf. *J. Geo. Res*. **1986**, 91 (C9), 10645-10659.

Crone, T. J., Tolstoy, M. Magnitude of the 2010 Gulf of Mexico Oil Leak. *Science*, **2010**, 330, 634.

Dagg, M.J. Physical and biological responses to the passage of a winter storm in the coastal and inner shelf waters of the northern Gulf of Mexico. *Cont. Shelf. Res*. **1988**, 8, 167-178.

Deslarzes, K.J.P., Boothe, P.N., Presley, B.J. and Steinmetz, G.L. Historical incorporation of barium in the reef building coral Montastrea annularis at the Flower Garden Banks, north-west Gulf of Mexico. *Mar. Pollut. Bull.* **1995**, 30 (11), 718-722.

Du, M., Kessler, J.D. Assessment of the spatial and temporal variability of bulk hydrocarbon respiration following the Deepwater Horizon oil spill. *Environ. Sci. Technol*. **2012**, 46(9), 10499-10507:doi 10.1021/es301363k.

Dymond, J., Suess, E., Lyle, M. Barium in deep-sea sediment: A geochemical proxy for paleoproductivity. *Paleoceanography* **1992**, 7, 163-181.

Emmett, B.A., Hudson, J.A., Coward, P.A., Reynolds, B. The impact of a riparian wetland on stream water recently afforested upland catchment. *J. Hydrology*, **1994**, 162, 337-353.

Fisher, J., Acreman, M.C. Wetland nutrient removal: a review of the evidence. *Hydrol. Earth Syst. Sc.* **2004**, 8(4), 673-685.

Flower, B.P., Hastings, D.W., Hill, H.W., Quinn, T.M. Phasing of deglacial warming and Laurentide Ice Sheet meltwater in the Gulf of Mexico. *Geology* **2004**, 32, 597-600.

Fowler, S.W.; Readman, J.W.; Oregioni, B.; Villeneuve, J.-P., McKay, K. Petroleum hydrocarbons and trace metals in nearshore gulf sediments and biota before and after the 1991 war: An assessment of temporal and spatial trends. *Mar. Pollut. Bull.* **1993**, 27, 171-182.

Guay, C.K., Falkner, K.K. A survey of dissolved barium in the estuaries of major Arctic rivers and adjacent seas. *Cont. Shelf Res*. **1998**, 18, 859-882.

Hall, J.M., Chan, L.,-H. Ba/Ca in Neogloboquarina pachyderma as an indicator of deglacial metwater discharge into the western Arctic Ocean. *Plaeoceanography* **2004**, 19, doi: 10.1029/2003PA000910.

Hanor, J.S., Chan, L.H. Non-conservative behavior of barium during mixing of Mississippi River and Gulf of Mexico waters. *Earth Planet. Sci. Lett.* **1977**, 37, 242–250.

Hazen, T.; Dubinsky, E.A.; DeSantis, T.Z.; Andersen, G.L.; Piceno, Y.M.; Singh, N.; Jansson, J.K.; Probst, A.; Borglin, S.; Fortney, J.L.; Stringfellow, W.T.; Bill, M., Conrad, M.E., Tom, L.A.; Chavarria, K.L.; Alusi, T.R.; Lamendella, R.; Joyner, D.C.; Spier, C.; Baelum, J.; Auer, M.; Zemla, M.L.; Chakraborty, R.; Sonnenthal, E.L.; D'haeseleer, P.; Holman, H.-Y.N.; Osman, S.; Lu, Z.; Nostrand, J.D.V.; Deng, Y.; Zhou, J., Mason, O.U. Deep-sea oil plume enriches indigenous oil-degrading bacteria. *Nature* **2010**, 330, 204-208.

Hill, H.W., Flower, B.P., Quinn, T.M., Hollander, D.J., Guilderson, T.P. Laurentide Ice Sheet meltwater and abrupt climate change during the last glaciations. *Paleoceanography* **2006**, 21, doi:10.1029/2005PA001186.

Hitchcock, G.L., Wiseman Jr, W.J., Boicourt, W.C., Mariano, A.J., Walker, N., Nelsen, T. A. and Ryan, E. Property fields in an effluent plume of the Mississippi river. *J. Mar. Sys*. **1997**, 12, 109-126.

Ho, T.-Y., Quigg, A., Finkel, Z.V., Milligan, A.J., Wyman, K., Falkowski, P.G., Morel, F.M.M., The elemental composition of some marine phytoplankton. *J. Phycol.* **2003**, 39, 1145–1159.

Honisch, B., Allen, K.A., Russell, A.D., Eggins, S.M., Bijma, J., Spero, H.J., Lea, D.W., Yu, J. Planktic foraminifers as recorders of seawater Ba/Ca. Mar. *Micropaleontol*. **2011**, 79, 52-57.

Jarosz, E., Murray, S.P. Velocity and transport characteristics of the Louisiana-Texas coastal current, in *New Developments in the Circulation of the Gulf of Mexico*, Sturges, W.and Lugo-Fernandez, A. Eds., AGU, *Monogr. Ser* **2005**, 143-156, doi: 10.1029/161GM11.

Kerr, S.C., Shafer, M.M., Overdier, J., Armstrong, D.E. Hydrologic and biogeochemical controls on trace element export from northern Wisconsin wetlands. *Biogeochemistry*, **2008**, 89, 273-294.

Kessler, J. D.; Valentine, D. L.; Redmond, M. C.; Du, M.; Chan, E. W.; Mendes, S. D.; Quiroz, E. W.; Villanueva, C. J.; Shusta, S. S.; Werra, L. M.; Yvon-Lewis, S., Weber, T. C. A persistent oxygen anomaly reveals the fate of spilled methane in the deep Gulf of Mexico. *Science* **2011**, 331, 312-315.

Khan, H., Brush, G.S. Nutrient and metal accumulation in a freshwater tidal marsh. *Estuaries*, **1994**, 17(2), 345-360.

Kujawinski, E.B.; Kido Soule, M.C.; Valentine, D.L.; Boysen, A.K.; Longnecker, K., Redmond, M.C. Fate of dispersant associated with the Deepwaer Horizon oil spill. *Environ. Sci. Technol.* **2011**, 45, 1298–306.

Lane, R.R., Day, J.W., Marx, B., Reyes, E., Kemp, G.P. Seasonal and spatial water quality changes in the outflow plume of the Atchafalaya River, Louisiana, USA. *Estuaries* **2002**, 25, 30-42.

Lea, D.W., Spero, H.J. Assessing the reliability of paleochemical tracers: Barium uptake in the shells of planktonic foraminifera. *Paleoceanography* 1994, 9, 445-452.

Mallini, L.J. Development of kinetic-colorimetric flow analysis techniques for determining dissolved manganese and iron and an assessment of the behavior of dissolved manganese in the far-field plume of the Mississippi River. *M.S. Thesis*, University of Southern Mississippi, May 1992.

Massoud, M.S. Al-Abdali, F., Al-Ghadban, A.N. The status of oil pollution in the Arabian Gulf by the end of 1993. *Environ. Int.* **1998**, 24 (1/2), 11-22.

Milliman, J.D., Meade, R. World-wide delivery of river sediment to the ocean. *J. Geol*. **1983**, 91, 1 –21.

Morel, F.M.M., Price, N.M. The biogeochemical cycles of trace metals in the oceans. *Science* **2003**, 300, 944-947.

Mulholland, P.J. Organic carbon flow in a swamp-stream ecosystem. *Ecol. Monogr.* **1981**, 51(3), 307-322.

Neff, J.M. Estimation of bioavailability of metals from drilling mud barite. *Intergr. Environ. Assess. Manag.* **2007**, 4 (2), 184-193.

Norisuye,K., Ezoe,M., Nakatsuka,S., Umetani,Y.S. Distribution of Bioactive trace metals (Fe, Co, Ni, Cu, Zn and Cd) in the Sulu Sea and its adjacent seas. *Deep-Sea Res. II*, **2007**, 54, 14-37.

Nowlin, W.D., Jr., Jochens, A.E., DiMarco, S.F., Reid, R.O., Howard, M.K. Low-frequency circulation over the Texas-Louisiana continental shelf, in *New Developments in the Circulation of the Gulf of Mexico*, Sturges, W.and Lugo-Fernandez, A. Eds., AGU, *Monogr. Ser*, **2005**, 1-22, doi: 10.1029/161GM11.

Olivie-Lauquet, G., Gruau, G., Dia, A., Riou, C., Jaffrezic, A., Henin, O. Release of trace elements in wetlands: role of seasonal variability. *Wat. Res.* **2001**, 35(4), 943-952.

Pakulski, J.D., Benner, R., Whitledge, T., Amon, R., Eadie, B., Cifuentes, L., Ammerman, J., Stockwell, D. Microbial Metabolism and Nutrien Cycling in the Mississippi and Atchafalaya River Plumes. *Estuar. Coast. Shelf Sci.* **2000**, 50, 173-184.

Portella, C.M.M.A., Tristao, M.L.B., Felcman, J. Evaluation of the possibility of contamination of sea water by metal ions present in fuel oil. *Fuel*, **2006**, 85, 2162-2170.

Powell, R.T., Wilson-Finelli, A. Importance of organic Fe complexing ligands in the Mississippi River plume. *Estuar. Coast. Shelf Sci*. **2003**, 58: 757-763.

Prego, R., Cobelo-Garcia, A. Zinc concentrations in the water column influenced by the oil spill in the vicinity of the Prestige shipwreck. *Ciencias Marinas* **2003**, 29 (1), 103-108.

Rucker, K., Schrautzer, J. Nutrient retention function of a stream wetland complex- A high-frequency monitoring approach. *Ecol. Eng.* **2010**, 36, 612-622.

Santos-Echeandia, J., Prego, R., Cobelo-Garcia, A. Influence of the heavy fuel spill from the Prestige tanker wreckage in the overlying seawater column levels of copper, nickel and vanadium (NE Atlantic ocean). *J. Mar. Sys.* **2008**, 72, 350-357.

Scavia, D., Rabalais, N.N., Turner, R.E., Justic, D., Wiseman, Jr. W.J. Predicting the response of Gulf of Mexico hypoxia to variations in Mississippi River nitrogen load. *Limnol. Oceanogr.* **2003**, 48(3), 951-956.

Seyler, P.T., Boaventura, G.R. Distribution and partition of trace metals in the Amazon basin. *Hydrol. Process.* **2003**, 17, 1345-1361.

Shaw, T.J., Moore, W.S., Kloepfer, J., Sochaski, M.A. The flux of barium to the coastal waters of the southeastern USA: The importance of submarine groundwater discharge. *Geochim. Cosmochim. Acta* **1998**, 62, 3047-3054.

Shiller, A.M. Comparison of nutrient and trace element distributions in the delta and shelf outflow regions of the Mississippi/Atchafalaya River. *Estuaries* **1993**, 16, 541-546.

Shiller, A.M. Dissolved trace elements in the Mississippi River: seasonal, interannual, and decadal varaibility. *Geochim. Cosmochim. Acta* **1997**, 61, 4321–4330.

Shiller, A.M., Mao, L. Dissolved vanadium on the Louisiana Shelf: effect of oxygen depletion. *Cont. Shelf Res.* **1999**, 19, 1007-1020.

Shiller, A.M., Boyle, E.D. Trace elements in the Mississippi River delta outflow region: Behavior at high discharge. *Geochim. Cosmochim. Acta* **1991**, 55, 3241–3251.

Shim, M-J., Swarzenski, P.W., Shiller, A.M. Dissolved and colloidal trace elements in the Mississippi River delta outflow after Hurricanes Katrina and Rita. *Cont. Shelf Res*. **2012**, 42, 1-9.

Sholkovitz, E.R. The flocculation of dissolved Fe, Mn, Cu, Ni, Co, and Cd during estuarine mixing. *Earth Planet. Sci. Lett.* **1978**, 41, 77–86.

Swarzenski, P.W., McKee, B.A. Seasonal uranium distribution in the coastal waters off the Amazon and Mississippi Rivers. *Estuaries* **1998**, 21, 379–390.

Tovar-Sanchez, Sanudo-Wilhelmy, S., Flegal, A.RTemporal and spatial variations in the biogeochemical cycling of cobalt in two urban estuaries: Hudson River Estuary and San Francisco Bay. *Estuar. Coastal Shelf Sci.* **2004**, 60, 717-728.

Tribovillard, N., Algeo, T.J., Lyons, T., Riboulleau, A. Trace metals as paleoredox and paleoproductivity proxies: An update. *Chem. Geol.* **2006**, 232(1-2), 12-32.

Trocine, R.P., Trefry, J.H. Particulate metal tracers of petroleum drilling mud dispersion in the marine environment. *Environ. Sci. Technol.* **1983**, 17(9), 507-512.

Turner, R.E., Rabalais, N.N. Changes in Mississippi River water quality this century. *BioScience* **1991**, 41(3), 140-147.

Valentine, D. L.; Kessler, J. D.; Redmond, M. C.; Mendes, S. D.; Heintz, M. B.; Farwell, C.; Hu, L.; Kinnaman, F. S.; Yvon-Lewis, S.; Du, M.; Chan, E. W.; Garcia Tigreros, F., Villanueva, C. J. Propane respiration jump-starts microbial response to a deep oil spill. *Science* **2010**, 330, 208–211.

Viers, J., Barrous, G., Pinelli, M., Seyler, P., Oliva, P., Dupre, B., Boaventura, G.B. The influence of the Amazonian floodplain ecosystems on the trace element dynamics of the Amazon River mainstem (Brzzil). *Sci. Total Environ*. **2005**, 339, 219-232.

Vymazal, J. Removal of nutrients in various types of constructed welands. *Sci. Total Environ.* **2007**, 380, 48-65.

Walker, N.D. Seasonal changes in surface temperature, shelf and slope circulation, and coastal upwelling in the northwestern Gulf of Mexico, in *New Developments in the Circulation of the Gulf of Mexico*, Sturges, W.and Lugo-Fernandez, A. Eds., AGU *Monogr. Ser*, **2005**, 295-314, doi: 10.1029/161GM11.

Wand, W.-X., Dei, R.C.H. Influences of phosphate and silicate on Cr(VI) and Se(IV) accumulation in marine phytoplankton. *Aquat. Toxicol.* **2001**, 52, 39-47.

Wang, D., Sanudo-Wilhelmy, S.A. Vanadium speciation and cycling in coastal waters. *Mar. Chem.* **2009**, 11, 52–58.

Wang, W-X., Guo, L. Bioavailability of colloid-bound Cd, Cr, and Zn to marine plankton. *Mar. Ecol. Prog. Ser.* **2000**, 202, 41-49.

Weis, J.S., Weis, P. Metal uptake, transport and release by wetland plants: implications for phytoremediation and restoration. *Environ. Int.* **2004**, 30, 685-700.

Wen, L.S., Shiller, A., Santschi, P.H. and Gill, G. Trace Element Behavior in Gulf of Mexico Estuaries. In *Biogeochemistry of Gulf of Mexico Estuaries*, T.S. Bianchi, J.R. Pennock, and R.R. Twilley, Eds., J. Wiley & Sons, New York, **1999**, Chpt. 10, pp. 303-346.

Wiseman, W.J., Rabalais, N.N., Turner, R.E., Dinnel, S.P., MacNaughton, A. Seasonal and interannual variability within the Louisiana coastal current: stratification and hypoxia. *J. Marine Syst*. **1997**, 12, 237-248.

Xu, Y. J. Organic nitrogen retention in the Atchafalaya River Swamp. *Hydrobiologia* **2006**, 560, 133-143.

Yamada, M.; Takada, H.; Toyoda, K.; Yoshida, A.; Shibata, A.; Nomura, H.; Wada, M.; Nishimura, M. and Okamoto, K. Study on the fate of petroleum-derived polycyclic aromatic hydrocarbons (PAHs) and the effect of chemical dispersant using an enclosed ecosystem, mesocosm. *Mar. Pollut. Bul*. **2003**, 47, 105-113.

CHAPTER II

TEMPORAL AND SPATIAL VARIATIONS OF DISSOLVED TRACE ELEMENT DISTRIBUTIONS IN LOUISIANA SHELF WATERS

Introduction

Estuaries are the interface between rivers and the ocean and play an important role in controlling the flux of trace elements to the ocean via intense chemical, physical, biological, and geological processes. The study of trace elements in estuaries is of importance because of their bioavailability and toxicity (Wen et al., 1999), as well as their ability to be tracers of key biogeochemical processes. However, biogeochemical characteristics and distributions of trace metals in estuaries are complicated due to temporal and spatial variability of sources and sinks including river input, atmospheric deposition, groundwater input, mixing with ocean water, input from the bottom, and biological productivity (Breuer et al., 1999; Tovar-Sanchez et al., 2004).

The Louisiana Shelf receives fresh water from the Mississippi and Atchafalaya Rivers (MR and AR, respectively), which are the dominant riverine sources of trace elements to the shelf. The AR is a major distributary of the MR, carrying 30% of the combined flow of the MR and the RR. While the main MR enters the northern Gulf of Mexico through the Birdfoot delta that extends to nearly the shelf break, the AR enters the shelf through the largest freshwater wetlands basin the United States (Ford and Nyman, 2011) and a broad shallow bay. That is, nearly the same river endmember mixes with seawater in two very different physiographic areas (Shiller, 1993a). Furthermore, the Louisiana Shelf is well-known for experiencing bottom water hypoxia occurring annually

(from spring to late fall) due to the combined effects of anthropogenic fluvial nutrient input together with strong vertical stratification (e.g., Rabalais et al., 2010).

Previously, many trace element studies have been conducted in Louisiana Shelf waters including the MR and AR plumes (e.g., Hanor and Chan, 1977; Shiller and Boyle, 1991; Shiller, 1993a; Shiller and Mao, 1999; Shim et al., 2012; Chapter III). For example, Shiller and Boyle (1991) observed largely conservative behavior of dissolved Cu, Fe, Mo, Ni and Zn in the MR plume during high river discharge, whereas Cd, Cr, and V showed non-conservative behavior. Similarly, Shim et al. (2012) also reported conservative behavior of Cu. Rapid removal of Ni was also observed at low salinity and was suggested to result from biological uptake (Shiller, 1993a), as well as adsorption onto suspended particles (Shim et al., 2012). Shim et al. (2012) reported the conservative behavior of Re and Cs and the desorption of Co in the MR delta outflow region. For Fe, Shim et al. (2012) observed rapid removal at low salinity in the MR plume, whereas Shiller and Boyle (1991) reported less intensive Fe removal at low salinity due to the alkaline nature of MR water (Shiller, 1997). This discrepancy may have resulted from the different filtration procedures between these two studies (Shim et al., 2012). Powell and Wilson-Finelli (2003) observed that a substantial fraction of the Fe in the MR plume was organically complexed. The observed non-conservative behavior of Cr in the MR outflow region suggested a temporal variability of the river endmember concentration (Shiller and Boyle, 1991), or photo-reduction of Cr(IV) to more particle-reactive Cr(III) (Shim et al., 2012). The non-conservative V behavior was observed in the surface waters in the MR plume area and has been suggested to result from biological uptake (Shiller and Boyle, 1991) as well as mixing with V-depleted bottom water (Shiller and Mao, 1999). In

contrast, a nearly conservative dissolved V distribution was observed in the MR plume area following the passage of a hurricane (Shim et al., 2012). Desorption of Ba from fluvial suspended particles has been comonly observed at low salinity during mixing of Mississippi plume waters (Hanor and Chan, 1977; Shim et al., 2012; Chapter III). Joung and Shiller (2014) (Chapter III) found slightly enriched Ba in the bottom waters apparently due to a flux from the sediments on the Louisiana Shelf. For Mn, a rapid increase was found at low salinity on the shelf near the delta, and it was suggested to result from desorption from the fluvial suspended matter (Shim et al., 2012). Mallini (1992) reported that the surface and bottom water enrichment of dissolved Mn in Louisiana Shelf waters was related to reductive dissolution and vertical mixing in July 1990 and 1991 during during stratification and hypoxia. In general, U has been found to behave conservatively (Swarzenski and McKee, 1998; Shim et al., 2012), whereas removal was observed during unusually high river flow (Swarzenski and McKee, 1998). In addition, Shiller (1993a) reported the contrasting behavior of Cd between the MR delta plume and the extended mixing zone of the Louisiana Shelf and suggested that the Cd behavior likely resulted from Cd desorption from suspended particles in the MR delta plume and the biological uptake in the shelf water.

Overall, these previous studies paint a complex picture of potential seasonal and spatial variability of trace element behavior in this system. Studies of dissolved trace elements together with nutrient and dissolved organic carbon (DOC) distributions in Louisiana Shelf waters including the low salinity mixing zones of the MR and AR are to follow. The ultimate goals of this study were to quantify the sources and sinks of trace elements in the Mississippi/Atchafalaya mixing zones, to compare trace element

distributions in different distributary mixing zones during different seasons and to investigate the origin of the different element distributions in the two mixing zones. The results can potentially provide critical information on environmental issues such as hypoxia on the Louisiana Shelf as well as pollutants source tracking.

Methods and Materials

Trace elements, nutrients, and dissolved organic carbon (DOC) samples were collected on the Louisiana Shelf including the MR and AR plumes during three cruises in May and November 2008 and June 2009 aboard the R/V Pelican (Figures 1 and Appendix). These cruises represent high, low, and mid-range Mississippi River water discharges, respectively (Figures 2). All trace element apparatus including syringes, filters, Teflon tubing, sample bottles, Niskin bottles and tubing connectors were acid cleaned as described by Shim et al. (2012) and Joung and Shiller (2013).

For the MR and AR plumes (i.e., the lowest salinity regions near or in the river mouths, depending on season), only surface samples were collected, and this was done using a small boat moving forward slowly. For the shelf, samples were collected at different depths including surface, near bottom, and middle depths. For the earlier two cruises (May and November 2008), a clean underway pumping system, driven by an air-powered plastic diaphragm pump, was employed for surface waters. A non-metallic, tow-fish was towed just below the surface, several meters off of the side of the ship. One end of acid-cleaned Teflon-lined polyethylene tubing was attached to and extended in front of the tow-fish running to the pump; from the pump, tubing was then run into a small plastic enclosure in the ship's lab where surface waters were sampled. These surface water samples were collected after allowing about 10-minutes of flushing of the pumping

system while the ship was moving. For the June 2009 sampling, a grab sampler was used. An acid-cleaned bottle was attached at the end of the PVC pole (~ 5 m length), and the bottle was rinsed with ambient water three times before collecting the sample while the ship was slowly moving forward. For deep water, a clean pumping system was used during the first cruise. This system was similar to the surface water sampling at this time, but the acid-cleaned tubing was connected to a non-metallic, Kevlar cable (~ 1 m above the weight), which held a non-metallic weight at the end. For the two later cruises, an external spring, Teflon-coated, Niskin bottle was used. The Niskin bottle was mounted on a PVC frame extending ~1 m below the bottle and which automatically closed the bottle when the frame hit the bottom. This system was also used for mid-depth sampling by using a plastic messenger to trigger the closing of the Niskin bottle.

Trace element samples were filtered using acid-cleaned 25 mm x 0.45 µm pore size polypropylene (Whatman Puradisc) and 25 mm x 0.02 µm pore size alumina (Whatman Anotop) syringe filters, allowing us to separate operationally-defined *total* and *truly dissolved* fractions, respectively. The colloidal phase (0.02 – 0.45 µm) is defined by the difference between the two fractions. Details of the sample processing can be found elsewhere (Shiller, 2003). The nutrient and DOC samples were also collected at the same time, but the samples were filtered using only 0.45 µm pore size filters. The trace element filtrates were then tightly capped and kept in clean, double zippered plastic bags. Nutrient and DOC samples were kept frozen until analysis.

Mixing experiments were conducted at sea using river water and seawater endmembers. Unfiltered river water and seawater were mixed in varying proportions and held at room temperature in the dark overnight. The experiments were done at sea, and it

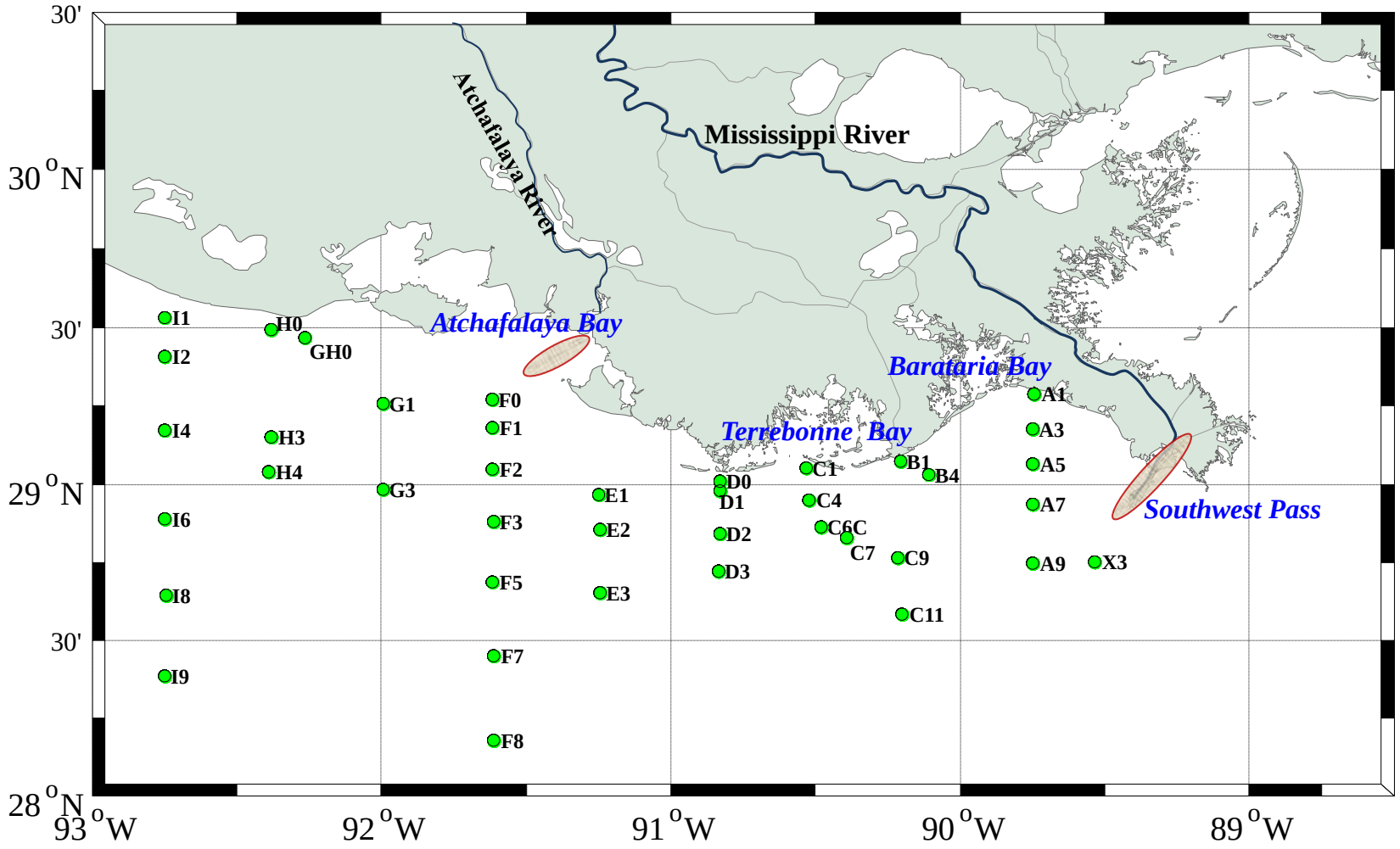

Figure 1. Louisiana Shelf sampling stations May 2008, November 2008, and June 2009 (green circles). Shaded areas by Southwest Pass and Atchafalaya Bay show general location of river endmember sampling (see, Appendix A, B for specific locations).

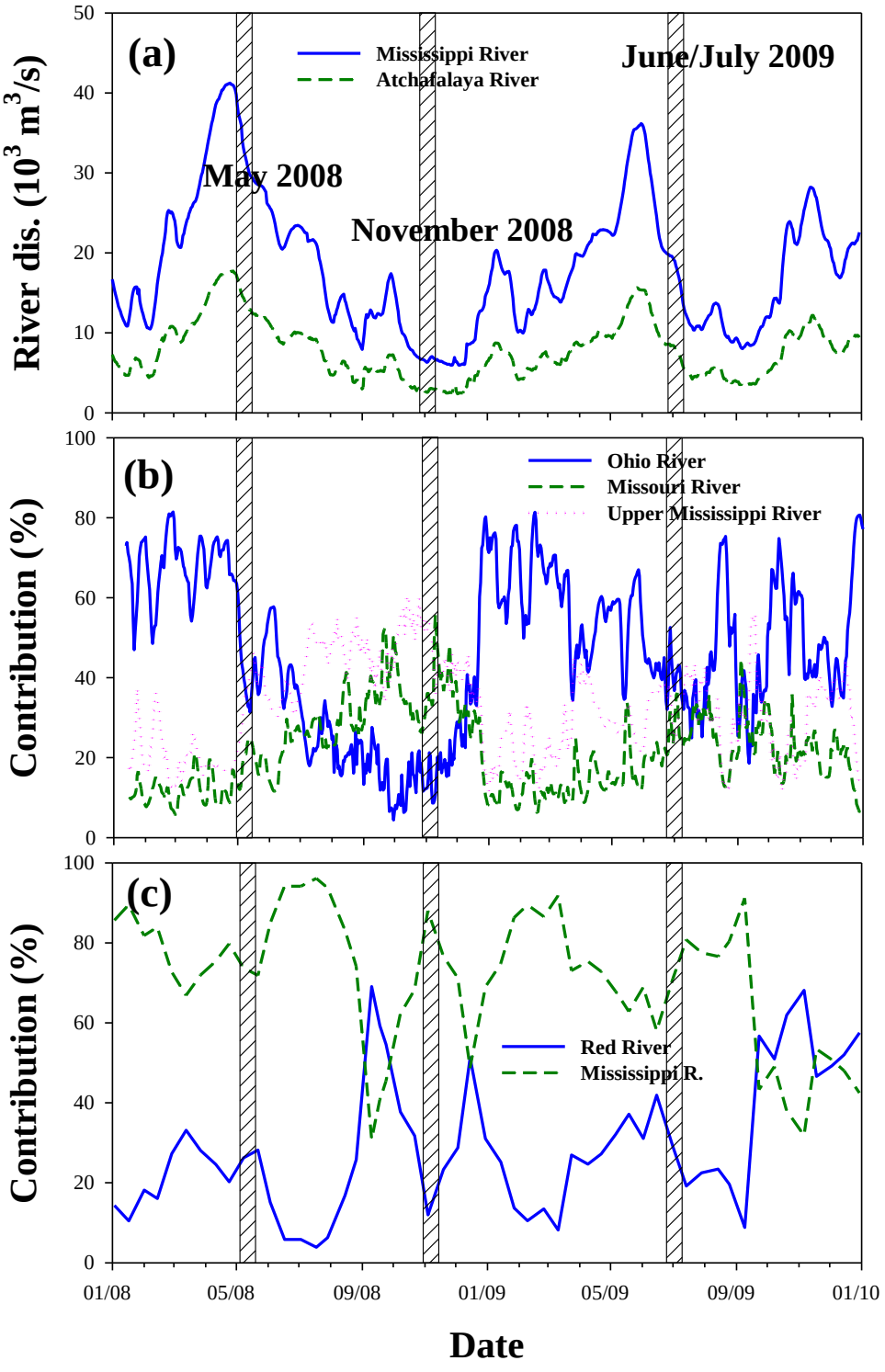

Figure 2. a) Discharges of Mississippi (MR) and Atchafalaya (AR) Rivers; b) relative contributions of major MR tributaries to the lower river; and c) relative contributions of the MR and Red River (RR) to the AR discharge.

was assumed that the ship's motion provided adequate mixing of the samples. The mixed samples were filtered in the same way as the field samples. The lowest salinity waters for the mixing experiment were collected from the AR (e.g., stn. AR1) for all of the study periods, and additionally from the MR (e.g., stn. MR8) only for June/July 2009. The overnight mixing time was chosen as being suffient for chemical reactions such as flocculation or desorption to occur (Boyle et al., 1977; Hanar and Chan, 1977; Sholkovitz, 1978; Li et al., 1984; Hatje et al., 2003), but not so long that the biological processes were likely to be dominant influences. Nonetheless, some biological effects on these mixing experiments cannot be ruled out.

Ancillary data such as salinity, temperature, and dissolved oxygen (DO) were obtained from a separate CTD cast. The DO sensor calibration was checked by Winkler titration. Nutrient analyses were performed at the University of South Florida or by the Geochemical & Environmental Research Group (Texas A&M). The oxygen isotope composition of the water was determined using isotope ratio infrared spectroscopy (L2120i cavity ringdown spectrometer, Picarro, Inc.), and the raw isotope data correction and calibration were made using the method of van Geldern and Barth (2012). Stadardization was accomplished using in-house standards calibrated to the VSMOW scale.

The Mississippi River discharge was obtained from U.S. Army Corps of Engineers (http://www.mvn.usace.army.mil/eng/edhd/wcontrol/discharge.asp) discharge records from the gage at Tarbert Landing, Mississippi. Relative major tributary contributions to the MR mainstem discharge were determined from USGS data from the Ohio River at Metropolis, IL, the Missouri, River at Hermann, MO, and the Mississippi

River at Grafton, IL for Ohio, Missouri and Upper Mississippi Rivers, respectively (water.usgs.gov). To adjust approximately for the travel time of water from these tributaries to the delta, the estimation of relative contributions used Upper Mississippi River, Missouri River, and Ohio River discharges from 15, 15, and 12 days, respectively, prior to our sampling. These travel times were adjusted by adding 2 days to the times used by Shiller (1997) in consideration of the extended distance from Baton Rouge to the birdfoot delta. For the Atchafalaya River, discharge was also obtained from the U.S. Army Corps of Engineers from the gage at Simmesport, LA.

Nutrient, DOC and trace element analysis

The frozen nutrient and DOC samples were thawed overnight at room temperature just before analysis. Nutrients were analyzed using a nutrient auto-analyzer applying standard methods. Detections limit of nutrient analysis were 0.1, 0.02, and 0.1 µmol/L for nitrate, phosphate, and silicate, respectively. The DOC samples were analyzed using a Shimadzu TOC-V total organic carbon analyzer employing a high temperature combustion method (Guo et al., 1995). For DOC measurements, samples were acidified with concentrated HCl to pH < 2 before analysis. Concentrations of DOC were automatically calculated using the calibration curves that were generated at the beginning of the analytical run. Certified DOC standards (University of Miami) were measured frequently during the run to check the performance of the instrument. The variation of 3-5 measurements of each sample was less than 2%.

For trace element analysis, the filtered samples were acidified to pH < 2 by the addition of 140 and 70 µl of clean 6 M HCl (Seastar baseline) for 30 (< 0.45 µm) and 15 (< 0.02 µm) ml samples, respectively, to prevent trace element loss onto the bottle wall,

precipitation, or biological interaction. Trace elements were measureed using a sector field-inductively coupled plasma-mass spectrometry (SF-ICP-MS; Thermo-Fisher Element 2). Analysis of seawater was performed either by diluting the sample 20-fold with 0.3 M ultrapure HNO_3 (Seastar Baseline) for Ba, Cs, Mo, Re, and U or by using a magnesium hydroxide co-precipitation technique for Fe, Cu, Ni, Mn, Co, Cr, and V (Shim et al., 2012; Wu and Boyle, 1997). In both cases, calibration was performed by isotope-dilution using enriched isotopic spikes obtained from Oak Ridge National Laboratory with the exception of Co, Cs, Mn and U, which were calibrated using external standards (see Shim et al. 2012 for details). Samples were prepared for analysis without UV oxidation. As noted by Shim et al. (2012), this yields reliable results for all trace elements with the possible exception of Co for which there may be a fraction that is not labile even after sample acidification (Saito and Moffett, 2001). However, given the high (compared with open ocean) Co values reported here, it is likely that we are recovering the substantial portion of the Co. To verify the accuracy of the analysis, the reference

Table 1

Detection limit and recovery of trace elements (n=40, nM)

	Co	Cr	Cs	Cu	Fe	Mo
Detection Limit	0.006	0.1	0.003	0.6	0.4	1
NASS5	0.190	2.1	2.000	4.7	3.7	100
Average	0.187	2.1	1.769	4.9	3.7	97
Standard deviation	0.006	0.1	0.115	0.2	0.4	6
Recovery (%)	99	100	88	104	99	97
	Mn	Ni	Re	U	V	
Detection Limit	0.3	0.9	0.004	0.04	0.6	
NASS5	16.7	4.3	0.036	10.92	23.6	
Average	16.7	4.0	0.037	11.17	21.1	
Standard deviation	0.5	1.0	0.006	1.37	2.2	
Recovery (%)	100	94	102	102	90	

seawater NASS-5 (NRC-Canada) was measured at the beginning and end of each analytical run. Analytical performance was checked by measuring a standard and blank after every 8 sample measurements. The detection limit and recovery of the standard material are shown in Table 1.

Results and Discussion

DOC and nutrients in river water

The MR discharge and major tributary contributions to the river are shown in Figure 2. During our high discharge sampling, the main contributor was the Ohio River, which accounted for more than 50% of the flow in the lower river. However, the Missouri and Upper Mississippi Rivers were the primary contributors during low river discharge, and all three tributaries had very similar contributions during the intermediate river discharge period.

The DOC and nutrient distributions are shown in Figure 3. The DOC and nutrient endmember concentrations varied seasonally in both the MR and AR, but the concentration range was similar to previously reported values (Shen et al., 2012; Duan et al., 2007; Bianchi et al., 2004; Dubois et al., 2010). These seasonal variations likely resulted from hydrologic factors such as changes in tributary mixing ratios (Duan et al., 2010) as well as inputs from the Red River (RR) and wetlands in the Atchafalaya River Basin (ARB) (Shen et al., 2012).

Different distributions of DOC and nutrients were observed between the low salinity AR and MR plumes. The distribution of DOC showed relatively higher concentrations in the AR than the MR plume, while nutrient concentrations were higher in the MR than the AR plume with the exception of phosphate and silicate during May

2008, when the concentrations were similar between the two plumes (Figure 3). Similar observations of nutrient and DOC distributions were reported previously in this system and were suggested to result from different conditions of suspended loads, mixing rates, and marsh interactions (Shen et al., 2012; Lohrenz et al., 2002; Shiller, 1993a), and different turbidities, which affect chlorophyll concentration by controlling light availability and species of phytoplankton (Pakulski et al., 2000). Total chlorophyll- a (Chl-a) concentrations showed the maximum concentration in low-middle salinity regions (Figure 3). These nutrient and total Chl-a distributions were similar to other studies in this system (Lohrenz et al., 1990, 2008; Shim et al., 2012) and suggest that the enhanced light availability with diminishing suspended load (Lohrenz et al., 1990), as well as increasing residence time with increasing salinity (Shiller, 1993b) in these regions that are the main reasons for increasing biological uptake of nutrients.

Distribution of trace elements in the shelf waters

Most of the trace elements in river waters showed seasonal variations, having higher concentrations of Fe, Mn, Cr, and Co during high river discharge (May 2008), while the concentrations of Cu, Mo, Re, U and V were high at low river flow (November 2008) (Figures 4-10). Previously, Shiller (1997, 2002) found distinctive differences of dissolved trace element concentrations in the major tributaries of MR and suggested that the observed seasonal variations of some trace elements in the lower MR (at Baton Rouge, LA) resulted from seasonal variations of the tributary mixing ratios as well as redox chemistry within the river system. During our shelf studies, the mixing ratios of the major MR tributaries varied significantly (Figure 2). With exception of Mn, a simple estimation of the MR trace element concentration based on Shiller's (1997) tributary endmembers

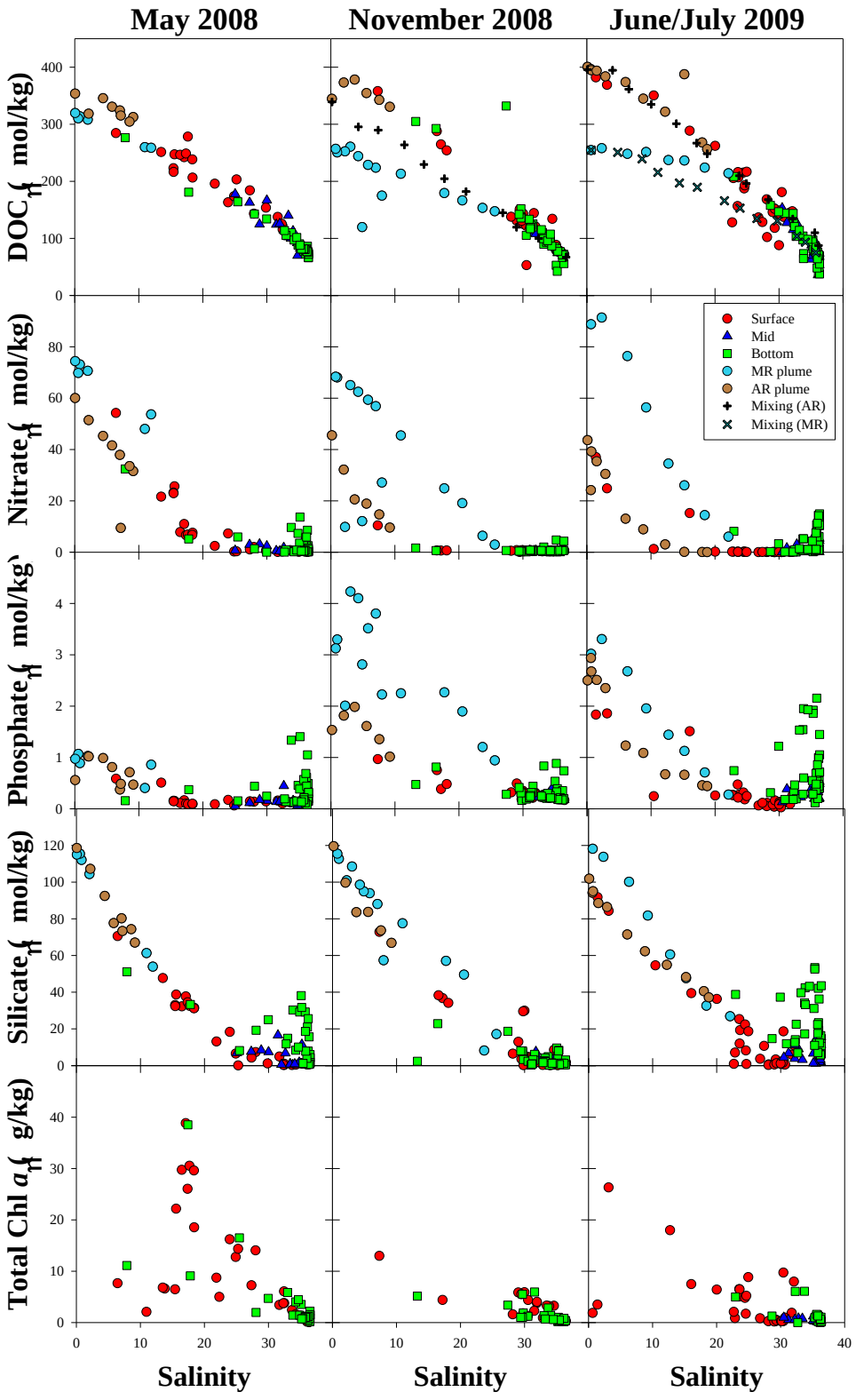

Figure 3. Distributions of DOC, nutrients, and total chlorophyll a. For, the MR and AR plumes have only surface water. Mixing experiment results are expressed black + and *x* for Atchafalaya (AR) and Mississippi (MR) Rivers, respectively.

and their mixing ratios during this study showed general agreement with the observed concentrations in the MR endmember (Appendix). During high and intermediate river flow, Mn was about 50-fold higher in the observed MR endmember than estimated, possibly due to seasonal variation in the rate of microbial Mn oxidation (Shiller and Stephens, 2005).

As mentioned above, the AR is composed of part of the MR and all of the RR discharge and flows through the ARB, which is the largest wetland in North America. During our sampling periods, the RR contributed 23% (April 24-May 8, 2008), 22% (October 22-November 4, 2008) and 35% (June 15-July1, 2009) of the water in the AR (Figure 2), suggesting that the additional inputs as well as interaction with floodplains in the ARB may have considerably affected the AR trace element concentrations (Chapter IV). During June/July 2009, the RR contribution to the AR decreased from 42% to 29% two weeks prior to our AR plume sampling (Figure 2). A plot of salinity versus the $\delta^{18}O$ of the water for the AR plume in June/July 2009 showed upward curvature below a salinity of 5, reflecting the more recent increased MR contribution to the AR as evidenced by the change to isotopicallly lighter values (Appendix A). This change of the RR contribution may have influenced the Co, Fe, and Mn distributions in the AR plume, which showed a low-salinity change at that time (June/July 2009; Figures 6, 7).

Distributions of Cs, Mo, and U

The truly dissolved (< 0.02 μm) phase was the dominant fraction for Mo, Cs, and U (Appendix B). Dissolved Cs and Mo in surface waters of the shelf showed generally conservative behavior in the field data regardless of season with some minor exceptions discussed below (Figure 4). Likewise, in the mixing experiments these elements also

showed conservative behavior. This generally conservative behavior was previously observed for Mo (Shim et al., 2012; Shiller and Boyle, 1991) and Cs (Shim et al., 2012) in this area. In the low salinity of the river plumes, Cs showed similar concentrations between the MR and AR plumes, while Mo showed slightly higher concentration in the MR than AR plume during November 2008 and June/July 2009, probably due to additional input in the ARB.

In May 2008 during high river flow, Cs at low salinity both in the field and the mixing experiment showed a slight removal possibly due to adsorption onto riverine particulate material during estuarine mixing (James and Palmer, 2000). However, this Cs removal at low salinity was not observed during the other two sampling times, which may be due to lower fluvial SPM during mid-low river discharge (waterdata.usgs.gov).

Bottom water Mo and Cs distributions generally agree well with the surface metal-salinity trend for all our study periods. During June/July when there was low bottom water DO, the bottom water Cs and Mo at high salinity showed slight removal (Figure 4 and A3). Because bottom DO was not correlated with salinity, an apparent bottom water Cs and Mo removal with oxygen was not all simply from the result of freshwater influences. For Mo, our observation in low DO bottom water is comparable to previous observations of diffusive Mo loss into anoxic sediments in oxygen-depleted waters (Emerson and Huested, 1991; Crusius et al., 1996; Morford et al., 2005, 2007) as well as removal via adsorption onto particles as a result of reduction of soluble Mo(VI) to reactive Mo(IV) in natural anoxic waters (Helz et al., 1996). In contrast, however, anthropogenic radio-Cs (Cs-137) has been observed to be released in anoxic sediments (Davison et al., 1993; Comans et al., 1989; Evans et al., 1983). Thus, the observation of

apparent bottom water Cs removal at low DO in this study remains unclear. Nonetheless, the shelf bottom acted as a sink for Cs and Mo at least in June/July 2009 during bottom water hypoxia.

For U, previous studies in this system reported conservative (Shim et al., 2012) and non-conservative (Swarzenski and McKee, 1998) distributions with the non-conservative behavior attributed to adsorption onto settling particles and/or interaction of water with salt marshes at low salinity (Swarzenski and McKee, 1998; Sarin and Church, 1994; Church et al., 1996). Slight removal of U in the field relative to the mixing experiment was observed at low salinity in the AR plume during November 2008. This U removal at low salinity may therefore have been related to the interaction with the extensive salt marshes surrounded in the micro-tidal Atachafalaya Bay system as has been observed in the lower Delaware salt marshes (Church et al., 1996). During June/July 2009, the variation of U in the low salinity MR and AR plumes may reflect the temporal change in the river endmember as evidenced by non-linearity of the $\delta^{18}O$-salinity relationship of the water (Appendix). Slightly higher U concentration in the MR than AR plume during June/July 2009 may be related to additional input in the ARB, similar to Mo. In June/July during bottom water hypoxia, the surface U distribution showed slightly lower concentration in the field than the mixing experiment, particularly in some high salinity waters as compared to the MR mixing experiment. This distribution is probably due to episodic vertical mixing as evidenced by other elements (Co, Mn, Cu, Ni; see below). During November 2008, a group of samples showed relatively low concentrations of U in some of high salinity surface waters (e.g., C6, D3, F5, F7, F8, I4, I8, I9 and X3) compared to other regions similar in salinity (Figure 4, Appendix). Because relatively low U

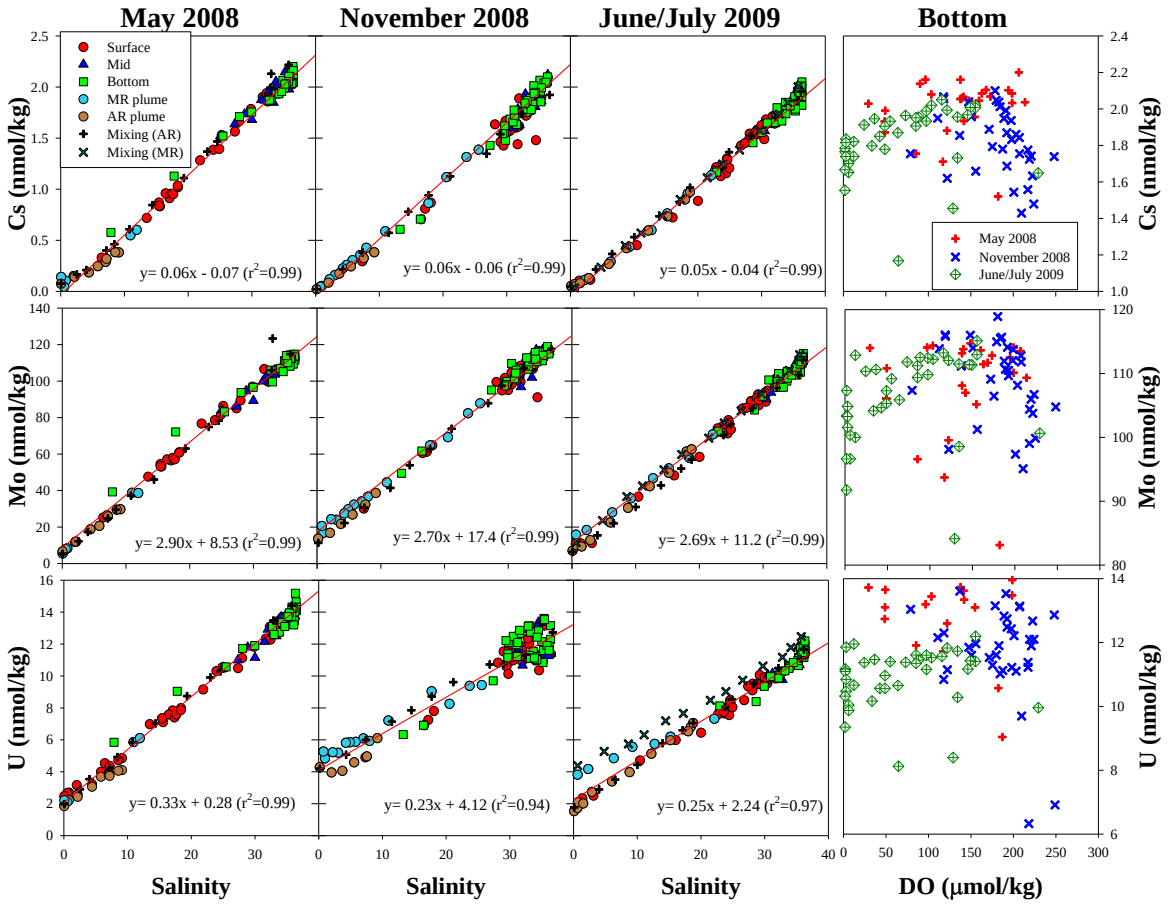

Figure 4. Distributions of Cs, Mo and U. The left three columns show concentrations versus salinity for each survey; the rightmost column of figures show bottom water DO versus concentration for all surveys. For, the MR and AR plumes have only surface water. Mixing experiment results are expressed black + and *x* for Atchafalaya (AR) and Mississippi (MR) Rivers, respectively. Regressions are generated for surface waters including the two river plumes (n= 44, 57 and 50 for May and November 2008, and June/July 2009), and p values for all regressions were < 0.0001).

concentrations were found in the bottom and middle depths of these stations, vertical exchange may affect the surface U distribution at this time. That is, U depleted bottom water during bottom water hypoxia may be mixed with surface water under weak water stratification conditions in November.

Bottom water U concentrations showed seasonal variations having the concentrations in the order June/July 2009 < November 2008 < May 2008. In June/July during bottom water hypoxia, the bottom water U at high salinity showed slight removal (Figure 4, Appendix), which may lead to lower U concentrations than during the other two times. This distribution suggests the shelf may act like a sink for U during bottom water hypoxia. The observed U removal at low DO is comparable to previous reported U geochemistry in oxygen-depleted waters (Klinkhammer and Palmer, 1991; McManus et al., 2005; Morford et al., 2005, 2007). During November 2008, bottom water U concentrations were intermediate compared to the other two periods, probably due to vertical mixing. The scenario, again, is that U depleted bottom water during hypoxia may have mixed with surface water, resulting in higher bottom water U in November compared to the June/July bottom water, as well as relatively lower U in some high salinity surface waters compared to the other surface water of similar salinity during November 2008.

Distributions of Cu and Ni

The behaviors of Ni and Cu were complex (Figure 5), but the concentrations of the elements were similar to the previous studies in this system (Shim et al., 2012; Shiller, 1993a; Shiller and Boyle, 1991). These elements were mostly in the truly dissolved phase (< 0.02 μm). In the associated mixing experiments, Cu and Ni showed largely

conservative behavior, implying that any non-conservative behavior of these elements in the field data is not likely the result of flocculation or adsorption reactions.

In bottom waters, slightly elevated concentrations of Ni and Cu relative to surface and middle depths during May and June/July were observed (Figure 5, Appendix). The bottom water enrichment of Cu and Ni is not surprising given that these elements are known to be mostly organically complexed and tend to be preferentially remineralized in reducing environments (Petersen et al. 1995; Waeles et al., 2005; Baeyens et al., 1998; Turner et al., 1998; Martino et al., 2004). Likewise, the bottom water Ni and Cu during May and June/July showed negative correlations with DO, suggesting either their dissolution and/or their diffusion from reducing sediments. During November 2008, bottom water Cu and Ni showed non-conservative behavior, probably due to the mixing of Cu and Ni enriched bottom water with surface waters.

In the low salinity of the AR and MR plumes, the AR plume Cu showed upward curvature indicative of Cu addition while the MR plume was generally conservative. This difference, therefore, most likely resulted from sedimentary inputs in the shallow Atchafalaya Bay and/or an increase of binding efficiency of Cu to organic matter (humic substances) with increasing salinity (Lores and Pennock, 1998). Generally, Ni in both river plumes showed conservative behavior.

Surface concentrations of Ni and Cu in the field data were frequently higher than in the mixing experiments. In part, we suggest that this phemomena reflects the different freshwater endmembers for the mixing experiment and field as evidenced by changes the $\delta^{18}O$ values at salinity ~ 5 in June/July 2009. During November 2009, Cu and Ni in high salinity surface and bottom waters were enriched relative to the mixing experiment.

Because the mixing experiment was conservative, this enrichment is not likely derived from desorption in surface waters. One might argue that the elevated surface as well as bottom water Cu and Ni may be derived from different freshwater sources in November when the freshwater residence time on the shelf is a few months (Dinnel and Wiseman, 1986). However, extrapolating the high salinity trend of Cu and Ni to zero salinity yielded to river endmembers > 40 and > 50 nmol/kg, respectively, which are greater than has been previously observed in the lower MR (Shiller, 1997). Thus, the elevation of Cu and Ni was derived from processes in the shelf rather than from changes in the river concentration. It was concluded that the enriched surface Cu and Ni likely reflects benthic input as evidenced by elevated Mn, Co, and Fe (see below).

During June/July 2009, the concentrations of Ni and Cu in surface waters from some shallow stations (e.g., E2, F3, F5, H0, H3, I1, I2, etc) were elevated. Mn, Co, and Fe at these stations were also increased at the surface, indicative of episodic vertical exchanges in relation to the seasonal changes in circulation on the shelf in which summer winds become more upwelling-favorable (Cochrane and Kelly, 1986). Thus, the episodic addition of the elements found in our study may reflect somewhat different distributions than those found in previous studies that reported fairly conservative mixing of Cu and low salinity removal of Ni (Shim et al., 2012; Shiller, 1993a; Shiller and Boyle, 1991). The observation of elevated surface water Cu and Ni concentration during strong water stratification (average surface-bottom salinity difference of 10) implies that episodic upward mixing may be important process altering the shelf surface water Cu and Ni distribution.

Distribution of Fe

Mostly, Fe was in the colloidal phase (0.02-0.45 µm), typically accounting for over 90% of the total dissolved phase (< 0.45 µm) in all surface water samples (n=149) during all sampling periods (Figure 6). It has been noted that our low end cutoff for the colloidal fraction is larger than the 10 kDa cutoff commonly used by other workers (e.g., Guo et al., 2000), and that very little organic matter is retained by the 0.02 µm filters (Shiller, 2003). Thus, most of the organically-complexed and bioavailable Fe was likely in our truly dissolved (< 0.02 µm) fraction, and the colloidal fraction in our study was mainly composed of suspended nanoparticles including Fe hydroxides (Shim et al., 2012; Stolpe et al., 2010).

During the study period, elevated bottom water Fe relative to surface and middle depths was observed (Figures 7, Appendix). However, there may have been different processes causing bottom water Fe increases for different seasons. The dissolved (< 0.02 µm) Fe showed an inverse correlation (r^2=0.39, n=33, p= 0.0003) with DO during June/July 2009 (Appendix). For May 2008, excluding some of low salinity samples, a negative correlation was also observed (r^2=0.33, n=26, p= 0.0021) with DO. This distribution suggests particulate or sedimentary Fe dissolution under reducing conditions for these two surveys. Generally, the bottom water increase in Fe concentration was not as great as the Mn concentration increases at low DO (see Figure 7 and next section), possibly due to the more rapid oxidation of Fe than Mn, the deeper (i.e., more reducing) sedimentary conditions needed for Fe reduction, and the possible incorporation of reduced Fe into sulfides. The bottom water Fe-DO relationship was not observed in the November study, probably due to generally higher bottom DO concentrations at this time.

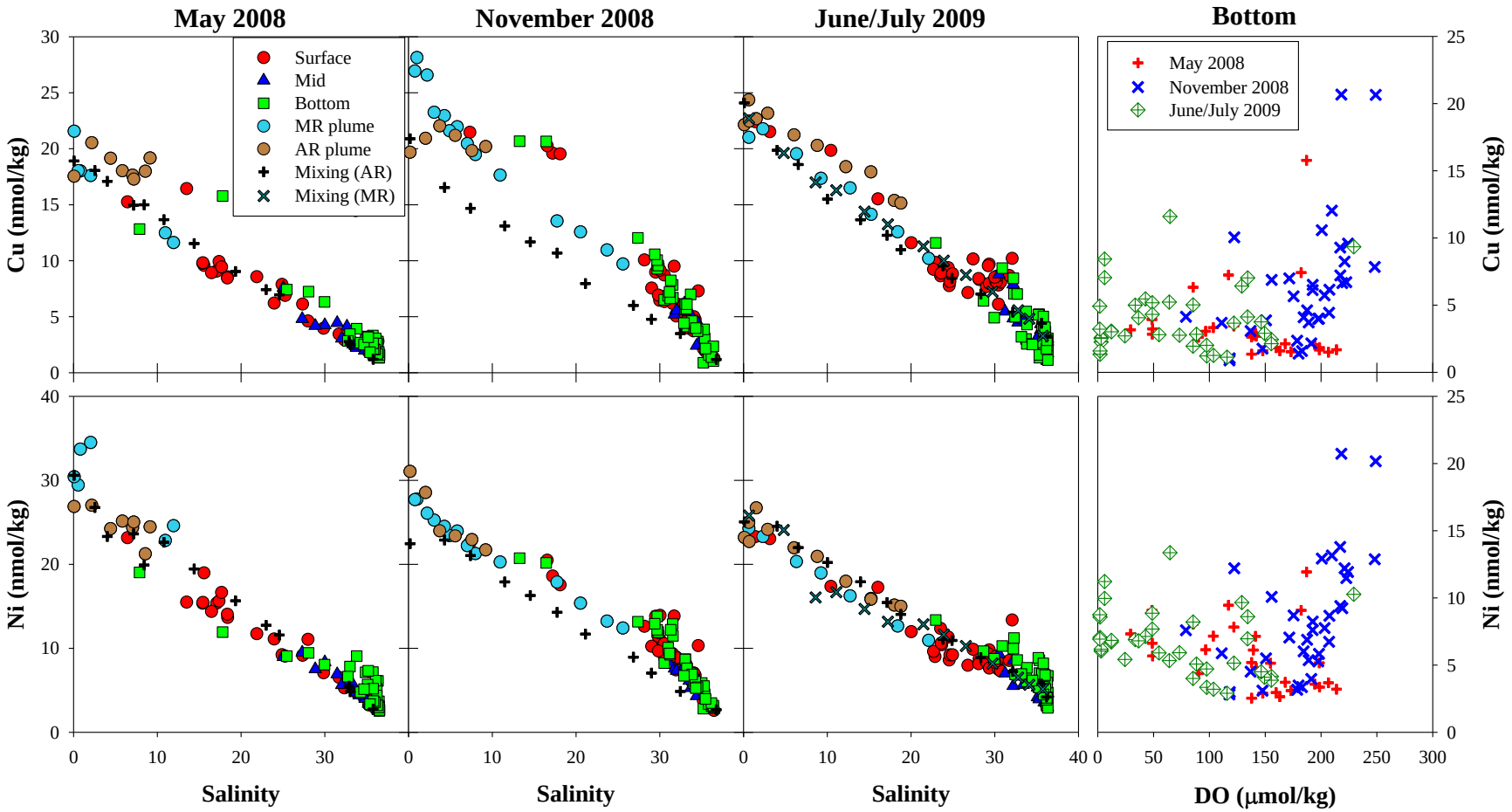

Figure 5. Distribution of Cu and Ni are shown. The left three columns show concentrations versus salinity for each survey; the rightmost column of figures show bottom water DO versus concentration for all surveys.

During all of the study periods, the surface water distribution of Fe was non-conservative in both the field data and mixing experiments (Figure 6), showing rapid removal at low salinity with low Fe concentrations (< 10 nmol/kg) at high salinities (S > 20). This Fe removal behavior is typical in estuarine systems (Powell et al., 1996; Shim et al., 2012) and mainly reflects colloidal organic flocculation/coagulation during estuarine mixing (Sholkovitz et al., 1978; Boyle et al., 1977). In the two low salinity river plumes, Fe (both phases) was higher in the AR than MR plume with the exception of slightly higher colloidal Fe in the MR than AR plume during May 2008. Again, this distribution is probably due to the higher river concentration of Fe in the AR, which is derived from inputs from the RR and wetland waters in the ARB. The colloidal Fe in the MR in May 2008 was much greater than during the other two study periods as well as previous studies (Shim et al., 2012; Shiller and Boyle, 1991). In June/July 2009, the Fe distribution in the field and the mixing experiments were not closely matched, probably due to the change of river endmember evidenced by the $\delta^{18}O$ distribution at this time (Appendix).

In comparison, while concentrations of colloidal Fe were closely matched between the field data and mixing experiment, the dissolved Fe (< 0.02 μm) in the field was always lower than the mixing experiment. One might argue that the higher dissolved Fe in the mixing experiments resulted from not enough time for Fe-flocculation/coagulation and thereby less Fe removal in our mixing experiment compared to the field. However, in the laboratory experiments of sea- and river water mixing, Boyle et al. (1977) reported that the kinetics of the Fe precipitation were extremely rapid with a time scale of a few minutes. Thus, the overnight mixing experiments should have allowed for plenty of the time for Fe removal in the mixing experiment samples, and therefore,

the deviation between the field data and mixing experiments likely resulted from other processes in the field rather than the artifacts of our mixing experiments.

The removal of dissolved (< 0.02 μm) Fe might be attributed to biological consumption (Ho et al., 2003; Powell et al., 1996; Shim et al., 2012). The nitrate distribution with salinity showed almost identical removal as the dissolved Fe distribution, similar to the observation by Shim et al. (2012). During May 2008, the salinity where nitrate and dissolved Fe approached zero, and the peak of the Chl-a distribution were well coincided (Figure 3). Based on a cellular Fe:N ratio of 0.47 nmol/μmol (Ho et al., 2003), if we assume that the decrease of nutrients is due to biological uptake, then the decrease of nitrate from 80 μmol/kg to 0.1 μmol/kg during May 2008 yields about 35 nmol/kg of potential Fe removal. Similarly, the potential Fe removal was found to be about ~ 33 and ~ 42 nmol/kg during November 2008 and June/July 2009, respectively. These potential Fe removals were of similar magnitude to the fluvial dissolved Fe concentrations, suggesting that biological activity may indeed greatly influence the surface Fe distribution of the shelf. Obviously, these estimates are crude and do not account for differences in the regeneration of nutrients and Fe.

Benthic inputs also may have influenced the surface Fe distribution during the November and June/July periods. At those times surface Fe (both colloidal and dissolved) from shallow, inshore stations was higher than other offshore surface waters with similar salinity. During low river flow in November, the water stratification was found to be much weaker than during the other seasons due to the thinner buoyant freshwater layer at the surface and mixing because of a passage of fall atmospheric fronts (Dagg et al., 2007). The average salinity differences between the surface and the bottom were smaller in

November 2008 (~ 2) than in May 2008 (~ 7) and June/July 2009 (~ 9), suggesting the conditions more conducive to vertical mixing. Other trace elements (e.g., Mn, Co, Ni, and Cu) were elevated as well, suggesting that vertical mixing altered the surface Fe distribution in November 2009.

During June/July, despite significant stratification, several inshore, shallow stations (A1, H0, and I1) showed elevated Fe relative to other offshore surface samples with similar salinities. This increase was probably due to episodic vertical exchange in these shallow waters and was also evidenced by increased concentrations of Mn, Cu, and Ni at the surface. Also, the salinity difference between surface and bottom at stations H0 and I1 was very weak < 2, and the surface DO in the A1 was 145 μmol/kg (about 50 μmol/kg lower than other surface waters), indicative of recent vertical mixing. This distribution implies that the vertical mixing may play an important role in surface biological activities by supplying bioactive trace elements.

Distribution of Mn

The distribution of Mn is shown in Figure 7. The truly dissolved (< 0.02 μm) phase of Mn was the predominant phase except for a few samples in the low salinity AR plume during November 2008 when colloidal Mn was up to 55% of the total dissolved (< 0.45 μm) fraction (Figure 7, Appendix).

Higher bottom water Mn relative to surface and middle depths was observed in all of our surveys. This distribution is consistent with other estuarine observations and most likely results from reductive dissolution of Mn oxides in the sediments (Almroth et al., 2009; Colbert and McManus, 2005; Klinkhammer and McManus, 2001; Sundby and Silverberg, 1981). The observed Mn elevation at low bottom water DO also suggests

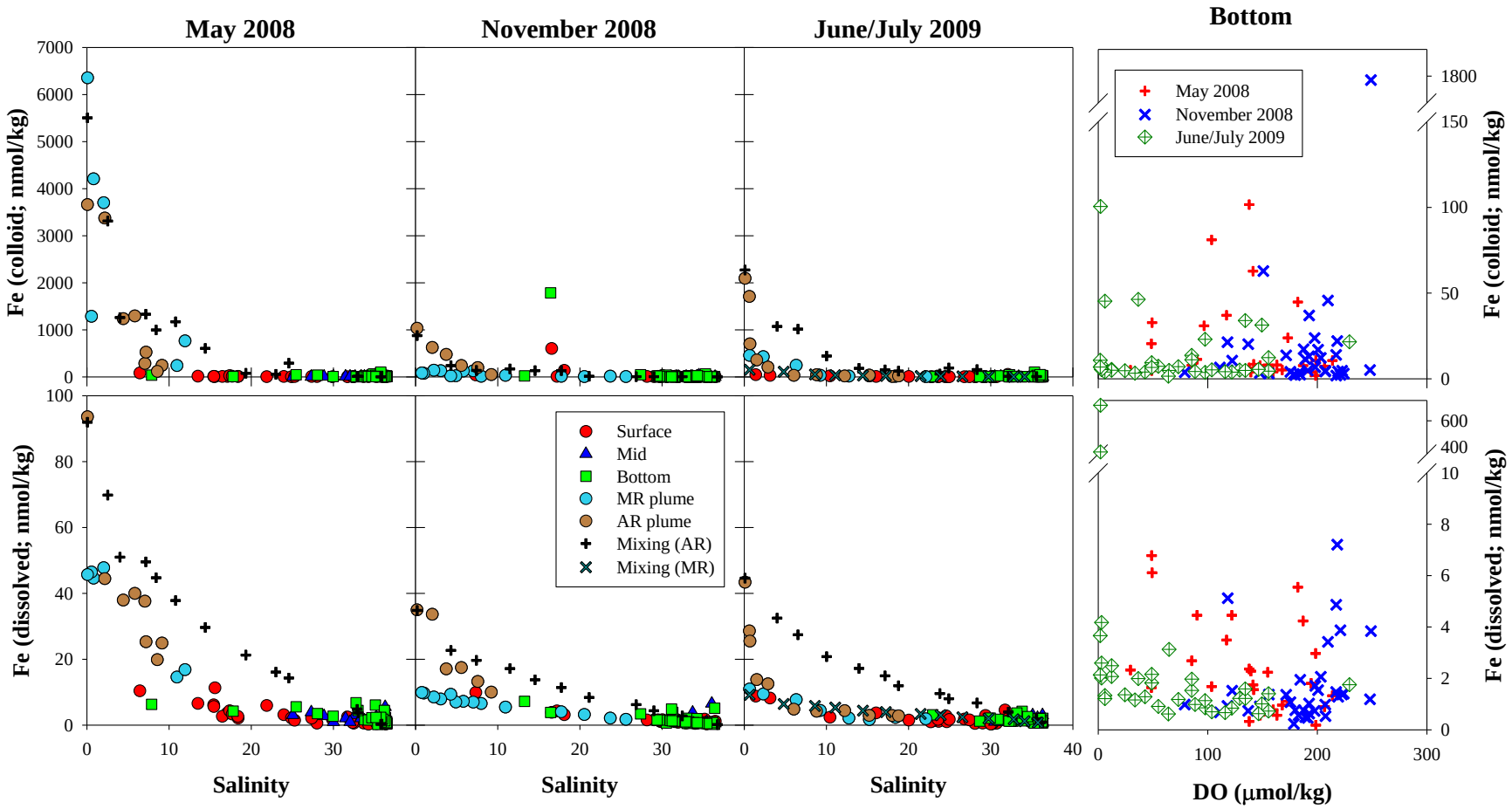

Figure 6. Distribution of colloid (0.02 – 0.45 µm; upper panel) and dissolved (< 0.02 µm; lower panel) Fe are shown. The left three columns show concentrations versus salinity for each survey; the rightmost column of figures show bottom water DO versus concentration for all surveys.

dissolution and/or diffusion from reducing shelf sediments. During November 2008, concentrations of Mn in the bottom water were not elevated as much as the other two periods, possibly due to precipitation of Mn-oxides and/or limiting reductive mobilization from sediments under well-oxygenated conditions (Shim et al., 2012). Overall, the seasonal variation of bottom water Mn distributions was likely controlled by oxygenation of the bottom waters.

During all sampling periods, surface Mn showed non-conservative behavior, with rapid removal at mid-salinity (S ~ 15) during May 2008 and upward curvature at low-mid salinity for November 2008 and June/July 2009. The field Mn data showed lower concentrations than the associated mixing experiment during May 2008, whereas the Mn concentrations were higher in the field than the mixing experiments during November 2008 and June/July 2009.

During November 2008, Mn showed maximum concentrations at low and mid-salinity, and this distribution has been commonly observed in other estuarine systems (Roitz et al., 2002; Yang and Sanudo-Wilhelmy, 1998) as well as in this system (Shim et al., 2012). Desorption of Mn from riverine suspended particulate matter (SPM) has been suggested based on river-seawater mixing experiments (Hatje et al., 2003; Li et al., 1984). However, the concentration of Mn in our field data was much greater than in our mixing experiments, suggesting an additional source of Mn. As has been mentioned in previous sections, vertical mixing could have readily occurred at this time, and similar concentrations of Mn and other elements (Cu, Ni) in surface and bottom waters, indicating the field Mn in November 2008 may be derived simply a result of vertical mixing at high salinity. For the low salinity MR plume, the maximum peak of Mn was

observed near the MR mouth and rapidly decreased toward the outer shelf. At this time of low river flow, the salt wedge can extend well upstream of the MR mouth (Figure A1), and the sediments deposited under freshwater regime may release Mn to the water column when they encounter salt water. For the low salinity AR plume samples, there were also some samples elevated above the mixing line, indicative of sedimentary Mn input in Atchafalaya Bay at this time (Shiller and Mao, 1999).

During June/July 2009, there was much higher Mn in the field data at low to intermediate salinity than in the mixing experiment (Figure 7). Although it has been noted above, a change in AR endmember at this time, low salinity samples in the MR plume are much higher than previously reported for the MR (Shiller, 1997), suggesting that the elevation in Mn at low-intermediate salinity is indicative of another source. Clearly the mixing experiment results argue against Mn desorption from the fluvial suspended load in June/July. We were not able to obtain near-bottom samples in the low salinity regions. However, given the very high Mn enrichment of the low DO bottom waters (Figure 7), it would seem that mixing with those waters is the most likely source of the low-salinity surface water Mn enrichment. In June/July despite increased water stratification, some high salinity surface samples also showed increased Mn relative to the mixing experiment and other high salinity surface waters. At these stations, elevated Ba, Co, Cu, Fe, and Ni were also observed in the surface waters. Thus, the increase of Mn in some high salinity surface waters was probably due to episodic vertical exchange even at strong water stratification periods when summer winds become more upwelling favorable (Cochrane and Kelly, 1986).

During high river flow (May 2008), Mn in the two rivers was much greater than the other two study periods as well as compared with Shiller's (1997) lower MR temporal study. This distribution is probably due to seasonal variation in the rate of microbial Mn oxidation (Shiller and Stephens, 2005). Mn at low salinity in the AR plume showed sharply fluctuating concentrations with salinity. We are not sure what processes are responsible for this Mn distribution, but possible processes are: different parcels of water on slightly different river-seawater mixing trends as evidenced by slightly lower salinity at AR8 than at AR5, eventhough AR8 was further from the AR mouth than AR5. Alternatively, inflow of water from surrounding bays (e.g., Vermilion Bay) (Walker and Hammack, 2000) with different Mn concentrations may have affected the AR plume. At this time, the field Mn was lower than that of the mixing experiment. Sinks for dissolved Mn include precipitation by formation of Mn-oxides or adsorption onto particles (Fe-hydroxides; Millward and Moore, 1982, and organic matter; Roitz et al., 2002; Moffett and Ho, 1996) and biological activity including uptake (Bruland et al., 1991; Sunda and Huntsman, 1997) and microbial oxidation (Shiller and Stephens, 2005). The distribution of Mn was similar to Fe (e.g., decreasing pattern) along the salinity gradient, indicating possible Mn removal together with Fe (Millward and Moore, 1982) particularly during May 2008 when Mn and Fe concentrations were much greater than the other two periods.

Biological assimilation of Mn by phytoplankton may be considerable at mid-salinity with high Chl a (~ 40 µg/kg Chl a). Based on ratios of Chl a to carbon of 125 (gC/gChl a) in this area (the highest value from Lohrenz et al., 1992) and a Redfield-type elemental ratio of Mn:C ($3.8\sim25.9 \times 10^{-6}$:1) in phytoplankton (Ho et al., 2003), phytoplankton uptake could account for up to 40% of the observed Mn concentrations in

the water during May 2008. The estimates during the other two periods were generally less than 10%.

Microbial Mn oxidation has been found to be an important process for Mn removal in river and estuarine waters with the oxidation rates 10-84 nM/day (Shiller and Stephens, 2005; Sunda and Huntsman, 1987). Considering the residence time of Louisiana Shelf water of from a few days to months (Dinnel and Wiseman, 1986; Moore and Krest, 2004), microbial Mn oxidation may also play an important role in the surface Mn removal.

Distribution of Co

The truly dissolved (< 0.02 μm) phase of Co was the predominant phase except that there was considerable colloidal Co in the two low salinity river plumes as well as some high salinity waters during November 2009 that accounted for up to ~ 40% of the Co (Figure 8, Appendix).

Enrichment of bottom water Co relative to surface and middle depths was observed during all our studies. During hypoxic conditions in June/July 2009, bottom water Co was negatively correlated with DO, suggesting that the Co increase was probably due to diffusion from anoxic sediments and/or dissolution from particles (Takata et al., 2010). At this time, the bottom water Co was also positively correlated with Mn (Appendix), indicating a similar behavior of Co and Mn and suggesting the release of Co occurs concomitantly with the reductive dissolution of Mn oxides (Santos-Echeandia et al., 2009; Shaw et al., 1990). During November 2008, elevated Co was observed in some bottom waters (e.g., A1, C1, E1, F1, and F2), and the increase may have originated from benthic mobilization of Co (Takata et al., 2010; Chiffoleau et al., 1994).

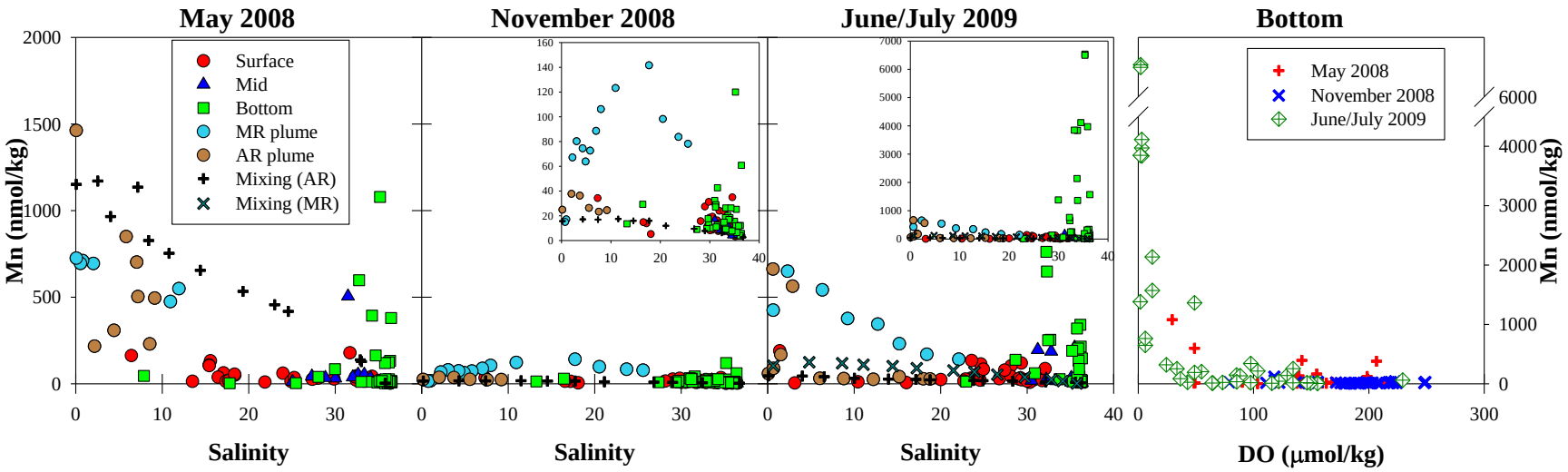

Figure 7. Distribution of the total dissolved (< 0.45 μm) Mn. The left three columns show concentrations versus salinity for each survey; the rightmost column of figures show bottom water DO versus concentration for all surveys. Insets are also expressed for November 2008 and June/July 2009, as well as for bottom water, and units are same as the original figures.

During all the sampling periods, Co showed non-conservative behavior, with maximum concentrations at low-intermediate salinity. This behavior has been observed in other estuarine systems (Tovar-Sanchez et al., 2004; Takata et al., 2010) as well as previously in this system (Shim et al., 2012) and appears to be due to Co desorption from riverine SPM (Takata et al., 2010; Hatje et al., 2003; Li et al., 1984). In the low salinity river plumes, the field Co data was generally similar to the mixing experiment, consistent with the idea of Co desorption. The low salinity AR plume Co showed fluctuation during May 2008, which probably reflects different water parcels similar to the Mn distribution at this time (see Mn section). During November, the MR plume Co showed higher concentrations than in the mixing experiment, particularly for mid-high salinities, possibly due to desorption from river sediments when salt intrusion reached the far upstream of MR at this time, similar to the Mn distribution. Thus, desorption of Co may play an important role on surface dissolved Co distribution at low-mid salinity in the shelf.

At intermediate to high salinity, the field Co concentrations were higher than the associated mixing experiments in at least two of our studies (November and June/July) (Figure 8). As discussed in previous sections (e.g., Cu, Ni, Mn, and Fe), the vertical mixing in both periods may affect the surface Co distributions. During November 2008, in addition to broad downward curvature, the surface Co showed the maximum peak at high salinity in shallow (< 20 m) stations (e.g., A1, C1, C4, C6, C7, D0, E1, F2, and F3). At this time, it seemed like that the enriched bottom water Co, leftover from when bottom water hypoxia occurred, may have vertically mixed in November when mixing readily occurs, similar to U and Cu (see U and Cu sections). Thus, benthic flux of Co is perhaps

the most important process altering the surface Co distribution in the shelf at least during low-intermediate river discharges.

During high river flow, concentrations of Co were slightly lower in the field data than in the mixing experiment, which contrasts with the other two periods. Biological assimilation of Co, based on ratios of Chl a to carbon of 125 (gC/gChl a) in this area and a Redfield-type elemental ratio of Co:C (1.3×10^{-7}:1) in phytoplankton (Bruland et al., 1991; Ho et al., 2003), suggests that the phytoplankton assimilation of Co could account for an uptake of up to 50% of the observed dissolved Co during May 2008, but generally less than 10% of the Co during the other sampling periods. Thus, the phytoplankton activity could also play an important role on the surface Co distribution, at least during bloom conditions in May.

Distribution of Cr

For Cr, the colloidal (0.02-0.45 μm) phase was dominant at low salinity, and the truly dissolved phase (< 0.02 μm) was dominant at intermediate to high salinity (Figure 9). The distribution of colloidal Cr showed non-conservative behavior in both the field data and the associated mixing experiments, revealing a downward curvature during high (May2008) and intermediate (June/July 2009) river discharges. During low river flow (November 2008), while the mixing experiment for colloidal Cr showed an increasing trend with salinity, the field colloidal Cr showed a plateau until mid-salinity (S ~ 27) and then increased at higher salinity. Dissolved (< 0.02 μm) Cr showed a different distribution in the field data from the mixing experiments. In the mixing experiments, dissolved Cr showed fairly conservative behavior during all our studies. In the field data, the dissolved Cr distributions showed downward curvature in all our studies showing low Cr at mid-high salinity.

Some of the bottom waters showed Cr depletion relative to the surface and middle depths particularly during May 2008 and June/July 2009. When plotted versus DO, bottom waters showed clear depletion of Cr with diminished oxygen. This distribution is not surprising given that soluble Cr(VI) can be reduced to particle-reactive Cr(III) in reducing environments (Richard and Bourg, 1991 and references therein). Note that one could also hypothesize that bottom water dissolved Cr could be high due to oxidation of Cr(III) to soluble Cr(VI) during Mn reduction (Eary and Rai, 1987; Richard and Bourg, 1991). However, given that it has already demonstrated that Mn increases and Cr decreases as bottom DO was diminished, this distribution is clearly not the case (Appendix). This is consistent with the major locus of reduction being in the sediments with the resulting dissolved Mn diffusing out from sediments into water column, while oxidized Cr diffuses into sediments to be reduced therein at the same time. During the November study, the bottom water Cr showed similar concentrations to the surface and showed a similar distribution with salinity. This distribution was possibly due to the vertical mixing together with horizontal mixing between the low Cr of mid-salinity and the high Cr of high-salinity waters.

Surface colloidal Cr during our studies showed removal at low salinity particularly in May 2008, probably due to colloid flocculation/coagulation. The associated mixing experiments also showed similar distributions, supporting the idea that colloidal flocculation is responsible for low salinity Cr removal (Figure 9). The low salinity MR plume showed higher colloidal Cr concentrations than in the low salinity AR plume with the exception of similar concentrations in November 2008, possibly due to variation of the inputs from the RR and wetlands in the ARB.

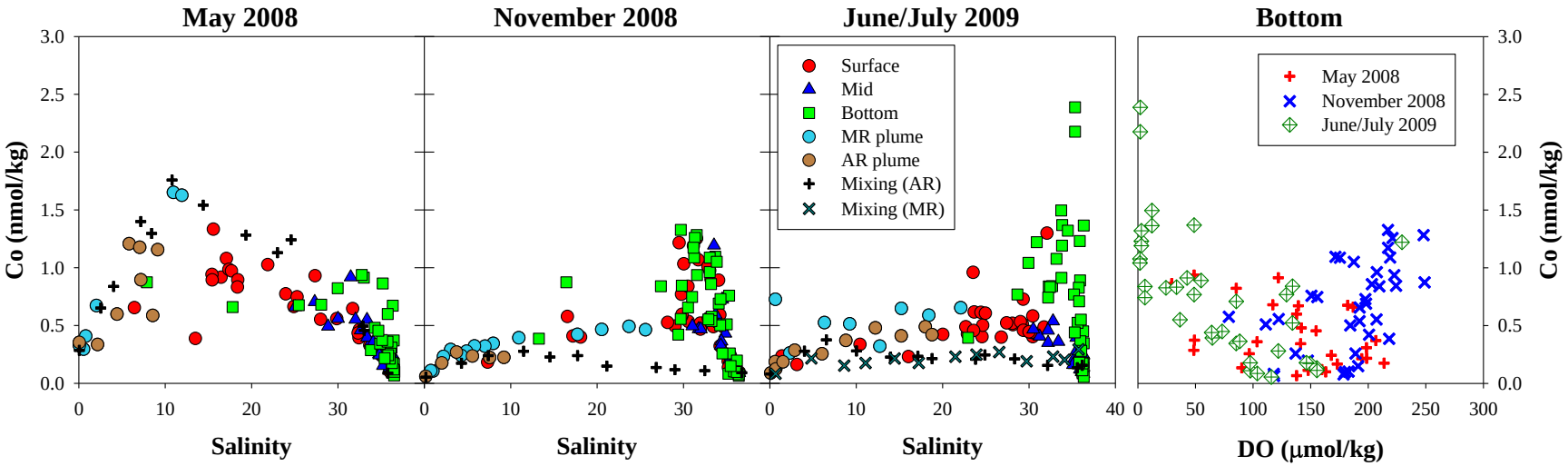

Figure 8. Distribution of the total dissolved (< 0.45 µm) Co. The left three columns show concentrations versus salinity for each survey; the rightmost column of figures show bottom water DO versus concentration for all surveys.

In addition to low salinity Cr removal, the field surface Cr concentrations at intermediate to high salinity were lower than in the mixing experiments, which is a similar observation to previous studies (Shim et al., 2012; Shiller and Boyle, 1991). Shiller and Boyle (1991) explained the removal Cr by the variation of river endmember Cr. However, as was noted by Shim et al. (2012), this removal seems to occur regardless of the river stage, making such an explanation unlikely. Thus, in situ processes such as biological uptake (Wang and Guo, 2000; Wang and Dei, 2001), photoreduction (Kiever and Helz, 1992) and vertical mixing with Cr-depleted bottom water may be responsible for the Cr removal in the shelf. Also, the fairly conservative behavior of the dissolved Cr in the mixing experiment supports the idea that the removal in the field is derived from the above processes rather than the flocculation at mid-high salinity in the field.

Biological uptake and/or related activities (e.g., production of organic ligands) has been suggested for Cr removal in the water column (Wang and Guo, 2000; Wang and Dei, 2001), and the organic ligands (colloid)-Cr complexation can increase Cr uptake by marine plankton (Wang and Guo, 2000). Interestingly, during May 2008, the salinity (~ 15) of the lowest Cr, the maximum Chl a, and the removal of Fe and nitrate coincided, suggesting that biological uptake may have contributed for the surface Cr removal during this period of apparent high biological productivity.

Photochemical reduction of Cr(VI) to Cr(III) in surface water has been suggested in other estuaries (Kieber and Helz, 1992; Abu-Saba and Flegal, 1995) and in this system (Shim et al., 2012). Shim et al. (2012) found that the Cr removal appeared in less turbid surface waters away from the most immediate river influence. Similarly, in our studies, the sharpest removal of surface Cr (or the largest difference between the field and the

mixing experiment) occurred at high salinity, suggesting that the light-induced Cr reduction and the removal by adsorption onto particles may play an important role in the apparent Cr removal in the surface waters during all of our studies (Kieber and Helz, 1992).

In addition to photochemical Cr removal, vertical mixing could result in apparent Cr removal from the surface waters. Depletion of the bottom water Cr was observed particularly during June/July 2009 and some of May 2008; thus the vertical mixing could enhance the apparent Cr removal in the surface water. During November 2008, the similar Cr concentration in the surface and bottom waters was suggestive of vertical mixing. The Cr depleted bottom water at the time of low DO may have mixed with surface water around our November sampling time. During June/July 2009, some surface water Cr at high salinity (> 25) was found to be very low in some stations with low bottom water Cr concentrations (e.g., C1, E2, F3, G3, H0, I1, etc), suggesting episodic vertical exchanges affecting surface Cr distribution as also evidenced by elevated concentrations of Co, Cu, Fe, Mn, and Ni. In the May study, the surface Cr distribution may also have influenced by vertical mixing. That is, the vertical mixing may have been occurred prior to our sampling, and the low Cr bottom water signal remained until the time of our sampling (see V section).

Distribution of Re and V

The distributions of Re and V showed non-conservative behavior in both the field and the associated mixing experiments (Figure 10). The truly dissolved (< 0.02 μm) phase was the main form of these elements.

Bottom water concentrations of V were depleted compared to surface and to middle depth waters in some stations during June/July 2009 when the bottom water DO concentrations were low. This distribution is probably due to reductive V removal under reducing environments (Emerson and Huested, 1991). Similar observation was previously reported for the Louisiana Shelf (Shiller and Mao, 1999). Vanadium showed a negative correlation with Mn when the DO < 65 μmol/kg, probably due to the diffusion into the overlying water column for Mn and into sediments for V (Appendix). This bottom water V distribution suggests that the shelf may act like a sink for V during bottom water hypoxia.

Seasonally, the V distribution in the surface water was complex in the field and the associated mixing experiments. This stems partly from the high standard error of our analytical method for V. Distributions of V in the field and the mixing experiment showed an initial decrease as salinity increased in both the low salinity MR and AR plumes during May 2008 and June/July 2009. Adsorption of V onto particulate matter and thereby removal from the water column may contribute to the V distribution (Prange and Kremline, 1985; Yeats, 1992; Auger et al., 1999; Takematsu et al., 1985). The V distributions were similar to colloidal Fe at the low salinity (S < 8) in May 2008, suggesting that the V removal at low salinity may have been associated with adsorption onto the Fe-colloidal flocculants (Auger et al., 1999). In June/July 2009, changes of freshwater sources as evidenced by the $\delta^{18}O$-salinity plot (Appendix) may have resulted in a rapid decrease of V in the AR plume. During November 2008, the low salinity MR plume V showed a decreasing trend in the channel until the MR mouth was reached. But, V in the AR plume showed fluctuation, probably due to the analytical scatter.

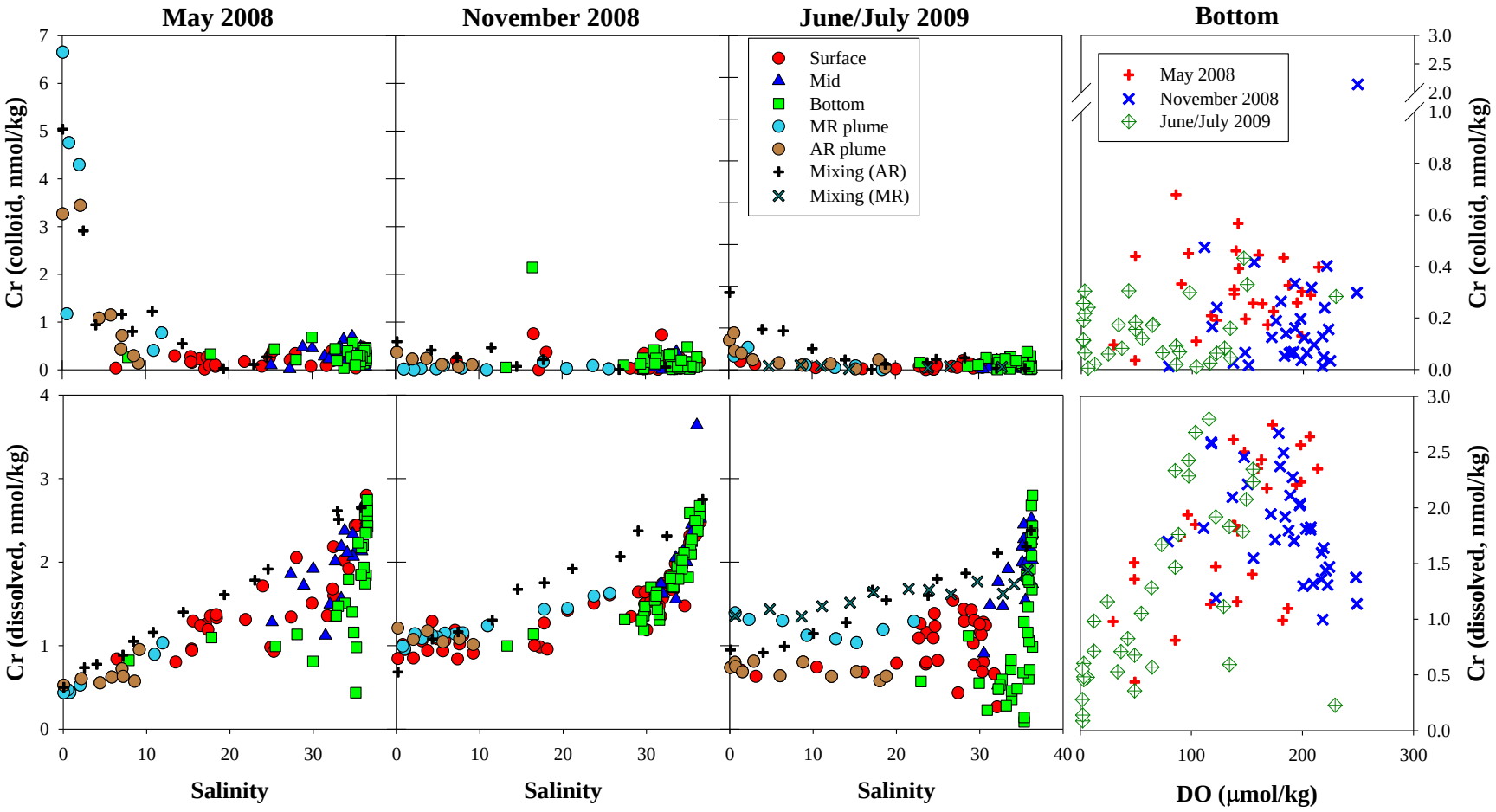

Figure 9. Distribution of the colloid (0.02 – 0.45 μm; upper panel) and dissolved (< 0.02 μm; lower panel) Cr along the salinity gradients. The left three columns show concentrations versus salinity for each survey; the rightmost column of figures show bottom water DO versus concentration for all surveys.

At salinity > 20, surface water V showed a decrease again, particularly in the May and June/July studies, and it resulted in the depletion of V relative to the mixing experiments (Figure 10). Previously, Shiller and Boyle (1987) suggested biological associated V removal based on the similarity between V and phosphate. However, we have not observed correlations of V with nutrients or the total Chl a, consistent with previous observation in this system (Shiller and Mao, 1999) and in the Long Island Sound (Wang and Sanudo-Wilhelmy, 2009). The bottom and middle depth V during May 2008 was similar to the surface. As suggested previously by Shiller and Mao (1999), the mid-salinity surface water V depletion probably results from vertical mixing of V-depleted bottom waters into the surface. Although we were not sure when the mixing occurred, Mn was slightly elevated in the surface water (Figure 7). Considering the rapid Mn-oxidation rate in natural waters (Sunda and Huntsman, 1986; Shiller and Stephens, 2005), the vertical mixing could have occured contemporaneously. During June/July 2009, as has been discussed in previous sections, surface V depletion may also be associated with vertical mixing of V depleted bottom. The episodic vertical mixing could be an important process on V distribution even during strong water stratification conditions.

During the November study with low river flow, most of the field surface V concentrations were higher than the associated mixing experiment. Similar V concentrations between surface and bottom water together with the elevated Mn, Co, and Fe concentrations suggest benthic inputs under well-mixed conditions. Previously, Shiller and Mao (1999) suggested the sedimentary input of V at low salinity regions of Atchafalaya Bay at almost the same time of year as we observed here, and benthic inputs

of dissolved V and desorption of V from resuspended particulate matter have also been suggested in the Long Island Sound (Wang and Sanudo Wilhelmy, 2009). Thus, benthic input may be an important process that affects V concentrations in shelf waters, at least in November.

In contrast to V or Mo, we did not observe depletion of Re nor a relationship with DO in the bottom water (Figure 10), even though both elements can be removed under reducing conditions (e.g., Morford et al., 2005, 2007). This contrasting behavior is likely related to the sulfur content in the water column (Helz and Dolor, 2012). Helz and Dolor (2012) reported that Re(VII) could be reduced to insoluable Re(IV) in the presense of sulfide at least > $10^{-3.0}$ M, whereas Mo could be reduced at the condition of $10^{-4.9}$ M of sulfide. Athough we did not measure the sulfur content in the water colmn, the different reaction of Mo and Re to S may result in the removal of Mo, but not for Re in this sytem during bottom water hypoxia. Also, more reducing conditions are needed for Re reduction than V reduction. For example, Crusius et al. (1996) reported that Re enrichment in sediments occurred at depths below Fe and U reduction. Since V is often incorporated with Fe-Mn (hydr)oxides (Auger et al., 1999; Takematsu et al., 1985), Re reduction may occur at the depths below V reduction. In this study, particularly in June/July with oxygen-depleted bottom waters, the release of Fe was not as prominent as Mn, though U and V removal was apparent. Thus, the system was not sufficiently reducing in either the bottom waters or near the sediment-water interface to lead to Re reduction.

Surface Re distributions were broadly conservative along the salinity gradient (Figure 10). Note that the high uncertainty of the Re measurements at these low

concentrations results in significant analytical scatter of the results. In previous work, others have occasionally observed non-conservative estuarine Re behavior which has been suggested to result of desorption from fluvial SPM (Colodner et al., 1993), the vertical exchange of Re depleted bottom water with the surface, remobilization of Re from the sediment to the water column during oxic condition (Morford et al., 2009; Rahaman and Singh, 2010), and the possible incorporation of Re in sulfide minerals (Miller et al., 2011; Xiong, 2003). Nonetheless, the concentrations of Re we observed were within the range previously reported in this system (Shim et al., 2012), and the conservative Re distributions are similar both to the previous study in this area and other estuaries in India and the Amazon plume (Shim et al., 2012; Rahaman and Singh, 2010; Colodner et al., 1993).

Estimation of shelf sink/source and influence of vertical mixing

Based on the differences between theoretical and field element concentration at salinity 23-36.5 in bottom waters, the removal of bottom water elements was estimated for the June/July during bottom water hypoxia. As an example, the theoretical Cr in the bottom water has been estimated by simple regression (or tie-line) of Cr between the lowest and highest bottom salinities. Also, the regression for the field bottom water Cr was generated using 2^{nd} order polynomial curve fit. The removal of Cr is determined by the area lying between the tie-line and the the 2^{nd} order polynomial curve. The estimationyielded that about 5 % of Cs, Mo and U, ~ 50% of Cr, and 30% of V may have been removed, regardless of removal mechanisms, relative to the theoretical concentrations at the bottom in June/July 2009. This estimation suggests that the shelf may act as a sink for these elements under the low DO conditions. At the same time,

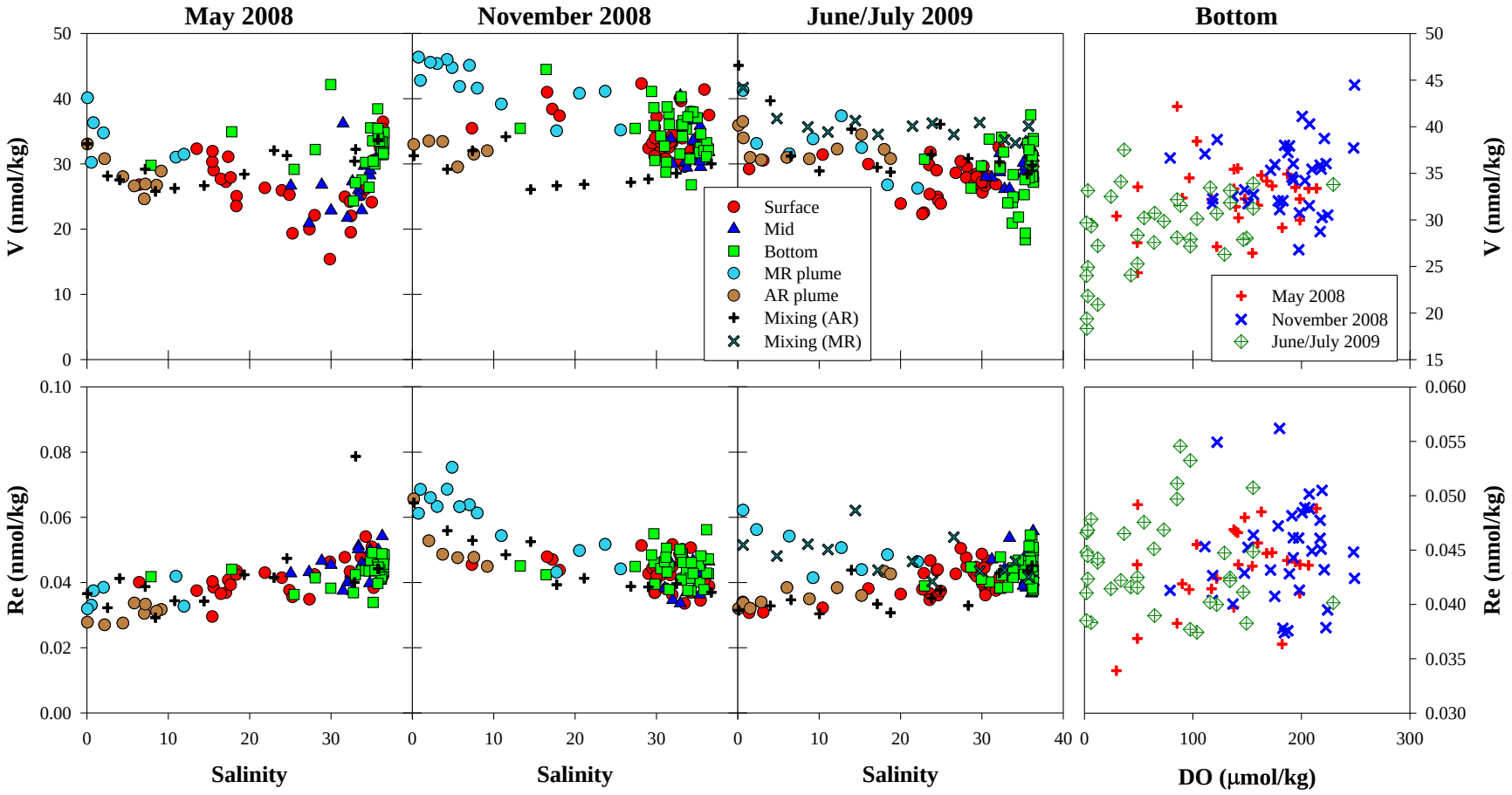

Figure 10. Distribution of the total dissolved (< 0.45 µm) V and Re are shown. The left three columns show concentrations versus salinity for each survey; the rightmost column of figures show bottom water DO versus concentration for all surveys.

bottom water Co, Cu, Fe, Mn, and Ni were enriched relative to surface waters, suggesting that the shelf bottom is a source for these elements during bottom water hypoxia. Moreover, in general, the bottom water hypoxia persists until fall (Rabalais et al., 2010) on the shelf, and the apparent removal/enrichment of those elements may be greater toward the end of the bottom water hypoxia relative to our June/July period.

As has been discussed, vertical mixing affects surface water trace element distributions in June/July 2009 during strong water stratification and bottom water hypoxia. To investigate how much the bottom water affects the surface element distributions, a simple calculation was made. For example, based on an average Mn concentration of 30 nmol/kg at salinity ~ 30, the increase of Mn concentration up to 100 nmol/kg in some high salinity surface waters is assumed to result from the bottom water. Using the highest bottom water Mn concentrations (~ 7 μmol/kg), this estimation suggests that < 1% bottom water input could account for the surface water Mn increase. Also, the influence of the vertical mixing was estimated to be roughly > 50% for Cu and Ni, ~ 1% for Fe, and ~ 14% for Co. For Cr and V, which showed removal at the surface, the calculation yields up to 50% of potential bottom water influences for both elements, assuming that the apparent Cr (or V) surface removal is derived only from the vertical mixing of Cr (or V) depleted bottom water with surface water, which is not.

Of course, the estimation of vertical mixing was overestimated by assuming only bottom water could affect the element distributions at the surface, which is not real. As discussed above, there are many other processes affecting trace element distributions at surface waters. Nonetheless, the estimation indicates that the element distribution at the surface could be very easily altered even with small contribution of bottom water

depending on bottom water concentration. The estimation implies that the vertical mixing could be an important mechanism supplying trace elements to the surface even during strong water stratification. Perhaps, this vertical mixing is the most important processes of trace element supply in some high salinity water with low river influence.

Conclusions

The large data set including different seasons and depths allow us to improve our understanding of trace element behavior in this region. The observed seasonal variation of trace elements in the rivers was probably due to seasonal changes in relative contributions of MR tributaries as well as inputs from Red River and wetlands in the Atchafalaya Basin. Distributions of Cs, Mo, and U showed conservative behavior along the salinity gradient regardless of season. Also, Re showed broadly conservative behavior.

During May 2008, colloidal flocculation was an important process removing Fe and Cr at low salinity, while biological uptake and photochemistry were important factors for Fe and Cr removal, respectively, at mid-high salinity. Removal of Mn at this time may also be related to biological activity as well as adsorption onto particulate matter. For Co, desorption from particulate matter was the main factor for the mid-salinity maximum as well as the considerable biological uptake. Cu and Ni at this time showed broadly conservative behaviors with slight sedimentary inputs at low salinity. For V, adsorptive removal at low salinity and vertical mixing with V depleted bottom water may play important role on surface V distribution. Bottom water Cu, Ni, Fe, Co, and Mn during May 2008 were elevated relative to their surface concentrations in some low DO waters, while bottom water Cr and V concentrations were decreased, probably due to reductive dissolution and/or diffusion in the sediments.

In November 2008 during low river discharge, surface distributions of all the studied elements were greatly influenced by vertical mixing, which is led by frequent passage of winter atmospheric fronts at this time of year. In addition, the surface Fe distribution was affected by colloidal flocculation and biological uptake. Also, Cu at low salinity in the AR plume may have been increased by sedimentary input. Desorptive addition of Co and Mn was observed in the two low salinity river plumes. For Cr, photochemical reactions may also lead to surface water Cr removal. The bottom water trace element distributions were influenced by vertical mixing.

In June/July 2009 during bottom water hypoxia, bottom water enrichment of some elements (Co, Cu, Fe, Mn, and Ni) was observed, probably due to reduction, dissolution, and/or diffusion from sediments. At the same time, in the bottom water Mo, Cr, V, and U were removed under low oxygen, probably due to the reduction/diffusion into the sediments. Interestingly, Cs also showed a decreasing trend when the bottom water DO decreased, which is somewhat different from previous studies of Cs-release under reducing environments. At this time, we observed rapid changes in the river source, evidenced by a non-linear low salinity $\delta^{18}O$-salinity relationship, and this change hindered comparing the field and mixing experiment results. However, biological uptake (Fe), desorption (Co, Mn) and photochemistry (Cr) likely play roles in the surface water distributions of these elements. In addition, perhaps most importantly, the surface distributions of all the studied trace elements showed an evident influence of episodic vertical mixing particularly in some shallow waters where Co, Cu, Fe, Mn, and Ni were elevated, while Cr, U, and V were decreased relative to other stations similar in salinity.

Different distributions of almost all of the studied elements were observed in the two low salinity distributary zones of the MR and the AR plumes. The different trace element concentrations in two rivers were primarily derived from the additional input of RR water and the interaction of the AR with floodplains/marshes in the ARB. Also, biogeochemical processes affecting the transport of fluvial SPM and the biological activity in the two plumes play an important role on the different trace element distributions.

Overall, the findings in our study suggest that during bottom water hypoxia, the Louisiana shelf is potentially a sink or source for certain elements. Assuming that the bottom water hypoxia persists until fall, the removal or enrichment would potentially be greater then than in June/July. Also, episodic vertical mixing could be an important mechanism for supplying the trace elements to the surface during bottom water hypoxia and other periods of strong water column stratification. This distribution implies that vertical mixing may play an important role on biological productivity by supplying some micro-nutrients (e.g., Fe, Mn, Co). Depending on the element, the alteration of some of trace element distributions may very easily occur even with a small scale of vertical mixing. Thus, this mixing should be accounted for in the studies of the Louisiana Shelf biogeochemistry, particularly in relation to hypoxia. Additionally, the AR influence on shelf trace element distributions needs to be accounted for in studies of Louisiana Shelf biogeochemistry.

APPENDIX A

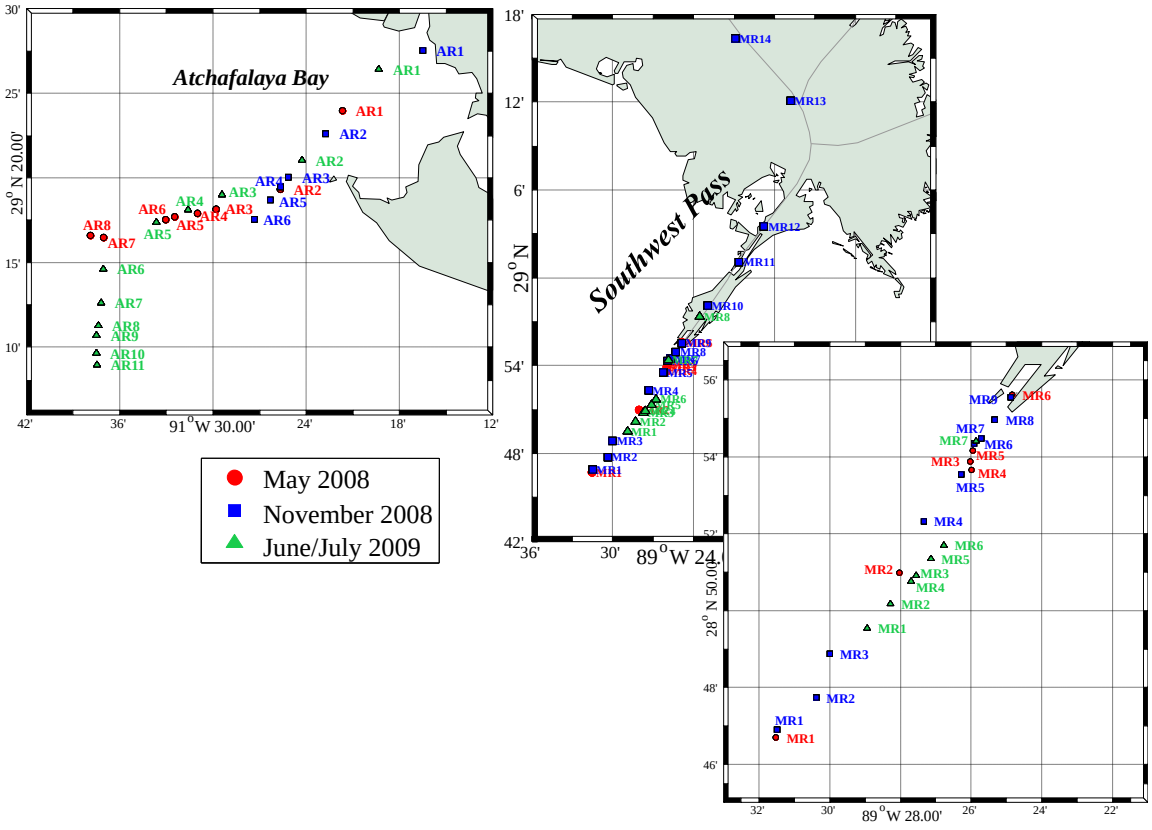

Figure. Sampling locations of the MR and AR plumes. Only surface waters were collected from these two river plumes.

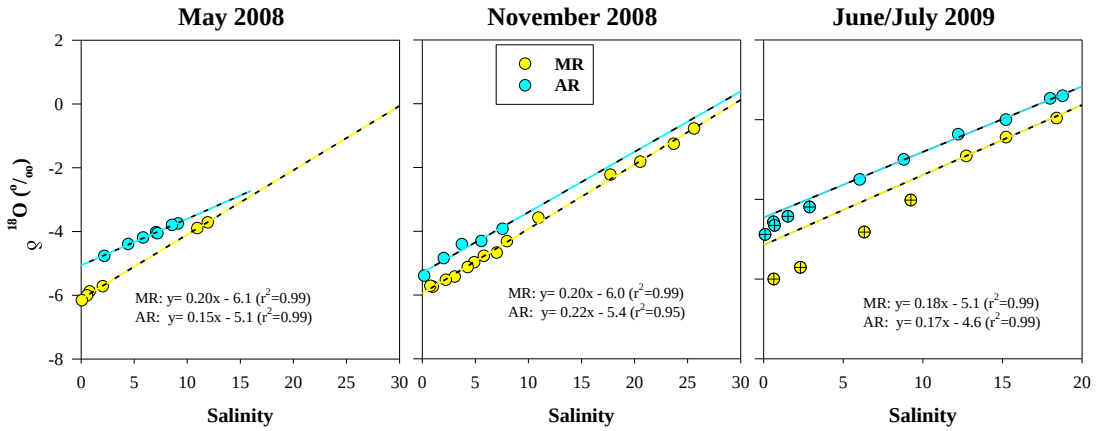

Figure. Distribution of $\delta^{18}O$ in the MR and AR plumes. Regression lines are also experessed, and for June/July, the low salinity data (cross circles) were excluded for the regression (see, text). All the p values were < 0.001.

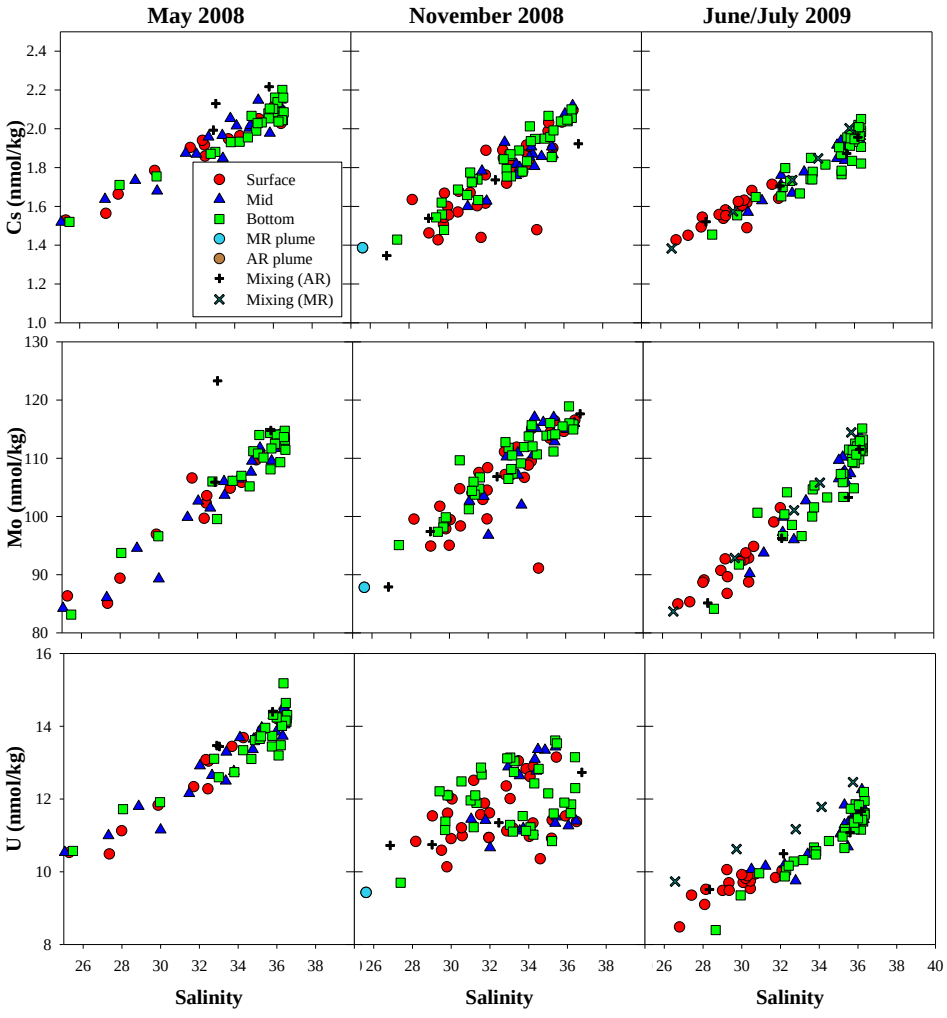

Figure. Distribution of Cs, Mo and U at salinity > 25.

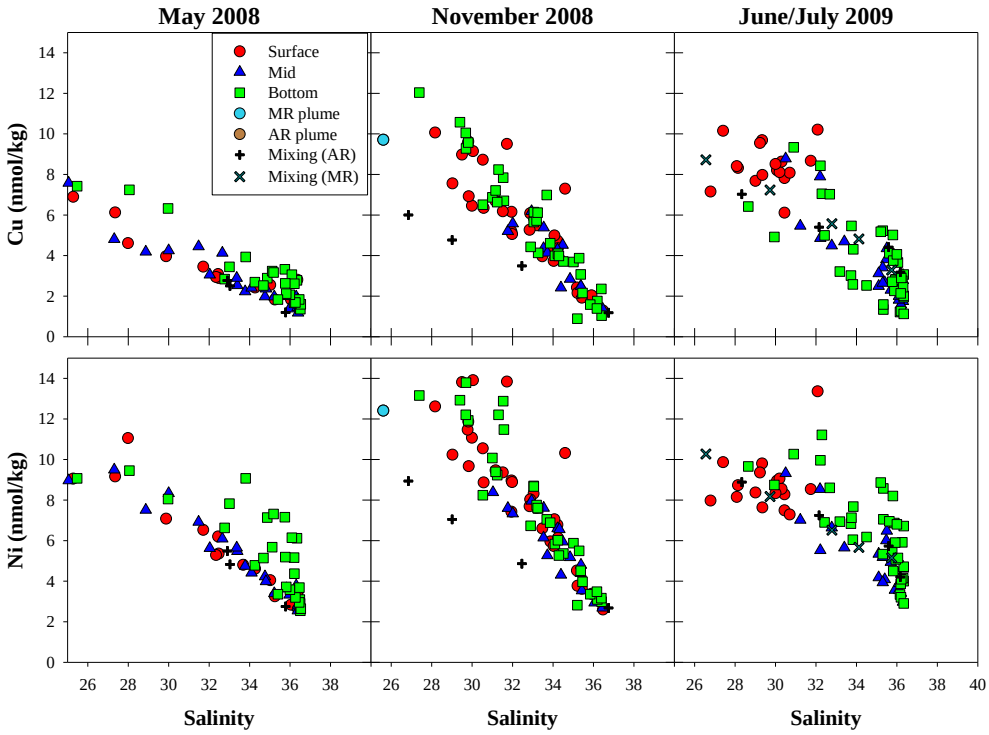

Figure. Distribution of Cu and Ni at salinity > 25.

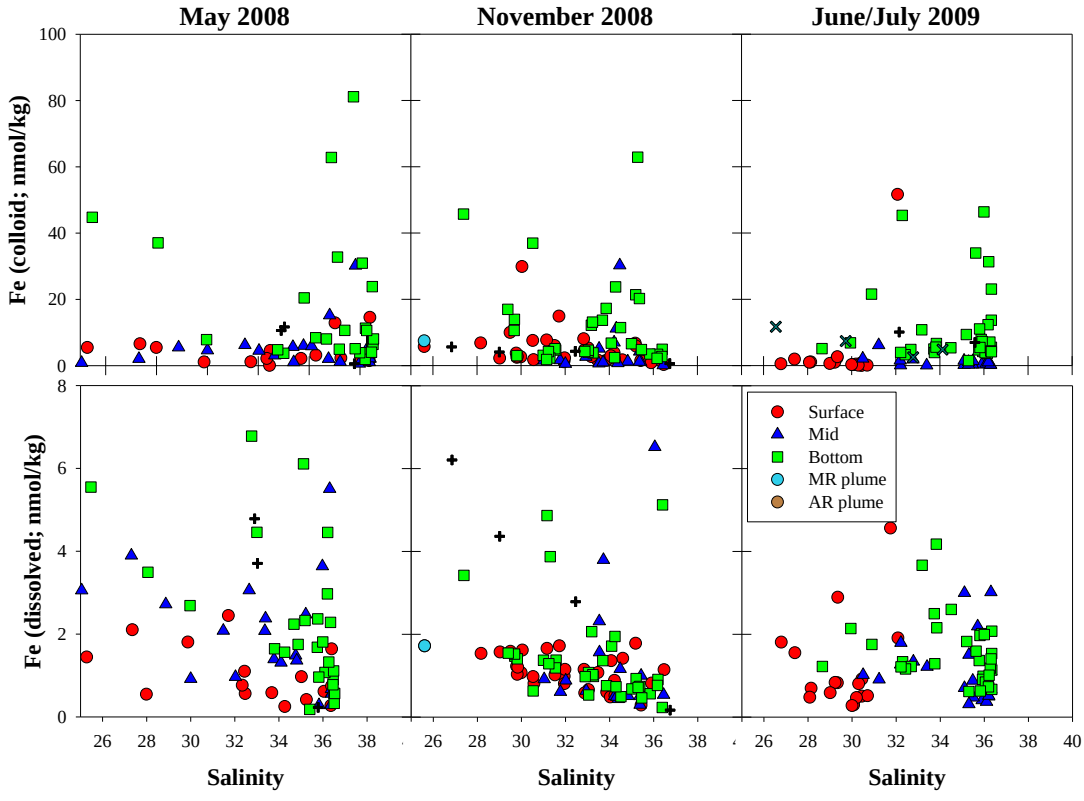

Figure. Distribution of Fe (colloid; upper panel, dissolved, lower panel) at salinity > 25.

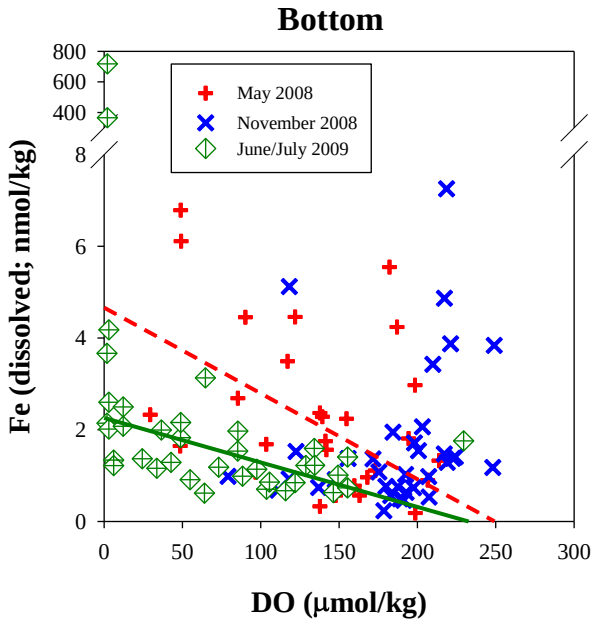

Figure. Distribution of the dissolved Fe (< 0.02 um) versus DO in bottom water is shown. Regressions for May 2008 (red dashed line) and June/July 2009 (dark green straight ling) are y= -0.019x + 4.7 (R^2=0.33, n=26, p= 0.0021) and y=-0.010x + 2.3 (R^2=0.37, n=33, p= 0.0003), respectively. And, some of low salinity waters with great Fe concentrations were excluded for the regressions.

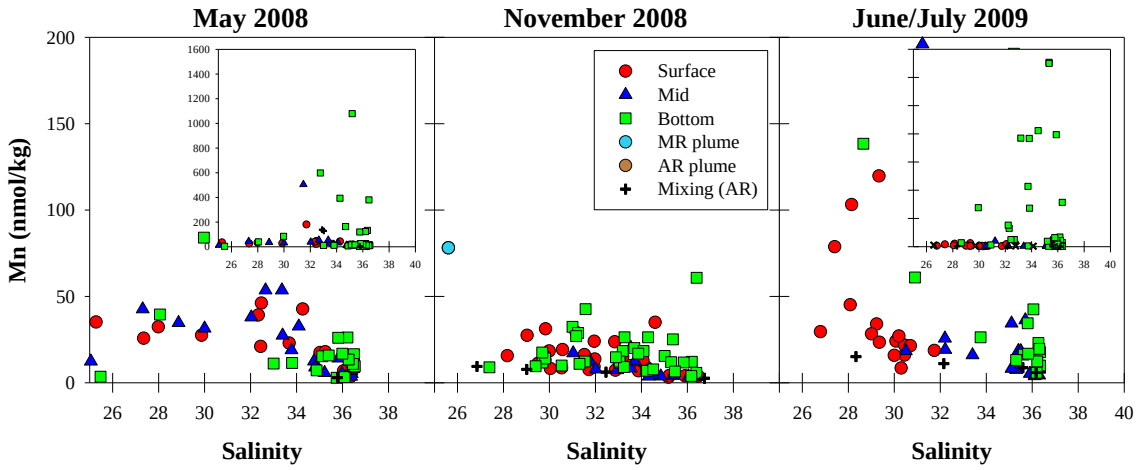

Figure. Distribution of Mn at salinity > 25.

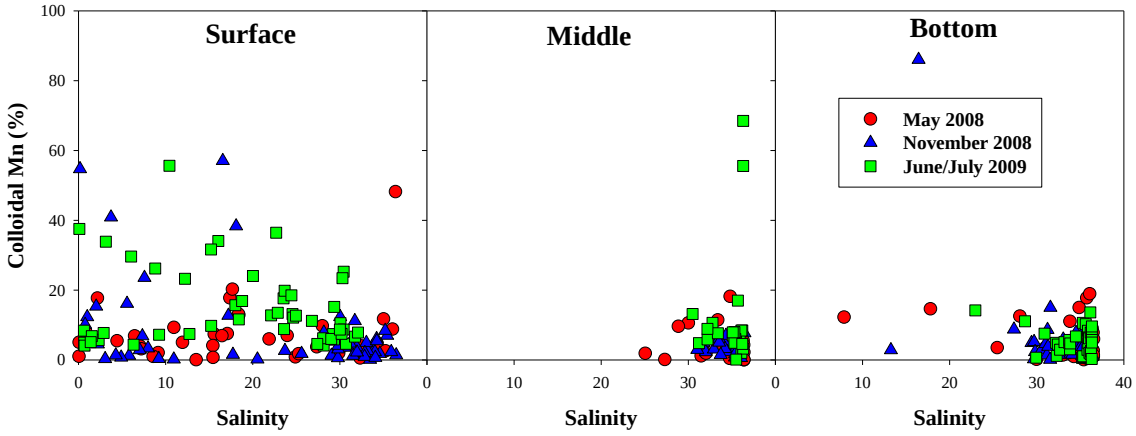

Figure. Distribution of colloidal (0.02-0.45 µm) Mn in surface, middle, and bottom depths.

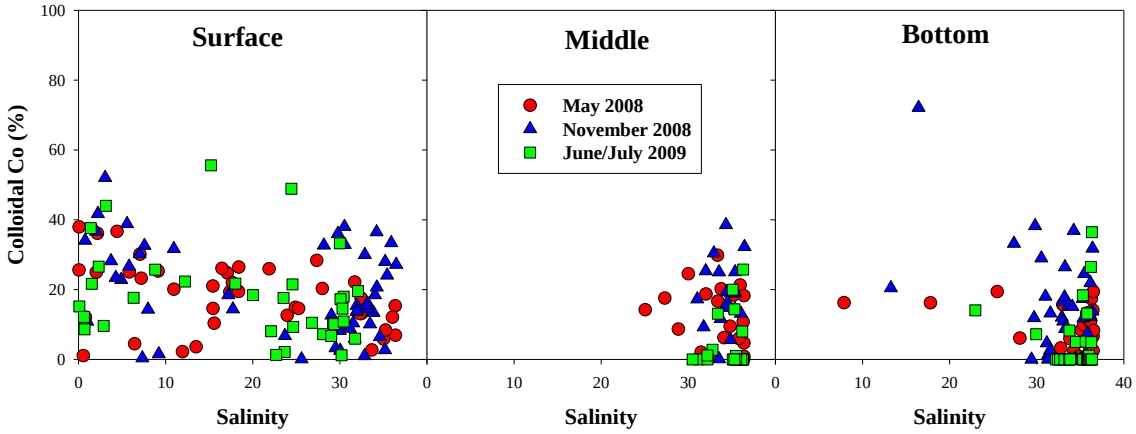

Figure. Distribution of colloidal (0.02-0.45 µm) Co in in surface, middle, and bottom depths.

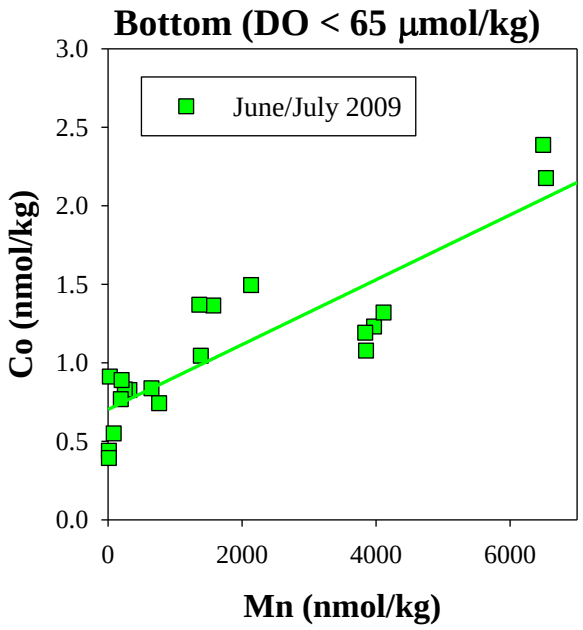

Figure. Dissolved Mn versus Co in low oxygen (<65 µmol/kg) bottom waters during June/July 2009. Regression equation is y= 0.0002x + 0.70 (R^2=0.76, n=20, p< 0.0001).

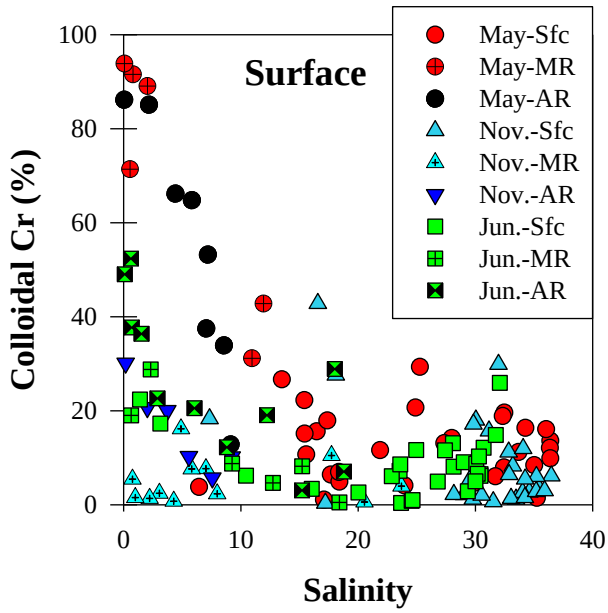

Figure. Distribution of colloidal (0.02-0.45 µm) Cr in surface waters.

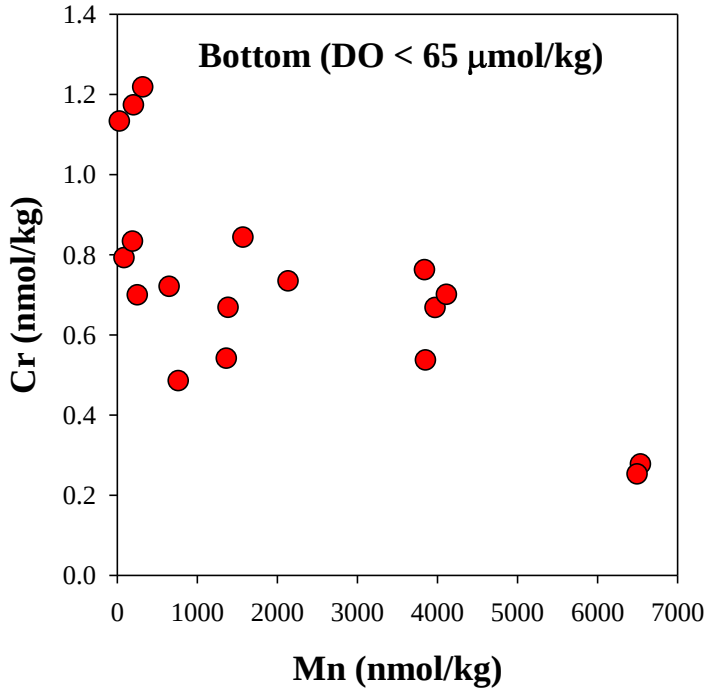

Figure. Dissolved Cr versus Mn in low oxygen (<65 µmol/kg) bottom waters during June/July 2009.

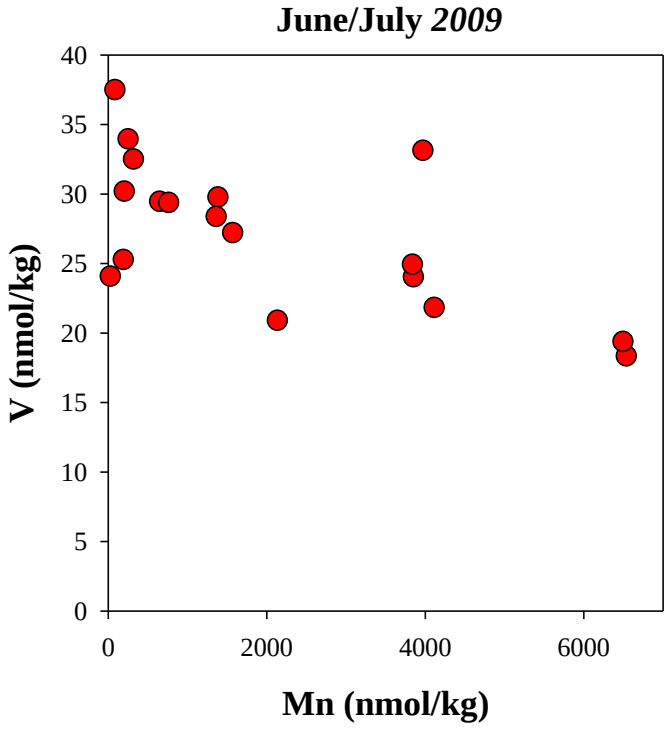

Figure. Distribution of the bottom water V with Mn at the DO < 65 µmol/kg during June/July 2009. Regression equation is y= -0.002x + 30.4 (r^2= 0.44, n=20, p= 0.0015).

APPENDIX B

Table

Estimation of trace elements based on tributary endmember and contribution, and compared with our MR endmember. The tributary trace elements endmebers were taken from Shiller (1997). Trace elements are in nmol/kg

	Date	Upper Mississippi River	Ohio River	Missouri River
Tributary Contribution (%)	5/1/2008	15.7	25.2	59.1
	10/30/2008	51.9	12.3	35.8
	6/28/2009	40.9	37.9	21.2

		Mn	Ni	Cu	Mo	Ba	U	V
Estimated (Shill, 1997)	5/1/2008	15	30.3	32.7	18.3	524	7.35	22.4
	10/30/2008	27	28.1	28.6	27.5	460	9.86	28.2
	6/28/2009	8	24.2	28.8	13.3	429	3.76	19.6
MR endmember	5/1/2008	725	30.4	21.6	5.5	393	2.47	40.1
	10/30/2008	15	27.7	26.9	20.5	568	4.94	46.4
	6/28/2009	425	24.3	21.0	15.8	573	3.82	41.2

Table

Results of May 2008

	Date	Bot. (m)	Sam. (m)	Lat.	Lon.	Salinity	Temp. (°C)	SPM (mg/kg)	DO (µmol/kg)	DOC
X3	5/1/08	90	0	28.758	89.537	22.3	22.8	4.1	245	
			80			36.5	20.1		170	
MR1	5/1/08	0	0	28.778	89.525	11.0		143.6		260
MR2	5/2/08	0	0	28.850	89.467	11.9		6.3		259
MR3	5/2/08	0	0	28.898	89.434	2.0				309
MR4	5/2/08	0	0	28.894	89.433	0.8				315
MR5	5/2/08	0	0	28.903	89.433	0.6				310
MR6	5/2/08	0	0	28.927	89.414	0.1				320
A9	5/2/08	82	0	28.751	89.750	28.0	23.1	1.9	420	143
			20			30.0	23.1	2.1	325	168
			70			36.5	20.4	2.5	207	76
A7	5/2/08	50	0	28.945	89.760	15.6	22.7	3.4	192	247
			18			32.7	22.3		161	114
			45			36.3	20.9	1.4	139	86
A5	5/2/08	30	0	29.074	89.757	17.1	23.3	4.3	598	242
			15			36.0	22.9		311	84
			26			36.2	22.3		198	82
A3	5/2/08	17	0	29.186	89.758	16.5	24.0	6.3	543	246
			14			33.8	21.9		49	110
A1	5/3/08	5	0	29.292	89.753	6.4	22.8	12.6	429	284
			4			7.9	23.3		461	277
C1	5/3/08	5	0	29.057	90.532	17.4	23.8	27.1	329	249
			3.5			17.4	23.8		326	
C4	5/3/08	13	0	28.951	90.533	17.7	23.8	5.0	336	278
			6			27.3	23.3	5.8	279	163
			11.5			33.0	23.1	11.5	122	106
C6	5/3/08	20	0	28.843	90.497	18.4	23.3	3.0	267	207
			8			33.8	23.3	1.4	241	100
			18			34.9	22.4	20.0	141	88
C7	5/3/08	20	0	28.827	90.396	18.4	23.8	1.7	335	238
			10			33.4	23.1	2.3	204	102
			20			35.7	22.6	14.0	104	78
C9	5/3/08	27	0	28.768	90.225	24.0	23.8	1.8	304	163
			10			34.8	23.2	0.4	218	92
			27			36.1	21.9	6.2	97	73
C11	5/4/08	51	0	28.587	90.207	32.4	23.4	1.4	244	122
			18			36.3	23.2	1.3	210	77
			49			36.5	20.4	2.4	173	66
F0	5/3/08	3.5	0	29.275	91.618	13.8	22.8	28.2	202	
			2.2			17.8	24.0	25.2	187	181

Table (continued).

	Date	Bot. (m)	Sam. (m)	Lat.	Lon.	Salinity	Temp. (°C)	SPM (mg/kg)	DO (µmol/kg)	DOC (µmol/kg)
AR1	5/4/08	0	0	29.400	91.362	0.1				354
AR2	5/4/08	0	0	29.323	91.429	2.2				318
AR3	5/4/08	0	0	29.303	91.497	4.4				346
AR4	5/4/08	0	0	29.299	91.517	5.8				331
AR5	5/4/08	0	0	29.295	91.542	7.1				324
AR6	5/4/08	0	0	29.293	91.551	9.1				313
AR7	5/4/08	0	0	29.275	91.618	8.6				305
AR8	5/4/08	0	0	29.277	91.632	7.2				316
F2	5/4/08	8.4	0	29.517	91.620	21.9	24.7	3.6	259	196
			6	29.517	91.620	25.5	23.6	5.3	182	164
F3	5/5/08	20	0	28.887	91.618	27.3	24.6	5.1	275	184
			10	28.887	91.618	33.4	23.2	4.3	181	140
			19	28.887	91.618	35.1	22.8	22.6	49	90
F5	5/5/08	30	0	28.699	91.621	31.7	23.7	8.8	204	138
			10	28.699	91.621	35.2	22.5	1.4	147	82
			28	28.699	91.621	36.2	21.9	8.8	90	79
F7	5/5/08	57	0	28.451	91.619	36.4	23.3	2.2	174	74
			28	28.451	91.619	36.4	22.5	1.1	178	73
			52	28.451	91.619	36.5	21.1	4.4	148	74
F8	5/5/08	82	0	28.178	91.620	36.4	23.6	0.3	174	70
			28	28.178	91.620	36.4	23.0	2.3	177	76
			82	28.178	91.620	36.5	19.9	4.8	138	66
I9	5/6/08	57	0	28.384	92.753	36.0	23.3	3.0	176	75
			28	28.384	92.753	36.4	22.0	1.2	180	81
			54	28.384	92.753	36.5	20.2	3.2	163	72
I8	5/6/08	37	0	28.648	92.759	36.4	22.9	1.8	177	74
			15	28.648	92.759	36.4	22.9	0.6	176	74
			34	28.648	92.759	36.5	21.9	1.5	160	76
I6	5/6/08	28	0	28.889	92.762	35.0	23.0	3.0	222	86
			13	28.889	92.762	35.8	22.9	2.4	218	78
			26	28.889	92.762	36.3	22.6	7.3	214	77
I4	5/6/08	20	0	29.031	92.761	33.7	23.6	15.8	232	107
			12	29.031	92.761	34.8	23.2	2.1	223	70
			19	29.031	92.761	36.0	22.8	2.7	194	80
I2	5/6/08	15	0	29.413	92.751	24.9	24.3	1.8	277	174
			7	29.413	92.751	25.1	23.7	5.3	237	178
			13.5	29.413	92.751	30.0	23.2	4.1	85	134
I1	5/6/08	11	0	29.536	92.754	13.5	24.4	3.3	260	251
			9.5	29.536	92.754	28.1	23.0	2.1	117	143

Table (continued).

	Date	Bot. (m)	Sam. (m)	Lat.	Lon.	Salinity	Temp. (°C)	SPM (mg/kg)	DO (µmol/kg)	DOC (µmol/kg)
H3	5/7/08	14	0	29.167	92.403	25.3	24.8	4.5	288	203
			9	29.167	92.403	31.5	23.3	3.9	95	124
			15	29.167	92.403	34.3	23.4	1.8	142	97
H4	5/7/08	22	0	29.040	92.391	34.3	24.2	2.1	234	104
			20	29.040	92.391	35.8	22.7	1.9	168	81
G3	5/7/08	21	0	28.974	92.007	32.5	23.8	2.2	220	115
			10	28.974	92.007	34.1	23.6	2.6	205	113
			19	28.974	92.007	35.8	23.0	5.3	138	82
F3(2)	5/7/08	20	0	28.893	91.623	29.9	24.1	3.8	253	154
			11	28.893	91.623	32.0	23.9	2.3	223	126
			19	28.893	91.623	32.8	22.9	5.7	49	114
E2(2)	5/7/08	16	0	28.745	91.254	32.3	24.3	1.5	254	125
			14	28.745	91.254	34.7	23.3	2.0	155	102
D3	5/8/08	18	0	28.725	90.837	35.3	23.9	1.5	199	82
			15	28.725	90.837	35.4	23.7	2.3	199	81
B4	5/8/08	16	0	29.035	90.120	15.4	24.0		266	223
			0	29.035	90.120	15.4	24.0	2.0	266	216
			9.5	29.035	90.120	28.9	22.6	1.2	187	125
			15	29.035	90.120	35.2	22.3	1.9	29	88

Abbreviation: Bot.: bottom depth, Sam.: sample depth, Lat.: latitude, Lon.: longitude, Temp.: temperature, DO: dissolved Oxygen, SPM: suspended particulate matter, DOC: dissolved organic carbon.

Table (continued).

	Bot.	Sam.	Total Chl a	NO_3	PO_4	SiO_3	NH_4	NO_2
	(m)		(µg/kg)	(µmol/kg)				
X3	90	0	5.0					
		80	0.2					
MR1	0	0	2.1	48.0	0.40	61.3	2.7	1.8
MR2	0	0		53.6	0.86	53.9	2.1	1.7
MR3	0	0		70.9	1.03	104.8	3.5	2.2
MR4	0	0		73.4	0.89	112.5	3.7	2.2
MR5	0	0		69.8	1.07	115.5	3.8	2.2
MR6	0	0		74.4	0.97	114.9	3.8	2.0
A9	82	0	14.0	2.0	0.14	7.3	0.2	0.4
		20		2.4	0.16	7.4	0.3	0.4
		70	0.4	2.5	0.49	4.5	0.1	0.1
A7	50	0	22.2	25.7	0.15	38.7	0.2	1.5
		18		1.8	0.45	6.7	1.9	0.7
		45	0.5	8.5	1.05	15.6	0.0	0.3
A5	30	0	38.8	10.9	0.16	37.7	0.3	1.3
		15		5.6	0.26	2.1	0.1	1.9
		26	0.6	2.5	0.61	7.9	0.2	0.6
A3	17	0	29.7	7.8	0.11	32.2	0.7	1.3
		14	1.4	9.7	1.34	30.3	4.3	1.3
A1	5	0	7.7	54.2	0.58	70.5	1.3	2.0
		4	11.1	32.5	0.16	51.3	0.9	1.7
C1	5	0	26.0	6.6	0.10	34.4	1.4	1.3
		4	38.5					
C4	13	0	30.5	6.9	0.09	32.5	1.0	1.3
		6		2.9	0.11	7.6	0.8	0.7
		12	5.9	0.9	0.14	14.9	2.0	0.7
C6	20	0	18.5	7.6	0.09	31.4	1.1	1.1
		8		0.1	0.11	0.4	0.2	0.1
		18	1.4	7.3	0.46	29.2	0.0	0.4
C7	20	0	29.6	6.7	0.10	31.1	0.8	1.1
		10		0.0	0.11	0.8	1.1	0.2
		20	1.2	3.2	0.57	29.2	0.1	1.2
C9	27	0	16.2	7.3	0.17	18.3	0.2	0.8
		10		0.2	0.11	0.4	0.1	0.1
		27	0.7	5.7	0.69	21.0	0.2	0.2
C11	51	0	6.1	0.3	0.10	0.2	0.1	0.1
		18		1.0	0.17	2.9	0.0	0.0
		49	0.2	1.7	0.30	3.8	0.2	0.2
F0	4	0	6.6					
		2	9.1	5.2	0.37	33.3	2.1	2.1

Table (continued).

	Bot.	Sam.	Total Chl. a	NO_3	PO_4	SiO_3	NH_4	NO_2
	(m)		(µg/kg)			(µmol/kg)		
AR1	0	0		60.0	0.56	118.6	3.8	3.8
AR2	0	0		51.4	1.02	107.2	3.1	3.1
AR3	0	0		45.2	0.99	92.4	3.1	3.1
AR4	0	0		41.6	0.81	77.7	3.2	3.2
AR5	0	0		37.9	0.37	80.3	3.1	3.1
AR6	0	0		31.6	0.47	67.0	3.0	3.0
AR7	0	0		33.5	0.71	74.4	2.9	2.9
AR8	0	0		9.4	0.48	73.4	2.7	2.7
F2	8	0	8.7	2.4	0.09	13.0	0.6	0.6
		6	16.5	5.9	0.15	8.1	1.9	1.9
F3	20	0	7.3	1.0	0.15	4.3	0.6	0.6
		10		0.2	0.12	0.6	0.1	0.1
		19	3.5	3.5	0.38	38.1	2.3	2.3
F5	30	0	3.4	0.1	0.16	4.9	0.6	0.6
		10		2.9	0.17	11.4	0.1	0.1
		28	0.5	5.9	0.44	25.5	0.0	0.0
F7	57	0	0.1	0.1	0.14	0.7	0.1	0.1
		28		0.2	0.14	1.3	0.0	0.0
		52	2.2	0.6	0.32	6.0	0.0	0.0
F8	82	0	0.1	0.2	0.13	0.9	0.0	0.0
		28		0.1	0.14	0.8	0.1	0.1
		82	0.9	1.1	0.32	4.3	0.1	0.1
I9	57	0	0.1	0.2	0.14	0.6	0.0	0.1
		28		0.2	0.16	0.6	0.1	0.1
		54	1.5	0.2	0.19	1.6	0.0	0.0
I8	37	0	0.1	0.2	0.13	0.7	0.1	0.1
		15		0.2	0.12	0.9	0.0	0.1
		34	1.5	0.1	0.15	0.8	0.2	0.1
I6	28	0	1.3	0.1	0.09	1.3	0.1	0.1
		13		0.1	0.08	0.1	0.1	0.1
		26	1.2	0.1	0.08	0.6	0.1	0.1
I4	20	0	2.4	0.8	0.12	0.2	0.0	0.1
		12		0.5	0.07	1.7	0.9	0.3
		19	1.1	0.7	0.12	3.9	0.7	0.3
I2	15	0	12.8	0.2	0.06	6.5	0.2	0.3
		7		0.7	0.05	6.8	0.5	0.3
		14	4.7	0.0	0.25	25.0	8.2	1.0
I1	11	0	6.8	21.6	0.51	47.7	1.1	1.0
		10	2.0	1.4	0.44	19.2	6.5	1.4

Table (continued).

	Bot.	Sam.	Total Chl a	NO_3	PO_4	SiO_3	NH_4	NO_2
	(m)		(µg/kg)	(µmol/kg)				
H3	14	0	14.4	0.3	0.11	0.0	0.1	0.3
		9		0.5	0.14	16.5	4.8	1.2
		15	4.0	0.2	0.13	8.4	1.0	0.8
H4	22	0	1.6	0.5	0.15	0.4	0.1	0.1
		20	1.2	0.7	0.22	7.8	0.1	2.2
G3	21	0	3.8	0.4	0.15	0.9	0.1	0.1
		10		0.3	0.16	0.8	0.1	0.2
		19	1.0	0.4	0.17	18.6	2.4	1.6
F3(2)	20	0		0.5	0.14	1.1	0.4	0.2
		11		0.4	0.14	0.5	0.1	0.1
		19		0.0	0.19	11.8	1.0	1.4
E2(2)	16	0	3.7	0.5	0.16	0.4	0.0	0.1
		14	4.5	0.8	0.15	10.1	2.1	0.4
D3	18	0	0.7	0.4	0.13	1.0	0.1	0.1
		15	0.8	0.4	0.14	1.1	0.0	0.1
B4	16	0	6.5	23.2	0.15	33.0	1.4	1.5
		0		22.9	0.14	32.3	1.3	1.5
		10		3.1	0.18	8.4	3.0	0.6
		15	0.7	13.7	1.41	31.7	0.9	0.9

Abbreviation: Bot.: bottom depth, Sam.: sample depth.

Table (continued).

Trace elements concentrations are in nmol/kg

	Bot.	Sam.	Co		Cr		Cs	Cu	Fe	
	(m)		col.	dis.	col.	dis	dis.	dis.	col.	dis.
MR1	0	0	0.331	1.319	0.4	0.9	0.549	12.5	239.6	14.6
MR2	0	0	0.036	1.590	0.8	1.0	0.602	11.6	761.9	16.8
MR3	0	0	0.168	0.507	4.3	0.5	0.151	17.7	3714.0	48.0
MR4	0	0	0.049	0.361	4.8	0.4	0.104	18.1	4221.8	44.7
MR5	0	0	<0.006	0.292	1.2	0.5	0.043	18.1	1286.7	46.5
MR6	0	0	0.124	0.203	6.7	0.4	0.141	21.6	6352.3	45.7
A9	82	0	0.112	0.441	0.3	2.1	1.663	4.6	5.5	0.5
		20	0.138	0.424	0.5	1.9	1.687	4.3	4.6	0.9
		70	0.024	0.346	0.3	2.6	2.200	1.5	7.4	0.9
A7	50	0	0.138	1.196	0.2	1.3	0.832	9.6	4.1	11.3
		18	<0.006	0.457	0.4	2.0	1.962	4.1	3.1	3.1
		45	<0.006	0.723	0.5	1.8	2.059	2.8	3.9	2.3
A5	30	0	0.267	0.812	<0.1	1.3	0.912	9.1	7.1	3.6
		15	0.029	0.107	0.3	2.7	2.078	1.4	0.6	3.6
		26	0.034	0.275	<0.1	2.6	2.085	1.7	1.9	3.0
A3	17	0	0.239	0.679	0.2	1.2	0.960	8.9	7.1	2.6
		14	0.017	0.270	<0.1	1.5	1.931	3.9	20.4	1.6
A1	5	0	0.029	0.625	<0.1	0.8	0.330	15.3	81.3	10.4
		4	0.142	0.734	0.3	0.8	0.579	12.9	36.8	6.3
C1	5	0	0.190	0.795	0.3	1.2	0.955	9.9	24.3	4.3
C4	13	0	0.214	0.759	<0.1	1.4	0.952	9.4	11.5	3.3
		6	0.124	0.581	<0.1	1.9	1.637	4.8	2.0	3.9
		12	0.143	0.772	0.2	1.5	1.882	3.4	3.7	4.5
C6	20	0	0.237	0.659	<0.1	1.3	1.019	8.6	8.1	2.1
		8	0.071	0.281	0.6	2.4	2.051	2.2	6.0	1.4
		18	<0.006	0.341	0.6	1.2	2.068	2.9	62.9	1.7
C7	20	0	0.162	0.671	<0.1	1.4	1.034	8.5	7.2	2.6
		10	0.066	0.330	0.5	2.2	1.848	2.5	1.0	2.4
		20	0.048	0.313	<0.1	1.9	2.079	3.3	81.1	1.7
C9	27	0	0.097	0.676	<0.1	1.7	1.385	6.2	7.6	3.1
		10	0.048	0.204	0.2	2.3	2.003	2.0	2.1	1.5
		27	0.027	0.229	0.5	1.9	2.161	3.1	30.9	1.1
C11	51	0	0.069	0.325	0.2	2.2	1.915	3.1	<0.4	1.1
		18	0.027	0.223	<0.1	2.4	2.124	2.0	2.0	5.5
		49	<0.006	0.163	0.2	2.7	2.068	1.5	23.8	1.1
F0	4	0								
		2	0.107	0.553	0.3	1.1	1.129	15.8	7.6	4.2

Table (continued).

Trace elements concentrations are in nmol/kg

	Bot.	Sam.	Co		Cr		Cs	Cu	Fe	
	(m)		col.	dis.	col.	dis	dis.	dis.	col.	dis.
AR1	0	0	0.090	0.263	3.3	0.5	0.074	17.5	3659.7	93.6
AR2	0	0	0.121	0.214	3.4	0.6	0.142	20.5	3373.9	44.5
AR3	0	0	0.219	0.379	1.1	0.6	0.186	19.1	1235.1	37.9
AR4	0	0	0.302	0.906	1.1	0.6	0.246	18.0	1293.6	40.0
AR5	0	0	0.354	0.823	0.4	0.7	0.288	17.7	282.6	37.6
AR6	0	0	0.292	0.865	<0.1	1.0	0.382	19.2	243.1	24.9
AR7	0	0	<0.006	0.632	0.3	0.6	0.384	18.0	114.6	19.9
AR8	0	0	0.208	0.688	0.7	0.6	0.318	17.3	523.8	25.3
F2	8	0	0.266	0.760	0.2	1.3	1.283	8.6	2.5	5.9
		6	0.131	0.545	0.4	1.0	1.520	7.4	44.8	5.5
F3	20	0	0.264	0.668	0.2	1.3	1.565	6.1	6.6	2.1
		10	0.164	0.386	0.3	1.6	1.966	2.9	5.6	2.1
		19	0.031	0.343	0.2	0.4	1.990	3.2	32.8	6.1
F5	30	0	0.143	0.503	<0.1	1.4	1.903	3.5	1.2	2.4
		10	0.028	0.124	<0.1	2.2	2.148	2.0	1.1	2.5
		28	<0.006	0.132	0.3	1.7	2.137	2.6	11.3	4.5
F7	57	0	<0.006	0.086	0.4	2.8	2.027	1.6	3.1	1.6
		28	<0.006	0.084	<0.1	2.6	2.074	1.2	2.1	0.6
		52	0.022	0.092	0.2	2.5	2.045	1.6	7.6	0.6
F8	82	0	0.015	0.080	0.4	2.6	2.045	2.8	1.5	0.3
		28	<0.006	0.092	0.2	2.5	2.153	1.4	1.1	0.3
		82	<0.006	0.072	0.3	2.6	2.160	1.4	6.4	0.3
I9	57	0	0.012	0.087	0.5	2.5	2.117	1.8	2.0	0.6
		28	<0.006	0.079	<0.1	2.5	2.112	1.8	2.2	0.7
		54	0.008	0.092	0.3	2.4	2.085	1.6	8.0	0.6
I8	37	0	0.007	0.092	0.3	2.5	2.096	1.7	14.6	0.7
		15	0.022	0.098	0.4	2.5	2.148	1.8	6.5	0.6
		34	0.017	0.103	0.4	2.4	2.044	1.8	4.1	0.8
I6	28	0	0.014	0.227	0.2	2.4	2.022	2.6	12.9	1.0
		13	0.012	0.190	0.5	2.1	1.978	2.0	30.2	0.3
		26	0.030	0.145	0.4	2.3	2.037	1.7	10.6	1.3
I4	20	0	0.009	0.321	0.3	2.0	1.948	14.5	2.2	0.6
		12	0.023	0.221	0.7	2.1	2.017	2.4	15.2	1.4
		19	<0.006	0.210	0.3	2.2	2.103	2.1	3.9	1.8
I2	15	0	0.099	0.565	0.3	1.0	1.394	7.9	1.3	2.1
		7	0.094	0.567	<0.1	1.3	1.519	7.6	0.8	3.1
		14	<0.006	0.861	0.7	0.8	1.755	6.3	7.8	2.7
I1	11	0	0.014	0.374	0.3	0.8	0.718	16.4	12.1	6.5
		10	0.041	0.639	0.2	1.1	1.710	7.2	37.0	3.5

Table (continued).

	Bot.	Sam.	Co		Cr		Cs	Cu	Fe	
	(m)		col.	dis.	col.	dis	dis.	dis.	col.	dis.
H3	14	0	0.109	0.639	0.4	0.9	1.529	6.9	5.5	1.4
		9	0.019	0.901	0.3	1.1	1.876	4.5	6.2	2.1
		15	0.011	0.469	0.4	1.8	1.933	2.7	8.4	1.6
H4	22	0	<0.006	0.316	0.4	1.9	1.964	2.4	3.2	0.3
		20	0.011	0.232	0.2	2.2	2.105	2.1	5.1	1.0
G3	21	0	0.061	0.404	0.4	1.6	1.858	2.9	4.5	0.6
		10	0.022	0.333	0.2	2.1	2.015	2.4	5.9	1.3
		19	<0.006	0.608	0.3	1.8	2.054	2.6	101.7	2.4
F3(2)	20	0	0.052	0.507	<0.1	1.5	1.785	4.0	1.1	1.8
		11	0.103	0.449	0.2	1.5	1.869	3.1	4.5	1.0
		19	0.030	0.908	0.4	1.4	1.874	2.8	4.8	6.8
E2(2)	16	0	0.057	0.378	0.4	1.7	1.940	2.9	2.1	0.8
		14	<0.006	0.471	0.3	1.4	1.956	2.5	8.0	2.2
D3	18	0	0.019	0.211	<0.1	2.4	2.052	1.8	2.3	0.4
		15	0.022	0.196	0.3	2.2	2.033	1.8	10.6	0.2
B4	16	0	0.197	0.744	0.3	1.0	0.869	9.8	6.8	6.1
		0	0.130	0.764	0.2	0.9	0.837	9.8	8.4	5.6
		10	0.043	0.452	0.5	1.7	1.740	4.2	5.5	2.7
		15	<0.006	0.913	<0.1	1.0	2.029	3.2	5.0	2.3

Table (continued).

	Bot.	Sam.	Mo	Mn		Ni	Re	U	V
	(m)		dis.	col.	dis.	dis.	dis.	dis.	dis.
MR1	0	0	39	44.2	430.4	22.8	0.042	5.86	31.0
MR2	0	0	39	27.5	521.5	24.6	0.033	6.10	31.5
MR3	0	0	12	39.1	658.5	34.6	0.039	3.17	34.9
MR4	0	0	8	58.6	654.8	33.8	0.038	2.69	36.4
MR5	0	0	8	34.4	661.0	29.5	0.033	2.67	30.2
MR6	0	0	6	36.5	688.9	30.4	0.032	2.47	40.1
A9	82	0	89	3.2	29.2	11.1	0.042	11.13	22.1
		20	90	3.3	28.2	8.4	0.046	11.15	23.0
		70	114	29.7	350.0	3.7	0.044	14.64	33.4
A7	50	0	53	9.8	122.6	19.0	0.038	7.11	29.0
		18	102	4.0	49.6	6.1	0.037	12.65	27.4
		45	114	12.0	120.3	6.1	0.047	15.18	31.4
A5	30	0	57	4.7	58.3	15.4	0.037	7.84	27.3
		15	112	0.4	4.9	3.3	0.043	13.85	31.2
		26	114	9.5	113.4	5.2	0.041	13.48	32.2
A3	17	0	57	2.7	35.6	14.4	0.037	7.58	27.7
		14	106	1.3	10.2	9.1	0.044	12.74	27.6
A1	5	0	25	11.2	151.8	23.2	0.040	4.54	26.8
		4	39	5.6	40.0	19.1	0.042	5.84	29.9
C1	5	0	58	2.5	11.4	15.6	0.041	7.40	31.1
C4	13	0	57	3.9	15.3	16.6	0.039	7.58	27.9
		6	86	<0.3	42.5	9.5	0.043	10.99	20.9
		12	100	<0.3	11.0	7.8	0.042	12.60	27.2
C6	20	0	61	6.4	43.5	13.7	0.044	7.98	25.0
		8	106	1.1	17.9	4.7	0.046	12.76	22.9
		18	111	1.1	6.1	7.1	0.047	13.62	35.5
C7	20	0	61	7.2	48.0	14.1	0.042	7.87	23.5
		10	104	3.1	24.3	5.5	0.051	13.29	26.0
		20	114	0.5	2.4	7.2	0.046	13.44	38.4
C9	27	0	79	4.2	56.4	11.1	0.041	10.31	25.9
		10	108	<0.3	12.4	4.2	0.040	13.36	28.2
		27	114	0.6	2.7	6.1	0.041	13.20	34.5
C11	51	0	102	<0.3	20.7	6.2	0.042	12.28	19.5
		18	112	<0.3	5.4	3.8	0.054	13.73	31.9
		49	113	<0.3	10.9	3.1	0.045	14.19	33.6
F0	4	2	72	0.5	2.7	11.9	0.044	9.04	35.0

Table (continued).

	Bot.	Sam.	Mo	Mn		Ni	Re	U	V
	(m)		dis.	col.	dis.	dis.	dis.	dis.	dis.
AR1	0	0	7	15.0	1447.8	26.9	0.028	1.90	33.0
AR2	0	0	12	38.4	178.6	27.0	0.027	2.58	30.8
AR3	0	0	19	16.9	291.4	24.2	0.028	3.22	28.0
AR4	0	0	21	<0.3	855.7	25.2	0.034	3.99	26.6
AR5	0	0	26	27.9	675.5	24.4	0.031	3.91	24.6
AR6	0	0	30	10.3	484.4	24.5	0.032	4.85	28.9
AR7	0	0	30	2.3	227.8	21.3	0.031	4.73	26.7
AR8	0	0	26	16.0	487.7	25.1	0.033	4.37	26.9
F2	8	0	77	0.6	9.5	11.7	0.043	9.15	26.3
		6	83	<0.3	3.4	9.1	0.036	10.57	29.2
F3	20	0	85	1.0	24.8	9.2	0.035	10.49	20.0
		10	106	2.5	51.1	5.6	0.050	12.49	25.0
		19	111	<0.3	15.6	5.7	0.049	13.65	33.5
F5	30	0	107	10.1	169.3	6.5	0.048	12.34	24.9
		10	112	0.2	5.6	3.4	0.045	13.95	33.6
		28	113	1.2	25.0	4.4	0.042	14.17	32.4
F7	57	0	112	3.6	3.9	3.5	0.048	14.22	36.4
		28	114	<0.3	5.1	2.8	0.045	14.04	34.3
		52	115	<0.3	16.4	2.9	0.048	14.12	32.3
F8	82	0	114	<0.3	3.7	3.3	0.048	14.34	35.3
		28	113	<0.3	3.5	2.7	0.048	14.55	32.8
		82	113	<0.3	9.0	2.5	0.047	14.22	33.3
I9	57	0	113	0.6	6.2	2.8	0.043	14.20	32.4
		28	113	<0.3	5.1	2.5	0.046	14.48	33.4
		54	111	0.6	9.1	2.6	0.049	14.31	34.8
I8	37	0	113	<0.3	6.9	2.6	0.042	14.33	32.8
		15	114	<0.3	7.0	2.8	0.043	14.30	34.8
		34	114	0.3	10.6	3.0	0.046	14.16	31.6
I6	28	0	110	2.0	15.4	4.0	0.051	13.69	24.1
		13	110	0.5	13.7	3.6	0.050	14.30	31.5
		26	109	<0.3	13.3	3.2	0.049	14.01	33.4
I4	20	0	105	0.4	22.5	4.8	0.048	13.44	25.2
		12	110	1.6	7.3	4.0	0.050	13.65	29.0
		19	112	<0.3	16.6	3.6	0.044	14.24	33.5
I2	15	0	82	<0.3	13.8	9.2	0.038	10.54	25.2
		7	84	<0.3	12.1	9.0	0.043	10.53	26.7
		14	97	<0.3	83.9	8.1	0.038	11.91	42.2
I1	11	0	48	<0.3	14.0	15.5	0.037	6.98	32.3
		10	94	4.9	34.6	9.5	0.041	11.72	32.2

Table (continued).

	Bot.	Sam.	Mo	Mn		Ni	Re	U	V
	(m)		dis.	col.	dis.	dis.	dis.	dis.	dis.
H3	14	0	86	0.6	34.5	9.1	0.036	10.53	19.3
		9	100	5.7	499.4	6.9	0.037	12.15	36.2
		15	107	3.8	389.7	4.8	0.044	13.34	30.2
H4	22	0	106	2.0	40.6	4.6	0.054	13.69	26.2
		20	112	<0.3	26.0	3.7	0.045	14.31	34.2
G3	21	0	104	1.8	44.3	5.4	0.043	13.04	22.0
		10	106	1.2	31.5	4.4	0.045	13.69	29.7
		19	108	4.9	115.1	5.2	0.040	13.74	35.4
F3(2)	20	0	97	0.5	26.9	7.1	0.046	11.83	15.4
		11	103	0.7	37.2	5.6	0.040	12.91	21.7
		19	106	21.6	577.2	6.6	0.037	13.11	24.4
E2A	16	0	100	<0.3	38.9	5.3	0.043	13.08	24.2
		14	105	<0.3	164.0	5.1	0.044	13.10	26.4
D3	18	0	110	0.5	17.5	3.3	0.038	13.90	30.6
		15	110	0.0	15.8	3.4	0.044	13.96	30.0
B4	16	0	54	4.4	104.2	15.4	0.030	7.34	30.3
		0	53	0.7	104.3	15.5	0.040	7.34	31.9
		10	95	3.3	31.4	7.5	0.047	11.80	26.9
		15	114	24.3	1054.2	7.3	0.034	13.72	30.4

Abbreviation: Bot.: bottom depth, Sam.: sample depth, col.: colloid (0.02-0.45 μm), dis.: dissolved (< 0.02 μm).

Table

Result from November 2008

	Date	Bot. (m)	Sam. (m)	Lat.	Lon.	Salinity	Temp. (°C)	DO (µmol/kg)	DOC (µmol/kg)	T. Chl a (µg/kg)
X3	10/31/08	95	0	28.758	89.537	34.6	23.4	211	134	3.3
			20			34.8	25.0	187	86	
			94			35.2	18.3	118	53	0.2
MR1	10/31/08	0	0	28.782	89.525	25.6			147	
MR2	10/31/08	0	0	28.796	89.506	23.7			153	
MR3	10/31/08	0	0	28.815	89.500	20.5			166	
MR4	10/31/08	0	0	28.872	89.456	17.7			179	
MR5	10/31/08	0	0	28.893	89.438	10.9			213	
MR6	10/31/08	0	0	28.906	89.432	8.0			175	
MR7	10/31/08	0	0	28.908	89.429	7.0			224	
MR8	10/31/08	0	0	28.999	89.422	5.8			229	
MR9	10/31/08	0	0	28.926	89.415	4.9			120	
MR10	10/31/08	0	0	28.969	89.383	4.3			244	
MR11	10/31/08	0	0	29.018	89.344	3.1			261	
MR12	10/31/08	0	0	29.058	89.313	2.2			253	
MR13	10/31/08	0	0	29.202	89.281	1.0			251	
MR14	10/31/08	0	0	29.272	89.349	0.8			257	
A1	11/1/08	7	0	29.287	89.752	30.0	21.2	227	125	5.9
			6			31.6	21.3	223	125	6.0
A3	11/1/08	16	0	29.170	89.762	30.6	21.9	233	53	4.4
			8.3			31.8	22.6	217	109	
			16			33.3	26.3	79	90	1.1
A5	11/1/08	30	0	29.067	89.752	31.9	22.7	230	111	3.8
			12			32.0	22.7	225	108	
			29			35.0	26.1	111	85	0.8
A7	11/1/08	47.5	0	28.937	89.758	29.0	22.1	257	131	5.8
			9.8			31.0	22.4	226	122	
			46			35.4	26.3	137	42	0.3
A9	11/1/08	83	0	28.744	89.776	32.0	23.7	228	121	4.0
			20			34.4	27.6	203	88	
			82			36.4	18.9	118	56	0.3
C11	11/2/08	52	0	28.576	90.214	35.4	25.2	188	81	0.3
			19.8			35.4	25.1	191	74	
			48			36.2	23.4	148	67	0.2
C9	11/2/08	31	0	28.763	90.225	33.9	24.1	207	95	3.2
			15.3			34.5	25.0	164	89	
			28			35.3	25.8	151	82	1.0
C7	11/2/08	21	0	28.830	90.395	33.5	23.7	211	100	3.3
			10			33.5	23.7	211	98	
			18			33.7	23.9	172	93	2.8

Table (continued).

	Date	Bot. (m)	Sam. (m)	Lat.	Lon.	Salinity	Temp. (°C)	DO (µmol/kg)	DOC (µmol/kg)	T. Chla (µg/kg)
C6	11/2/08	20	0	28.860	90.498	34.0	23.5	202	98	1.2
			16.5			34.1	23.6	198	93	1.4
C4	11/2/08	13	0	28.943	90.533	31.5	22.2	207	117	2.3
			10.5			33.0	23.3	175	110	1.3
C1	11/2/08	5	0	29.055	90.533	29.5	20.5	230	151	5.5
			4			29.7	20.5	217	152	5.5
D3	11/2/08	18	0	28.713	90.839	33.2	23.0	209	107	
			0						105	
			17			33.2	23.0	203	101	
E2A	11/3/08	16.5	0	28.743	91.255	33.0	22.7	208	102	
			13			33.1	22.7	207	104	
F0	11/3/08	3	0	29.784	92.033	7.3	19.1	312	358	13.0
			2			13.3	19.5	219	306	5.2
F1	11/3/08	6	0	29.185	91.618	17.2	21.1	269	264	4.4
			5			27.4	21.1	210	332	3.4
AR 1	11/3/08	0	0	29.626	91.257	0.2	19.1		345	
AR 2	11/3/08	0	0	29.377	91.379	2.0	19.7		373	
AR 3	11/3/08	0	0	29.334	91.420	3.7	20.6		378	
AR 4	11/3/08	0	0	29.325	91.428	5.6	20.6		355	
AR 5	11/3/08	0	0	29.311	91.439	7.6	20.7		343	
AR 6	11/3/08	0	0	29.293	91.456	9.2	20.9		331	
F2	11/3/08	8	0	29.053	91.619	29.8	21.6	224	135	1.8
			7			29.8	21.6	224	136	1.9
F3	11/4/08	18.5	0	28.884	91.618	30.5	22.0	210	122	1.3
			17.5			30.5	22.7	193	106	1.2
F5	11/4/08	29	0	28.688	91.629	34.2	23.9	186	99	
			15.3			34.2	23.9	185	91	
			28			34.2	23.9	184	96	
F7	11/4/08	52	0	28.449	91.617	35.2	24.7	189	89	0.8
			20.3			35.4	24.9	189	83	
			51			35.8	25.6	183	77	0.4
F8	11/4/08	82	0	28.180	91.622	36.5	25.8	189	72	0.3
			30			36.5	25.8	189	72	
			81			36.4	25.3	179	72	0.4
I9	11/4/08	56	0	28.392	92.764	35.9	25.3	192	77	0.2
			19.8			36.1	25.4	190	74	
			55			36.2	25.3	180	71	0.8
I8	11/5/08	36	0	28.641	92.764	35.2	24.6	191	79	0.7
			20.7			35.4	24.8	193	81	
			35			35.5	24.9	191	77	0.5

Table (continued).

	Date	Bot. (m)	Sam. (m)	Lat.	Lon.	Salinity	Temp. (°C)	DO (µmol/kg)	DOC (µmol/kg)	T. Chla (µg/kg)
I6	11/5/08	26	0	28.893	92.762	34.2	23.8	192	93	0.7
			12.1			34.3	23.9	190	91	
			25			34.5	24.0	189	86	0.6
I4	11/5/08	19	0	29.181	92.761	32.9	23.0	202	102	0.9
			10.3			32.9	23.0	200	104	
			17.5			33.2	23.2	192	99	0.7
I2	11/5/08	14	0	29.411	92.756	29.8	21.8	208	133	1.3
			13			29.7	23.8	123	136	1.0
I1	11/5/08	10	0	29.539	92.759	28.2	21.5	223	138	1.6
			9			29.4	21.3	201	142	1.0
H0	11/5/08	3	0	29.492	92.388	16.6	21.1	249	287	
			2			16.4	21.1	249	293	
GH0	11/6/08	3.5	0	29.470	92.268	18.1	20.8	251	254	
			2.5			31.5	20.8	248	120	
E1	11/6/08	5.5	0	28.968	91.252	31.7	21.5	221	144	
			4.5			31.3	21.5	221	123	
D0	11/6/08	4	0	29.016	90.833	30.0	20.6	226	143	
C6(2)	11/6/08	18	0	28.872	90.493	32.8	23.4	223	106	
			11.3			33.5	23.9	200	106	
			17			33.9	24.2	187	96	
C7(2)	11/6/08	20	0	28.837	90.398	34.1	24.4	209	100	
			12.3			33.7	24.2	203	101	
			19			34.3	24.2	198	107	
B4	11/6/08	16	0	29.032	90.111	32.0	23.6	226	112	
			15			32.9	23.6	207	115	
B1	11/6/08	8	0	29.077	90.208	29.8	22.6	247	131	
			7			31.0	22.7	156	133	
C1(2)	11/7/08	5	0	29.059	90.549	31.2	22.5	219	121	
			4			31.2	22.6	219	119	
C1W	11/7/08	5	3	29.058	90.533	31.2	22.5	217	117	

Abbreviation: Bot.: bottom depth, Sam.: sample depth, Lat.: latitude, Lon.: longitude, Temp.: temperature, DO: dissolved Oxygen, DOC: dissolved organic carbon, T. Chl a., total chlorophyll a.

Table (continued).

Trace elements are in nmol/kg

	Bot.	Sam.	NO_3	PO_4	SiO_3	NH_4	NO_2	Co		Cr		Cs
	(m)				(µmol/kg)			col.	dis.	col.	dis.	dis.
X3	95.0	0.0	0.7	0.35	8.5	0.3	0.1	0.032	0.458	<0.1	1.5	1.476
		20.0	0.1	0.27	1.2	1.5	0.7	0.024	0.408	<0.1	2.0	1.857
		94.0	4.8	0.88	4.7	0.0	0.2	<0.006	0.092	0.2	2.6	2.061
MR1	0.0	0.0	2.9	0.94	17.1	0.2	0.5	<0.006	0.463	<0.1	1.6	1.387
MR2	0.0	0.0	6.4	1.20	8.1	0.6	0.5	0.033	0.459	<0.1	1.5	1.314
MR3	0.0	0.0	19.1	1.89	49.5	0.1	0.6	<0.006	0.481	<0.1	1.4	1.117
MR4	0.0	0.0	24.8	2.27	57.0	0.2	0.7	0.061	0.362	<0.1	1.3	0.864
MR5	0.0	0.0	45.5	2.25	77.6	0.7	0.5	0.125	0.270	<0.1	1.2	0.590
MR6	0.0	0.0	27.1	2.23	57.4	0.9	0.3	0.049	0.296	<0.1	1.1	0.427
MR7	0.0	0.0	56.9	3.80	88.1	0.9	0.4	0.097	0.224	<0.1	1.2	0.355
MR8	0.0	0.0	59.4	3.52	93.9	1.1	0.4	0.086	0.237	<0.1	1.1	0.305
MR9	0.0	0.0	12.1	2.81	94.9	0.8	0.1	0.063	0.214	<0.1	1.1	0.259
MR10	0.0	0.0	62.5	4.10	98.6	0.9	0.3	0.056	0.184	<0.1	1.3	0.225
MR11	0.0	0.0	65.0	4.23	108.5	1.0	0.3	0.152	0.140	<0.1	1.1	0.159
MR12	0.0	0.0	9.8	2.01	101.0	0.8	0.1	0.097	0.135	<0.1	1.1	0.119
MR13	0.0	0.0	68.0	3.30	112.7	0.7	0.2	0.011	0.094	<0.1	1.0	0.053
MR14	0.0	0.0	68.4	3.12	115.5	0.8	0.2	0.037	0.072	<0.1	1.0	0.046
A1	7.0	0.0	0.7	0.35	29.9	0.2	0.2	0.067	0.752	<0.1	1.5	1.601
		6.0	0.9	0.44	6.1	0.4	0.2	0.124	0.813	<0.1	1.3	1.633
A3	16.0	0.0	0.6	0.25	4.7	0.1	0.1	0.176	0.359	<0.1	1.6	1.677
		8.3	0.5	0.30	7.6	0.1	0.1	0.043	0.427	<0.1	1.7	1.783
		16.0	2.0	0.83	3.0	0.0	0.4	0.050	0.527	<0.1	1.7	1.757
A5	30.0	0.0	0.6	0.26	2.1	0.3	0.1	0.073	0.400	<0.1	1.7	1.762
		12.0	0.7	0.23	4.4	0.1	0.1	0.119	0.350	<0.1	1.6	1.628
		29.0	0.9	0.54	9.5	0.4	0.3	<0.006	0.520	0.5	1.8	1.949
A7	47.5	0.0	0.8	0.49	12.9	0.1	0.2	0.062	0.433	<0.1	1.6	1.462
		9.8	0.7	0.25	3.6	0.1	0.1	0.085	0.410	<0.1	1.7	1.599
		46.0	0.7	0.39	8.3	0.2	0.3	0.030	0.228	<0.1	2.1	1.854
A9	83.0	0.0	0.5	0.31	2.1	0.2	0.3	0.071	0.449	<0.1	1.6	1.616
		20.0	0.4	0.23	2.2	0.0	0.4	0.070	0.294	<0.1	2.1	1.869
		82.0	4.3	0.74	3.0	0.0	0.2	0.021	0.044	<0.1	2.6	2.056
C11	52.0	0.0	0.6	0.18	0.7	0.1	0.1	0.058	0.183	<0.1	2.3	1.900
		19.8	0.5	0.21	1.5	0.1	0.3	0.045	0.191	<0.1	2.4	1.866
		48.0	0.8	0.35	0.3	0.1	0.4	0.024	0.172	<0.1	2.5	2.038
C9	31.0	0.0	0.5	0.23	0.3	0.0	0.2	0.069	0.450	<0.1	2.0	1.778
		15.3	0.1	0.39	3.3	0.1	0.9	0.118	0.607	<0.1	2.1	1.806
		28.0	0.1	0.33	7.9	0.0	1.0	0.132	0.627	<0.1	2.2	1.958
C7	21.0	0.0	0.7	0.25	1.8	0.1	0.1	0.050	0.440	<0.1	2.0	1.786
		10.0	0.6	0.26	3.5	0.1	0.1	0.141	0.424	<0.1	2.1	1.759
		18.0	0.5	0.20	4.8	0.6	0.2	0.170	0.925	<0.1	1.9	1.889

Table (continued).

	Bot.	Sam.	NO_3	PO_4	SiO_3	NH_4	NO_2	Co		Cr		Cs
	(m)				(µmol/kg)			col.	dis.	col.	dis.	dis.
C6	20.0	0.0	0.6	0.22	0.1	0.1	0.1	0.102	0.451	<0.1	2.0	1.882
		16.5	0.4	0.22	0.2	0.6	0.3	0.104	0.585	<0.1	2.0	1.832
C4	13.0	0.0	0.4	0.21	1.2	0.3	0.3	0.130	1.123	<0.1	1.5	1.603
		10.5	0.3	0.23	2.7	0.5	0.4	0.179	0.909	0.2	1.7	1.793
C1	5.0	0.0	0.1	0.36	3.5	0.5	0.7	0.040	1.176	<0.1	1.3	1.427
		4.0	0.2	0.33	7.4	0.5	0.6	0.158	1.169	<0.1	1.4	1.558
D3	18.0	0.0	0.4	0.27	2.3	0.6	0.4	0.131	0.769	<0.1	1.7	1.824
		0.0	0.5	0.23	3.8	0.7	0.4	0.131	0.687	<0.1	1.8	1.801
		17.0	0.3	0.24	4.2	0.6	0.5	0.153	0.706	<0.1	1.8	1.860
E2	16.5	0.0	0.3	0.23	2.0	0.4	0.5	0.151	0.824	<0.1	1.8	1.719
		13.0	0.3	0.23	2.6	0.4	0.5	0.105	0.857	<0.1	1.8	1.754
F0	3.0	0.0	10.4	0.97	72.8	0.4	0.4	<0.006	0.184	0.2	0.8	0.296
		2.0	1.7	0.47	2.3	0.3	0.3	0.079	0.309	<0.1	1.0	0.612
F1	6.0	0.0	0.6	0.38	36.7	0.1	0.1	0.076	0.335	<0.1	1.0	0.810
		5.0	0.7	0.28	18.7	0.5	0.1	0.279	0.562	<0.1	1.3	1.430
AR1	0.0	0.0	45.5	1.53	119.6	0.7	0.1	<0.006	0.060	0.4	0.8	0.021
AR2	0.0	0.0	32.1	1.81	99.7	1.1	0.1	0.065	0.112	0.2	0.9	0.086
AR3	0.0	0.0	20.5	1.98	83.6	0.9	0.2	0.076	0.194	0.2	0.9	0.174
AR4	0.0	0.0	18.9	1.61	83.7	0.6	0.2	0.092	0.145	<0.1	0.9	0.245
AR5	0.0	0.0	14.7	1.35	73.6	0.5	0.2	0.072	0.150	<0.1	1.0	0.326
AR6	0.0	0.0	9.6	1.01	66.9	0.4	0.2	<0.006	0.221	<0.1	0.9	0.383
F2	8.0	0.0	0.6	0.18	29.5	0.1	0.1	0.277	0.493	<0.1	1.5	1.507
		7.0	0.6	0.16	3.3	0.2	0.1	0.323	0.521	<0.1	1.5	1.478
F3	18.5	0.0	0.5	0.20	4.0	0.1	0.2	0.319	0.520	<0.1	1.5	1.572
		17.5	0.1	0.19	2.3	0.2	0.7	0.191	0.467	0.2	1.7	1.690
F5	29.0	0.0	0.3	0.27	3.1	0.2	0.5	0.216	0.377	<0.1	1.9	1.908
		15.3	0.1	0.27	1.9	0.1	0.7	0.076	0.439	<0.1	1.9	1.854
		28.0	0.1	0.26	1.4	0.1	0.7	0.185	0.317	<0.1	1.9	2.012
F7	52.0	0.0	0.4	0.21	0.1	0.1	0.4	<0.006	0.185	<0.1	2.2	1.988
		20.3	0.6	0.20	0.8	0.1	0.2	0.030	0.180	<0.1	2.2	1.859
		51.0	0.2	0.22	1.3	0.1	0.6	0.008	0.095	<0.1	2.5	2.038
F8	82.0	0.0	0.7	0.17	1.7	0.1	0.1	0.026	0.069	0.2	2.5	2.095
		30.0	0.6	0.17	1.6	0.1	0.1	0.029	0.061	<0.1	2.5	2.120
		81.0	0.7	0.20	0.4	0.1	0.1	0.011	0.067	<0.1	2.7	2.100
I9	56.0	0.0	0.7	0.18	1.8	0.0	0.1	0.055	0.110	<0.1	2.3	2.034
		19.8	0.7	0.17	1.5	0.0	0.1	0.016	0.109	<0.1	3.6	2.077
		55.0	0.6	0.17	1.2	0.1	0.2	0.022	0.077	0.3	2.4	2.047
I8	36.0	0.0	0.6	0.20	2.5	0.1	0.2	0.038	0.099	<0.1	2.3	2.032
		20.7	0.6	0.19	0.1	0.1	0.2	0.036	0.107	<0.1	2.3	1.907
		35.0	0.7	0.18	0.5	0.1	0.1	0.037	0.113	<0.1	2.3	1.992

Table (continued).

	Bot.	Sam.	NO_3	PO_4	SiO_3	NH_4	NO_2	Co		Cr		Cs
	(m)			(μmol/kg)				col.	dis.	col.	dis.	dis.
I6	26.0	0.0	0.5	0.21	1.1	0.6	0.3	0.067	0.256	<0.1	1.9	1.817
		12.1	0.1	0.23	1.3	0.4	0.7	0.126	0.201	<0.1	2.0	1.907
		25.0	0.4	0.21	1.3	0.4	0.4	<0.006	0.286	<0.1	2.1	1.948
I4	19.0	0.0	0.5	0.25	1.7	0.2	0.3	0.168	0.393	<0.1	1.7	1.849
		10.3	0.5	0.25	1.2	0.2	0.3	0.164	0.375	0.2	1.7	1.931
		17.5	0.5	0.27	2.1	0.4	0.3	0.143	0.396	0.3	1.7	1.869
I2	14.0	0.0	0.4	0.29	5.8	0.1	0.4	<0.006	0.617	<0.1	1.4	1.542
		13.0	0.3	0.31	8.0	1.0	0.5	<0.006	0.605	0.2	1.2	1.623
I1	10.0	0.0	0.5	0.32	6.4	1.2	0.3	0.172	0.355	<0.1	1.3	1.635
		9.0	0.4	0.42	8.0	0.8	0.4	<0.006	0.445	<0.1	1.3	1.543
H0	3.0	0.0	0.7	0.75	38.2	0.2	0.1	0.254	0.324	0.8	1.0	0.706
		2.0	0.6	0.81	22.8	0.3	0.1	0.630	0.244	2.1	1.1	0.707
GH0	3.5	0.0	0.7	0.48	34.1	0.1	0.1	<0.006	0.401	0.4	1.0	0.868
		2.5	0.5	0.31	2.8	0.1	0.3	0.033	1.237	0.3	1.4	1.722
E1	5.5	0.0	0.7	0.28	3.3	0.0	0.1	0.064	1.004	<0.1	1.3	1.439
		4.5	0.5	0.31	3.2	0.1	0.3	<0.006	1.394	0.4	1.4	1.742
D0	4.0	0.0	0.6	0.31	3.2	0.1	0.1	0.026	1.007	0.3	1.2	1.556
C6(2)	18.0	0.0	0.7	0.23	0.3	0.0	0.1	0.010	1.000	0.2	1.8	1.890
		11.3	0.7	0.27	0.8	0.3	0.1	<0.006	1.192	<0.1	1.6	1.818
		17.0	0.4	0.30	0.2	0.5	0.4	<0.006	1.097	<0.1	1.8	1.780
C7(2)	20.0	0.0	0.6	0.23	1.5	0.0	0.2	<0.006	0.962	0.3	1.9	1.915
		12.3	0.6	0.23	1.1	0.1	0.2	0.069	0.526	0.4	1.8	1.801
		19.0	0.6	0.21	1.2	0.2	0.2	<0.006	0.781	0.2	2.0	1.936
B4	16.0	0.0	0.6	0.28	1.9	0.2	0.2	0.065	0.404	0.7	1.7	1.889
		15.0	0.7	0.25	1.5	0.2	0.2	0.066	0.487	0.3	1.8	1.843
B1	8.0	0.0	0.8	0.17	0.1	0.0	0.1	<0.006	0.600	0.3	1.6	1.668
		7.0	0.7	0.22	0.3	0.0	0.1	0.135	0.613	0.4	1.5	1.659
C1(2)	5.0	0.0	0.8	0.30	1.4	0.2	0.1	0.105	1.084	0.3	1.5	1.671
		4.0	0.7	0.26	0.9	0.1	0.1	0.010	1.079	0.2	1.6	1.724
C1W	5.0	3.0	0.8	0.24	0.8	0.3	0.1	0.055	1.118	<0.1	1.6	1.775

Abbreviation: Bot.: bottom depth, Sam.: sampling depth, col.: colloid (0.02-0.45 μm), dis.: dissolved (<0.02 μm).

Table (continued).

	Bot.	Sam.	Cu	Fe		Mn		Ni	Mo	Re	U	V
	(m)		dis.	col.	dis.	col.	dis.	dis.	dis.	dis.	dis.	dis.
X3	95.0	0.0	7.3	1.7	1.4	0.6	34.2	10.3	91	0.044	10.33	31.2
		20.0	2.8	1.2	0.5	<0.3	3.6	5.2	116	0.044	13.34	33.4
		94.0	0.9	21.3	0.9	1.5	118.2	2.8	116	0.040	10.81	31.7
MR1	0.0	0.0	9.7	5.7	1.7	1.4	76.7	12.4	88	0.044	9.43	35.2
MR2	0.0	0.0	11.0	13.8	2.1	2.2	81.4	13.2	82	0.052	9.38	41.1
MR3	0.0	0.0	12.6	5.8	3.2	<0.3	98.0	15.4	69	0.050	8.25	40.8
MR4	0.0	0.0	13.6	11.1	4.0	2.1	139.4	17.9	65	0.043	9.04	35.0
MR5	0.0	0.0	17.7	30.1	5.4	<0.3	123.4	20.3	45	0.055	7.09	39.3
MR6	0.0	0.0	19.5	11.8	6.5	3.6	102.7	21.3	37	0.061	5.93	41.6
MR7	0.0	0.0	20.5	125.0	7.0	2.5	86.1	22.2	35	0.064	6.10	45.1
MR8	0.0	0.0	22.0	122.5	7.2	0.9	71.7	24.0	32	0.063	5.88	41.9
MR9	0.0	0.0	21.6	20.7	7.0	0.5	63.4	23.4	30	0.075	5.85	44.8
MR10	0.0	0.0	23.0	19.4	9.3	1.0	73.4	24.5	27	0.069	5.81	46.0
MR11	0.0	0.0	23.3	128.2	7.9	<0.3	80.0	25.3	24	0.063	5.03	45.4
MR12	0.0	0.0	26.6	140.0	8.5	3.0	64.0	26.1	24	0.066	5.22	45.6
MR13	0.0	0.0	28.1	72.3	9.7	2.1	14.9	27.7	17	0.069	4.84	42.8
MR14	0.0	0.0	26.9	81.7	9.9	1.5	13.4	27.7	21	0.061	4.94	46.4
A1	7.0	0.0	6.5	2.6	1.1	0.7	17.7	11.1	95	0.041	10.92	32.7
		6.0	6.7	4.7	1.4	6.4	36.2	11.5	107	0.038	12.67	36.0
A3	16.0	0.0	6.3	1.8	0.8	0.8	18.3	8.9	98	0.042	10.99	32.4
		8.3	5.2	1.6	0.6	0.6	11.8	7.6	103	0.046	11.41	33.9
		16.0	4.1	3.8	1.0	1.2	25.1	7.6	107	0.041	13.06	36.7
A5	30.0	0.0	5.2	1.1	1.0	<0.3	9.2	7.4	100	0.045	10.94	33.2
		12.0	5.6	0.5	0.9	<0.3	7.6	7.3	97	0.035	10.66	30.0
		29.0	3.7	6.6	0.7	0.6	14.9	5.9	114	0.045	12.15	37.1
A7	47.5	0.0	7.6	2.2	1.6	<0.3	27.0	10.2	95	0.043	11.53	32.4
		9.8	7.0	1.5	0.9	0.5	16.7	8.4	103	0.038	11.45	33.6
		46.0	3.1	20.2	0.7	<0.3	24.8	4.5	111	0.040	13.61	32.5
A9	83.0	0.0	6.2	1.5	0.8	0.9	23.1	9.0	105	0.036	10.94	33.5
		20.0	2.4	0.7	<0.4	<0.3	4.0	4.3	117	0.043	12.77	30.8
		82.0	1.0	4.9	5.1	0.6	60.2	3.0	116	0.043	12.30	32.3
C11	52.0	0.0	1.9	1.5	0.3	0.4	5.0	3.6	116	0.034	13.15	31.4
		19.8	2.1	1.1	1.0	<0.3	6.2	3.5	113	0.042	11.51	29.5
		48.0	1.8	3.4	0.9	0.5	11.6	3.1	116	0.043	11.85	33.2
C9	31.0	0.0	4.3	1.5	0.6	<0.3	6.7	6.0	107	0.042	12.83	30.9
		15.3	4.5	30.3	1.2	<0.3	4.8	5.9	115	0.047	13.36	33.5
		28.0	3.9	62.9	0.7	0.4	11.5	5.5	114	0.045	11.60	31.7
C7	21.0	0.0	4.0	1.6	1.1	<0.3	9.8	6.6	112	0.034	13.05	29.6
		10.0	4.4	0.6	2.3	0.5	7.9	6.1	111	0.043	12.64	30.2
		18.0	7.0	13.7	1.4	0.9	19.3	7.1	109	0.043	11.53	35.3

Table (continued).

	Bot.	Sam.	Cu	Fe		Mn		Ni	Mo	Re	U	V
	(m)		dis.	col.	dis.	col.	dis.	dis.	dis.	dis.	dis.	dis.
C6	20.0	0.0	3.7	2.1	0.5	<0.3	12.2	5.7	109	0.042	10.97	30.8
		16.5	4.0	6.8	1.7	<0.3	18.1	5.8	114	0.041	11.22	30.7
C4	13.0	0.0	6.2	6.0	1.0	<0.3	16.0	9.4	108	0.043	11.57	32.5
		10.5	5.7	4.0	1.1	<0.3	11.7	8.7	106	0.041	11.29	35.9
C1	5.0	0.0	9.0	10.0	1.6	0.6	10.6	13.8	102	0.044	10.59	33.2
		4.0	9.3	13.9	1.5	0.6	11.1	13.8	99	0.046	11.38	35.9
D3	18.0	0.0	5.5	2.7	1.0	<0.3	14.7	7.6	107	0.050	11.20	33.9
		0.0	5.6	8.9	1.0	0.5	18.5	7.7	108	0.045	11.60	39.2
		17.0	5.7	12.2	2.1	<0.3	18.1	7.8	108	0.049	11.10	34.2
E2A	16.5	0.0	5.9	5.3	0.7	0.6	11.0	8.3	112	0.047	12.01	39.6
		13.0	6.1	4.6	0.5	0.7	11.6	8.7	112	0.049	13.14	40.3
F0	3.0	0.0	21.6	38.7	9.9	2.3	32.0	22.7	30	0.046	4.92	35.6
		2.0	20.8	22.1	7.3	0.4	13.2	20.9	50	0.045	6.37	35.7
F1	6.0	0.0	19.6	9.5	4.3	1.8	12.1	18.6	61	0.047	7.26	38.5
		5.0	12.0	45.7	3.4	0.8	8.1	13.2	95	0.045	9.71	35.5
AR1	0.0	0.0	19.7	1031.0	34.9	13.6	11.3	31.1	14	0.066	3.91	33.0
AR2	0.0	0.0	20.9	622.7	33.6	5.8	31.9	28.5	17	0.053	3.96	33.5
AR3	0.0	0.0	22.0	475.6	17.1	14.8	21.4	24.0	22	0.049	4.06	33.4
AR4	0.0	0.0	21.2	239.5	17.5	4.2	22.0	23.4	27	0.048	4.59	29.5
AR5	0.0	0.0	19.8	194.2	13.2	5.5	17.8	22.9	32	0.048	4.96	31.5
AR6	0.0	0.0	20.2	47.5	10.0	<0.3	24.3	21.7	39	0.045	6.11	32.0
F2	8.0	0.0	9.5	3.7	1.2	<0.3	15.4	11.5	99	0.037	10.13	31.2
		7.0	9.6	3.0	1.4	<0.3	13.8	11.9	100	0.039	12.10	30.5
F3	18.5	0.0	8.7	7.6	1.0	<0.3	8.3	10.6	105	0.045	11.21	33.3
		17.5	6.5	37.0	0.6	<0.3	9.7	8.3	110	0.044	12.50	34.3
F5	29.0	0.0	4.7	3.9	0.9	0.5	8.4	6.8	109	0.051	11.34	32.0
		15.3	4.3	7.0	0.5	<0.3	6.5	6.6	115	0.043	11.09	37.8
		28.0	4.1	2.4	1.9	<0.3	6.6	6.0	116	0.037	11.02	38.0
F7	52.0	0.0	2.4	6.7	1.8	<0.3	3.2	4.5	113	0.042	10.92	32.5
		20.3	2.5	1.1	0.5	<0.3	4.2	4.4	114	0.036	11.33	30.4
		51.0	1.6	3.5	0.6	<0.3	11.7	3.4	115	0.038	11.90	32.1
F8	82.0	0.0	1.3	<0.4	1.1	<0.3	3.7	2.6	117	0.039	11.38	37.5
		30.0	1.4	<0.4	0.5	<0.3	3.3	2.7	116	0.046	11.40	31.8
		81.0	2.4	2.7	<0.4	<0.3	5.7	3.2	115	0.047	13.15	32.0
I9	56.0	0.0	2.0	0.8	0.8	<0.3	3.9	3.4	115	0.041	11.53	41.4
		19.8	1.6	<0.4	6.5	<0.3	3.7	2.9	115	0.047	11.26	32.0
		55.0	1.4	2.2	0.8	<0.3	3.9	3.5	119	0.056	11.61	31.1
I8	36.0	0.0	2.2	5.9	0.7	<0.3	3.7	3.8	114	0.044	11.42	34.1
		20.7	2.5	4.2	<0.4	<0.3	4.2	4.8	117	0.046	13.43	35.8
		35.0	2.2	4.8	0.5	0.6	6.0	4.0	114	0.048	13.53	34.6

Table (continued).

	Bot.	Sam.	Cu	Fe		Mn		Ni	Mo	Re	U	V
	(m)		dis.	col.	dis.	col.	dis.	dis.	dis.	dis.	dis.	dis.
I6	26.0	0.0	4.4	2.1	0.5	0.4	6.2	6.1	115	0.037	12.90	37.9
		12.1	4.1	11.2	0.5	<0.3	3.4	6.6	111	0.043	13.09	36.7
		25.0	3.7	11.4	0.5	0.6	7.1	5.4	111	0.043	12.83	37.9
I4	19.0	0.0	6.1	4.7	0.6	<0.3	7.1	8.0	107	0.049	11.12	40.0
		10.3	6.2	2.6	0.6	<0.3	7.2	8.0	110	0.034	12.88	40.5
		17.5	6.1	13.1	1.0	<0.3	8.9	7.6	110	0.046	12.74	36.0
I2	14.0	0.0	9.6	2.5	1.0	0.4	12.7	11.9	98	0.045	11.61	35.6
		13.0	10.1	10.6	1.5	<0.3	17.5	12.2	98	0.055	11.17	38.7
I1	10.0	0.0	10.1	6.8	1.5	1.2	14.4	12.6	100	0.051	10.83	42.3
		9.0	10.6	17.0	1.5	0.5	9.1	12.9	97	0.048	12.21	41.1
H0	3.0	0.0	20.3	600.3	3.8	8.4	6.3	20.5	61	0.048	6.91	41.0
		2.0	20.7	1785.6	3.8	25.2	4.1	20.2	62	0.042	6.92	44.5
GH0	3.5	0.0	19.5	137.7	3.1	2.0	3.2	17.6	65	0.044	7.80	37.4
		2.5	7.8	5.0	1.2	<0.3	12.2	12.8	104	0.044	12.74	37.4
E1	5.5	0.0	9.5	14.9	1.7	0.8	6.7	13.8	103	0.042	11.88	33.3
		4.5	8.2	2.3	3.9	0.4	10.5	12.2	104	0.043	11.90	38.7
D0	4.0	0.0	9.1	29.9	1.6	1.0	7.2	13.9	99	0.042	12.00	37.2
C6(2)	18.0	0.0	5.3	8.1	1.1	<0.3	23.5	7.7	111	0.049	12.36	30.5
		11.3	5.4	5.1	1.6	1.0	19.2	7.6	107	0.047	11.12	30.3
		17.0	4.6	17.2	0.8	<0.3	16.6	6.9	112	0.038	11.12	37.2
C7(2)	20.0	0.0	5.0	2.9	1.4	<0.3	12.8	7.1	109	0.043	12.61	30.9
		12.3	4.1	1.0	3.8	<0.3	12.3	5.3	102	0.037	11.19	29.4
		19.0	4.0	23.7	0.7	1.2	25.1	5.3	112	0.046	12.43	26.8
B4	16.0	0.0	5.1	2.3	1.2	<0.3	13.4	8.9	108	0.052	11.62	34.5
		15.0	4.4	4.2	1.0	<0.3	14.5	6.7	113	0.050	13.12	31.5
B1	8.0	0.0	6.9	2.7	1.2	1.3	29.9	9.7	99	0.037	12.10	33.9
		7.0	6.9	3.1	1.4	1.5	30.9	10.1	101	0.046	11.96	32.7
C1(2)	5.0	0.0	6.7	7.7	1.7	1.4	27.7	9.5	104	0.038	12.51	30.8
		4.0	6.6	4.2	1.3	2.5	26.3	9.2	106	0.050	12.10	30.3
C1W	5.0	3.0	7.2	1.8	4.9	0.4	26.6	9.4	104	0.048	11.22	28.7

Abbreviation: Bot.: bottom depth, Sam.: sampling depth, col.: colloid (0.02-0.45 μm), dis.: dissolved (<0.02 μm).

Table

Results from June/July 2009

	Date	Bot. (m)	Sam. (m)	Lat.	Lon.	Salinity	Temp. (°C)	DO (µmol/kg)	DOC	T. Chl a (µg/kg)
X3	6/28/09	93	0	28.753	89.534	26.8	30.4	200	137	0.8
			40			36.3	23.4	192	74	0.4
			92			36.2	16.4	106	39	0.0
MR 1	6/28/09	0	0	28.826	89.482	22.1			214	
MR 2	6/28/09	0	0	28.837	89.471	18.4			224	
MR 3	6/28/09	0	0	28.846	89.462	15.2			236	
MR 4	6/28/09	0	0	28.849	89.459	12.7			237	18.0
MR 5	6/28/09	0	0	28.856	89.452	9.2			251	
MR 6	6/28/09	0	0	28.862	89.446	6.3			248	
MR 7	6/28/09	0	0	28.907	89.431	2.3			258	
MR 8	6/28/09	0	0	28.956	89.392	0.6			255	1.9
A1	6/29/09	6.8	0.3	29.290	89.745	23.5	29.7	142	157	6.5
			5.8			28.7	28.5	129	157	1.3
A3	6/29/09	15.5	0	29.177	89.751	23.7	30.1	182	207	5.1
			7			32.8	25.2	64	127	0.8
			16			35.9	24.4	3	78	0.2
A5	6/29/09	31	0	29.068	89.750	24.4	30.0	194	215	4.8
			13.5			35.7	24.8	116	79	0.1
			20			36.2	24.4	146	68	
			30			36.3	22.1	12	69	0.2
A7	6/29/09	50	0	28.940	89.749	24.6	30.6	197	187	1.7
			20			35.9	24.9	162	74	0.4
			49			36.3	18.9	85	57	0.2
A9	6/29/09	80	0	28.750	89.749	22.9	31.3	200	206	0.9
			14			35.5	25.6	107	86	
			30			36.1	24.7	189	72	0.1
			40			36.3	21.8	119	68	0.3
			79			36.2	16.8	104	48	0.0
C11	6/30/09	52	0	28.587	90.201	22.7	30.3	212	128	2.1
			30			36.3	21.8	128	53	0.3
			51			36.3	19.3	98	38	0.1
C9	6/30/09	31	0	28.767	90.216	24.6	30.1	224	193	5.2
			20			36.1	24.5	149	36	0.2
			30			36.3	22.7	73	49	0.5
C7	6/30/09	20.7	0	28.830	90.392	23.6	30.4	237	216	6.5
			9.5			35.1	24.8	61	63	1.2
			19.7			35.9	24.3	88	48	1.2

Table (continued).

	Date	Bot.	Sam.	Lat.	Lon.	Salinity	Temp.	DO	DOC	T. Chl a
							(°C)	(µmol/kg)		(µg/kg)
C6	6/30/09	19.7	0	28.866	90.483	20.0	30.6	238	262	6.4
			10			35.4	25.0	92	75	1.1
			18.7			35.9	24.4	55	70	0.9
C4	6/30/09	13.8	0	28.950	90.523	25.0	30.1	157	217	8.8
			5.3			31.2	25.6	58	127	0.5
			12.8			35.8	24.4	24	80	1.5
C1	6/30/09	6.2	0	29.055	90.533	30.4	27.7	181	181	9.7
			5.2			33.7	25.6	12	97	6.1
D2	6/30/09	16.2	0	28.843	90.833	16.0	30.3	223	289	7.5
			15.2			35.3	24.5	2	82	0.9
			15.2			35.3	24.5	2	81	
AR 1	7/1/09	0	0	29.440	91.322	0.1			400	
AR 2	7/1/09	0	0	29.351	91.405	0.6			397	
AR 3	7/1/09	0	0	29.317	91.490	0.7			395	
AR 4	7/1/09	0	0	29.302	91.527	1.5			394	
AR 5	7/1/09	0	0	29.290	91.561	2.9			384	
AR 6	7/1/09	0	0	29.244	91.618	6.0			374	
AR 7	7/1/09	0	0	29.211	91.620	8.8			345	
AR 8	7/1/09	0	0	29.188	91.623	12.2			322	
AR 9	7/1/09	0	0	29.178	91.625	15.2			388	
AR 10	7/1/09	0	0	29.161	91.625	18.0			268	
AR 11	7/1/09	0	0	29.149	91.625	18.8			257	
F0	7/1/09	5	0	29.272	91.619	3.1	30.0	137	369	26.3
			4			23.0	29.1	65	208	5.0
F1	7/1/09	5	0	29.181	91.618	1.4	30.2	210	382	3.5
			4			32.3	26.8	6	127	6.1
F2	7/1/09	7	0	29.050	91.617	10.4	31.1	218	350	
			6			32.7	26.3	134	104	
F3	7/1/09	20	0	28.883	91.616	29.3	30.7	199	118	0.5
			6.5			30.5	28.5	150	153	1.0
			19			35.6	25.7	134	78	1.6
F5	7/1/09	30	0	28.691	91.617	29.2	31.2	196	152	0.3
			10			35.5	34.1	195	97	0.5
			29			36.1	24.0	122	76	0.9
F7	7/2/09	53	0	28.464	91.612	28.1	30.5	193	102	0.3
			20			35.3	27.1	198	70	0.2
			40			36.2	22.8	201	76	0.4
			52			36.3	21.2	155	70	1.1

Table (continued).

	Date	Bot.	Sam.	Lat.	Lon.	Salinity	Temp.	DO	DOC	T. Chl a
							(°C)	(µmol/kg)		(µg/kg)
F8	7/2/09	84	0	28.181	91.613	28.1	31.0	193	168	0.3
			20			35.3	26.7	204	85	0.3
			82			36.3	18.8	116	55	0.2
I9	7/2/09	56	0	28.391	92.752	29.0	31.0	196	146	0.2
			20			35.1	26.6	201	88	0.4
			55			36.2	20.9	155	69	0.5
I8	7/3/09	37	0	28.646	92.748	29.4	30.9	193	152	0.4
			12.5			32.2	27.4	153	115	0.5
			36			36.2	22.2	149	71	0.7
I6	7/3/09	27.4	0	28.892	92.750	30.1	30.9	193	142	0.3
			18.5			33.4	26.9	144	107	0.8
			26.4			35.8	24.9	146	79	1.3
I4	7/3/09	20.7	0	29.174	92.750	30.4	32.0	193	143	0.3
			19.7			35.3	26.1	64	97	
I2	7/3/09	14	0	29.409	92.750	30.7	31.9	196	138	1.0
			13			33.8	26.9	43	104	
I1	7/3/09	10.4	0	29.532	92.750	31.7	32.1	208	145	1.9
			5.7			32.2	28.5	107	138	
			9.5			32.4	33.8	34	121	
H0	7/3/09	2	0	29.494	92.385	32.1	31.9	229	147	8.0
			1			30.9	31.9	230	144	
H3	7/3/09	14	0	29.154	92.382	30.2	31.7	193	142	0.3
			13			35.2	26.0	49	94	
G1	1/0/00	8	0	29.260	91.998	30.8	30.8	187		3.6
			7			32.2	26.1	6	144	
G3	7/4/09	20	0	28.983	91.998	30.3	31.1	196	149	
			19			35.8	25.6	85	84	
E2	7/4/09	8.5	0	28.857	91.248	27.4	31.3	206	129	
			7.5			33.8	25.7	49	73	
E3	7/4/09	21.7	0	28.656	91.248	30.0	31.4	196	88	
			20.7			36.0	24.2	37	64	
D1	7/4/09	7.7	0	28.982	90.833	31.5	28.8	76		
			6.7			33.8	24.9	3	65	
			6.7			34.5	24.9	3	98	
D0	7/4/09	7.8	1.5	29.013	90.833	33.2	25.3	2	114	
D0(W)	7/4/09	6.5	1.5	29.018	90.833	29.9	25.5	2	147	

Abbreviation: Bot.: bottom depth, Sam.: sample depth, Lat.: latitude, Lon.: longitude, Temp.: temperature, DO: dissolved Oxygen, DOC: dissolved organic carbon, T. Chl a., total chlorophyll a.

Table (continued).

Trace elements are in nmol/kg

	Bot.	Sam.	NO_3	PO_4	SiO_3	NH_4	NO_2	Co		Cr		Cs
	(m)		(µmol/kg)					col.	dis.	col.	dis.	dis.
X3	93	0.0	0.0	0.06	3.6	0.2	0.1	0.042	0.357	<0.1	1.5	1.427
		40.0	0.1	0.20	1.4	0.1	0.1	0.022	0.062	0.0	2.3	1.960
		92.0	14.4	1.00	10.1	0.1	0.3	<0.006	0.230	0.3	2.3	1.933
MR1	0	0.0	6.0	0.27	26.8	0.5	0.0	0.053	0.600	<0.1	1.3	1.134
MR2	0	0.0	14.4	0.71	32.6	1.8	0.2	<0.006	0.634	<0.1	1.2	0.956
MR3	0	0.0	26.0	1.12	47.5	1.6	0.3	<0.006	0.679	<0.1	1.0	0.762
MR4	0	0.0	34.5	1.44	60.5	1.6	0.3	<0.006	0.838	<0.1	1.1	0.599
MR5	0	0.0	56.3	1.95	81.7	1.8	0.5	<0.006	0.664	<0.1	1.1	0.435
MR6	0	0.0	76.3	2.68	100.1	2.3	0.6	0.093	0.432	<0.1	1.3	0.291
MR7	0	0.0	91.4	3.31	113.8	2.6	0.5	0.070	0.192	0.5	1.3	0.113
MR8	0	0.0	88.8	3.02	118.2	2.6	0.6	0.081	0.646	0.3	1.4	0.047
A1	6.8	0.3	0.2	0.47	25.3	4.7	0.8	0.169	0.791	<0.1	0.8	1.228
		5.8	0.2	0.31	14.6	3.4	0.3	<0.006	0.771	<0.1	1.1	1.454
A3	15.5	0.0	0.1	0.27	19.3	1.0	0.1	0.013	0.604	<0.1	1.2	1.213
		7.0	3.1	0.31	9.0	2.1	0.2	0.015	0.523	<0.1	1.5	1.668
		16.0	10.6	2.15	42.1	0.3	1.5	<0.006	1.465	<0.1	0.6	1.835
A5	31	0.0	0.1	0.32	22.3	1.8	0.0	0.299	0.313	<0.1	1.1	1.155
		13.5	6.7	0.45	10.0	0.1	0.2	<0.006	0.266	<0.1	2.0	1.922
		20.0	1.6	0.19	2.4	0.0	0.1	<0.006	0.123	<0.1	2.5	1.986
		30.0	14.9	1.45	43.5	0.0	0.2	<0.006	1.535	<0.1	1.0	1.821
A7	50	0.0	0.2	0.20	8.2	0.9	0.0	0.087	0.316	<0.1	1.4	1.299
		20.0	0.8	0.28	3.5	0.1	0.4	<0.006	0.131	<0.1	2.2	1.939
		49.0	13.0	1.05	14.7	0.1	0.2	<0.006	0.442	<0.1	2.3	1.906
A9	80	0.0	0.2	0.27	7.0	1.0	0.0	<0.006	0.542	<0.1	1.3	1.215
		14.0	5.9	0.30	12.1	0.2	0.3	0.004	0.392	<0.1	1.5	1.886
		30.0	0.2	0.32	1.8	0.2	0.1	<0.006	0.109	<0.1	2.4	2.011
		40.0	4.4	0.49	11.3	0.2	0.2	<0.006	0.156	<0.1	2.0	1.975
		79.0	14.2	0.98	9.3	0.1	0.3	<0.006	0.173	<0.1	2.7	2.020
C11	52	0.0	0.2	0.27	0.9	0.9	0.0	0.006	0.483	<0.1	1.1	1.181
		30.0	5.3	0.53	15.5	0.1	0.4	<0.006	0.266	<0.1	1.7	1.939
		51.0	10.4	0.71	10.5	0.0	0.2	<0.006	0.379	<0.1	2.4	1.988
C9	31	0.0	0.2	0.18	0.8	0.9	0.0	0.047	0.455	<0.1	1.2	1.291
		20.0	2.4	0.36	4.7	0.0	0.5	<0.006	0.134	<0.1	2.2	1.971
		30.0	6.1	0.55	16.3	0.1	0.3	0.022	0.428	<0.1	1.7	1.964
C7	20.7	0.0	0.1	0.22	12.0	0.4	0.2	<0.006	0.510	<0.1	0.8	1.127
		9.5	1.7	0.41	6.6	0.0	1.0	<0.006	0.212	<0.1	2.0	1.847
		19.7	5.8	0.57	19.2	0.1	0.7	<0.006	0.381	<0.1	1.8	1.955

Table (continued).

	Bot.	Sam.	NO_3	PO_4	SiO_3	NH_4	NO_2	Co		Cr		Cs
	(m)			(µmol/kg)				col.	dis.	col.	dis.	dis.
C6	19.7	0.0	0.2	0.26	36.3	0.5	0.1	0.078	0.345	<0.1	0.8	0.886
		10.0	6.0	0.48	13.7	0.0	0.7	<0.006	0.246	<0.1	1.8	1.898
		18.7	8.0	0.70	23.3	0.0	0.4	<0.006	0.974	<0.1	1.1	1.933
C4	13.8	0.0	0.1	0.25	18.6	3.9	0.1	<0.006	0.641	<0.1	0.8	1.207
		5.3	1.6	0.39	6.8	0.8	1.1	<0.006	0.468	<0.1	1.5	1.633
		12.8	7.5	0.69	22.3	2.8	0.7	<0.006	0.835	<0.1	1.2	1.913
C1	6.2	0.0	0.0	0.10	18.6	0.1	0.0	0.105	0.478	<0.1	0.8	1.490
		5.2	5.2	1.54	34.1	0.6	2.6	<0.006	1.758	<0.1	0.7	1.740
D2	16.2	0.0	15.2	1.51	39.4	0.6	2.3	<0.006	0.347	<0.1	0.7	0.724
		15.2	0.5	1.92	53.4	6.9	0.5	<0.006	2.566	0.2	<0.1	1.766
		15.2	0.2	1.86	52.6	6.9	0.4	<0.006	2.556	<0.1	<0.1	1.784
AR1	0.0	0.0	43.6	2.50	101.8	2.5	0.6	0.013	0.076	0.7	0.7	0.052
AR2	0.0	0.0	24.1	2.94	94.1	2.6	0.6	0.023	0.163	0.9	0.8	0.069
AR3	0.0	0.0	39.2	2.67	95.0	2.4	0.7	0.011	0.113	0.5	0.8	0.050
AR4	0.0	0.0	35.4	2.51	88.6	2.2	0.8	0.040	0.146	0.4	0.7	0.080
AR5	0.0	0.0	30.4	2.35	86.4	2.2	0.9	0.027	0.259	0.2	0.8	0.130
AR6	0.0	0.0	13.0	1.23	71.4	2.7	0.4	<0.006	0.299	0.2	0.6	0.269
AR7	0.0	0.0	8.9	1.09	62.3	3.2	0.4	0.095	0.275	<0.1	0.8	0.422
AR8	0.0	0.0	3.0	0.67	54.9	2.9	0.3	0.107	0.373	<0.1	0.6	0.595
AR9	0.0	0.0	0.1	0.66	48.2	3.1	0.2	0.228	0.182	<0.1	0.7	0.734
AR10	0.0	0.0	0.0	0.46	40.5	1.8	0.2	0.106	0.383	0.2	0.6	0.899
AR11	0.0	0.0	0.0	0.44	37.1	1.6	0.2	<0.006	0.450	<0.1	0.6	0.974
F0	5.0	0.0	24.8	1.85	84.3	3.0	0.8	0.073	0.093	<0.1	0.6	0.115
		4.0	8.2	0.74	38.7	1.2	1.8	0.055	0.339	0.2	0.6	1.168
F1	5.0	0.0	37.0	1.84	91.8	2.9	0.7	0.089	0.148	0.2	0.7	0.105
		4.0	0.7	0.34	14.1	1.7	0.6	<0.006	1.005	0.2	0.5	1.701
F2	7.0	0.0	1.2	0.24	54.5	2.1	0.4	<0.006	0.340	<0.1	0.7	0.455
		6.0	0.1	0.20	6.9	0.3	0.0	<0.006	0.855	<0.1	0.6	1.734
F3	20.0	0.0	0.0	0.05	1.5	0.3	0.0	<0.006	0.752	<0.1	0.8	1.581
		6.5	0.0	0.13	4.4	0.1	0.0	<0.006	0.476	<0.1	0.9	1.570
		19.0	0.5	0.12	12.3	0.0	1.8	0.027	0.496	0.2	1.8	1.955
F5	30.0	0.0	0.0	0.04	3.3	0.2	0.0	0.053	0.461	<0.1	1.0	1.537
		10.0	0.0	0.20	1.1	0.1	0.0	<0.006	0.289	<0.1	2.0	1.828
		29.0	1.1	0.20	12.3	0.1	2.3	<0.006	0.295	<0.1	1.9	1.993
F7	53.0	0.0	0.1	0.11	0.6	0.3	0.0	<0.006	0.513	<0.1	1.3	1.544
		20.0	0.0	0.37	1.4	0.2	0.0	<0.006	0.181	<0.1	2.5	1.914
		40.0	0.1	0.42	3.2	0.3	0.4	0.010	0.120	0.2	2.3	1.996
		52.0	1.4	0.40	6.2	0.2	0.9	<0.006	0.149	<0.1	2.3	2.020

Table (continued).

	Bot.	Sam.	NO_3	PO_4	SiO_3	NH_4	NO_2	Co		Cr		Cs
	(m)			(μmol/kg)				col.	dis.	col.	dis.	dis.
F8	84.0	0.0	0.1	0.05	0.3	0.6	0.0	0.038	0.482	0.2	1.4	1.493
		20.0	0.0	0.29	1.4	0.2	0.0	0.024	0.146	0.2	2.3	1.937
		82.0	10.6	0.72	6.4	0.1	0.1	0.020	0.035	<0.1	2.8	2.050
I9	56.0	0.0	0.1	0.08	0.5	0.2	0.0	0.036	0.497	<0.1	1.4	1.558
		20.0	0.1	0.28	1.2	0.1	0.1	0.032	0.129	0.2	2.2	1.916
		55.0	2.8	0.47	5.8	0.1	0.2	<0.006	0.115	<0.1	2.2	2.007
I8	37.0	0.0	0.0	0.16	1.2	0.1	0.0	0.046	0.412	<0.1	1.3	1.552
		12.5	0.4	0.22	3.7	0.1	0.4	<0.006	0.370	<0.1	1.8	1.762
		36.0	0.8	0.44	5.8	0.0	2.3	0.046	0.126	0.3	2.1	2.008
I6	27.4	0.0	0.1	0.13	0.8	0.0	0.0	0.077	0.368	<0.1	1.2	1.595
		18.5	0.2	0.22	3.1	0.2	1.1	0.047	0.314	<0.1	1.9	1.778
		26.4	1.0	0.37	7.1	0.1	1.0	<0.006	0.199	0.4	1.8	1.968
I4	20.7	0.0	0.1	0.14	0.6	0.0	0.0	0.044	0.359	<0.1	1.3	1.619
		19.7	1.1	0.29	11.0	0.2	1.8	0.081	0.359	0.2	1.3	1.869
I2	14.0	0.0	0.0	0.11	0.5	0.1	0.0	<0.006	0.468	0.2	1.2	1.682
		13.0	0.6	0.28	17.3	0.0	3.1	0.075	0.837	0.3	0.8	1.851
I1	10.4	0.0	0.0	0.09	5.8	0.2	0.0	0.029	0.458	<0.1	0.7	1.713
		5.7	0.1	0.19	11.2	0.0	1.2	0.005	0.452	0.2	0.5	1.711
		9.5	0.9	0.47	22.5	1.3	5.2	<0.006	0.887	0.2	0.5	1.791
H0	2.0	0.0	0.1	0.26	11.0	0.0	0.0	0.254	1.045	<0.1	0.3	1.641
		1.0	0.1	0.18	11.9	0.0	0.0	<0.006	1.227	0.3	0.2	1.649
H3	14.0	0.0	0.1	0.11	2.2	0.1	0.0	<0.006	0.440	<0.1	1.1	1.605
		13.0	4.3	0.55	31.1	0.1	4.9	<0.006	0.838	0.2	0.7	1.905
G1	8.0	7.0	0.1	0.18	12.6	0.3	0.1	<0.006	0.812	<0.1	0.5	1.655
G3	20.0	0.0	0.0	0.03	1.4	0.1	0.0	0.064	0.377	<0.1	0.7	1.632
		19.0	1.1	0.48	17.5	0.1	6.1	0.093	0.616	<0.1	1.5	1.951
E2	8.5	0.0	0.1	0.11	10.7	0.2	0.0	<0.006	0.535	<0.1	0.4	1.451
		7.5	5.3	0.60	33.2	0.1	0.2	<0.006	1.477	0.2	0.4	1.780
E3	21.7	0.0	0.1	0.08	1.1	0.5	0.0	0.148	0.297	<0.1	1.3	1.625
		20.7	11.2	0.86	36.2	0.1	0.3	<0.006	0.545	<0.1	0.7	1.946
D1	7.7	6.7	1.1	1.95	42.4	0.6	3.7	<0.006	1.377	0.3	0.5	1.740
		6.7	1.1	1.93	43.2	1.8	3.7	0.066	1.254	0.2	0.5	1.815
D0	7.8	1.5	1.4	1.53	39.7	2.1	6.7	<0.006	1.149	0.3	0.3	1.668
D0(W)	6.5	1.5	3.3	1.22	37.4	3.8	5.8	0.076	0.970	<0.1	0.6	1.559

Abbreviation: Bot.: bottom depth, Sam.: sampling depth, col.: colloid (0.02-0.45 μm), dis.: dissolved (<0.02 μm).

Table (continued).

	Bot.	Sam.	Cu	Fe		Mo	Mn		Ni	Re	U	V
	(m)		dis.	col.	dis.	dis.	col.	dis.	dis.	dis.	dis.	dis.
X3	93.0	0.0	7.2	0.5	1.8	85	3.3	26.2	8.0	0.043	8.48	28.6
		40.0	1.7	<0.4	0.7	112	4.3	3.4	3.0	0.056	11.44	30.1
		92.0	1.2	3.7	0.9	110	46.3	294.3	3.3	0.053	11.16	27.9
MR1	0.0	0.0	10.2	2.8	1.9	71	18.0	123.2	10.9	0.046	7.30	26.2
MR2	0.0	0.0	12.6	8.5	2.3	58	19.7	149.9	12.6	0.048	6.80	26.7
MR3	0.0	0.0	14.1	17.8	1.7	52	22.5	208.6	15.9	0.044	6.20	32.5
MR4	0.0	0.0	16.5	15.4	2.1	47	25.6	318.8	16.2	0.051	5.75	37.3
MR5	0.0	0.0	17.3	31.2	4.4	36	27.2	349.6	19.0	0.041	5.56	33.8
MR6	0.0	0.0	19.5	244.9	7.7	28	23.6	518.4	20.3	0.054	4.85	31.5
MR7	0.0	0.0	21.8	426.7	9.4	18	36.9	613.6	23.3	0.056	4.17	33.1
MR8	0.0	0.0	21.0	517.1	10.9	16	21.1	403.7	24.3	0.062	3.82	41.2
A1	6.8	0.3	8.6	14.2	2.3	74	5.7	26.4	12.4	0.037	7.82	29.8
		5.8	6.4	5.1	1.2	84	15.3	123.0	9.7	0.045	8.39	26.3
A3	15.5	0.0	9.2	5.7	1.1	75	5.6	22.5	10.4	0.047	7.65	31.8
		7.0	4.5	1.8	1.3	96	19.8	166.6	6.6	0.044	9.75	26.1
		16.0	2.3	7.9	2.0	105	331.6	3638.7	6.9	0.042	11.86	33.1
A5	31.0	0.0	9.4	4.0	1.5	71	11.7	51.4	11.3	0.044	7.55	29.0
		13.5	2.3	<0.4	2.2	107	6.2	30.1	4.9	0.046	11.48	31.2
		20.0	1.6	1.2	0.5	111	0.4	4.1	3.4	0.043	11.83	32.2
		30.0	3.1	5.5	2.1	113	150.5	1420.4	6.7	0.044	11.95	27.2
A7	50.0	0.0	7.8	<0.4	2.8	79	2.7	18.1	8.6	0.044	8.47	24.9
		20.0	2.3	<0.4	<0.4	111	0.4	4.9	3.6	0.051	11.58	27.9
		49.0	1.9	13.7	1.5	111	9.0	137.8	4.0	0.050	11.61	28.1
A9	80.0	0.0	9.9	0.8	1.2	74	3.6	22.8	9.0	0.043	7.71	21.7
		14.0	3.8	<0.4	0.9	107	14.1	195.3	6.0	0.049	10.68	30.3
		30.0	1.8	0.5	<0.4	113	<0.3	3.8	3.6	0.037	11.59	29.4
		40.0	2.8	<0.4	3.0	112	<0.3	4.2	4.6	0.042	11.59	31.8
		79.0	1.3	5.2	0.7	112	16.8	197.5	3.2	0.037	11.53	30.1
C11	52.0	0.0	9.2	1.0	1.0	72	5.6	9.8	9.6	0.038	7.60	22.3
		30.0	3.0	<0.4	1.1	112	5.7	2.6	4.7	0.040	11.63	30.9
		51.0	2.0	23.1	1.1	112	1.6	16.1	4.7	0.038	11.60	27.2
C9	31.0	0.0	8.1	1.2	1.0	77	13.9	100.7	9.2	0.036	8.34	24.4
		20.0	2.0	<0.4	1.0	111	0.4	4.6	3.9	0.048	11.46	30.7
		30.0	2.8	7.1	1.2	112	1.5	21.5	5.9	0.047	11.38	29.9
C7	20.7	0.0	8.9	1.7	1.7	72	11.8	121.9	10.6	0.035	7.75	25.3
		9.5	2.5	<0.4	0.7	106	2.4	32.0	4.2	0.046	11.05	28.5
		19.7	2.8	4.2	1.0	113	8.6	124.9	5.1	0.055	11.45	31.6

Table (continued).

	Bot.	Sam.	Cu	Fe		Mo	Mn		Ni	Re	U	V
	(m)		dis.	col.	dis.	dis.	col.	dis.	dis.	dis.	dis.	dis.
C6	19.7	0.0	11.6	6.6	1.5	58	5.9	18.6	12.0	0.036	6.45	23.9
		10.0	2.7	<0.4	1.5	108	1.1	17.4	4.1	0.038	11.24	33.3
		18.7	2.8	7.3	0.9	109	9.7	193.8	5.9	0.048	11.40	30.2
C4	13.8	0.0	8.8	1.3	1.7	73	10.6	73.0	9.2	0.037	8.04	23.9
		5.3	5.5	6.2	0.9	94	9.5	187.0	7.0	0.047	10.17	28.0
		12.8	2.7	4.7	1.4	110	20.7	298.3	5.4	0.041	11.37	32.5
C1	6.2	0.0	6.1	0.8	0.9	89	4.0	12.0	8.3	0.038	9.54	26.9
		5.2	3.0	5.0	2.5	100	103.7	2032.1	6.8	0.044	10.66	20.9
D2	16.2	0.0	15.5	7.4	3.7	48	2.2	4.3	17.3	0.038	5.99	30.0
		15.2	1.3	-170.8	717.5	107	52.6	6484.9	7.1	0.045	11.17	18.3
		15.2	1.6	100.5	365.1	103	67.0	6428.9	8.6	0.047	11.09	19.4
AR 1	0.0	0.0	22.1	2092.8	43.4	7	22.0	36.7	23.2	0.032	1.54	35.9
AR 2	0.0	0.0	24.4	1707.1	28.6	11	55.6	607.2	25.0	0.034	1.73	36.5
AR 3	0.0	0.0	22.5	698.3	25.5	10	3.6	85.4	22.7	0.034	2.09	34.0
AR 4	0.0	0.0	22.7	356.8	13.8	9	11.5	156.7	26.7	0.032	2.01	31.0
AR 5	0.0	0.0	23.2	205.5	12.5	13	43.5	519.8	24.1	0.034	2.73	30.6
AR 6	0.0	0.0	21.2	31.6	4.8	23	9.3	22.1	22.0	0.038	3.39	31.0
AR 7	0.0	0.0	20.3	43.5	4.2	31	7.8	22.1	20.9	0.035	3.98	30.8
AR 8	0.0	0.0	18.4	16.9	4.4	42	5.9	19.5	18.0	0.038	5.13	32.2
AR 9	0.0	0.0	17.9	34.1	2.9	50	12.9	27.9	15.8	0.036	5.98	34.5
AR 10	0.0	0.0	15.4	7.2	2.9	61	4.5	24.3	15.1	0.043	6.54	32.2
AR 11	0.0	0.0	15.2	16.1	2.8	63	4.7	22.9	15.0	0.043	7.06	30.8
F0	5.0	0.0	21.9	30.5	8.3	11	1.7	3.3	23.4	0.031	2.55	31.1
		4.0	11.6	4.9	3.1	73	1.8	11.2	13.4	0.039	8.13	30.8
F1	5.0	0.0	22.5	44.2	8.8	11	9.7	180.9	23.4	0.031	2.35	29.3
		4.0	7.1	45.3	1.3	100	7.6	640.8	11.2	0.048	10.05	29.5
F2	7.0	0.0	20.0	19.6	2.4	37	6.3	5.1	17.5	0.032	4.74	31.6
		6.0	7.0	4.8	1.2	99	7.5	246.9	8.6	0.043	10.30	31.9
F3	20.0	0.0	9.7	2.3	0.8	87	7.0	112.7	9.8	0.045	9.69	28.5
		6.5	8.8	2.1	1.0	90	2.4	16.0	9.3	0.041	10.07	28.0
		19.0	4.1	33.9	1.6	111	1.7	14.6	7.0	0.042	11.73	33.2
F5	30.0	0.0	9.5	1.0	0.8	93	2.5	31.4	9.4	0.042	10.05	27.9
		10.0	4.3	1.4	0.5	105	<0.3	18.3	6.4	0.046	11.31	29.9
		29.0	3.7	3.9	0.8	112	0.9	41.6	5.1	0.040	11.83	30.7
F7	53.0	0.0	8.3	1.1	0.7	89	4.3	98.8	8.7	0.045	9.51	29.6
		20.0	2.6	<0.4	1.5	107	0.4	7.9	5.2	0.041	11.84	29.6
		40.0	2.7	1.0	0.5	114	<0.3	4.6	4.0	0.045	12.26	31.8
		52.0	2.4	4.4	1.4	115	<0.3	19.6	4.2	0.051	12.19	33.9

Table (continued).

	Bot.	Sam.	Cu	Fe		Mo	Mn		Ni	Re	U	V
	(m)		dis.	col.	dis.	dis.	col.	dis.	dis.	dis.	dis.	dis.
F8	84.0	0.0	8.4	1.0	0.5	89	2.8	42.3	8.2	0.048	9.10	27.9
		20.0	3.4	1.1	<0.4	110	0.6	7.0	3.9	0.040	11.29	30.4
		82.0	1.1	4.1	0.7	113	0.5	9.5	2.9	0.040	11.57	33.5
I9	56.0	0.0	7.7	0.6	0.6	91	1.7	26.5	8.4	0.043	9.48	26.8
		20.0	3.1	1.5	3.0	110	0.6	7.6	5.3	0.039	11.04	30.2
		55.0	2.1	12.3	0.7	113	<0.3	5.7	3.9	0.045	11.41	31.2
I8	37.0	0.0	8.0	2.6	2.9	90	3.6	19.9	7.6	0.042	9.49	28.0
		12.5	4.9	<0.4	1.8	100	1.1	18.0	5.5	0.038	10.20	31.6
		36.0	2.9	31.3	1.0	111	<0.3	12.1	4.1	0.038	11.43	28.0
I6	27.4	0.0	8.2	<0.4	<0.4	92	2.5	21.5	9.0	0.039	9.71	25.6
		18.5	4.7	<0.4	1.2	103	1.2	14.8	5.7	0.054	10.48	26.2
		26.4	3.8	5.4	0.6	111	0.5	16.3	4.5	0.041	11.17	27.9
I4	20.7	0.0	7.8	<0.4	0.5	93	1.9	19.9	7.5	0.036	9.74	26.7
		19.7	5.2	1.5	0.6	106	1.4	11.8	5.3	0.045	10.65	27.6
I2	14.0	0.0	8.1	<0.4	0.5	95	1.0	20.4	7.3	0.047	9.94	28.1
		13.0	5.5	3.9	1.3	105	1.5	24.8	7.1	0.042	10.57	24.1
I1	10.4	0.0	8.7	<0.4	4.6	99	1.2	17.4	8.5	0.038	9.84	26.8
		5.7	7.9	1.5	1.3	97	2.3	23.4	8.5	0.038	9.93	28.7
		9.5	5.0	3.3	1.2	104	11.1	239.7	6.9	0.042	10.13	34.0
H0	2.0	0.0	10.2	51.6	1.9	101	6.8	80.3	13.4	0.041	10.03	32.6
		1.0	9.3	21.6	1.8	101	4.6	56.4	10.3	0.040	9.96	33.8
H3	14.0	0.0	8.1	<0.4	0.5	92	2.0	25.0	9.1	0.040	9.82	29.6
		13.0	5.2	9.3	1.8	107	1.1	189.4	8.9	0.042	10.97	25.3
G1	8.0	7.0	8.4	4.0	1.2	97	37.5	726.4	10.0	0.038	9.89	29.4
G3	20.0	0.0	8.6	0.1	0.8	94	2.0	6.5	8.6	0.044	9.89	27.2
		19.0	5.0	11.1	2.0	109	2.3	32.1	8.2	0.051	11.35	32.2
E2	8.5	0.0	10.2	1.9	1.6	85	3.6	75.2	9.9	0.050	9.36	30.4
		7.5	4.3	6.6	2.2	105	64.5	1299.2	7.7	0.042	10.57	28.4
E3	21.7	0.0	8.5	0.3	0.3	92	1.4	14.4	8.3	0.049	9.92	27.2
		20.7	4.1	46.3	2.0	111	5.3	80.2	6.8	0.047	11.47	37.5
D1	7.7	6.7	2.6	5.6	4.2	102	116.8	3723.0	6.0	0.044	10.48	24.9
		6.7	2.5	5.4	2.6	103	276.6	3836.0	6.2	0.047	10.84	21.8
D0	7.8	1.5	3.2	10.8	3.7	97	196.0	3654.9	6.9	0.039	10.33	24.0
D0(W)	6.5	1.5	4.9	6.9	2.1	92	9.1	1376.0	8.8	0.041	9.38	29.8

Abbreviation: Bot.: bottom depth, Sam.: sampling depth, col.: colloid (0.02-0.45 μm), dis.: dissolved (<0.02 μm).

Table

Results of the mixing experiments from May 2008. Trace elements are in nmol/kg

	Co		Cr		Cs	Cu	Fe	
Salinity	col.	dis.	col.	dis.	dis.	dis.	col.	dis.
0.1	0.125	0.160	5.0	0.5	0.075	18.9	5504.3	92.0
2.5	0.257	0.393	2.9	0.7	0.166	18.1	3309.2	69.8
4.0	0.110	0.728	0.9	0.8	0.209	17.1	1261.1	51.0
7.2	0.494	0.904	1.2	0.9	0.401	15.0	1330.0	49.5
8.4	0.289	1.007	0.8	1.1	0.462	15.0	997.6	44.7
10.8	0.630	1.128	1.2	1.2	0.608	13.7	1170.9	37.8
14.4	<0.006	1.659	0.5	1.4	0.844	11.5	603.6	29.6
19.3	0.221	1.058	<0.1	1.6	1.107	9.0	77.8	21.2
23.0	0.242	0.887	<0.1	1.8	1.366	7.4	54.8	16.1
24.6	0.212	1.029	0.3	1.9	1.467	7.0	290.6	14.3
32.9	0.040	0.453	<0.1	2.6	1.986	2.8	10.6	4.8
33.0	0.053	0.405	<0.1	2.5	2.128	2.5	11.7	3.7
35.8	0.009	0.079	0.0	2.7	2.217	1.2	0.6	<0.4

	Mo	Mn		Ni	Re	U	V
Salinity	dis.	col.	dis.	dis.	dis.	dis.	dis.
0.1	5	1.5	1149.6	30.6	0.028	1.97	33.1
2.5	12	0.6	1170.2	26.7	0.032	2.90	28.1
4.0	17	18.0	947.3	23.3	0.041	3.54	27.5
7.2	25	100.8	1034.5	23.6	0.039	4.26	29.2
8.4	30	14.7	812.5	19.9	0.029	4.92	25.8
10.8	37	12.3	741.4	22.6	0.034	5.83	26.2
14.4	46	28.8	626.2	19.4	0.034	7.02	26.7
19.3	63	11.4	521.8	15.6	0.042	8.73	28.4
23.0	75	21.2	435.0	12.7	0.041	9.89	32.0
24.6	78	19.1	399.1	11.6	0.047	10.29	31.3
32.9	106	<0.4	141.4	5.5	0.040	13.42	30.3
33.0	123	1.0	127.1	4.8	0.000	13.43	32.2
35.8	115	<0.4	3.5	2.8	0.044	14.40	33.7

Abbreviation: col.: colloid (0.02-0.45 µm), dis.: dissolved (<0.02 µm).

Table

Results of the mixing experiments from November 2008. Trace elements are in nmol/kg

	Co		Cr		Cs	Cu	Fe	
Salinity	col.	dis.	col.	dis.	dis.	dis.	col.	dis.
0.2	<0.006	0.057	0.6	0.7	0.021	20.9	877.3	34.8
4.3	<0.006	0.204	0.4	1.1	0.214	16.5	239.0	22.7
7.4	0.024	0.216	0.3	1.2	0.379	14.7	136.3	19.7
11.5	0.044	0.233	0.5	1.3	0.572	13.1	168.2	17.1
14.5	<0.006	0.297	<0.1	1.7	0.779	11.7	133.8	13.7
17.7	0.007	0.232	0.2	1.8	0.940	10.7	133.5	11.4
21.1	<0.006	0.174	<0.1	1.9	1.127	8.0	12.3	8.4
26.9	<0.006	0.175	<0.1	2.1	1.344	6.0	5.6	6.2
29.0	<0.006	0.142	<0.1	2.4	1.538	4.8	4.1	4.4
32.5	<0.006	0.131	<0.1	2.3	1.737	3.5	4.3	2.8
36.7	0.012	0.080	<0.1	2.7	1.922	1.2	0.6	<0.4

	Mo	Mn		Ni	Re	U	V	DOC
Salinity	dis.	col.	dis.	dis.	dis.	dis.	dis.	(µmol/kg)
0.2	11	11.5	4.1	22.5	0.064	3.87	31.3	339
4.3	22	3.7	13.4	22.9	0.056	5.03	29.2	295
7.4	31	2.6	14.3	21.0	0.053	5.31	31.9	290
11.5	41	2.7	14.7	17.9	0.048	6.13	34.0	264
14.5	54	1.7	14.2	16.3	0.053	7.85	25.8	230
17.7	63	2.6	13.3	14.3	0.039	8.71	26.4	205
21.1	74	<0.4	11.5	11.7	0.041	9.62	26.5	182
26.9	88	<0.4	9.2	8.9	0.039	10.71	26.7	145
29.0	97	<0.4	7.4	7.0	0.039	10.74	27.1	119
32.5	107	<0.4	5.7	4.9	0.040	11.35	27.9	100
36.7	118	<0.4	2.5	2.7	0.037	12.73	29.3	67

Abbreviation: col.: colloid (0.02-0.45 µm), dis.: dissolved (<0.02 µm).

Table

Results of the mixing experiments from June/July 2009 (Mississippi River). Trace elements are in nmol/kg

	Co		Cr		Cs	Cu	Fe	
Salinity	col.	dis.	col.	dis.	dis.	dis.	col.	dis.
0.7	<0.006	0.083	<0.1	1.4	0.034	22.7	151.2	9.2
4.8	0.039	0.176	<0.1	1.4	0.236	19.6	109.3	6.4
8.6	<0.006	0.244	<0.1	1.3	0.448	17.0	53.0	5.8
11.1	<0.006	0.308	<0.1	1.5	0.571	16.3	34.8	5.3
14.4	<0.006	0.340	<0.1	1.5	0.740	14.4	29.9	4.4
17.2	<0.006	0.403	<0.1	1.6	0.899	13.2	20.5	4.0
21.5	<0.006	0.388	<0.1	1.7	1.111	11.3	16.1	3.4
23.9	<0.006	0.358	<0.1	1.7	1.245	10.0	15.1	3.0
26.6	<0.006	0.308	<0.1	1.6	1.383	8.7	11.7	2.4
29.7	<0.006	0.349	<0.1	1.8	1.574	7.2	7.4	2.0
32.8	<0.006	0.296	<0.1	1.6	1.735	5.6	2.5	1.8
34.1	<0.006	0.311	<0.1	1.7	1.847	4.8	4.8	1.2
35.7	<0.006	0.322	<0.1	1.9	2.002	3.3	<0.4	0.8

	Mo	Mn		Ni	Re	U	V	DOC
Salinity	dis.	col.	dis.	dis.	dis.	dis.	dis.	(µmol/kg)
0.7	11	2.6	101.0	25.8	0.051	4.39	41.7	255
4.8	24	6.1	118.4	24.1	0.048	5.27	37.0	251
8.6	37	3.2	115.1	16.0	0.052	5.74	35.7	239
11.1	42	<0.4	110.6	16.7	0.050	6.31	34.9	216
14.4	51	2.6	99.2	14.7	0.062	7.19	36.6	197
17.2	60	<0.4	92.3	13.2	0.044	7.65	34.5	190
21.5	69	<0.4	78.0	12.9	0.046	8.47	35.8	166
23.9	77	2.7	65.1	11.6	0.040	9.02	36.2	153
26.6	84	<0.4	53.9	10.3	0.054	9.73	34.5	135
29.7	93	<0.4	38.7	8.2	0.043	10.62	36.3	131
32.8	101	0.6	23.1	6.5	0.044	11.17	33.7	104
34.1	106	0.0	15.5	5.7	0.046	11.78	33.2	93
35.7	114	<0.4	2.3	5.2	0.042	12.46	35.8	75

Table

Results of the mixing experiments from June/July 2009 (Atchafalaya River). Trace elements are in nmol/kg

	Co		Cr		Cs	Cu	Fe	
Salinity	col.	dis.	col.	dis.	dis.	dis.	col.	dis.
0.1	<0.006	0.079	1.9	0.9	0.048	24.1	2270.2	44.6
4.0	0.151	0.127	1.0	0.9	0.214	19.9	1070.3	32.5
6.5	0.239	0.136	0.9	1.0	0.366	18.6	1015.6	27.4
10.0	0.088	0.192	0.5	1.1	0.531	15.5	443.8	20.8
14.0	<0.006	0.236	0.2	1.3	0.735	13.7	180.8	17.2
17.1	<0.006	0.258	<0.1	1.7	0.875	12.3	149.6	14.9
18.8	<0.006	0.243	<0.1	1.5	1.015	11.0	123.9	12.0
23.8	<0.006	0.240	0.2	1.6	1.223	9.5	60.4	9.6
24.9	0.054	0.191	0.3	1.8	1.362	8.4	188.6	8.0
28.3	0.027	0.184	0.3	1.9	1.520	7.0	154.8	6.7
32.2	<0.006	0.197	<0.1	2.1	1.705	5.4	10.1	4.0
35.6	<0.006	0.160	<0.1	2.2	1.872	4.4	6.9	1.9
36.2	<0.006	0.163	<0.1	2.4	1.956	3.2	<0.4	0.9

	Mo	Mn		Ni	Re	U	V	DOC
Salinity	dis.	col.	dis.	dis.	dis.	dis.	dis.	(µmol/kg)
0.1	6	24.7	20.7	25.046	0.031	1.78	45.098	396
4.0	15	14.1	30.1	24.526	0.033	2.89	39.684	395
6.5	22	10.8	30.0	21.978	0.035	3.51	31.21	361
10.0	31	4.5	27.3	20.204	0.030	4.43	28.917	335
14.0	43	1.8	25.1	17.913	0.044	5.79	35.316	301
17.1	52	1.1	24.1	15.439	0.033	6.60	29.483	267
18.8	57	<0.4	22.2	14.038	0.031	7.05	28.738	248
23.8	70	<0.4	18.8	11.067	0.035	8.06	31.438	210
24.9	76	2.1	15.3	10.935	0.038	8.52	36.071	196
28.3	85	1.3	13.9	8.887	0.033	9.51	30.831	168
32.2	96	<0.4	11.2	7.2432	0.043	10.49	30.323	134
35.6	103	<0.4	8.6	5.7318	0.043	11.07	28.435	110
36.2	112	<0.4	6.1	4.2055	0.045	11.66	29.792	87

Abbreviation: col.: colloid (0.02-0.45 µm), dis.: dissolved (<0.02 µm).

REFERENCES

Abu-Saba, K.E., Flegal, A.R. Chromium speciation in SanFrancisco Bay: superposition of geochemical processes causes complex spatial distribution of inorganic species. *Mar. Chem*. **1995**, 49, 189-200.

Almroth, E., Tenberg, A., Andersson, J.H., Pakhomova, S., Hall, P.O.J. Effects of resuspension on bentic fluxes of oxygen, nutrients, dissolved inorganic carbon, iron and manganese in the Gulf of Finland, Baltic Sea. *Cont. Shelf Res*. **2009**, 29, 807-818.

Auger, Y., Bodineau, L., Leclercq, S., Wartel, M. Some aspects of vanadium and chromium chemistry in the English Channel. *Cont. Shelf Res*. **1999**, 19, 2003–2018.

Baeyens, W., Goeyens, L., Monteny, F., Elskens, M. Effect of organic complexation on the behavior of dissolved Cd, Cu and Zn in the Scheldt estuary. *Hydrobiologia* **1998**, 366, 81-90.

Bianchi, T.S., Filley, K. Dria, K., Hatcher, P.G. Temporal variability in sources of dissolved organic carbon in the lower Mississippi River. *Geochim. Cosmochim. Acta* **2004**, 68, 959-967.

Boyle, E.A., Edmond, J.M., Sholkovitz, E.R. The mechanism of iron removal in estuaries. *Geochim. Cosmochim. Acta* **1977**, 41, 1313-1324.

Breckel, E.J., Emerson, S., Balistrieri, LS. Authigenesis of trace metals in energetic tropical shelf environments. *Cont. Shelf Res*. **2005**, 25, 1321-1337.

Breuer, E., Sanudo-Wilhelmy, S.A., Aller, R.C. Trace metals and dissolved organic carbon in an estuary with restricted river flow and a brown tide bloom. *Estuaries* **1999**, 22, 603-615.

Bruland, K.W., Donat, J.R., Hutchins, D.A. Interactive influences of bioactive trace metals on biological production in oceanic waters. *Limnol Oceanogr.* **1991**, 36, 1555-1577.

Chiffoleau, J.-F., Cossa, D., Auger, D., Truquet, I. Trace metal distribution, partition and fluxes in the Seine estuary (France) in low discharge regime. *Mar. Chem.* **1994**, 47, 145-158.

Church, T.M., Sarin, M.M., Fleisher, M.Q., Ferdelman, T.G. Salt marshes: an important coastal sink for dissolved uranium. *Geochim. Cosmochim. Acta* **1996**, 60, 3879-3887.

Cochrane, J.D., Kelly, F.J. Low-frequency circulation on the Texas-Louisiana continental shelf. *J. Geo. Res.* **1986**, 91, 10645-10659.

Colbert, D., McManus, J. Importance of seasonal variability and coastal processes on estuarine manganese and barium cycling in a Pacific Northwest estuary. *Cont. Shelf Res*. 2005, 25, 1395-1414.

Colodner, D., Sachs, J., Ravizza, G., Turekian, K.K., Edmond, J., Boyle, E., The geochemical cycle of rhenium: a reconnaissance. *Earth Planet. Sci. Lett.* **1993**, 117, 205–221.

Comans, R.N.J., Middelburg, J.J., Zonderhuts, J., Woittiex, J.R.W., De Lange, G.J., Das, H.A., van der Weuden, C.H. Mobilization of radioceasium in pore water of lake sediments. *Nature* **1989**, 339, 367-369.

Crusius, J., Calvert, S., Pedersen, T., Sage, D. Rhenium and molybdenum enrichments in sediments as indicators of oxic, suboxic and sulfidic conditions of deposition. *Earth Planet. Sci. Lett.* **1996**, 145, 65-78.

Dagg, M.J., Ammerman, J.W., Amon, R.M.W., Gardner, W.S., Green, R.E., Lohrenz, S.E. A review of water column processes influencing hypoxia in the northern Gulf of Mexico. *Estuar. Coast.* **2007**, 30, 735-752.

Davison, W., Hilton, J., Hamilton-Taylor, J., Livens, F., Kelly, M. The transport of Chernobyl-derived Cs-137 through two freshwater lakes in Cumbria. *J. Environ. Radioact*. **1993**, 19, 125-153.

Dinnel, A.P. and Wiseman Jr, W.J. Fresh water on the Louisiana and Texas shelf. *Cont. Shelf Res*. **1986**, 6, 765-784.

Duan, S.W., Bianchi, T.S., Shiller, A.M., Dria, K. Hatcher, P. Seasonal variations in abundance and bulk composition of dissolved organic matter in the Lower Mississippi and Pearl Rivers (USA). *J. Geophys. Res.-Biosciences* **2007**, 112, Go2024. Doi:10.1029/2006JG000206.

Duan, S.W., Bianci, T., Santschi, P., Amon, M.W. Effects of tributary inputs on nutrient export from the Mississippi and Atchafalaya Rivers to the Gulf of Mexico. *Mar. Freshwater Res*. **2010**, 61, 1029-1038.

Dubois, K.D., Lee, D., Veizer, J. Isotopic constraints on alkalinity, dissolved organic carbon, and atmospheric carbon dioxide fluses in the Mississippi River. *J. Geophys. Res. Biogeosciences* **2010**, 115: G02018, doi: 10.1029/2009JG001102.

Eary, L.E., Rai, D. Kinetics of chromium(III) oxidation to chromium(VI) by reaction with manganese dioxide. *Environ. Sci. Technol.* **1987**, 21, 1187–1193.

Emerson, S.R., Huested, S.S. Ocean anoxia and the concentrations of molybdenum and vanadium in seawater. *Mar. Chem.* **1991**, 34, 177-196.

Evans, D.W., Alberts, J.J., Clark III, R.A. Reversible ion-exchange fixation of cesium-137 leading to mobilization from reservoir sediments. *Geochim. Cosmochim. Acta* **1983**, 47, 1041-1049.

Ford, M., Nyman, J.A. Preface: an overview of the Atchafalaya River. *Hydrobiologia*, **2011**, 658, 1-5.

Guo, L., Santschi, P.H., Warnken, K.W. Dynamics of dissolved organic carbon (DOC) in oceanic environments. *Limnol. Oceanogr.* **1995**, 40, 1392-1403.

Guo, L., Santschi, P.H., Warnken, K.W. Trace metal composition of colloidal organic material in marine environments. *Mar. Chem.* **2000**, 70, 257-275.

Hanor, J.S., Chan, L.H. Non-conservative behavior of barium during mixing of Mississippi River and Gulf of Mexico waters. *Earth Planet. Sci. Lett.* **1977**, 37, 242–250.

Hatje, V., Payne, T.E., Hill, D.M., McOrist, G., Birch, G.F., Szymczak, R. Kinetics of trace element uptake and release by particles in estuarine waters: effects of pH, Salinity, and particle loading. *Environ. Int.* **2003**, 29, 619-269.

Helz, G.R., Miller, C.V., Charnock, J.M., Mosselmans, J.F.W., Patrick, R.A.D. Mechanism of molybdenum removal from the sea and its concentration in black shales: EXAFS evidence. *Geochim. Cosmochim. Acta* **1996**, 60(19): 3631-3642.

Helz, G.R., Dolor, M.K. What regulates rhenium deposition in euxinc basins? *Chem. Geol*. **2012**, 304-305, 131-141.

Ho, T.-Y., Quigg, A., Finkel, Z.V., Milligan, A.J., Wyman, K., Falkowski, P.G., Morel, F.M.M.. The elemental composition of some marine phytoplankton. *J. Phycol.* **2003**, 39, 1145–1159.

James, R.H., Palmer, M. Marine geochemical cycles of the alkali elements and boron: the role of sediments. *Gcochim. Cosmochim. Acta* **2000**, 64(18), 3111-3122.

Joung, D.J., Shiller, A.M. Trace element distributions in the water column near the Deepwater Horizon well blowout. *Environ. Sci. Technol.* **2012**, 47, 2161-2168.

Kieber, R.J., Helz, G.R. Indirect photoreduction of aqueous chromium(VI). *Environ. Sci. Technol.* **1992**, 26, 307-312.

Klinkhammer, G.P., McManus, J. Dissolved manganese in the Columbia River estuary: production in the water column. *Geochim. Cosmochim. Acta* **2001**, 65, 2835-2841.

Klinkhammer, G.P., Palmer, M.R. Uranium in the oceans: Where it goes and why. *Geochim. Cosmochim. Acta* **1991**, 55(7): 1799-1806.

Li, Y.-H., Burkhardt, L., Teraoka, H. Desorption and coagulation of trace elements during estuarine mixing. *Geochim. Cosmochim. Acta* **1984**, 48, 1879-1884.

Lohrenz, S. E., Redalje, D. G., Cai, W.-J., Acker, J., Dagg, M. A retrospective analysis of nutrients and phytoplankton productivity in the Mississippi River Plume, Continental Shelf Research, *Cont. Shelf Res*. **2008**, 28, 1466-1475.

Lohrenz, S.E., Dagg, M.J., Whitledge, T.E. Enhanced primary production at the plume/oceanic interface of the Mississippi River. *Cont. Shelf Res*. **1990**, 10, 639–664.

Lohrenz, S.E., Redalje, D.G., Fahnenstiel, G.L., Lang, G.A. Regulation and distribution of primary production in the northern Gulf of Mexico. In *Nutrient Enhanced Coastal Ocean Productivity*. Publication Number TAMU-SG-92-109, Sea Grant Program, Texas A&M University, Galveston, Texas, 1992; pp 95-104.

Lores, E.M., Pennock, J.R. The effect of salinity on binding of Cd, Cr, Cu and Zn to dissolved organic matter. *Chemosphere* **1998**, 37, 861-874.

Mallini, L.J. Development of kinetic-colorimetric flow analysis techniques for determining dissolved manganese and iron and an assessment of the behavior of dissolved manganese in the far-field plume of the Mississippi River. *M.S. Thesis,* University of Southern Mississippi, May 1992.

Martino, M.,Turner, A., Nimmo, M. Distribution, speciation and particle water interactions of nickel in the Mersey estuary, UK. *Mar. Chem.* **2004**, 88, 161–177.

McManus, J., Berelson, W.M.., Klinkhammer, G.P., Hammond, D.E., Holm, C. Authigenic uranium: relationship to oxygen penetration depth and organi carbon rain. *Geochim. Cosmochim. Acta* **2005**, 69, 95-108.

Miller, C.A., Peucker-Ehrenbrink, B., Walker, B.D. Marcantonio, F. Re-assessing the surface cycling of molybdenum and rhenium. *Geochim. Cosmochim. Acta* **2011**, 75, 7146-7179.

Millward, G.E., Moore, R.M. The adsorption of Cu, Mn and Zn by iron oxyhydroxide in model estuarine solutions. *Wat. Res.* **1982**, 16, 981-985.

Moffett, J.W., Ho, J. Oxidation of cobalt and manganese in seawater via a common microbially catalyzed pathway. *Geochim. Cosmochim. Acta* **1996**, 60, 3415-3424.

Moore, W. S., Krest, J. Distribution of ^{223}Ra and ^{224}Ra in the plumes of the Mississippi and Atchafalaya Rivers and the Gulf of Mexico. *Mar. Chem.* **2004**, 86, 105-119.

Morford, J.L., Emerson, S.R., Breckel, E.J., Kim S.H. Diagenesis of oxyanions (V, U, Re, and Mo) in pore waters and sediments from a continental margin. *Geochim. Cosmochim. Acta* **2005**, 69, 5021-5032.

Morford, J.L., Martic, W.R., Francois, R. Carney, C.M. A model for uranium, rhenium, and molybdenum diagenesis in marine sediments based on results from coastal locations. *Geochim. Cosmochim. Acta* **2009**, 73, 2938-2960.

Morford, J.L., Martic, W.R., Kalnejais, L.H., Francois, R., Bothner, M., Karle, I.-M. Insights on geochemical cycling of U, Re and Mo from seasonal sampling in Boston Harbor, Massachusetts, USA. *Geochim. Cosmochim. Acta* **2007**, 71, 895-917.

Pakulski, J.D., Benner, R., Whitledge, T., Amon, R., Eadie, B., Cifuentes, L., Ammerman, J., Stockwell, D. Microbial Metabolism and Nutrien Cycling in the Mississippi and Atchafalaya River Plumes. *Estuar. Coast. Shelf Sci.* **2000**, 50, 173-184.

Petersen, W., Wallman, K., Pinglin, L., Schroeder, F., Knauth, H.D. Exchange of trace elements at the sediment-water interface during early diagenesis processes. *Mar. Freshwater Res.* **1995**, 46, 19-26.

Powell, R.T., Landing, W.M., Bauer, J.E. Colloidal trace metals, organic carbon and nitrogen in a southeastern U.S. estuary. *Mar. Chem.* **1996**, 55, 165-176.

Powell, R.T., Wilson-Finelli, A. Importance of organic Fe complexing ligands in the Mississippi River plume. *Estuar. Coas. Shelf Sci.* **2003**, 58, 757–763.

Prange, A., Kremling, K. Distribution of dissolved molybdenum, uranium and vanadium in Baltic Sea waters. *Mar. Chem.* **1985**, 16, 259 – 274.

Rabalais, N.N., Diaz, R.J., Levin, L.A., Turner, R.E., Gilbert, D., Zhang, J. Dynamics and distribution of natural and human-caused hypoxia. *Biogeosciences* **2010**, 7, 585-619.

Rahaman, W., Singh, S.K. Rhenium in rivers and estuaries of India: sources, transport and behavior. *Mar. Chem.* **2010**, 118, 1–10.

Richard, F.C., Bourg, A.C.M. Aqueous geochemistry of chromium: a review. *Wat. Res.* **1991**, 25, 807-8016.

Roitz, J.S., Flegal, A.R., Bruland, K.W. The biogeochemical cycling of manganese in San Francisco Bay: temporal and spatial variations in surface water concentrations. *Estuar. Coas. Shelf Sci.* **2002**, 54, 227-239.

Saito, M.A., Moffett, J.W. Complexation of cobalt by natural organic ligands in the Sargasso Sea as determined by a new high-sensitivity electrochemical cobalt speciation method suitable for open ocean work. *Mar. Chem.* **2001**, 75, 49-68.

Santos-Echeandia, J., Prego, R., Cobelo-Garcia, A., Millward, G.E. Porewater geochemistry in a Galician Ria (NW Iberian Peninsula): Implications for benthic fluxes of dissolved trace elements (Co, Cu, Ni, Pb, Zn). *Mar. Chem.* **2009**, 117, 77-87.

Sarin, M.M., Church, T.M. Behaviour of uranium during mixing in the Delaware and Chesapeake estuaries. *Estuar. Coast. Shelf Sci.* **1994**, 39, 619-631.

Shaw, T.J., Gieskes, J.M., Jahnke, R.A. Early diagenesis in differing depositional environments: The response of transition metals in pore water. *Geochim. Cosmochim. Acta* **1990**, 54, 1233-1246.

Shen, Y., Fichot, C.G., Benner, R. Floodplain influence on dissolved organic matter composition and export from the Mississippi-Atchafalaya River system to the Gulf of Mixico. *Limnol. Oceanogr.* **2012**, 57, 1149-1160.

Shiller, A.M., Boyle, E.A., 1987. Dissolved vanadium in rivers and estuaries. *Earth Planet. Sci. Lett.* **1987**, 86, 214-224.

Shiller, A.M. Comparison of nutrient and trace element distributions in the delta and shelf outflow regions of the Mississippi/Atchafalaya River. *Estuaries* **1993**a, 16, 541-546.

Shiller, A.M. A mixing rate approach to understanding nutrient distributions in the plume of the Mississippi River. *Mar. Chem.* **1993**b, 43, 211-216.

Shiller, A.M. Dissolved trace elements in the Mississippi River: seasonal, interannual, and decadal varaibility. *Geochim. Cosmochim. Acta* **1997**, 61, 4321–4330.

Shiller, A.M. Seasonality of dissolved rare earth elements in the lower Mississippi River. *Geochem. Geophys. Geosyst.* **2002**, 3, 1-14.

Shiller, A.M. Syringe filtration methods for examining dissolved and colloidal trace element distributions in remote field locations. *Environ. Sci. Technol.* **2003**, 37, 3953 - 3957.

Shiller, A.M., Mao, L. Dissolved vanadium on the Louisiana Shelf: effect of oxygen depletion. *Cont. Shelf Res.* **1999**, 19, 1007-1020.

Shiller, A.M., Stephens, T.H. Microbial manganese oxidation in the lower Mississippi River: methods and evidence. *Geomicrobiol. J.* 2005, 22, doi:10.1080/01490450590945924.

Shiller, A.M., Boyle, E.D. Trace elements in the Mississippi River delta outflow region: Behavior at high discharge. *Geochim. Cosmochim. Acta* **1991**, 55, 3241–3251.

Shim, M-J., Swarzenski, P.W., Shiller, A.M. Dissolved and colloidal trace elements in the Mississippi River delta outflow after Hurricanes Katrina and Rita. *Cont. Shelf Res*. **2012**, 42, 1-9.

Sholkovitz, E.R. The flocculation of dissolved Fe, Mn, Cu, Ni, Co, and Cd during estuarine mixing. *Earth Planet. Sci. Lett.* **1978**, 41, 77–86.

Stolpe, B., Guo, L., Shiller, A.M., Hassellov, M. Size and composition of colloidal organic matter and trace elements in the Mississippi River, Pearl River and the northern Gulf of Mexico, as characterized by flow field-flow fractionation. *Mar. Chem.* **2010**, 118, 119–128.

Sunda, W.G., Huntsman, S. Relationships among growth rate, cellular manganese concentrations, and manganese transport kinetics in estuarine and oceanic species of the diatom Thalassiosira. *J. Phycol.* **1986**, 22, 259-270.

Sunda, W.G., Huntsman, S. Interrelated influence of iron, light, and cell size on marine phytoplankton growth. *Nature* **1997**, 390, 389-392.

Sunda, W.G., Huntsman, S.A. Microbial oxidation of manganese in a North Carolina estuary. *Limnol. Oceanogr.* **1987**, 32, 552-564.

Sundby, B., Silverberg, N. Pathways of manganese in an open estuarine system. *Geochim. Cosmochim. Acta* **1981**, 45, 293-307.

Swarzenski, P.W., McKee, B.A. Seasonal uranium distribution in the coastal waters off the Amazon and Mississippi Rivers. *Estuaries* **1998**, 21, 379–390.

Takata, H., Aono, T., Tagami, K., Uchica, S. Processes controlling cobalt distribution in two temperate estuaries, Sagami Bay and Wakasa Bay, Japan. *Estuar. Coast. Shelf Sci.* **2010**, 89, 294-305.

Takematsu, N., Sato, Y., Okabe, S. and Nakayama, E. The partition of vanadium and molybdenum between manganese oxides and sea water. *Geochim. Cosmochim. Acta* **1985**, 49, 2395-2399.

Tovar-Sanchez, Sanudo-Wilhelmy, S., Flegal, A.R. Temporal and spatial variations in the biogeochemical cycling of cobalt in two urban estuaries: Hudson River Estuary and San Francisco Bay. *Estuar. Coast. Shelf Sci.* **2004**, 60, 717-728.

Turner, A., Nimmo, M., Thuresson, K.A. Speciation and sorptive behavior of nickel in an organic-rich estuary (Beaulieu, UK). *Mar. Chem*. **1998**, 63, 105-118.

van Geldern, R., Barth, J.A.C. Optimization of instrument setup and post-run corrections for oxygen and hydrogen stable isotope measurements of water by isotope ratio infrared spectroscopy (IRIS). *Limnol. Oceanogr.:Methods* **2012**, 10, 1024-1036.

Waeles, M., Riso, R.D., Corre, P.L. Seasonal variations of dissolved and particulate copper species in estuarine waters. *Estuar. Coast. Shelf Sci.* **2005**, 62, 313-323.

Walker, N.D., Hammack, A.D. Impacts of winter storms on circulation and sediment transport: Atchafalaya-Vermilion Bay region, Louisiana, U.S.A. *J. Coastal Res.* **2000**, 16, 996-1010.

Wang, W-X., Guo, L. Bioavailability of colloid-bound Cd, Cr, and Zn to marine plankton. *Mar. Ecol. Prog. Ser.* **2000**, 202, 41-49.

Wand, W.-X., Dei, R.C.H. Influences of phosphate and silicate on Cr(VI) and Se(IV) accumulation in marine phytoplankton. *Aquat. Toxicol.* **2001**, 52, 39-47.

Wang, D., Sanudo-Wilhelmy, S.A. Vanadium speciation and cycling in coastal waters. *Mar. Chem.* **2009**, 11, 52–58.

Wen, L.S., Shiller, A., Santschi, P.H., Gill, G. Trace Element Behavior in Gulf of Mexico Estuaries. In *Biogeochemistry of Gulf of Mexico Estuaries*, T.S. Bianchi, J.R. Pennock, and R.R. Twilley, eds., J. Wiley & Sons, New York, 1999, Chpt. 10, pp. 303-346.

Wu, J., Boyle, E.A. Low blank preconcentration technique for the determination of lead, copper, and cadmium in small volume seawater samples by isotope dilution ICP MS. *Anal. Chem.* **1997**, 69, 2464–2470.

Xiong, Y. Solubility and speciation of rhenium in anoxic environments at ambient temperature and applications to the Black Sea. *Deep-Sea Res. I* 2003, 50, 681-690.

Yang, M.Y., Sanudo-Wilhelmy, S.A. Cadmium and manganese distributions in the Hudson River estuary: interannual and seasonal variability. *Earth Planet. Sci. Lett.* **1998**, 160, 403-418.

Yeats, P.A. The distribution of dissolved vanadium in eastern Canadian coastal waters. *Estuar. Coast. Shelf Sci.* **1992**, 34, 85–93.

CHAPTER III

DISSOLVED BARIUM BEHAVIOR IN LOUISIANA SHELF WATERS AFFECTED BY THE MISSISSIPPI/ATCHAFALAYA RIVER MIXING ZONE

Introduction

Barium is an important ocean geochemical tracer that has been used in several specific ways: a) as a paleo-productivity tracer in the form of barite preserved in marine sediments (e.g., Dymond et al., 1992), b) as an indicator of paleoceanographic changes in ocean circulation as recorded in the Ba/Ca ratio of benthic foraminifera (Lea and Boyle, 1989), c) as a stable analogue for radium (Chan et al., 1976), and d) as a tracer of fresh water influence in the coastal ocean both through direct measurement of seawater concentrations (Guay and Falkner, 1997, 1998) as well as by proxy measurement of Ba/Ca ratios in corals (Alibert et al., 2003) and foraminifera (Williams et al., 2010). The use of Ba as a coastal fresh water indicator has also been applied to fisheries research, wherein changes in Ba/Ca ratios in fish otoliths help reveal migration and spawning patterns (e.g., Thorrold et al., 1997).

In order to fully exploit Ba as a coastal fresh water tracer, it is necessary to understand the fresh water source composition, how this composition might be changed in the estuarine environment, and what might be the temporal variability of the input as well as of the influencing estuarine processes. In rivers, geology (i.e., rock type) appears to be the major influence on dissolved Ba concentrations (Dalai et al., 2002) with changes in tributary flow contributions being an important control on seasonal variability in Ba concentrations in a large floodplain river (Shiller, 1997).

* This chapter of the dissertation has been submitted for publication to Geochimica et Cosmochimica Acta: Joung, D.J. and Shiller, A.M. Dissolved barium behavior in Louisiana Shelf waters affected by the Mississippi/Atchafalaya River Mixing Zone.

In estuaries, Hanor and Chan (1977) first reported non-conservative behavior of Ba, which they attributed to Ba desorption from clays. This desorption was experimentally confirmed via sediment desorption experiments (Li and Chan 1979) and seawater-fresh water mixing experiments (Li et al., 1984). While salinity-induced desorption may be the dominant process affecting the dissolved Ba flux through estuaries (Coffey et al., 1997), it is not the only process that can affect this element's distribution. In particular, there can be seasonal productivity-related depletion of Ba (Stecher and Kogut, 1999; Guay and Falkner, 1998), and there is some evidence suggesting removal associated with co-precipitation in Fe oxyhydroxides and subsequent flocculation of this material (Coffey et al., 1997). Perhaps of more importance in coastal and estuarine environments is the influence of benthic inputs, either from submarine groundwater discharge (Shaw et al., 1998), benthic dissolution of marine barite (Colbert and McManus, 2005; Falkner et al., 1993), or desorption from river sediments deposited at high discharge in estuarine swamps/marshes (Carroll et al., 1993).

Herein, studies of the dissolved Ba distribution in the mixing zone of the Mississippi River (MR) and the Atchafalaya River (AR) including Louisiana Shelf waters are reported. The Atchafalaya is a major distributary of the Mississippi River, mandated to contain 30% of the combined flow of the Mississippi and the Red Rivers. While the mainstem of the Mississippi River enters the northern Gulf of Mexico through a birdfoot delta that extends to nearly the shelf break, the Atchafalaya enters the Gulf through a broad shallow bay. Thus, nearly the same river endmember mixes with seawater in two very different physiographic areas (Shiller, 1993). Furthermore, the Louisiana Shelf, where much of the extended mixing of these river waters takes place, is a region of high

primary productivity and seasonal bottom water hypoxia, resulting from high anthropogenic fluvial nutrient fluxes combined with significant vertical stratification (Rabalais et al., 2010). This region therefore serves as a unique testbed to examine estuarine Ba geochemistry, and our results may be pertinent to the interpretation of foraminiferal Ba/Ca ratios as a proxy for meltwater input to the northern Gulf (e.g., Williams et al., 2010).

Methods and Materials

The sample collection was conducted on the Louisiana Shelf including the MR and the AR plumes during three cruises in May and November 2008, and June/July 2009, which represent high, low, and intermediate Mississippi River water discharges, respectively (Figures. 11, 12, Appendix). Samples were also collected from the Atchafalaya River Basin (ARB) including the Red River (RR), Mississippi River (Knox Landing), and swamp waters. The ARB sampling campaigns were conducted in April and November 2010 and in June 2011, which represent intermediate, low, and high river discharges.

Samples were collected at different depths on the shelf, but only surface samples were taken in the lowest salinity regions of the two river plumes. For May and November 2008, surface waters were taken using a clean underway pumping system that was driven by an air-powered plastic diaphragm pump. Acid-cleaned Teflon-lined polyethylene tubing was attached to a non-metallic tow-fish which was towed just below the surface, several meters off the side of the ship. Water from this system was sampled in a small plastic enclosure in the ship's lab. These surface water samples were taken after flushing the pumping system about 10 minutes while the ship was moving. During June/July 2009,

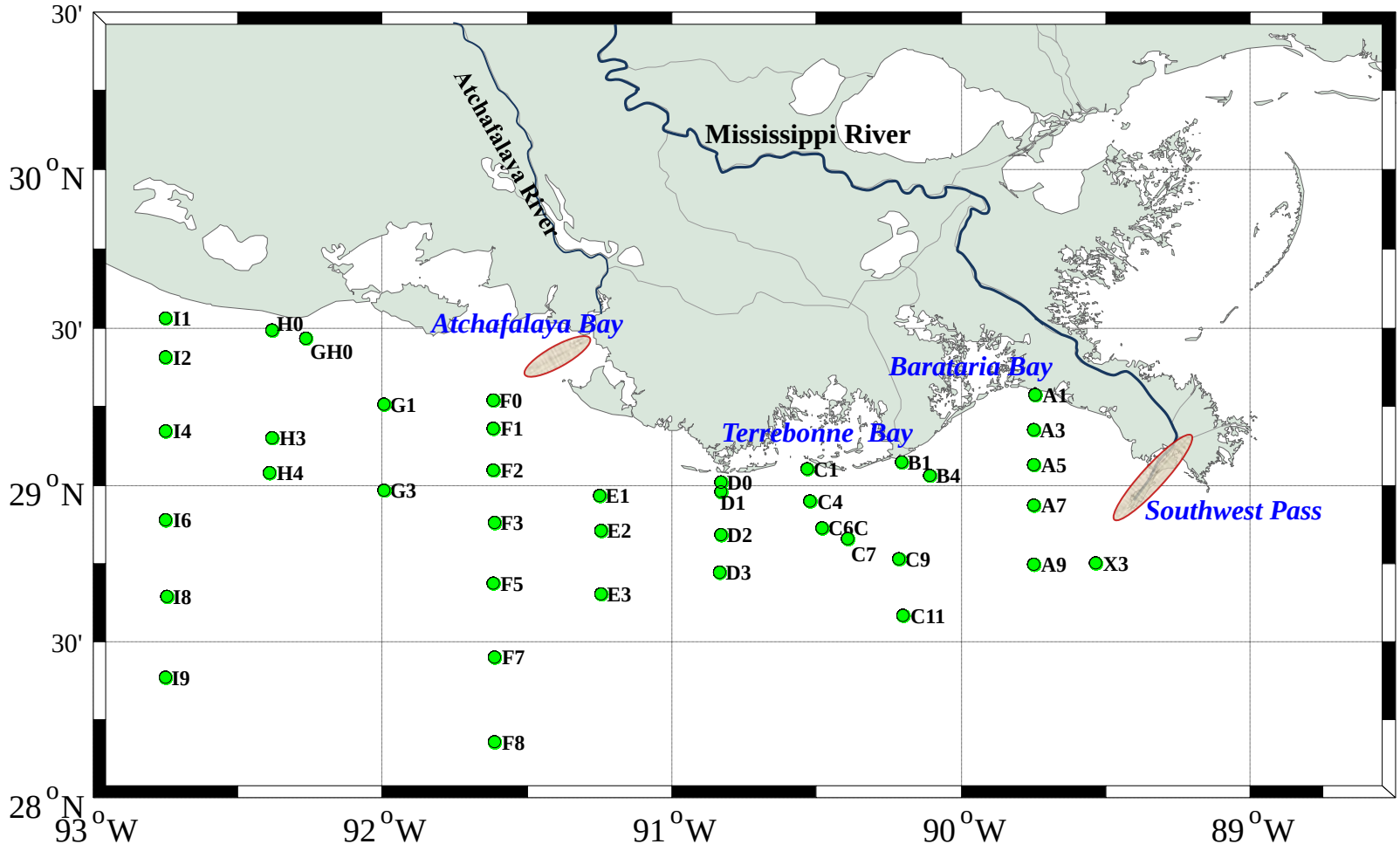

Figure 11. Louisiana Shelf sampling stations during May 2008, November 2008, and June/July 2009. Shaded areas by Southwest Pass and Atchafalaya Bay show the general location of low salinity sampling (see, Appendix and Tables 1-3 for specific locations).

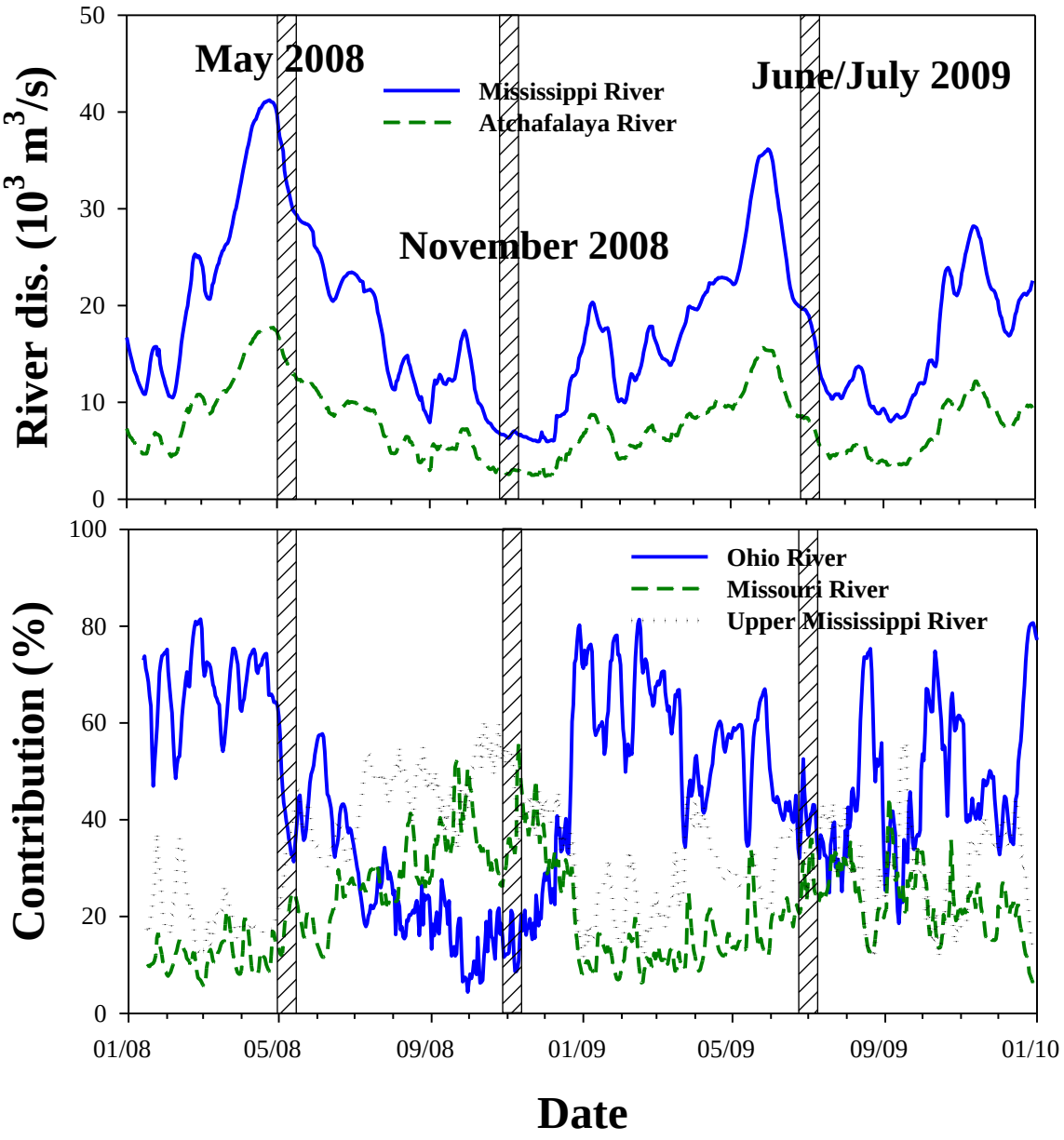

Figure 12. River discharges and relative contributions of Mississippi River tributaries to the total discharge.

the surface samples were collected using a grab sampler which consisted of a non-metallic PVC pole with polycarbonate bottle holder attached at the end of the pole. This sampling was also carried out while the ship was slowly moving. For deep water samples, acid-cleaned Teflon-coated tubing was attached to a non-metallic cable holding an epoxy-coated weight at the end, and this tube was connected to the same pump system as

the surface water collection. This pumping system was used to collect deep water samples during the first cruise. For the two later cruises, an external spring, Teflon-coated Niskin bottle was used. The Niskin bottle was mounted on a PVC frame extending ~1 m below the bottle and automatically closed the bottle when the frame hit the bottom.

Soon after the water samples were collected, the samples were filtered using acid-cleaned 25 mm x 0.45 μm pore size polyethylene (Whatman Puradisc PP) and 25 mm x 0.02 μm pore size alumina (Whatman Anotop) syringe filters, providing us with operationally-defined *total* and *truly dissolved* fractions, respectively. The colloidal phase (0.02 – 0.45 μm) was defined by the difference between the two fractions. Details of the sample processing can be found elsewhere (Shiller, 2003). The filtered water samples were brought to our shore-based clean lab and acidified to pH < 2 by adding 70 μl and 140 μl of 6 M ultrapure hydrochloric acid (Seastar Baseline) for the 15 ml and 30 ml samples, respectively.

Barium was determined with a high resolution inductively coupled plasma mass spectrometer (HR-ICP-MS, ThermoFisher Element 2) using an isotope dilution method (Shim et al., 2012). In this study, Ba was calibrated by adding a known amount of ^{135}Ba enriched isotopic spike obtained from Oak Ridge National Laboratory and measuring the $^{135/138}$Ba ratio. Samples were diluted 20-fold by the addition of 0.3 M of ultrapure dilute nitric acid (Seastar Baseline) prior to analysis. For verifying the accuracy of analysis, the certified reference seawater NASS-5 (NRC-Canada) was measured during all analytical runs. Our NASS-5 result (37.3 ± 1.1 nM, n=40) agrees well with previous results (37.0 nM, Field et al., 2007 and 37.5 nM, Shim et al., 2012). The detection limit of the method was estimated to be 1.2 nM.

Mixing experiments were conducted at sea using river water and seawater. Unfiltered river water and seawater were mixed in varying proportions and held in the dark for overnight, with the ship's motion providing constant sample mixing. The mixed samples were filtered in the same way as the field samples. The lowest salinity waters we obtained from the MR and the AR were used as the river endmembers. The MR mixing experiment was conducted only during June/July 2009.

Ancillary data such as salinity, temperature, and dissolved oxygen (DO) were obtained from instruments mounted on the ship's CTD-rosette system. The DO sensor calibration was calibrated by Winkler titrations. The oxygen isotope composition of the water was measured using isotope ratio infrared spectroscopy (L2120i cavity ringdown spectrometer, Picarro, Inc.), and the raw isotope data correction and calibration were made using the method of van Geldern and Barth (2012).

The Mississippi River discharge was obtained from the U.S. Army Corps of Engineers discharge records from the gage at Tarbert Landing, MS (http://rivergages.mvr.usace.army.mil). This gage is below the diversion of water into the Atchafalaya River. Major tributary contributions to the mainstem flow were estimated from USGS discharge data from the Ohio River at Metropolis, IL, the Missouri River at Hermann, MO, and the Mississippi River at Grafton, IL for Ohio, Missouri, and Upper Mississippi Rivers, respectively (http://water.usgs.gov). To adjust approximately for the travel time of water from these tributaries to the sampling sites, about 15 days and 12 days were applied for the Upper Mississippi and Missouri Rivers and the Ohio River, respectively. These travel times were adjusted by adding 2 days to the times used by Shiller (1997) in consideration of the extended distance from Baton Rouge to the birdfoot

delta. For the Atchafalaya River Basin, discharges were also obtained from the US Army Corps of Engineers from the gages at Simmesport, Acme, Alexandria, Wax Lake, and Morgan City, LA.

Mississippi River discharge and major tributary contributions to the river are shown in Figure 2. During May 2008, the MR discharge from the gage at Tarbert Landing, MS, was about 35×10^3 m^3/sec while this was about 8×10^3 and 15×10^3 m^3/sec during November 2008 and June 2009, respectively. Note that the Tarbert Landing gage is below the Old River Control Structure (where some MR water is diverted into the AR) and thus represents approximately 70% of the total flow of the river. During the high discharge sampling (May 2008), the MR mainstem was dominated by contributions from the Ohio River. However, the Upper Mississippi and Missouri Rivers were the primary MR contributors during low river discharge (November 2008), and all three tributaries had very similar contributions during the intermediate discharge period (June/July 2009).

Results and Discussion

Results from the three field surveys are shown in Tables 2-4 and for the mixing experiments in Table 5. Concentrations of Ba in the <0.02 µm and <0.45 µm filtrates were almost always within analytical error of each other. That is, there was no significant colloidal Ba, at least by the definition of the colloidal phase we use here (0.02 - 0.45 µm). Thus, only the fraction <0.45 µm results are focused.

Surface water Ba distributions and the associated mixing experiments (Figure 13, Appendix) show some distinct as well as subtle differences between our three sampling campaigns. During high discharge (May 2008), there is obvious, non-conservative behavior at lower salinities in the immediate vicinity of the mouths of both the MR and

Table 2

Results from May 2008. (units: µmol/kg for DO, mg/kg for SPM, µg/kg for Chl a, nmol/kg for Ba)

	Date	Bot.	Sam. (m)	Lat.	Lon.	S	Tem. (°C)	DO	SPM	Chl a	Ba 0.45*	Ba 0.02*	$\delta^{18}O$ (‰)
X3	5/1/08	90	0	28.758	89.537	22.3	22.8	245.2	4.1	5.0			
			80			36.5	20.1	170.1		0.2			
MR1	5/1/08	0	0	28.778	89.525	11.0			143.6	2.1	391	392	-3.9
MR2	5/2/08	0	0	28.850	89.467	11.9			6.3		393	386	-3.7
MR3	5/2/08	0	0	28.898	89.434	2.0					483	473	-5.7
MR4	5/2/08	0	0	28.894	89.433	0.8					451	438	-5.9
MR5	5/2/08	0	0	28.903	89.433	0.6					426	419	-6.0
MR6	5/2/08	0	0	28.927	89.414	0.1					393	370	-6.2
A9	5/2/08	82	0	28.751	89.750	28.0	23.1	419.6	1.9	14.0	139	137	-0.5
			20			30.0	23.1	325.3	2.1		139	136	-0.5
			70			36.5	20.4	206.6	2.5	0.4	66	64	1.1
A7	5/2/08	50	0	28.945	89.760	15.6	22.7	192.3	3.4	22.2	321	315	-3.0
			18			32.7	22.3	160.9			100	99	0.3
			45			36.3	20.9	139.3	1.4	0.5	86	89	1.1
A5	5/2/08	30	0	29.074	89.757	17.1	23.3	597.9	4.3	38.8	294	290	-2.7
			15			36.0	22.9	311.4			65	59	1.1
			26			36.2	22.3	198.4		0.6	65	62	1.1
A3	5/2/08	17	0	29.186	89.758	16.5	24.0	542.8	6.3	29.7	296	290	-2.8
			14			33.8	21.9	48.6		1.4	133	134	0.5
A1	5/3/08	5	0	29.292	89.753	6.4	22.8	428.6	12.6	7.7	400	396	
			4			7.9	23.3	461.5		11.1	360	353	
C1	5/3/08	5	0	29.057	90.532	17.4	23.8	329.4	27.1	26.0	297	293	-2.7
			3.5			17.4	23.8	325.8		38.5			
C4	5/3/08	13	0	28.951	90.533	17.7	23.8	336.0	5.0	30.5	300	297	
			6			27.3	23.3	279.1	5.8		173	173	-0.8
			11.5			33.0	23.1	121.9	11.5	5.9	123	121	
C6	5/3/08	20	0	28.843	90.497	18.4	23.3	267.0	3.0	18.5	274	275	-2.2
			8			33.8	23.3	240.5	1.4		87	87	0.7
			18			34.9	22.4	141.3	20.0	1.4	89	90	1.1
C7	5/3/08	20	0	28.827	90.396	18.4	23.8	335.2	1.7	29.6	279	276	-2.3
			10			33.4	23.1	204.0	2.3		116	95	0.6
			20			35.7	22.6	103.5	14.0	1.2	83	83	1.2
C9	5/3/08	27	0	28.768	90.225	24.0	23.8	304.2	1.8	16.2	190	190	-1.2
			10			34.8	23.2	218.5	0.4		80	81	0.8
			27			36.1	21.9	96.6	6.2	0.7	77	77	1.0
C11	5/4/08	51	0	28.587	90.207	32.4	23.4	244.3	1.4	6.1	110	110	
			18			36.3	23.2	209.6	1.3		68	67	1.0
			49			36.5	20.4	173.1	2.4	0.2	58	60	

Table 2 (continued).

	Date	Bot. (m)	Sam. (m)	Lat.	Lon.	S	Tem. (°C)	DO	SPM	Chl a	Ba 0.45*	Ba 0.02*	$\delta^{18}O$ (‰)
F0	5/3/08	3.5	0	29.275	91.618	13.8	22.8	202.2	28.2	6.6			
			2.2			17.8	24.0	187.0	25.2	9.1	302	305	-1.8
AR1	5/4/08	0	0	29.400	91.362	0.1					480	466	
AR2	5/4/08	0	0	29.323	91.429	2.2					544	544	-4.8
AR3	5/4/08	0	0	29.303	91.497	4.4					568	555	-4.4
AR4	5/4/08	0	0	29.299	91.517	5.8					586	591	-4.2
AR5	5/4/08	0	0	29.295	91.542	7.1					562	565	-4.0
AR6	5/4/08	0	0	29.293	91.551	9.1					529	533	-3.8
AR7	5/4/08	0	0	29.275	91.618	8.6					464	465	-3.8
AR8	5/4/08	0	0	29.277	91.632	7.2					477	483	-4.1
F2	5/4/08	8.4	0	29.517	91.620	21.9	24.7	258.8	3.6	8.7	238	248	-1.5
			6			25.5	23.6	182.2	5.3	16.5	208	209	-1.0
F3	5/5/08	20	0	28.887	91.618	27.3	24.6	275.4	5.1	7.3	190	194	
			10			33.4	23.2	181.1	4.3		123	123	0.3
			19			35.1	22.8	49.2	22.6	3.5	103	104	
F5	5/5/08	30	0	28.699	91.621	31.7	23.7	204.5	8.8	3.4	140	126	0.2
			10			35.2	22.5	147.2	1.4		80	75	1.1
			28			36.2	21.9	90.2	8.8	0.5	77	77	1.2
F7	5/5/08	57	0	28.451	91.619	36.4	23.3	174.2	2.2	0.1	65	55	1.2
			28			36.4	22.5	178.4	1.1		63	56	1.2
			52			36.5	21.1	147.8	4.4	2.2	71	70	1.2
F8	5/5/08	82	0	28.178	91.620	36.4	23.6	173.7	0.3	0.1	64	56	1.2
			28			36.4	23.0	176.8	2.3		54	56	1.1
			82			36.5	19.9	137.8	4.8	0.9	71	70	1.3
I9	5/6/08	57	0	28.384	92.753	36.0	23.3	175.9	3.0	0.1	60	59	
			28			36.4	22.0	180.5	1.2		56	56	1.2
			54			36.5	20.2	163.0	3.2	1.5	90	74	
I8	5/6/08	37	0	28.648	92.759	36.4	22.9	176.6	1.8	0.1	55	55	1.2
			15			36.4	22.9	176.0	0.6		55	56	1.3
			34			36.5	21.9	159.7	1.5	1.5	66	62	1.3
I6	5/6/08	28	0	28.889	92.762	35.0	23.0	221.6	3.0	1.3	73	74	1.1
			13			35.8	22.9	217.7	2.4		75	69	1.1
			26			36.3	22.6	213.8	7.3	1.2	65	60	1.2
I4	5/6/08	20	0	29.031	92.761	33.7	23.6	232.3	15.8	2.4	88	89	0.5
			12			34.8	23.2	222.7	2.1		81	80	0.8
			19			36.0	22.8	194.4	2.7	1.1	67	66	1.2
I2	5/6/08	15	0	29.413	92.751	24.9	24.3	277.3	1.8	12.8	209	206	-1.1
			7			25.1	23.7	236.9	5.3		211	210	-1.1
			13.5			30.0	23.2	85.4	4.1	4.7	177	174	-0.3
I1	5/6/08	11	0	29.536	92.754	13.5	24.4	260.1	3.3	6.8	360	359	-3.0
			9.5			28.1	23.0	117.1	2.1	2.0	185	183	-0.5

Table 2 (continued).

	Date	Bot. (m)	Sam. (m)	Lat.	Lon.	S	Tem. (°C)	DO	SPM	Chl a	Ba 0.45*	Ba 0.02*	$\delta^{18}O$ (‰)
H3	5/7/08	14	0	29.167	92.403	25.3	24.8	287.9	4.5	14.4	204	202	-1.1
			9			31.5	23.3	95.4	3.9		158	153	-0.2
			15			34.3	23.4	141.9	1.8	4.0	93	92	0.8
H4	5/7/08	22	0	29.040	92.391	34.3	24.2	234.1	2.1	1.6	81	82	0.7
			20			35.8	22.7	168.0	1.9	1.2	71	70	1.1
G3	5/7/08	21	0	28.974	92.007	32.5	23.8	220.5	2.2	3.8	104	100	0.4
			10			34.1	23.6	205.4	2.6		82	81	0.8
			19			35.8	23.0	137.8	5.3	1.0	83	82	1.1
F3(2)	5/7/08	20	0	28.893	91.623	29.9	24.1	252.7	3.8		148	149	-0.1
			11			32.0	23.9	223.2	2.3		113	112	0.4
			19			32.8	22.9	48.9	5.7		112	107	0.7
E2	5/7/08	16	0	28.745	91.254	32.3	24.3	254.2	1.5	3.7	115	103	0.5
			14			34.7	23.3	154.7	2.0	4.5	104	102	0.8
D3	5/8/08	18	0	28.725	90.837	35.3	23.9	199.0	1.5	0.7	65	66	1.1
			15			35.4	23.7	198.7	2.3	0.8	65	64	1.2
B4	5/8/08	16	0	29.035	90.120	15.4	24.0	265.9		6.5	322	324	-2.9
			0			15.4	24.0	265.9	2.0		318	321	-3.0
			9.5			28.9	22.6	186.7	1.2		154	153	-0.4
			15			35.2	22.3	29.5	1.9	0.7	103	102	0.9

Abbreviation: Bot.: bottom depth, Sam.: sampling depth, Lat.: latitude, Lon.: Longitude, S: salinity, Tem.: temperature, DO: dissolved oxygen, SPM: suspended particulate matter, Chl a: chlorophyll a.

*: < 0.45 µm and < 0.02 µm.

AR, with conservative behavior at higher salinities. The mixing experiment at that time likewise shows low-salinity non-conservative behavior suggestive of Ba desorption from the suspended load as previously reported for this system by Hanor and Chan (1977). Also, the fluvial endmember Ba concentration for the AR is nearly 100 nM higher than for the MR, though the desorption humps for both distributaries are similar in magnitude as is the salinity of maximum Ba.

During low discharge (November 2008), the field data show apparent non-conservative behavior somewhat different from the high discharge distribution. While

Table 3

Results from November 2008. (units: µmol/kg for DO, mg/kg for SPM, µg/kg for Chl a, nmol/kg for Ba)

	Date	Bot. (m)	Sam. (m)	Lat.	Lon.	S	Tem. (°C)	DO	Chl a	Ba 0.45*	Ba 0.02*	$\delta^{18}O$ (‰)
X3	10/31/08	95	0	28.758	89.537	34.6	23.4	211	3.3	199	201	0.1
			20			34.8	25.0	187		82	89	1.0
			94			35.2	18.3	118	0.2	50	50	1.0
MR1	10/31/08	0	0	28.782	89.525	25.6				255	253	-0.8
MR2	10/31/08	0	0	28.796	89.506	23.7				289	286	-1.3
MR3	10/31/08	0	0	28.815	89.500	20.5				326	324	-1.8
MR4	10/31/08	0	0	28.872	89.456	17.7				347	377	-2.2
MR5	10/31/08	0	0	28.893	89.438	10.9				455	454	-3.6
MR6	10/31/08	0	0	28.906	89.432	8.0				490	481	-4.3
MR7	10/31/08	0	0	28.908	89.429	7.0				498	495	-4.7
MR8	10/31/08	0	0	28.999	89.422	5.8				512	509	-4.8
MR9	10/31/08	0	0	28.926	89.415	4.9				524	522	-5.0
MR10	10/31/08	0	0	28.969	89.383	4.3				537	534	-5.1
MR11	10/31/08	0	0	29.018	89.344	3.1				545	538	-5.4
MR12	10/31/08	0	0	29.058	89.313	2.2				553	548	-5.5
MR13	10/31/08	0	0	29.202	89.281	1.0				568	551	-5.7
MR14	10/31/08	0	0	29.272	89.349	0.8				568	557	-5.7
A1	11/1/08	7	0	29.287	89.752	30.0	21.2	227	5.9	173	182	0.3
			6			31.6	21.3	223	6.0	184	201	0.5
A3	11/1/08	16	0	29.170	89.762	30.6	21.9	233	4.4	175	169	0.2
			8.3			31.8	22.6	217		144	142	0.4
			16			33.3	26.3	79	1.1	107	118	0.8
A5	11/1/08	30	0	29.067	89.752	31.9	22.7	230	3.8	139	139	0.3
			12			32.0	22.7	225		137	141	0.2
			29			35.0	26.1	111	0.8	94	96	0.7
A7	11/1/08	47.5	0	28.937	89.758	29.0	22.1	257	5.8	185	203	-0.2
			9.8			31.0	22.4	226		159	173	0.1
			46			35.4	26.3	137	0.3	75	79	0.9
A9	11/1/08	83	0	28.744	89.776	32.0	23.7	228	4.0	155	164	0.1
			20			34.4	27.6	203		78	83	0.8
			82			36.4	18.9	118	0.3	48	48	1.0
C11	11/2/08	52	0	28.576	90.214	35.4	25.2	188	0.3	67	71	1.3
			19.8			35.4	25.1	191		65	69	1.0
			48			36.2	23.4	148	0.2	58	57	1.0
C9	11/2/08	31	0	28.763	90.225	33.9	24.1	207	3.2	99	105	0.8
			15.3			34.5	25.0	164		92	97	0.8
			28			35.3	25.8	151	1.0	85	84	1.0

Table 3 (continued).

	Date	Bot. (m)	Sam. (m)	Lat.	Lon.	S	Tem. (°C)	DO	Chl a	Ba 0.45*	Ba 0.02*	$\delta^{18}O$ (‰)
C7	11/2/08	21	0	28.830	90.395	33.5	23.7	211	3.3	103	108	0.7
			10			33.5	23.7	211		110	107	0.6
			18			33.7	23.9	172	2.8	107	107	0.8
C6	11/2/08	20	0	28.860	90.498	34.0	23.5	202	1.2	102	104	0.8
			16.5			34.1	23.6	198	1.4	123	130	1.0
C4	11/2/08	13	0	28.943	90.533	31.5	22.2	207	2.3	140	154	0.5
			10.5			33.0	23.3	175	1.3	142	140	0.6
C1	11/2/08	5	0	29.055	90.533	29.5	20.5	230	5.5	243	262	0.3
			4			29.7	20.5	217	5.5	263	262	0.2
D3	11/2/08	18	0	28.713	90.839	33.2	23.0	209		131	131	0.6
			17			33.2	23.0	203		127	126	0.8
			0							124	128	0.7
E2	11/3/08	16.5	0	28.743	91.255	33.0	22.7	208		118	129	0.9
			13			33.1	22.7	207		131	138	0.7
F0	11/3/08	3	0	29.784	92.033	7.3	19.1	312	13.0	499	502	-3.6
			2			13.3	19.5	219	5.2	426	429	-2.5
F1	11/3/08	6	0	29.185	91.618	17.2	21.1	269	4.4	380	376	-1.9
			5			27.4	21.1	210	3.4	209	219	-0.1
AR1	11/3/08	0	0	29.626	91.257	0.2	19.1			510	513	-5.4
AR2	11/3/08	0	0	29.377	91.379	2.0	19.7			523	521	-4.8
AR3	11/3/08	0	0	29.334	91.420	3.7	20.6			502	498	-4.4
AR4	11/3/08	0	0	29.325	91.428	5.6	20.6			493	497	-4.3
AR5	11/3/08	0	0	29.311	91.439	7.6	20.7			480	485	-3.9
AR6	11/3/08	0	0	29.293	91.456	9.2	20.9			443	469	-3.1
F2	11/3/08	8	0	29.053	91.619	29.8	21.6	224	1.8	178	184	0.4
			7			29.8	21.6	224	1.9	174	192	0.0
F3	11/4/08	18.5	0	28.884	91.618	30.5	22.0	210	1.3	164	172	0.3
			17.5			30.5	22.7	193	1.2	127	138	0.6
F5	11/4/08	29	0	28.688	91.629	34.2	23.9	186		105	105	0.7
			15.3			34.2	23.9	185		100	102	0.8
			28			34.2	23.9	184		102	102	1.0
F7	11/4/08	52	0	28.449	91.617	35.2	24.7	189	0.8	72	72	1.1
			20.3			35.4	24.9	189		69	75	1.1
			51			35.8	25.6	183	0.4	64	64	1.1
F8	11/4/08	82	0	28.180	91.622	36.5	25.8	189	0.3	52	51	1.2
			30			36.5	25.8	189		55	55	1.2
			81			36.4	25.3	179	0.4	57	58	1.2
I9	11/4/08	56	0	28.392	92.764	35.9	25.3	192	0.2	66	65	1.1
			19.8			36.1	25.4	190		62	62	1.0
			55			36.2	25.3	180	0.8	60	59	1.1

Table 3 (continued).

	Date	Bot.	Sam. (m)	Lat.	Lon.	S	Tem. (°C)	DO	Chl a	Ba 0.45*	Ba 0.02*	$\delta^{18}O$ (‰)
I8	11/5/08	36	0	28.641	92.764	35.2	24.6	191	0.7	76	75	1.1
			20.7			35.4	24.8	193		75	82	1.1
			35			35.5	24.9	191	0.5	76	77	1.0
I6	11/5/08	26	0	28.893	92.762	34.2	23.8	192	0.7	96	106	0.9
			12.1			34.3	23.9	190		103	103	0.9
			25			34.5	24.0	189	0.6	97	98	1.0
I4	11/5/08	19	0	29.181	92.761	32.9	23.0	202	0.9	127	128	0.7
			10.3			32.9	23.0	200		129	131	0.7
			17.5			33.2	23.2	192	0.7	124	127	0.7
I2	11/5/08	14	0	29.411	92.756	29.8	21.8	208	1.3	184	199	0.3
			13			29.7	23.8	123	1.0	202	206	0.3
I1	11/5/08	10	0	29.539	92.759	28.2	21.5	223	1.6	209	207	0.3
			9			29.4	21.3	201	1.0	224	227	0.2
H0	11/5/08	3	0	29.492	92.388	16.6	21.1	249		436	454	-1.9
			2			16.4	21.1	249		464	461	-1.9
GH0	11/6/08	3.5	0	29.470	92.268	18.1	20.8	251		374	362	-1.7
			2.5			31.5	20.8	248		180	184	0.5
E1	11/6/08	5.5	0	28.968	91.252	31.7	21.5	221		224	245	0.4
			4.5			31.3	21.5	221		178	181	0.5
D0	11/6/08	4	0	29.016	90.833	30.0	20.6	226		240	239	0.3
C6(2)	11/6/08	18	0	28.872	90.493	32.8	23.4	223		121	123	0.6
			11.3			33.5	23.9	200		119	118	0.6
			17			33.9	24.2	187		105	106	0.6
C7(2)	11/6/08	20	0	28.837	90.398	34.1	24.4	209		108	106	0.8
			12.3			33.7	24.2	203		96	96	0.8
			19			34.3	24.2	198		94	94	0.8
B4	11/6/08	16	0	29.032	90.111	32.0	23.6	226		180	136	0.4
			15			32.9	23.6	207		126	125	0.6
B1	11/6/08	8	0	29.077	90.208	29.8	22.6	247		168	170	0.0
			7			31.0	22.7	156		168	164	0.1
C1-1	11/7/08	5	0	29.059	90.549	31.2	22.5	219		156	159	0.3
			4			31.2	22.6	219		153	151	0.4
C1W	11/7/08	5	3	29.058	90.533	31.2	22.5	217		153	155	0.3

Abbreviation: Bot.: bottom depth, Sam.: sampling depth, Lat.: latitude, Lon.: Longitude, S: salinity, Tem.: temperature, DO: dissolved oxygen, Chl a: chlorophyll a.

*: < 0.45 μm and < 0.02 μm.

Table 4

Results from June/July 2009. (units: µmol/kg for DO, mg/kg for SPM, µg/kg for Chl a, nmol/kg for Ba)

	Date	Bot. (m)	Sam. (m)	Lat.	Lon.	S	Tem. (°C)	DO	Chl a	Ba		$\delta^{18}O$
										0.45	0.02	(‰)
X3	6/28/09	93	0	28.753	89.534	26.8	30.4	200	0.8	154	151	-0.2
			40			36.3	23.4	192	0.4	63	63	1.2
			92			36.2	16.4	106	0.0	48	48	1.0
MR1	6/28/09	0	0	28.826	89.482	22.1				274	269	-1.2
MR2	6/28/09	0	0	28.837	89.471	18.4				327	324	-2.0
MR3	6/28/09	0	0	28.846	89.462	15.2				391	395	-2.4
MR4	6/28/09	0	0	28.849	89.459	12.7			18.0	452	452	-2.9
MR5	6/28/09	0	0	28.856	89.452	9.2				485	484	-4.0
MR6	6/28/09	0	0	28.862	89.446	6.3				506	502	-4.8
MR7	6/28/09	0	0	28.907	89.431	2.3				560	544	-5.7
MR8	6/28/09	0	0	28.956	89.392	0.6			1.9	573	559	-6.0
A1	6/29/09	6.8	0.3	29.290	89.745	23.5	29.7	142	6.5	286	283	-1.0
A1			5.8			28.7	28.5	129	1.3	231	229	-0.5
A3	6/29/09	15.5	0	29.177	89.751	23.7	30.1	182	5.1	269	265	-1.0
			7			32.8	25.2	64	0.8	175	172	0.0
			16			35.9	24.4	3	0.2	109	109	0.9
A5	6/29/09	31	0	29.068	89.750	24.4	30.0	194	4.8	287	286	-1.5
			13.5			35.7	24.8	116	0.1	91	92	1.0
			20			36.2	24.4	146		67	68	1.0
			30			36.3	22.1	12	0.2	96	96	1.0
A7	6/29/09	50	0	28.940	89.749	24.6	30.6	197	1.7	194	194	-0.7
			20			35.9	24.9	162	0.4	76	76	1.2
			49			36.3	18.9	85	0.2	65	65	1.0
A9	6/29/09	80	0	28.750	89.749	22.9	31.3	200	0.9	208	205	-0.9
			14			35.5	25.6	107		117	116	0.9
			30			36.1	24.7	189	0.1	67	66	1.1
			40			36.3	21.8	119	0.3	74	73	1.1
			79			36.2	16.8	104	0.0	46	45	0.9
C11	6/30/09	52	0	28.587	90.201	22.7	30.3	212	2.1	111	36	-1.1
			30			36.3	21.8	128	0.3	76	76	1.2
			51			36.3	19.3	98	0.1	60	60	1.1
C9	6/30/09	31	0	28.767	90.216	24.6	30.1	224	5.2	79	52	-0.9
			20			36.1	24.5	149	0.2	78	78	1.1
			30			36.3	22.7	73	0.5	83	83	1.0
C7	6/30/09	20.7	0	28.830	90.392	23.6	30.4	237	6.5	235	210	-1.2
			9.5			35.1	24.8	61	1.2	107	107	0.6
			19.7			35.9	24.3	88	1.2	95	94	1.0

Table 4 (continued).

	Date	Bot. (m)	Sam. (m)	Lat.	Lon.	S	Tem. (°C)	DO	Chl a	Ba 0.45	Ba 0.02	$\delta^{18}O$ (‰)
C6	6/30/09	19.7	0	28.866	90.483	20.0	30.6	238	6.4	331	323	-1.8
			10			35.4	25.0	92	1.1	94	95	0.8
			18.7			35.9	24.4	55	0.9	98	97	1.0
C4	6/30/09	13.8	0	28.950	90.523	25.0	30.1	157	8.8	284	281	-0.7
			5.3			31.2	25.6	58	0.5	178	180	-0.1
			12.8			35.8	24.4	24	1.5	102	101	0.9
C1	6/30/09	6.2	0	29.055	90.533	30.4	27.7	181	9.7	219	218	0.0
			5.2			33.7	25.6	12	6.1	184	184	0.5
D2	6/30/09	16.2	0	28.843	90.833	16.0	30.3	223	7.5	377	383	-2.3
			15.2			35.3	24.5	2	0.9	132	133	0.8
			15.2			35.3	24.5	2		135	134	0.8
AR1	7/1/09	0	0	29.440	91.322	0.1				437	421	-4.9
AR2	7/1/09	0	0	29.351	91.405	0.6				523	495	-4.6
AR3	7/1/09	0	0	29.317	91.490	0.7				496	512	-4.7
AR4	7/1/09	0	0	29.302	91.527	1.5				484	490	-4.4
AR5	7/1/09	0	0	29.290	91.561	2.9				518	526	-4.2
AR6	7/1/09	0	0	29.244	91.618	6.0				505	500	-3.5
AR7	7/1/09	0	0	29.211	91.620	8.8				469	469	-3.0
AR8	7/1/09	0	0	29.188	91.623	12.2				449	450	-2.4
AR9	7/1/09	0	0	29.178	91.625	15.2				411	409	-2.0
AR10	7/1/09	0	0	29.161	91.625	18.0				376	372	-1.5
AR11	7/1/09	0	0	29.149	91.625	18.8				355	363	-1.4
F0	7/1/09	5	0	29.272	91.619	3.1	30.0	137	26.3	489	482	-4.0
			4			23.0	29.1	65	5.0	313	316	-1.1
F1	7/1/09	5	0	29.181	91.618	1.4	30.2	210	3.5	467	472	-4.3
			4			32.3	26.8	6	6.1	216	214	0.5
F2	7/1/09	7	0	29.050	91.617	10.4	31.1	218		478	478	-3.0
			6			32.7	26.3	134		183	184	0.5
F3	7/1/09	20	0	28.883	91.616	29.3	30.7	199	0.5	157	154	0.1
			6.5			30.5	28.5	150	1.0	175	177	0.1
			19			35.6	25.7	134	1.6	94	96	1.1
F5	7/1/09	30	0	28.691	91.617	29.2	31.2	196	0.3	171	174	0.1
			10			35.5	34.1	195	0.5	105	104	0.5
			29			36.1	24.0	122	0.9	90	90	1.0
F7	7/2/09	53	0	28.464	91.612	28.1	30.5	193	0.3	136	129	-0.1
			20			35.3	27.1	198	0.2	86	87	0.9
			40			36.2	22.8	201	0.4	72	74	1.0
			52			36.3	21.2	155	1.1	74	75	1.2
F8	7/2/09	84	0	28.181	91.613	28.1	31.0	193	0.3	127	125	-0.1
			20			35.3	26.7	204	0.3	85	85	1.0
			82			36.3	18.8	116	0.2	53	53	1.1

Table 4 (continued).

	Date	Bot. (m)	Sam. (m)	Lat.	Lon.	S	Tem. (°C)	DO	Chl a	Ba 0.45*	Ba 0.02*	$\delta^{18}O$ (‰)
I9	7/2/09	56	0	28.391	92.752	29.0	31.0	196	0.2	137	136	0.0
			20			35.1	26.6	201	0.4	90	92	1.0
			55			36.2	20.9	155	0.5	75	78	1.3
I8	7/3/09	37	0	28.646	92.748	29.4	30.9	193	0.4	143	144	0.1
			12.5			32.2	27.4	153	0.5	133	133	0.5
			36			36.2	22.2	149	0.7	81	82	1.3
I6	7/3/09	27.4	0	28.892	92.750	30.1	30.9	193	0.3	130	131	0.3
			18.5			33.4	26.9	144	0.8	120	119	0.8
			26.4			35.8	24.9	146	1.3	87	88	1.4
I4	7/3/09	20.7	0	29.174	92.750	30.4	32.0	193	0.3	131	126	0.4
			19.7			35.3	26.1	64		121	121	1.0
I2	7/3/09	14	0	29.409	92.750	30.7	31.9	196	1.0	127	126	0.3
			13			33.8	26.9	43		127	129	1.0
I1	7/3/09	10.4	0	29.532	92.750	31.7	32.1	208	1.9	193	197	0.2
			5.7			32.2	28.5	107		199	200	0.3
			9.5			32.4	33.8	34		157	155	0.5
H0	7/3/09	2	0	29.494	92.385	32.1	31.9	229	8.0	239	237	0.4
			1			30.9	31.9	230		238	237	0.4
H3	7/3/09	14	0	29.154	92.382	30.2	31.7	193	0.3	148	148	0.2
			13			35.2	26.0	49		134	134	0.8
G1	7/4/09	8	7	29.260	91.998	32.2	26.1	6		208	205	0.3
G3	7/4/09	20	0	28.983	91.998	30.3	31.1	196		168	155	0.3
			19			35.8	25.6	85		109	106	1.0
E2	7/4/09	8.5	0	28.857	91.248	27.4	31.3	206		252	246	-0.1
			7.5			33.8	25.7	49		174	166	0.8
E3	7/4/2009	21.7	0	28.656	91.248	30.0	31.4	196		147	143	1.0
			20.7			36.0	24.2	37		115	112	0.9
D1	7/4/2009	7.7	6.7	28.982	90.833	33.8	24.9	3		148	144	0.7
			6.7			34.5	24.9	3		142	138	0.8
D0	7/4/09	7.8	1.5	29.013	90.833	33.2	25.3	2		176	174	0.6
D0(W)	7/4/09	6.5	1.5	29.018	90.833	29.9	25.5	2		220	217	0.3

Abbreviation: Bot.: bottom depth, Sam.: sampling depth, Lat.: latitude, Lon.: Longitude, S: salinity, Tem.: temperature, DO: dissolved oxygen, Chl a: chlorophyll a.

*: < 0.45 µm and < 0.02 µm.

there might be a small abrupt increase in Ba at the very lowest salinities, there is also a broad upward curvature throughout the entire distribution that was not observed at high discharge. There are also some high salinity surface water samples that appear distinctly

above the overall trend in Ba versus salinity. The mixing experiment in this instance is conservative, again contrasting with the high discharge behavior. Also at this time, the MR outflow appears to have slightly higher Ba than the AR outflow, again in contrast with high discharge (though we were unable to sample the true MR endmember in November 2008).

At intermediate discharge during summer hypoxia (June/July 2009), there again appears to be an abrupt jump in Ba at the lowest salinities, though both mixing experiments show conservative behavior. At higher salinities, Ba is more scattered than during the other sampling periods. In part, between salinities 15 and 30 the Ba distribution might be described by two different conservative trends with some additional scatter (e.g., the low Ba at stations C9 and C11). Similar to low discharge, the MR outflow appears to have higher Ba than the AR outflow at the lowest salinities.

During at least the high flow and hypoxia surveys, bottom water Ba appears to be enriched compared to surface and mid-depth waters (Figure 13, Appendix), suggesting that Ba input to the shelf bottom. This effect was most pronounced during the June/July 2009 cruise, which occurred when we observed the most depleted bottom water oxygen conditions (Figure 14).

The questions raised by these distributions are several-fold. First, why is it only during high discharge that the mixing experiments support desorptive input of dissolved Ba? If desorption is not occurring during the low and intermediate discharge surveys, then what explains the non-conservative behavior in those distributions? What accounts for the behavior of Ba in shelf bottom waters? And, finally, why are there differences

Table 5

Results from mixing experiments during May and November 2008 and June/July 2009. MR mixing experiment was conducted only during June/July 2009

May 2008			November 2008		
AR			AR		
Salinity	Ba (nmol/kg)		Salinity	Ba (nmol/kg)	
	0.45 µm	0.02 µm		0.45 µm	0.02 µm
0.1	498	466	0.2	479	512
2.5	492	470	4.3	436	478
4.0	533	521	7.4	411	446
7.2	441	431	11.5	366	391
8.4	464	465	14.5	320	342
10.8	431	425	17.7	279	299
14.4	377	374	21.1	236	252
19.3	307	309	26.9	174	192
23.0	253	254	29.0	136	144
24.6	235	232	32.5	101	108
32.9	107	106	36.7	49	51
33.0	118	101			
35.8	55	54			

June/July 2009					
	MR			AR	
Salinity	Ba (nmol/kg)		Salinity	Ba (nmol/kg)	
	0.45 µm	0.45 µm		0.45 µm	0.02 µm
0.7	537	537	0.1	435	418
4.8	501	501	4.0	433	421
8.6	450	450	6.5	406	400
11.1	416	416	10.0	370	363
14.4	378	378	14.0	329	326
17.2	348	348	17.1	302	295
21.5	300	300	18.8	280	275
23.9	269	269	23.8	235	233
26.6	229	229	24.9	217	213
29.7	186	186	28.3	180	176
32.8	144	144	32.2	145	141
34.1	120	120	35.6	117	114
35.7	79	79	36.2	88	86

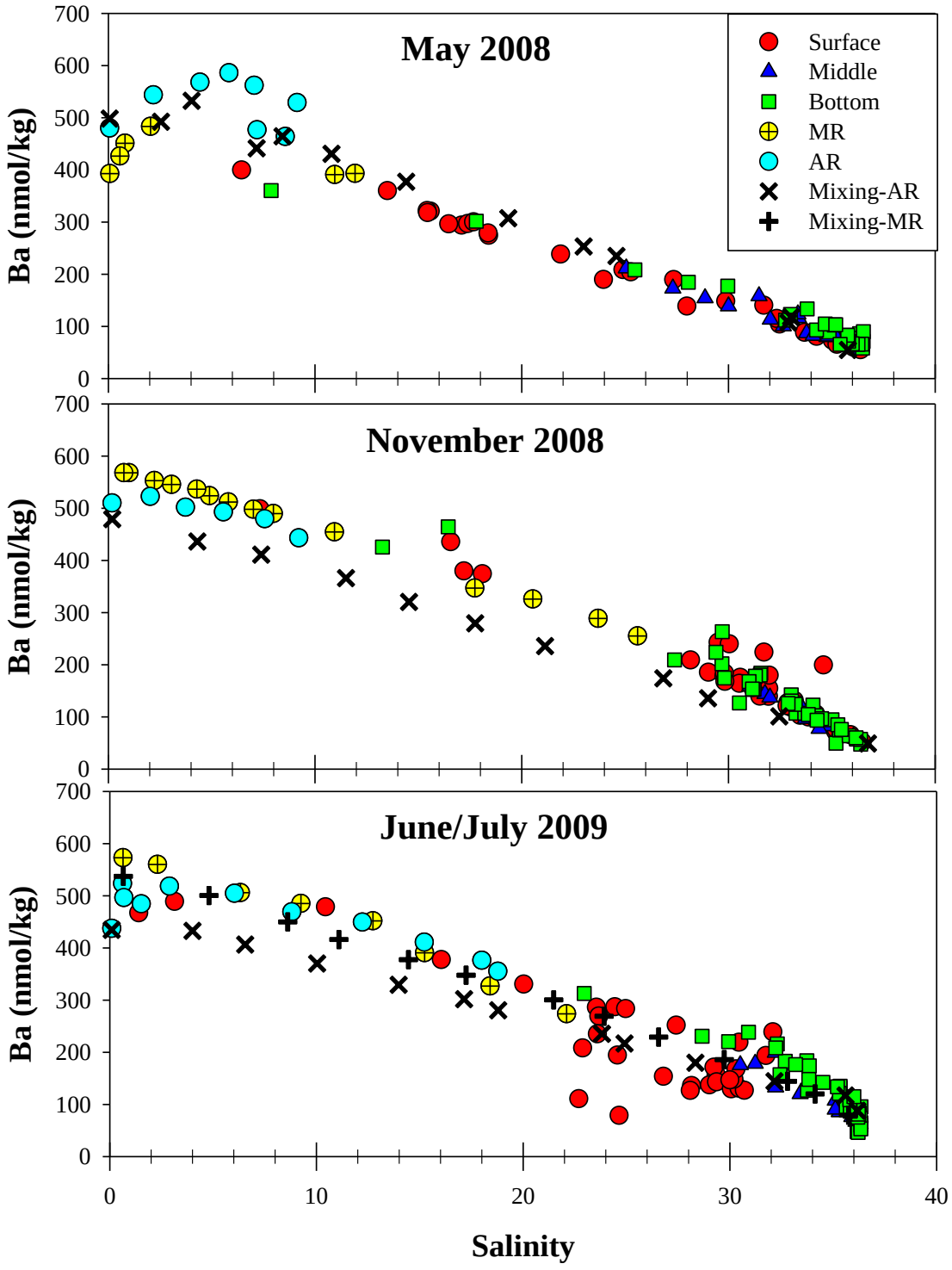

Figure 13. Total dissolved Ba (< 0.45 µm) distributions for three cruises. Mixing experiments are also plotted. For the Mississippi River endmember, the mixing experiment was only conducted during June/July 2009.

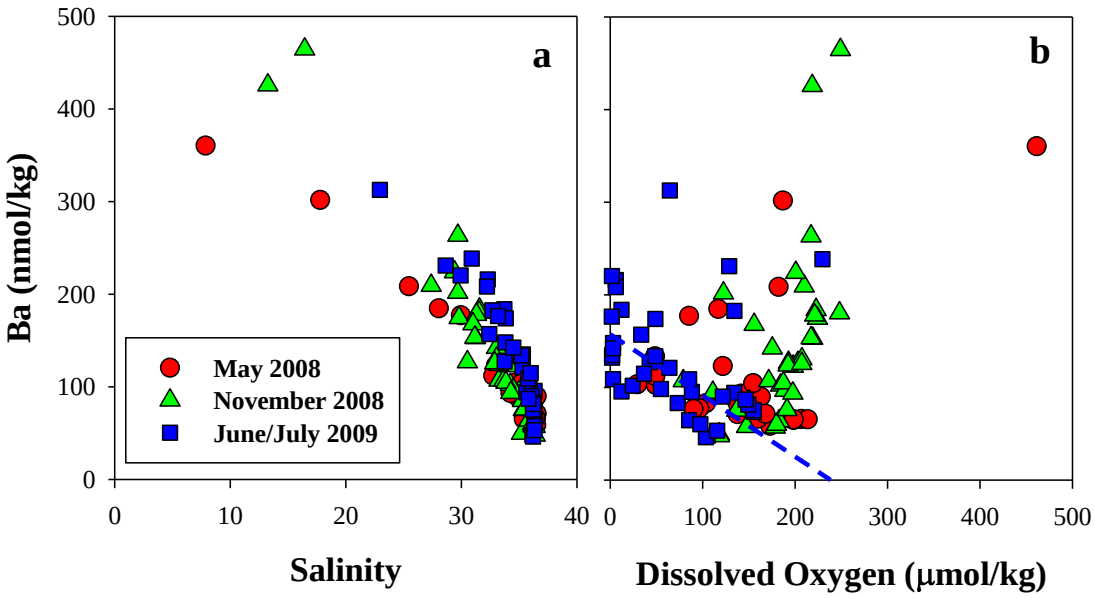

Figure 14. Bottom water Ba versus a) salinity and b) dissolved oxygen (DO). For the June/July 2009 Ba-DO regression (dashed blue line), several stations of higher DO and low salinity (indicating surface water intrusion) were excluded. The regression was Ba = -0.59 × DO + 150 (r^2 = 0.49, n = 31, p< 0.0001).

between the MR and the AR endmembers? We consider these questions below and then discuss the implications for paleoceanographic use of Ba as a freshwater proxy.

Ba input to shelf bottom waters

As noted above, Ba appears to be enriched in shelf bottom waters for at least two of our cruises. This distribution is not simply a consequence of upwelling of deeper Ba-enriched offshore waters onto the shelf: Ba does not increase strongly with depth in the northern Gulf of Mexico. For instance, even at 1600 m, dissolved Ba is only ~60 nM (Joung and Shiller, 2013).

Input of Ba to shelf bottom waters should not be surprising in this environment, however. Krest et al. (1999) observed excess Ra in the Louisiana Shelf bottom waters and suggested submarine groundwater discharge (SGD) or release of formation waters associated with oil/gas drilling as the source. McCoy et al. (2007) likewise suggested

formation water input and/or seawater recirculation as minor fluid inputs to the shelf bottom, though they still measurably contribute to isotopic inputs to these waters. Kolker et al. (2013) more recently provided evidence for SGD input to the delta and coastal bays in this region based partly on the distribution of ^{222}Rn, the daughter product of ^{226}Ra. These processes are also likely to be sources of Ba in this environment given the chemical similarity of Ba to Ra. Drilling activities under some circumstances may also result in the release of Ba-enriched drilling muds (e.g., Joung and Shiller, 2013). Additionally, dissolution of barite in reducing shelf sediments is another possible dissolved Ba source (Colbert and McManus, 2005; Falkner et al., 1993). For the June/July 2009 cruise, which occurred during summertime shelf hypoxia, dissolved Ba in shelf bottom waters varied inversely with dissolved oxygen (Figure 14). While this is compatible with anoxic barite dissolution being a significant source of bottom water barium, we note that this Ba-oxygen relationship could simply reflect the dual role of summertime water stratification both in inhibiting re-oxygenation of bottom waters as well as in trapping benthic-sourced Ba (regardless of input mechanism).

Also of some relevance is how much particulate Ba is supplied by the river. Shiller (1997) found that the lower Mississippi River carried 5 µmol/g particulate Ba or close to 1200 nM Ba at typical suspended loads. While it is unclear how much of this is either desorbable or able to be regenerated in the sediments, certainly there is significant fluvial particulate Ba for these processes. That is, while we cannot dismiss possible Ba input from oil and gas operations on the Louisiana Shelf, there is not necessarily a mass-balance requirement for it. Nonetheless, our data do not allow us to distinguish the particular source/mechanism of Ba input to shelf bottom waters. Clearly though, benthic

input is an important component of the Ba mass balance in this system just as it is in others (e.g., Colbert and McManus, 2005).

Ba input to surface waters

As described above, the high discharge (May 2008) Ba distribution along with its associated mixing experiment is non-conservative in a manner generally consistent with previous observations and experiments indicating salinity-induced desorption of Ba from the fluvial suspended load (Hanor and Chan, 1977; Li and Chan, 1979; Li et al., 1984). This process is generally viewed as the dominant modifier of the Ba flux through estuaries (Coffey et al., 1997).

Despite this *classic* picture, the high discharge Ba distribution is odd in that at a salinity of 10, Ba concentrations in the AR outflow suddenly drop and converge with the MR outflow trend in a single, conservative distribution out to high salinity (Figure 13). A related phenomenon is observed in the distribution of the $\delta^{18}O$ of the water versus salinity (Figure 15), where the trend for the AR outflow also converges into a main $\delta^{18}O$-S trend that is largely defined by the MR and the offshore high salinity Gulf endmembers. This distribution is not surprising given that during fall through spring, outflow waters are generally directed towards the west via the Louisiana Coastal Current (Cochrane and Kelly, 1986). Indeed, even when river discharge is exceptionally high, the influence of AR water on our sampling grid is likely to be confined to the more landward stations south and west of Atchafalaya Bay (Falcini et al., 2012). In other words, for most of our shelf stations MR outflow should be the dominant freshwater influence, and this evidence is borne out by both the Ba and $\delta^{18}O$ data.

It also notes that despite the enrichment of Ba in bottom waters during May 2008 (Figure 13, Appendix), there seems to be minimal influence of the bottom Ba input on the surface water Ba distribution. During this high flow survey, the surface-bottom salinity difference averaged 8. Thus, vertical stratification appears to have limited the upward mixing of Ba-enriched bottom waters.

In contrast to high discharge, the low discharge (November 2008) Ba distribution shows only a small, low-salinity concentration increase associated with the AR outflow. Possibly, the lack of low-salinity Ba increase in the MR outflow at this time is an artifact of our only being able to sample that outflow down to a salinity of 1, and thus missing the desorption hump almost entirely. A lower amount of desorption (relative to high discharge) is to be expected at this time as USGS data for Tarbert Landing, MS (water.usgs.gov), indicate that the low discharge, suspended matter concentration of the river was more than two-fold lower than the high discharge suspended matter concentration. Nonetheless, because there was broad upward curvature in the Ba distribution throughout the salinity range during November 2008, extrapolation of the high salinity surface water Ba data yields an effective river endmember of >800 nM Ba, suggesting substantial Ba input during river-seawater mixing.

Dion (1983) suggested that similar differences in the low/high discharge Ba distributions in the Amazon River plume might be explained through a kinetic/hydrodynamic mechanism. The concept is simply that at low discharge (as compared with high) a given suspended particle is likely to travel further through the salinity gradient before its Ba is desorbed, leading to a broader, more extended desorption maximum during low discharge. Coffey et al. (1997) likewise adapted this concept to

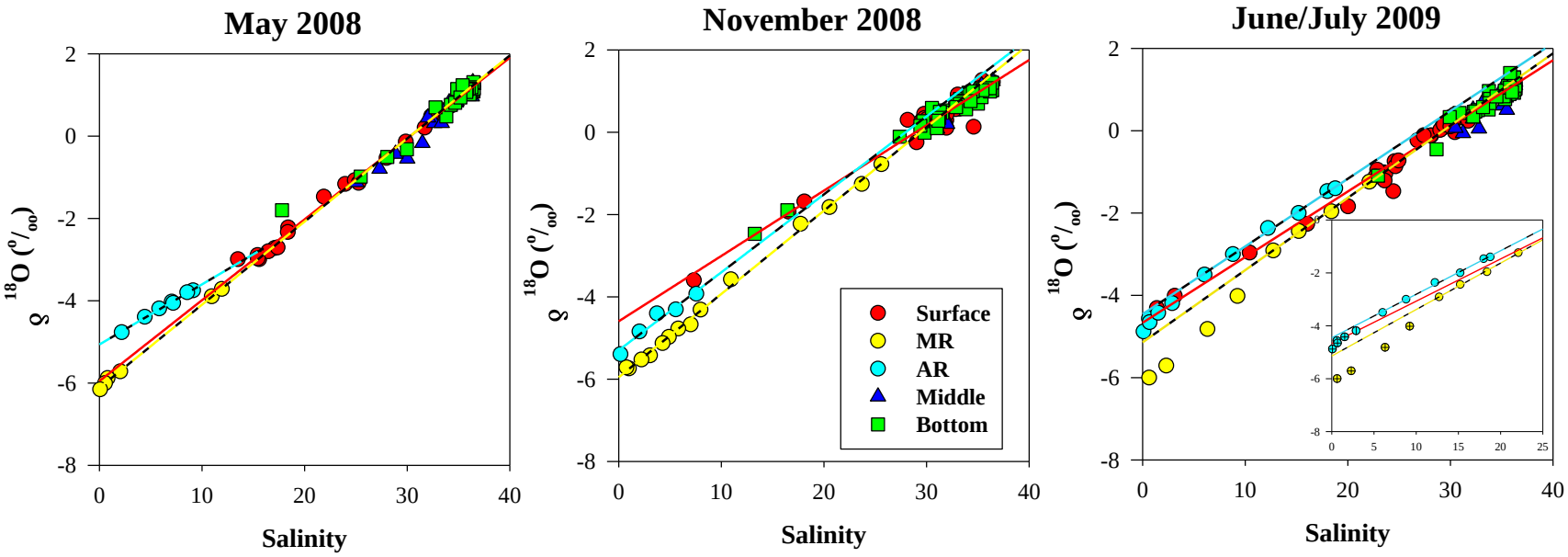

Figure 15. Surface water distribution of $\delta^{18}O$ of the water versus salinity. Regression equations for surface waters are y=0.20x – 6.0 (r^2= 0.99, n=25), y= 0.16x – 4.6 (r^2= 0.95, n= 36) and y= 0.16x – 4.7 (r^2=0.98, n=31). For two river plumes, see (Chapter II Appendix A). All p vales are < 0.0001.

explain differences in the location of Ba release among various estuaries. It seems that this mechanism is unrealistic. First, our mixing experiment shows scant evidence for Ba input, though one might argue that our surface grab sample under-sampled the suspended load. Second, it is difficult to explain why there would be desorption over a broad salinityrange while the field data still show a small low-salinity jump in Ba (presumably indicative of desorption). More importantly, however, is that the Dion/Coffey mechanism requires that desorption be slow relative to mixing. However, as was pointed out by Coffey et al. (1997), most Ba desorption occurs within 60 minutes of mixing; yet, the process of transporting MR and AR waters through the shelf mixing zone takes days (Moore and Krest, 2004) if not months (Dinnel and Wiseman, 1986). Thus, desorption is too fast for the kinetic/hydrodynamic mechanism to be relevant to this situation, nor is it likely to be a factor globally in any but the smallest mixing zones.

Another possible explanation for the November 2008 surface water Ba distribution is that the upward curvature of the field data represents a change in the river Ba concentration over the timescale of mixing (Loder and Reichard, 1981; Officer and Lynch, 1981). For the plume of the MR, mixing times can be a number of months at low discharge (Dinnel and Wiseman, 1986). While the more Ba-rich Missouri River was indeed the dominant source of water to the lower Mississippi a month before our sampling (Figure 12), the Missouri River's Ba concentration was probably not high enough to be the dominant cause of the upward curvature in our November surface water distribution (e.g., Shiller, 1997); i.e., it could not explain an extrapolated river endmember of >800 nM Ba.

Thus, it can be concluded that the non-conservative Ba input to the surface waters during November 2008 was simply from upward mixing of Ba-enriched shelf bottom waters. That is, the surface distribution reflects mixing of more than just two endmembers, resulting in an appearance of non-conservative behavior (Shiller, 1996). In contrast to high discharge, the surface-bottom salinity difference averaged only 2 during our low flow survey (with a median difference of only 0.7). With vertical stratification low at this time of year due to the decreased fresh water input and increased mixing by winter fronts, such upward mixing would occur readily. Indeed, bottom and surface water samples fall on the same Ba-salinity trend, consistent with this sort of vertical exchange. This process also likely explains a similar, broad Ba-salinity curvature observed in this system by Shim et al. (2012).

In the June/July 2009 Ba distribution, it showed again the low-salinity jump in Ba concentration in the AR outflow (Figure 13). However, it can be noted that a plot of salinity versus the $\delta^{18}O$ of the water shows some curvature at low salinity in the AR plume, reflecting a recent change to an isotopically-lighter AR endmember (Figure 15). This distribution is consistent with the fact that during June/July 2009, the RR contribution to the AR decreased from 42% to 29% two weeks prior to our AR plume sampling (i.e., the RR is isotopically heavier than the MR water). Thus, endmember variability likely explains the scatter in the low salinity Ba distribution at this time. Beyond this initial curvature, the AR outflow Ba-salinity trend continues towards a high-Ba, high-salinity bottom water endmember, intersecting inshore surface water samples (e.g., A1, C1, E2, and H0). In high-salinity bottom waters at this time, not only was the Ba enrichment related to bottom water oxygen depletion (Figure 14) but also the most

Ba-enriched bottom waters were the most inshore (i.e., shallowest) waters as evidenced by a plot of bottom Ba versus bottom depth (Appendix). This makes sense since the most inshore bottom waters are likely to have spent the most time traversing the shelf and interacting with the bottom. Although stratification was high at this time (average surface-bottom salinity difference of 10), upward mixing of Ba-enriched bottom water is also supported by observation of high dissolved Co, Cu, Fe, and Mn in these inshore waters (Chapter II). It can be noted that this contrasts with the situation in May 2008 when the scant evidence of upward mixing of Ba-enriched bottom waters was observed. This difference likely results both from the greater bottom Ba enrichment during summer hypoxia as well as the seasonal change in circulation on the shelf wherein summer winds become more upwelling-favorable (Cochrane and Kelly, 1986).

For the MR outflow during the June/July 2009 hypoxia survey, there is no apparent low-salinity jump in Ba, but there is a slight upward curvature out to mid-salinity. As was the case in the low discharge survey, it was unable to sample quite as low a salinity in the MR outflow as the AR outflow and thus might have missed some very low salinity desorption input of Ba. The MR outflow Ba-salinity trend intersects offshore surface water stations (e.g., X3, A7, A9, C7, and F8) continuing towards complete Ba depletion by salinity 35 (Figure 13). Two offshore stations (C9 and C11) fall well below the trend, showing very significant Ba depletion. While Ba depletion in this region has not been reported before, in the Delaware estuary Stecher and Kogut (1999) reported rapid, episodic Ba removal that they attributed to barite precipitation during late stages of a diatom bloom. For the MR plume, Lohrenz et al. (2008) found that productivity tends to peak in April/May coinciding with high discharge and it was also

observed that chlorophyll a in surface waters was higher during our May 2008 survey (6 - 30 µg/kg) than during the June/July 2009 survey (1 - 6 µg/kg). Interestingly, Flow Cam data (J. Paul, USF, pers. comm.) indicates that the surface water diatom abundance was comparatively high during June/July 2009 at the most Ba-depleted stations (C9 and C11). Observations in this study are thus consistent with the Stecher and Kogut (1999) Ba removal mechanism.

There is one final difference among the three surveys to consider. For the May 2008 survey, the apparent desorption hump spans a salinity range of 10 whereas the small increases was observed in the AR outflow in the other two surveys occur at a salinity below 2. This distribution stands in contrast to the Dion/Coffey hydrodynamic mechanism, which predicts the broadest desorption hump at low discharge rather than high as observed in this study. This study suggests that the difference does have a hydrodynamic component. Specifically, during May 2008, discharge was great enough so that the distributary channels were completely fresh and the mixing of river and seawater began in open waters beyond the river channels. In contrast, during the other two surveys, mixing began within the channels of the MR and AR. At high discharge, fresh water rapidly spreads out from the river mouths, potentially mixing with estuarine waters of a variety of salinities, thereby broadening the desorption maximum. But, when the initial mixing occurs within the distributaries, the constriction of the channels and the nature of gravitational circulation result in a simpler mixing regime and hence a much sharper and quicker desorption maximum.

Ba in the MR and AR endmembers

Another important aspect regarding the Ba distribution in the Louisiana Shelf is the different Ba endmembers of the MR and AR. At high discharge (May 2008), Ba was ~100 nmol/kg higher in the AR than in the MR. In contrast, at low and intermediate discharges (November 2008 and June 2009, respectively), Ba in the MR was generally higher than in the AR. As mentioned above, the AR water is derived mostly from the MR with a variable addition of water from the RR. Also, while the lower MR is highly channelized, the AR flows through the extensive wetlands of the Atchafalaya River Basin (ARB). During our ARB study, Ba concentrations in the RR were 480, 580, and 270 nmol/kg for April and November 2010, and June 2011, respectively. At the same time, Ba concentrations in the MR were 447, 546 and 456 nmol/kg, respectively (Table 6). The dissolved Ba concentrations in ARB swamp waters were found to be ~3 µmol/kg during intermediate (April 2010) and low (November 2010) river discharges. But, during high river flow (June 2011), the Ba concentration of the swamp water was 0.5 µmol/kg, similar to the MR Ba concentration, likely because opening of the Morganza Spillway during the lower MR flood that year inundated the ARB with MR water. Clearly our limited sampling of the RR and ARB was not sufficient to provide us with a predictive capability for the difference between the AR and MR endmembers, but nonetheless provides insight into how the AR can be either higher or lower in Ba than the MR.

Implications for paleoceanographic applications of Ba as a coastal salinity proxy

Ample studies have used the planktonic foraminiferal Ba/Ca ratio as an indicator of paleo-freshwater input because other proxies (e.g., oxygen isotopes) are affected by additional factors such as temperature (e.g., Hill et al., 2006; Flower et al., 2004; Hall and

Table 6

Results of dissolved Ba from the Red River (RR), Mississippi River (MR) and Atchafalaya basin swamp waters (ARS)

Stations	Date	Discharge*	Contribution to the AR**	Ba
		(m^3/sec)	(%)	(nmol/kg)
MR	Apr-10	8.7E+03	86	447
RR		1.2E+03	14	481
ARS				2802
MR	Nov-10	2.7E+03	95	546
RR		2.8E+02	5	583
ARS				3387
MR	Jun-11	13.5E+03	74	456
RR		1.9E+03	26	271
ARS				530

* River discharges were obtained from USGS and the US Army Corps Engineers river monitoring sites at Alexandria and Acne, LA for the Red River and at Tarbert Landing for the Mississippi River.

**: Atchafalaya River

Chan, 2004). However, the foraminiferal Ba/Ca ratio appears to be affected dominantly by only the Ba/Ca ratio of seawater (Lea and Spero, 1994; Honisch et al., 2011); and thus, it should reflect the salinity of the water at the time of foraminifers' calcite formation. Using a contemporary Ba-salinity relationship from a given coastal region, thus provides a means for inferring past salinities or freshwater inputs from planktonic foraminiferal Ba/Ca. This work on the Louisiana Shelf Ba distribution suggests possible caveats in this approach due to changing Ba-salinity surface water relationships including seasonal changes in the endmember composition (including desorbable suspended Ba), seasonal changes in stratification resulting in variation of bottom inputs, long-term changes in distributary systems, and possible anthropogenic effects on coastal hypoxia, submarine groundwater discharge, and oil drilling operations. The Louisiana Shelf system today is,

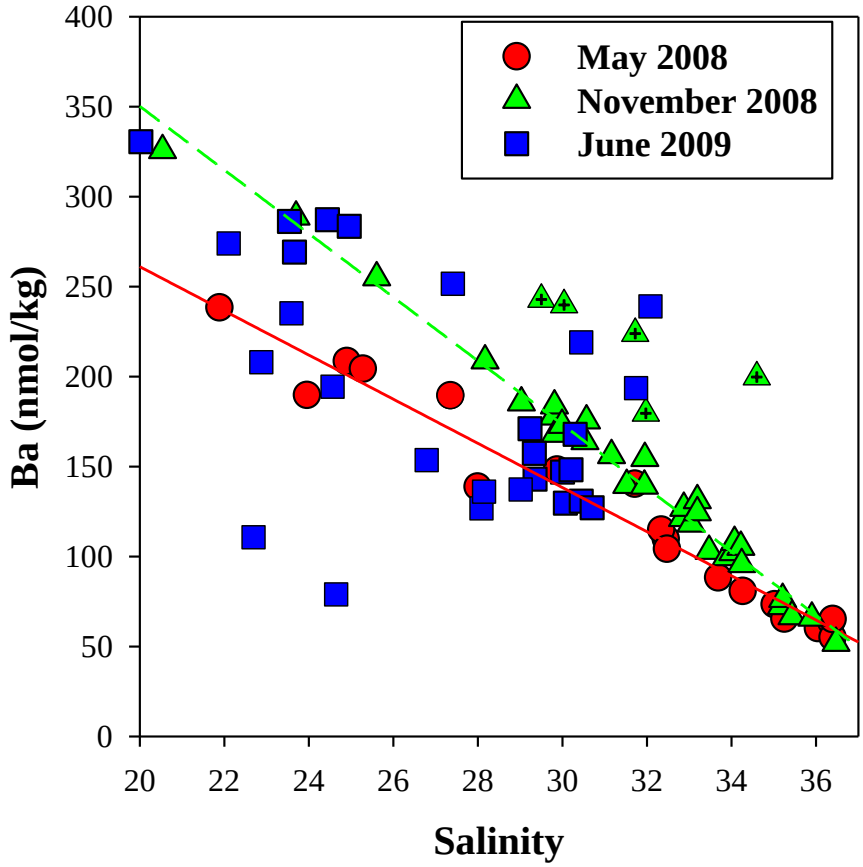

Figure 16. Surface Ba distribution versus salinity (> 20). Regressions for May (red solid) and November (green dashed) 2008 are y= -12.4x + 506 (r^2=0.96, p<0.0001) and y= -17.7x + 704 (r^2=0.98, p< 0.0001), respectively. For November 2008 regression, 5 data points (cross triangle) were not considered (see text). The regression for June/July 2009 was not generated in this figure.

perhaps, uniquely complicated in these various factors and thus might be viewed as a worst-case scenario. Nonetheless, a better understanding of the extent of and controls on benthic inputs (natural and otherwise) in this system and others is likely a key factor for the coastal Ba mass balance and hence the improved paleoceanographic application.

To better demonstrate the potential paleoceanographic uncertainty, Figure 16 provides an expanded view of high salinity surface water Ba-salinity relationships. As an example, at a salinity of 30, there is a seasonal uncertainty of ~40 nmol/kg in dissolved

Ba on the Louisiana Shelf which translates to a change of 0.68 µmol/mol in the foraminiferal Ba/Ca ratio when using the distribution coefficient of Lea and Spero (1994). Stated the opposite way, an uncertainty of 0.68 µmol/mol in the foraminiferal Ba/Ca ratio, would lead to an uncertainty in predicted salinity of 2 - 3 psu. These seasonal variations in surface water Ba-salinity relationships could be even more significant at low salinity, which, again, leads to greater over (or under)-estimation of paleo-salinity changes in low salinity estuarine system. Thus, as is the case with nearly all paleoceanographic proxies, the planktonic foraminiferal Ba/Ca ratio should be used in conjunction with other constraining proxies and with an eye towards possible coastal oceanographic and geochemical confounding factors.

Conclusions

Significant spatial and temporal variations in the dissolved Ba distribution on the Louisiana Shelf were observed during our three surveys. During high discharge (May 2008), both field data and a mixing experiment indicate non-conservative behavior consistent with salinity-induced desorption of Ba from the fluvial suspended load. The desorption humps for the MR and AR outflows are similar even though the AR Ba concentration was substantially higher than the MR concentration. Shelf bottom water Ba during the high discharge survey also appeared to be enriched relative to surface waters, though there was little evidence of significant input of this bottom Ba to surface waters.

At low discharge (November 2008), there was scant evidence of Ba desorption, likely because of the lower fluvial suspended load. However, a broad upward curvature was observed in the Ba-salinity distribution which was not observed during high discharge. This broad upward curvature appears to be due to upward mixing of Ba-

enriched shelf bottom waters, which occurs more readily at this time of year due to lessened freshwater inflow, and hence diminished vertical stratification as well as to mixing due to the passage of fall/winter storm fronts.

At intermediate discharge during summer hypoxia season (June/July 2009), evidence for desorption was again limited. Bottom water Ba enrichment at this time appears to be related to oxygen depletion. Significant scatter in the high salinity surface water Ba distribution may appear to result from episodic input of enriched bottom waters. It was also observed some Ba depletion associated with a diatom bloom.

These contrasting Ba distributions appear to reflect seasonal changes in suspended matter input, benthic inputs, and stratification/vertical mixing. The origin of the benthic inputs, whether from SGD input, sediment regeneration, or anthropogenic inputs, remains unresolved. However, this seasonal variation is clearly a question of importance for understanding the Ba distribution in this and other coastal/estuarine systems. Benthic inputs influenced at least two of our Ba surveys as much if not more than desorptive input.

This study of Ba distribution in the Louisiana Shelf implies possible caveats in the utilization of Ba as a proxy for paleo-salinity changes due to the contemporary seasonal variation of surface Ba-salinity relationships, which could lead to a considerable uncertainty in predicted salinity. The Louisiana Shelf, however, may prove a worst-case scenario due to its multiple endmembers and possible influences of anthropogenic hypoxia as well as inputs from oil/gas drilling operations. Clearly, though, a better understanding of benthic inputs of Ba is an important key in tying down the coastal/estuarine Ba mass balance.

APPENDIX A

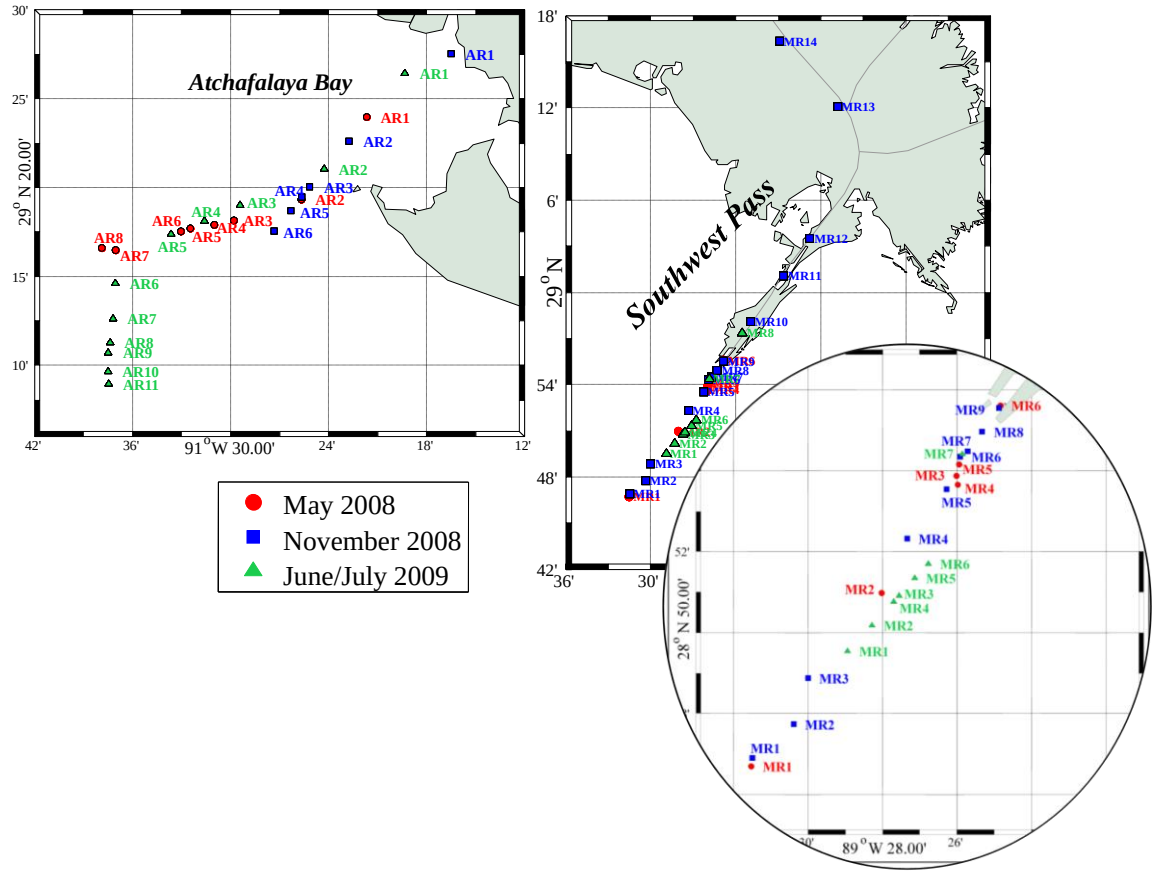

Figure. Sampling locations of the two river plumes.

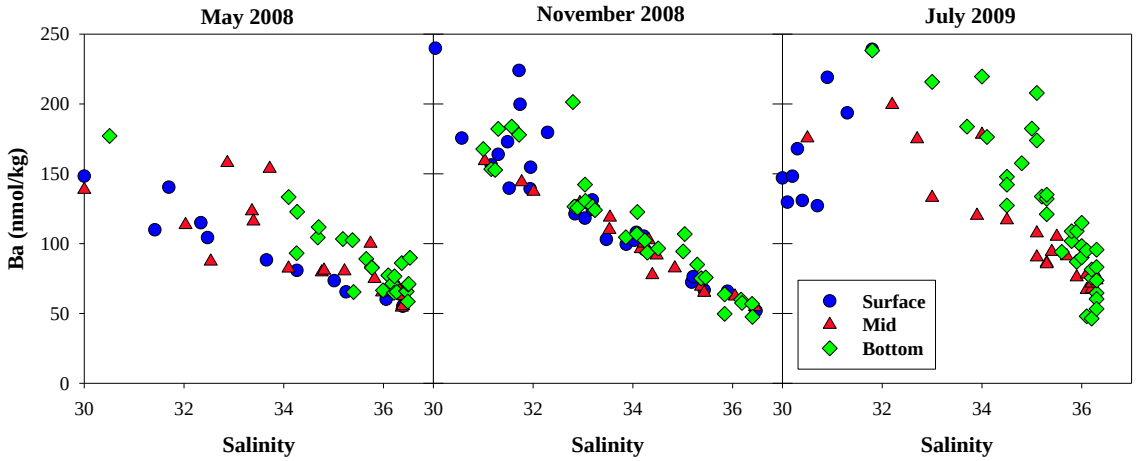

Figure. High salinity (>30) Ba distribution.

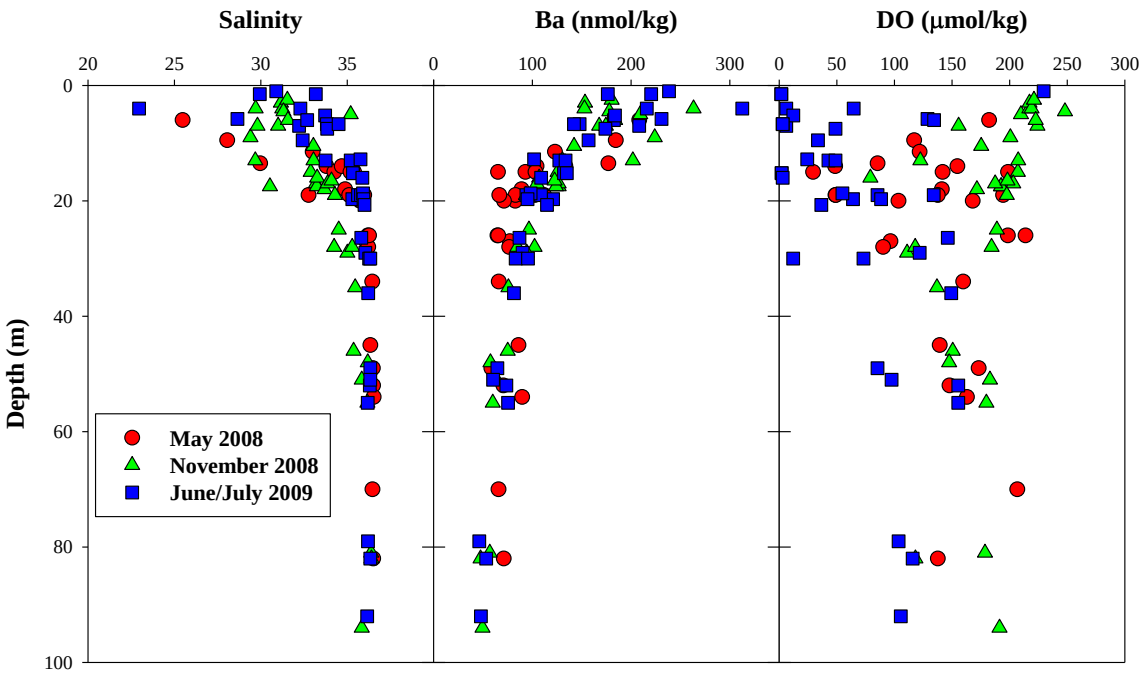

Figure. Bottom water salinity, Ba concentration, and dissolved oxygen (DO) with depth for samples with salinity > 20.

REFERENCES

Alibert, C., Kinsley, L., Fallon, S. J., McCulloch, M. T., Berkemmans, R., McAllister, F. Source of trace element variability in Great Barrier Reef corals affected by the Burdekin flood plumes. *Geochim. Cosmochim. Acta* **2003**, 67, 231-246.

Carroll, J., Falkner, K. K., Brown, E. T., Moore, W. S. The role of the Ganges-Brahmaputra mixing zone in supply Ba and ^{226}Ra to the Bay of Bengal. *Geochim. Cosmochim. Acta* 1993, 57, 2981–2990

Chan, L.H., Edmond, J.M., Stallard, R.F., Broecker, W.S., Chung, U.C., Weiss, R.F., Ku, T.L. Radium and barium at GEOSECS stations in the Atlantic and Pacific. *Earth Planet. Sci. Lett*. **1976**, 32, 258-267.

Cochrane, J.D., Kelly, F.J. Low-frequency circulation on the Texas-Louisiana continental shelf. *J. Geo. Res*. **1986**, 91, 10645-10659.

Coffey, M., Dehairs, F., Collette, O., Luther, G., Church, T., Jickells, T. The Behaviour of Dissolved Barium in Estuaries. *Estuar. Coastal Shelf Sci*. **1997**, 45, 113–121.

Colbert, D., McManus, J. Importance of seasonal variability and coastal processes on estuarine manganese and barium cycling in a Pacific Northwest estuary. *Cont. Shelf Res*. **2005**, 25, 1395-1414.

Dalai, T. K., Krishnaswami, S., Sarin, M. M. Barium in the Yamuna River system in the Himalaya: Sources, fluxes, and its behavior during weathering and transport. *Geochem. Geophy. Geosy*. **2002**, 3, 1076-1099.

Dinnel, A.P., Wiseman Jr, W.J. Fresh water on the Louisiana and Texas shelf. *Cont. Shelf Res*. **1986**, 6, 765-784.

Dion, E.P. Trace Elements and Radionuclides in the Connecticut River and Amazon River Estuary. Ph.D. Thesis, Yale Univ. January 1983.

Dymond, J., Suess, E., Lyle, M. Barium in deep-sea sediment: A geochemical proxy for paleoproductivity. *Paleoceanography* **1992**, 7, 163-181.

Falcini, F., Khan, N.S., Macelloni, L., Horton, B.P., Lutken, C.B., McKee, K.L., Santoleri, R., Colella, S., Li, C., Volpe, G., D'Emidio, M., Salusti, A., Jerolmack, D. Linking the historic 2011 Mississippi River flood to coastal wetland sedimentation. *Nat. Geosci*. **2012**, 5, doi:10.1038/ngeo1615.

Falkner, K.K., Klinkhammer, G.P., Bowers, T.S., Todd, J.F., Lewis, B.L., Landing, W.M., Edmond, J.M. The behavior of barium in anoxic marine waters. *Geochim. Cosmochim. Acta* **1993**, 57, 537-554.

Field, M.P., LaVigne, M., Murphy, K.R., Ruis, G.M., Sherrell, R.M. Direct determination of P, V, Mn, As, Mo, Ba and U in seawater by SF-ICP-MS. 2007 European Winter Conference on Plasma Spectrochemistry, Taormina, Italy (abstr), **2007**.

Flower, B.P., Hastings, D.W., Hill, H.W., Quinn, T.M. Phasing of deglacial warming and Laurentide Ice Sheet meltwater in the Gulf of Mexico. *Geology* **2004**, 32, 597-600.

Guay, C.K., Falkner, K.K. Baruim as a tracer of Arctic halocline and river waters. *Deep-Sea Res. II* **1997**, 44, 1543-1569.

Guay, C.K., Falkner, K.K. A survey of dissolved barium in the estuaries of major Arctic rivers and adjacent seas. *Cont. Shelf Res*. **1998**, 18, 859-882.

Hall, J.M., Chan, L.,-H. Ba/Ca in Neogloboquarina pachyderma as an indicator of deglacial metwater discharge into the western Arctic Ocean. *Plaeoceanography* **2004**, 19, doi: 10.1029/2003PA000910.

Hanor, J.S., Chan, L.H. Non-conservative behaviour of barium during mixing of Mississippi River and Gulf of Mexico waters. *Earth Planet. Sci. Lett*. **1977**, 37, 242–250.

Hill, H.W., Flower, B.P., Quinn, T.M., Hollander, D.J., Guilderson, T.P. Laurentide Ice Sheet meltwater and abrupt climate change during the last glaciations. *Paleoceanography* **2006**, 21, doi:10.1029/2005PA001186.

Honisch, B., Allen, K.A., Russell, A.D., Eggins, S.M., Bijma, J., Spero, H.J., Lea, D.W., Yu, J. Planktic foraminifers as recorders of seawater Ba/Ca. Mar. *Micropaleontol*. 2011, 79, 52-57.

Joung, D.J., Shiller, A.M. Trace element distributions in the water column near the Deepwater Horizon well blowout. *Environ. Sci. Technol*. **2013**, 47, doi:10.1021/es303167p.

Kolker, A.S., Cable, J.E., Johannesson, K.H., Allison, M.A., Inniss, LV. Pathways and processes associated with the transport of groundwater in deltaic systems. *J. hydrol*. **2013**, 498, 319-334.

Krest, J., Moore, W.S., Rama, J. ^{226}Ra and ^{228}Ra in the mixing zones of the Mississippi and Atchafalaya Rivers: indicators of groundwater input. *Mar. Chem.* **1999**, 64, 129-152.

Lea, D., Boyle, E. Barium content of benthic foraminifera controlled by bottom-water composition. *Nature* **1989**, 388, 751-753.

Lea, D.W., Spero, H.J. Assessing the reliability of paleochemical tracers: Barium uptake in the shells of planktonic foraminifera. *Paleoceanography* **1994**, 9, 445-452.

Li, Y.-H., Chan, L. -H. Desorption of Ba and ^{226}Ra from river-borne sediments in the Hudson estuary. *Earth Planet. Sci. Lett*. **1979**, 43, 343-350.

Li, Y.-H., Burkhardt, L., Teraoka, H. Desorption and coagulation of trace elements during estuarine mixing. *Geochim. Cosmochim. Acta* **1984**, 48, 1879-1884.

Loder, T.C., Reichard, R.P. The dynamics of conservative mixing in estuaries. *Estuaries* **1981**, 4, 64-69.

Lohrenz, S.E., Redalje, D.G., Cai, W.-J., Acker, J., Dagg, M. A retrospective analysis of nutrients and phytoplankton productivity in the Mississippi River plume. *Cont. Shelf Res*. **2008**, 28, 1466-1475.

McCoy, C.A., Corbett, D.R., McKee, B.A., Top, A. An evaluation of submarine groundwater discharge along the continental shelf of Louisiana using a multiple tracer approach. *J. Geophys. Res.* **2007**, 112, C03013, doi: 10.1029/2006JC003505.

Moore, W. S., Krest, J. Distribution of ^{223}Ra and ^{224}Ra in the plumes of the Mississippi and Atchafalaya Rivers and the Gulf of Mexico. *Mar. Chem.* **2004**, 86, 105-119.

Officer, C.B., Lynch, D.R. Dynamics of mixing in estuaries. *Estuar. Coast. Shelf Sci*. **1981**, 12, 525-533.

Rabalais, N.N., Diaz, R.J., Levin, L.A., Turner, R.E., Gilbert, D., Zhang, J. Dynamics and distribution of natural and human-caused hypoxia. *Biogeosci.* **2010**, 7, 585-619.

Shaw, T.J., Moore, W.S., Kloepfer, J., Sochaski, M.A. The flux of barium to the coastal waters of the southeastern USA: The importance of submarine groundwater discharge. *Geochim. Cosmochim. Acta* **1998**, 62, 3047-3054.

Shiller, A.M. Comparison of nutrient and trace element distributions in the delta and shelf outflow regions of the Mississippi/Atchafalaya River. *Estuaries* **1993**, 16, 541-546.

Shiller, A.M. The effect of recycling traps and upwelling on estuarine chemical flux estimates. *Geochim. Cosmochim. Acta* **1996**, 60, 3177-3185.

Shiller, A.M. Dissolved trace elements in the Mississippi River: Seasonal, interannual, and decadal variability. *Geochim. Cosmochim. Acta* **1997**, 61, 4321-4330.

Shiller, A.M. Syringe filtration methods for examining dissolved and colloidal trace element distributions in remote field locations. *Environ. Sci. Technol*. **2003**, 37, 3953 - 3957.

Shim, M.-J., Swarzenski, P.W., Shiller, A.M. Dissolved and colloidal trace elements in the Mississippi River delta outflow after Hurricanes Katrina and Rita. *Cont. Shelf Res*. **2012**, 42, 1-9.

Stecher III, H.A., Kogut, M.B. Rapid barium removal in the Delaware estuary. *Geochim. Cosmochim. Acta* **1999**, 63, 1003-1012.

Thorrold, S.R., Jones, C.M., Campana, S.E. Response of otolith microchemistry to envionmental variations experiences by larval and juvenile Atlantic croaker (Micropogonias undulatus). *Limnol. Oceanogr*. **1997**, 42, 102-111.

van Geldern, R., Barth, J.A.C. Optimization of instrument setup and post-run corrections for oxygen and hydrogen stable isotope measurements of water by isotope ratio infrared spectroscopy (IRIS). *Limnol. Oceanogr.:Methods* **2012**, 10, 1024-1036.

Williams, C., Flower, B.P., Hastings, D.W., Shiller, A.M., Goddard, E.A. A multi-proxy approach to deglacial paleo-salinity reconstructions based on Gulf of Mexico. AGU Fall Meeting **2010** (abstr).

CHAPTER IV

DISTRIBUTIONS OF DISSOLVED ORGANIC CARBON, NUTRIENTS, AND TRACE ELEMENTS IN THE ATCHAFALAYA RIVER BASIN AND THE EFFECT OF THE ATCHAFALAYA RIVER BASIN ON LOUISIANA SHELF WATERS

Introduction

Freshwater wetlands, including marshes, floodplains, and swamps, are an interface between the land and river water, and play an important role in regulating water quality in rivers and ultimately the estuaries and coastal zones fed by those rivers. Within wetlands systems, the nutrients, dissolved organic matter (DOM), and major and trace element distributions can be affected by biological uptake, microbial activity, adsorption onto particles, redox processes, and sedimentation. For example, when floodplains are covered with water by the so-called flood pulse (Junk et al., 1989), the nutrients from river waters can enhance biological productivity in flooded soils and in ambient waters (Bayley, 1995; Fisher and Acreman, 2004). During flooding, trace elements can also be enriched in plant roots, leaves, and stems in wetlands (Weis and Weis, 2004). Bacterial activity in wetlands has been found to be important in DOC production from litter material or removal by respiration (Chow et al., 2012; Mullholland, 1981), and in nutrient and trace element re-mineralization in natural and constructed wetlands (Kosolapov et al., 2004; Gadd, 2004; Olivie-Lauquet et al., 2001; Baldwin and Mitchell, 2000; Vymazal, 2007; Olivie-Lauquet et al., 2001). Denitrification is widely observed in anoxic wetland environments (Booth et al., 2005). Reduced metals can also be re-precipitated onto particles under oxic conditions (Du Laing et al., 2009; Foster and Charlesworth, 1996; Sheoran and Sheoran, 2006). Because of these effects on elemental fluxes, wetlands are

commonly utilized for the treatment of waste waters polluted with nutrients, heavy metals, and organic contaminants (Verhoeven et al., 2006 and references therein; Mays and Edwards, 2001).

Wetlands are sometimes regarded as sinks for the chemical constituents. For example, Emmett et al. (1994) reported a considerable reduction of loads of nitrate (28%), phosphate (94%), silica (21%), DOC (34%), Al (21%), and Fe (54%) after flood water flowed through a wetland of a recently afforested catchment in Wales, UK. Fisher and Aceman (2004) reported that about 80% and 84% of studied 57 wetlands (including both natural and constructed) are found to be reducing N and P, respectively, in the water flowing through the wetlands. By analyzing marsh sediments in a tidal freshwater marsh, Khan and Brush (1994) reported nutrient and trace metal accumulations over several decades related to pollutants from agricultural runoff and wastewater discharge. They suggested that the mechanism of the storage in the high marsh is associated with vegetation and litter uptake and immobilization of these substances as well as direct adsorption of nutrients and metals onto sedimentary organic matter.

Other evidence, however, indicates that some floodplains can act as a source of nutrients and DOC depending on hydrologic conditions (e.g., flooding, precipitation) (Rucker and Schrautzer, 2010; Kerr et al., 2008; Christopher et al., 2006; Seyler and Boaventura, 2003). For example, Mulholland (1981) reported a net annual fluvial export of 21 gC/m^2, which is mostly in dissolved form in watersheds drained by swamp streams in the southeastern United States. Noe and Hupp (2007) found net dissolved inorganic nitrogen (DIN) and phosphate (DIP) export in a largely forested watershed during short-hydroperiod floodings (1-2 days). Using data from 57 wetlands from around the world,

Fisher and Acreman (2004) revealed that about 10% and 13% of studied wetlands act as a source for phosphorus and nitrogen species, respectively.

Trace elements in fluvial systems have also been reported to have seasonal variations related to wetland interactions. For instance, Olivie-Lauquet et al. (2001) found seasonal variation of metal concentrations in a wetland and its recipient streams and river waters, depending on river-wetland connections in relation to redox potential and organic carbon content. Kerr et al. (2008) concluded that the most important effect on trace element export from wetland sediments to streams is seasonal hydrological changes such as the extent of flooding, which flushes DOC and metals from wetland sediments and dilutes groundwater sourced metals.

The Mississippi and Atchafalaya Rivers (MR and AR, respectively) have received attention as the primary source of nutrients to the Louisiana Shelf, an area of seasonal bottom-water hypoxia (Rabalais et al., 1996, 2010; Turner et al., 2007). The Atchafalaya River Basin (ARB) is the largest wetland in North America carrying about 30% of the total flow from the MR and Red Rivers (RR) (Ford and Nyman, 2011). Although the AR is a significant contributor of water, nutrients, and other fluvial materials to the shelf, studies of how the ARB wetlands modify the fluxes of nutrients and DOC are limited (Shen et al., 2012; Turner et al., 2007; Lane et al., 2002), and the basin's effect on trace element fluxes has yet to be determined.

So far, studies in the ARB have found significant alteration of DOC and nutrients in the basin. DOC was found to be about 150% higher in AR compared to MR due to the input from wetlands water in the ARB (Shen et al., 2012). Lambou and Hern (1983) explained that the increased DOC in AR waters was due to primary production within

overflow areas during high river discharge relative to low river discharge. Turner and Rabalais (1991) reported relatively lower nitrate and silicate (31% and 6%, respectively) and higher total phosphorous (30%) in the AR than in the MR, and suggested that these differences were probably due to differences in the contribution from the RR. However, nitrate input from the RR was found to be negligible, accounting for < 3% in comparison to total loading of nitrate from the MR (Turner et al., 2007). Xu (2006a) reported about 27% removal of total Kjeldahl nitrogen by comparing composition of waters entering and exiting the ARB. The removal was closely related to the interaction of river water with the swamp, where denitrification was found to be a major process for nitrogen removal (Xu, 2006a; Lindau et al., 2008; Scaroni et al., 2011).

To date, no studies have examined the effect of the ARB on trace element fluxes to the Louisiana Shelf, though their important roles as micronutrients and toxicants could affect primary productivity and fisheries in the shelf water. However, numerous processes occur in the ARB that could affect trace elements including biological uptake, microbial remineralization of organic matter, and changing redox state as well as input from the RR. For example, Viers et al. (2005) reported that plants along a river and wetlands in the Amazon accumulated metals (Al, Cu, Fe, Mn, Rb) at a rate up to 20% of the dissolved flux of the Solimoes River. And, Olivie-Lauguet et al. (2001) suggested that trace element release in wetlands in France appears to be closely related to microorganism activities, which catalyzed the change in redox condition and induced an increase of DOC.

Here, the results ofthe studies of DOC, nutrient, and trace element distributions in the ARB including the main river channels and surrounded swamps are reported in this

chapter. This study addresses the role of ARB on the transport of chemical constituents to the Louisiana Shelf under differing river discharges.

Methods and Materials

Site description

The Atchafalaya River basin (ARB) has one of the largest and widest floodplains in North America (Ford and Nyman, 2011) (Figure 17). Agriculture is common upstream in the ARB, while downstream retains the *pristine* river floodplain forest including its bayous, lakes, and swamps, which extend about 120 km in length (north to south) and 25-35 km in width (Ford and Nyman, 2011). The east and west boundaries are constrained by levees to prevent flooding, and these levees have isolated large portions of the floodplain from the AR at all but the highest river stages during the spring flood pulse (Fontenot et al., 2001). Construction activities related to navigation, flood control, and oil and gas canals have altered the historic water flow patterns, reduced water circulation, and a large portion of wetland areas in the ARB are experiencing low dissolved oxygen concentrations (Fontenot et al., 2001; Sabo et al., 1999).

Sampling locations (Figure 17) were chosen to include the major water sources to the ARB (MR and RR), the main exits for water into the Atchafalaya Bay (including the mouth of the AR and the Wax Lake outlet), plus other sites in the main channels and swamps throughout the basin. Swamp sampling sites (ARS1-3) were located in the upper part of the Atchafalya swamp, and also include the swamp inner-channel (ARS3), which frequently connects to main river channel. However, during June 2011, when parts of the ARB were flooded due to the opening of the Morganza Spillway, some adjustment of the sampling locations was necessary.

Figure *17*. Sampling locations in the Atchafalaya River basin. The white rectangle in the US map shows the location of the study area. White circles represent sampling locations, and red circles are town/cities.

Sample collection

Sampling campaigns were conducted during April and November 2010, and June 2011 corresponding to the intermediate, low and high river discharges, respectively (Figure 18). During June 2011, unusually high MR discharge resulted in the opening of the Morganza Spillway, inundating large areas of swamp and floodplains in the ARB.

Surface waters were collected for nutrient, dissolved organic carbon (DOC), and trace element samples. Soon after collection, nutrient and DOC samples were filtered in the field using 0.45 µm pore size filters (Whatman Puradisc) and kept in an iced cooler for transport back to the lab where they were frozen until analysis. Trace elements samples were collected at the same time as nutrients and DOC, using clean sampling techniques. An acid-cleaned polyethylene bottle was attached to a non-metallic pole (approximately 5 m length), and the bottle was rinsed 3 times with ambient water. Soon after sample collection, the sample bottle was tightly capped and doubly bagged in new plastic zipper bags and stored in an iced cooler. These samples were then filtered using 0.45 µm (Whatman Puradisc) and 0.02 µm (Whatman Anotop) pore size filters, using acid-cleaned syringes for total and truly dissolved fractions, respectively (Shiller, 2003). The colloidal (0.02-0.45 µm) phase was determined by the difference of the total (< 0.45 µm) and truly (< 0.02 µm) dissolved sizes. This filtration was conducted in a small plastic tent within 2-8 hours of sample collection. A small boat was used for the stations that were not accessible by foot. For ancillary data, portable sensors were used for the determination of conductivity, salinity, and temperature (Model 30, YSI Inc.) and pH (Oakton pH 110 series, USA).

Nutrient, DOC, and trace element analysis

The frozen nutrient and DOC samples were thawed overnight at room temperature just before the measurements. Nutrients were analyzed using an Astoria-Pacific A2C2 nutrient auto-analyzer (Astoria-Pacific International, Oregon USA). The detection limits for nutrient measurement were 0.1, 0.05 and 1 µmol/L for nitrate, phosphate and silicate, respectively. Concentrations of DOC were determined using a Shimadzu TOC-V total organic carbon analyzer employing the high temperature combustion method (Guo et al., 1995). For DOC measurements, samples were acidified with concentrated HCl to pH < 2 before analysis. Concentrations were automatically calculated using the calibration curves that were generated at the beginning of the analytical run. Certified DOC standards (University of Miami) were measured frequently during the run to check the performance of the instrument. Three to five measurements were made for each sample, and the precision were < 2%.

The filtered trace element samples were acidified to pH < 2 by addition of ultra-clean 6 M HCl (Seastar Baseline) at least a week before analysis. For analysis, these samples were then diluted to 33% by addition of 0.3 M HNO_3 containing 17 nM In as an internal standard. Arsenic, Ba, Cd, Co, Cr, Cs, Cu, Fe, Mn, Mo, Ni, Pb, Rb, Re, Sr, U, V, and Zn were analyzed using a sector field-inductively coupled plasma-mass spectrometer (SF-ICP-MS; Thermo-Fisher Element 2). To determine concentrations, standard curves were generated at the beginning of each of the analytical runs. The analytical performance was checked by measuring a standard and blank after every 8 sample measurements during each analytical run. The detection limits are shown in Table 7.

Table 7

Detection limit of the studied trace elements (nmol/kg; n=26)

	As	Ba	Cd	Co	Cr	Cs	Cu	Fe	Mn
Detection Limit	0.7	0.3	0.01	0.02	0.08	0.002	0.04	0.6	0.05
	Mo	Ni	Pb	Rb	Re	Sr	U	V	Zn
Detection Limit	0.04	0.2	0.002	0.01	0.001	1.2	0.02	0.2	0.5

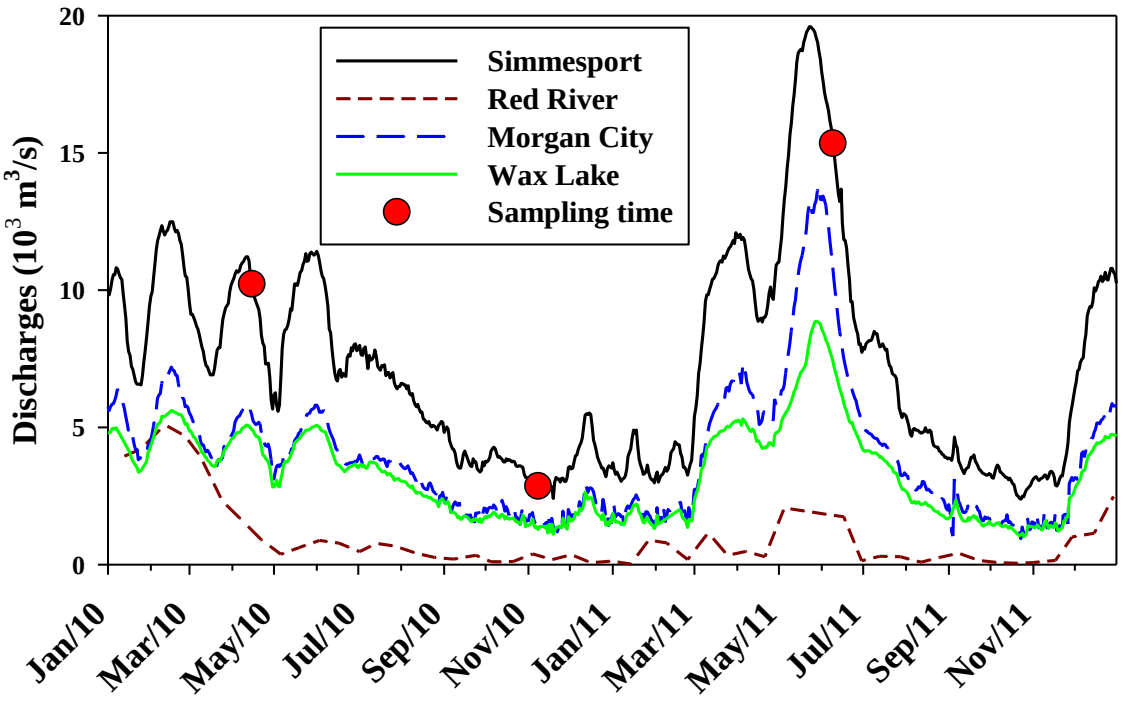

Figure 18. River discharges (10^3 m^3/s) in the Atchafalaya River Basin and sampling time.

River discharge, input and export fluxes estimation

Hydrological data was obtained from the US Army Corps of Engineers (http://www.mvn.usace.army.mil/). For the RR input to the ARB, the discharge from Alexandria and Acne, LA were combined (Figure 1). For the MR flow into the ARB, the discharge was obtained by subtracting of the RR input from the discharge at Simmesport, LA. The MR flow to the Louisiana Shelf was taken from the gage at Tarbert Landing, MS, which is located below the Old River Control Structure where the MR division is located.

The export flux from the ARB was estimated by combining the export flux of the AR mainstem (AR10) with that from the Wax Lake outlet (ARWL). At each site, the flux was calculated by multiplying the concentration of material at AR10 and ARWL with discharge at Morgan City and Wax Lake, respectively. The input flux of material to the ARB was estimated by combining the input fluxes of the RR and MR, with the flux at each site calculated by multiplying the river concentrations with the discharges from the RR and MR.

Results and Discussion

River discharges varied significantly with season (Figure 18). Discharge for the AR at Simmesport, LA was 10.2 x 10^3 and 2.8 x 10^3 m^3/s during April and November 2010, respectively; whereas, it was 15.9 x 10^3 m^3/s during June 2011. Other ancillary parameters such as pH, conductivity, and temperature, as well as the results of DOC, nutrients, and trace elements are listed in Tables Appendix and Figures 19-22.

DOC concentrations were higher in the RR than the MR during our study (Figure 3 and Tables A1-A3). The DOC concentrations showed low variability along the river flow from AR1 to AR outlets (AR10 and ARWL) with the exception of the DOC maximum at the middle of basin (AR4) during April and November 2010. At the most eastern (ARE1) and western (ARW1) sides of basin, the DOC concentrations were higher than in the AR main channel and decreased toward the main channel in April and November 2010. In swamp waters (ARS1-3), DOC concentrations were in general about 2-3-fold higher than the concentrations in the AR main channel waters throughout the seasons.

Nitrate and silicate concentrations were higher in the MR than RR in all sampling periods. Phosphate was also slightly higher in the MR than the AR during April and

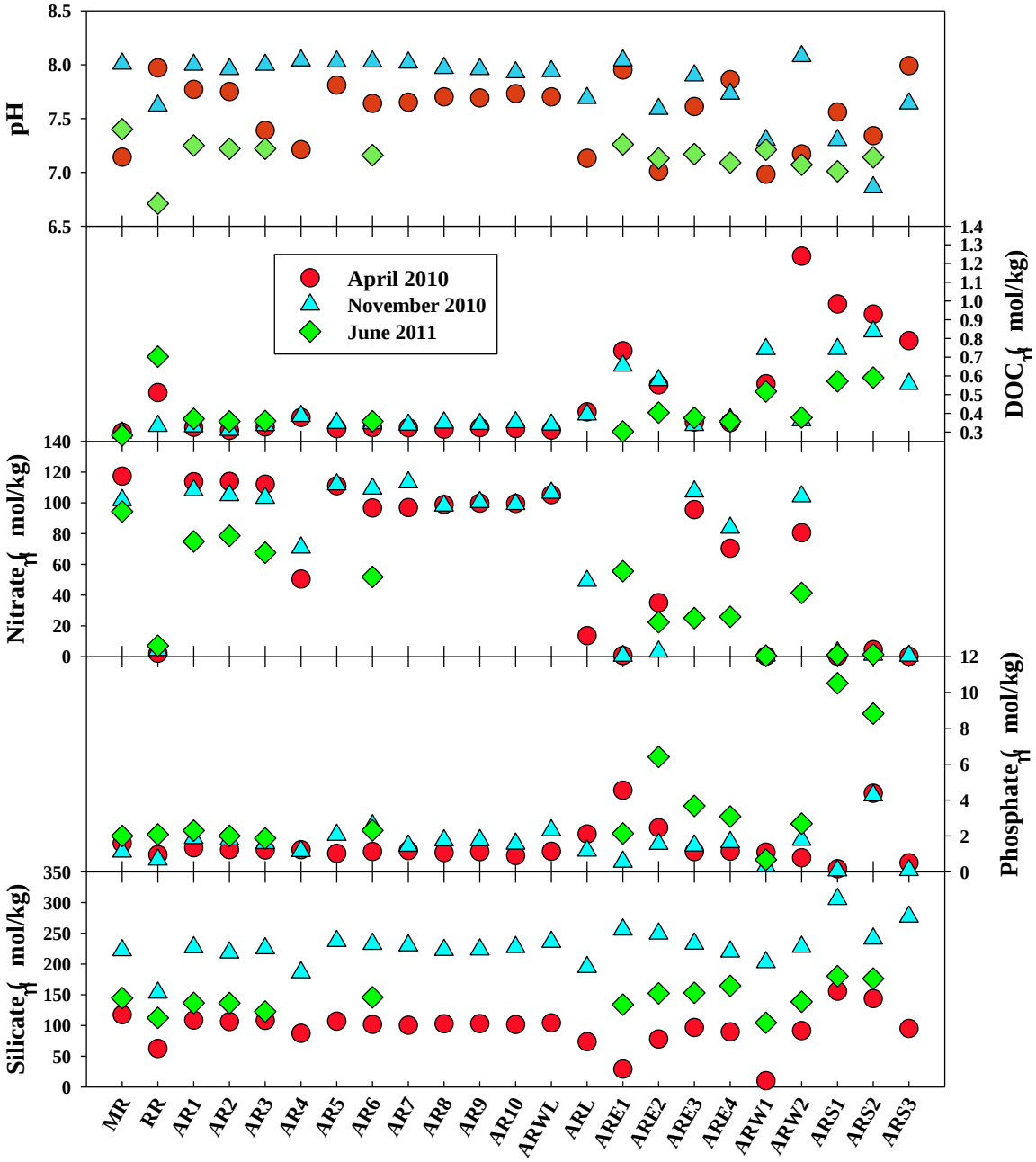

Figure 19. Distributions of pH, DOC, nitrate, phosphate and silicate during April (circle) and November (triangle) 2010, and June 2011 (diamond).

November 2010, although concentrations were comparable in both rivers during June 2011. At the mid-basin station where the DOC maximum was observed (AR4), nitrate and silica showed a minimum during April and November 2010; however, phosphate

showed a minimum only in November and not in April 2010. In the lower basin (AR6-10) and the Wax Lake (ARWL) outlet, nutrient concentrations generally showed little variability. At the most east (ARE1) and west (ARW1) sides of the basin, nitrate concentrations were lower than in the AR main channel and increased toward the main channel in April and November 2010. Phosphate showed in general decreased toward the main channel in April 2010 and June 2011, while it showed increasing during November 2010. During November 2010, silica decreased toward the AR mainstem, whereas during April 2010 and June 2011, it showed an increasing trend. Swamp waters showed very low nitrate concentrations regardless of season. Phosphate concentrations in waters from swamps were lower than the concentrations in the mainstem of the AR except during June 2011 as well as waters from the ARS2. Silica concentrations in swamp waters were higher in comparison to main channel waters. Ammonia and nitrite were generally very low throughout the basin, less than 1% of the nitrate concentrations, except the swamp waters, where ammonia was as high as 20 μmol/kg during November 2010.
Dissolved trace element distributions are shown in Figures 20-22 (or Appendix). Most of the studied trace elements were mainly in the truly dissolved fraction except Cr, Cs, Fe, Pb, and Zn. Fe and Pb were mostly in the colloidal phase accounting for > 80% of the total dissolved (< 0.45 μm) pool. For Cr, Cs, and Zn, the colloidal (0.02-0.45 μm) phase was considerable accounting for over 50% for many samples.

Dissolved Cd, Cu, Re, U, and Mo concentrations were higher in the MR than in the RR during our sampling campaigns, whereas Cs, Fe, Mn and Rb were higher in the RR. Other elements such as Ba, Co, Cr, Ni, Pb, Sr, V and Zn showed seasonality. For example, Ba was higher in MR than RR during June 2011, but it was lower in MR than

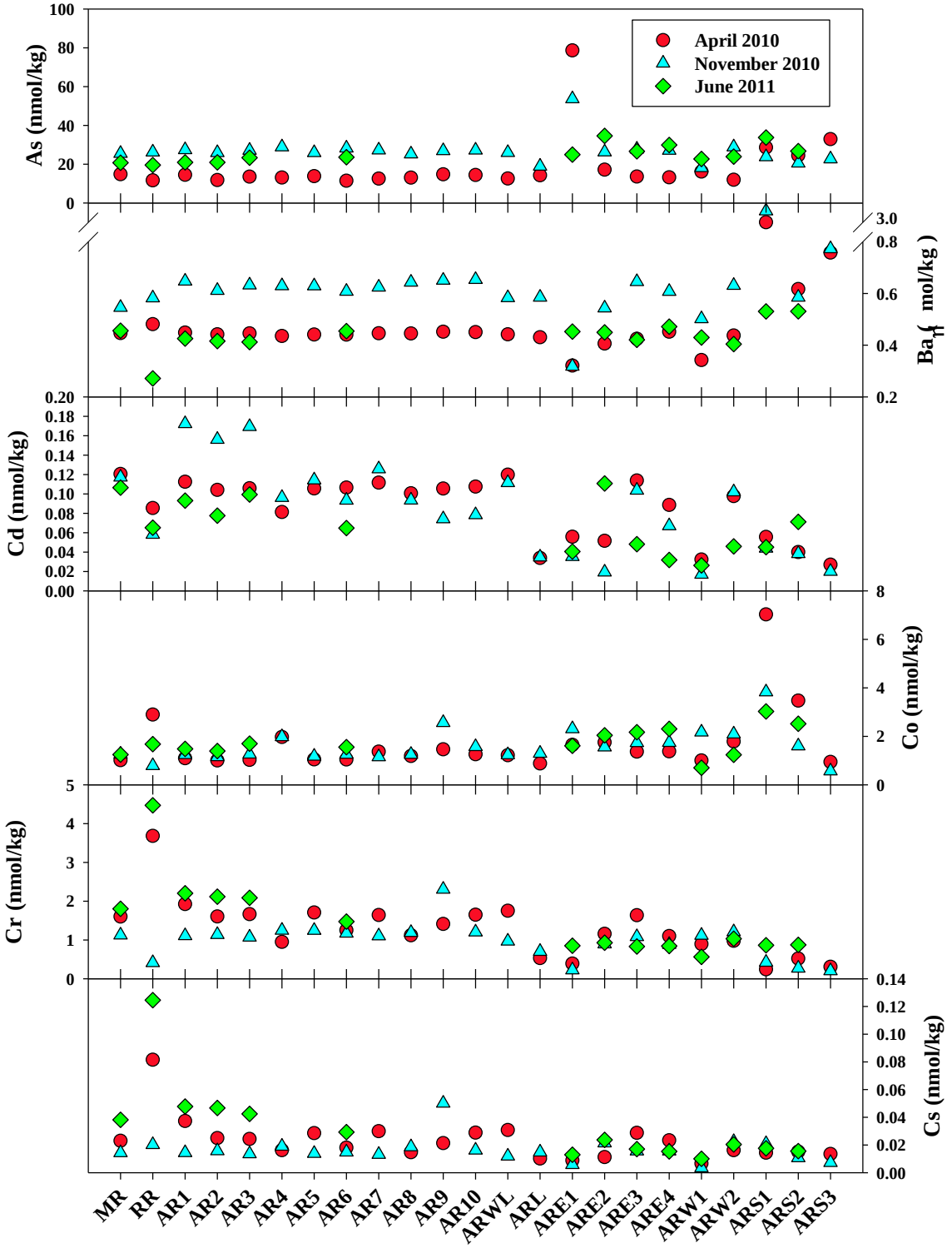

Figure 20. Distributions of As, Ba, Cd, Co, Cr, and Cs during April (circle) and November (triangle) 2010, and June 2011 (diamond).

RR during the other sampling campaigns. In general, Cd, Cr, Cs Fe, Mn, Pb, and Zn were higher during April 2010 and June 2011 than during November 2010 in the mainstem of the AR. In contrast, concentrations of As, Ba, Cu, Mo, Ni, Re, Sr, U, and V were higher in the AR mainstem during November 2010 than the other two periods. Other elements, including Co and Rb did not show significant seasonal variation. In the mid-basin (AR4) where the DOC maximum and low nitrate concentration were observed, dissolved Cd, Re, U, and Ni concentrations showed a minimum, whereas a maximum was observed for Fe, Mn and Co. In swamp waters, Fe, Mn, and Co were enriched in comparison to the main channel waters, whereas Cd, Ni, Cs, Re, V, Cr, Pb, Cu, and Mo were relatively low in swamp waters. Other elements such as As, Ba, Rb, Sr, and Zn showed similar concentrations in the mainstem and swamp waters.

Distributions of DOC, nutrients, and trace elements

Seasonal variations of DOC, nutrients, and trace elements were observed in the ARB as well as the MR and RR (Figure 19-22, Appendix). In the MR water, DOC, nutrient, and trace element concentrations were similar to previous reports (Shen et al., 2012; Duan et al., 2007; Bianchi et al., 2004; Dubois et al., 2010; Shiller, 1997, 2002). The seasonal variations of DOC, nutrients, and some trace elements in the MR have been suggested to result from temporal changes in tributary contributions (e.g., Ohio, Missouri, and Upper Mississippi Rivers) to the MR main stem (Duan and Bianchi, 2006; Duan et al., 2007; Shiller, 1997, 2002) and from redox effects (Shiller, 1997, 2002; Shiller and Stephens, 2005). Similar processes likely cause the seasonal concentration variations in the RR.

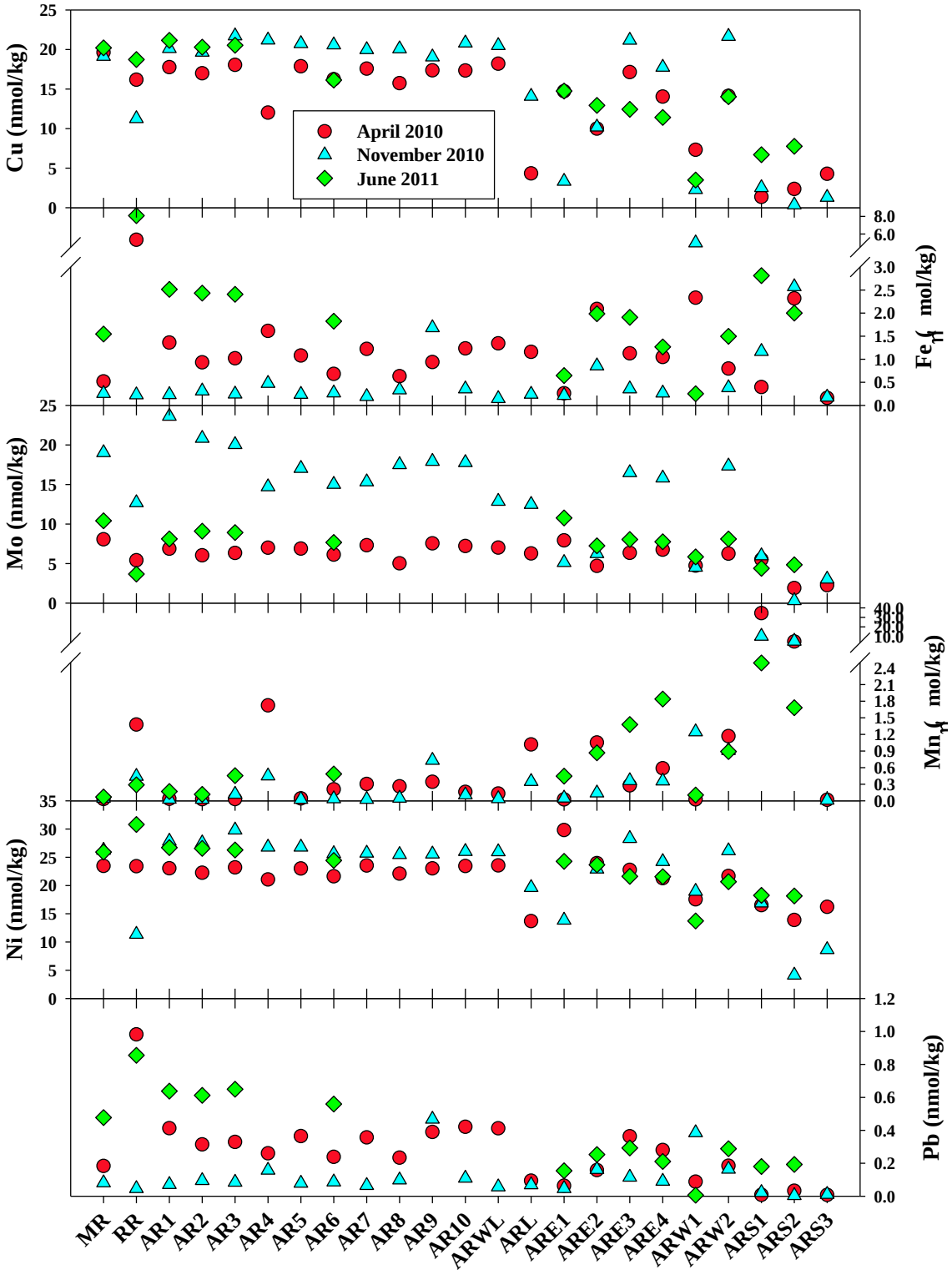

Figure 21. Distributions of Cu, Fe, Mo, Mn, Ni, and Pb during April (circle) and November (triangle) 2010, and June 2011 (diamond).

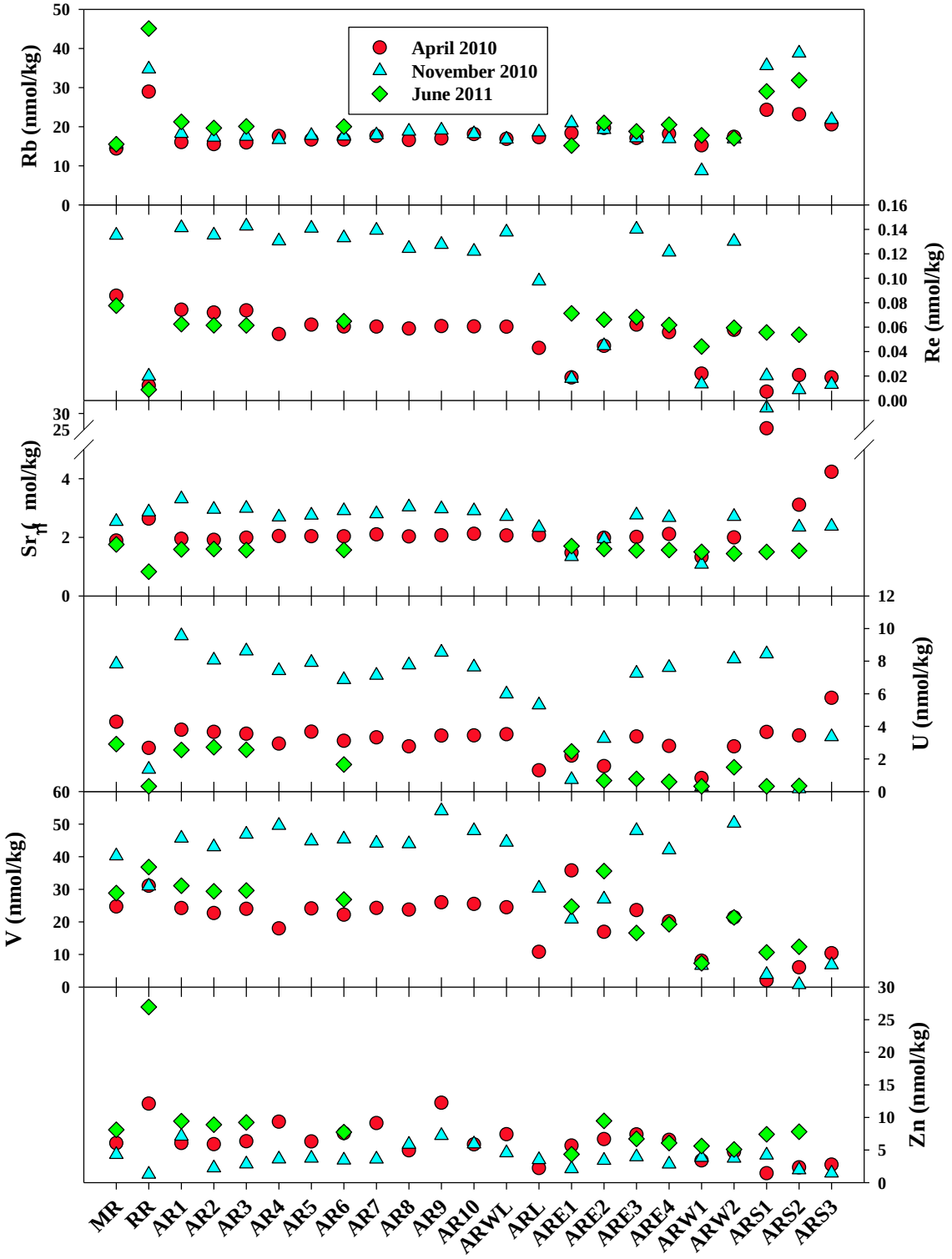

Figure 22. Distributions of Rb, Re, Sr, U, V, and Zn during April (circle) and November (triangle) 2010, and June 2011 (diamond).

In the ARB waters, DOC and nutrient concentrations were similar to what has been observed previously in this environment (Shen et al., 2012; Lambou and Hern, 1983; Turner et al., 2007; Xu, 2006a, b; Turner and Rabalais, 1991). The enrichment of DOC in swamp waters as well as eastern (ARE1) and western (ARW1) basin waters likely reflects decomposition of plant detritus (Lambou and Hern, 1983). The depletion of nitrate and phosphate in the swamp as well as the east and west sides of ARB, may be attributed to biological activity such as uptake and/or denitrification as well as ammonification (Lindau et al., 2008; Scaroni et al., 2010, 2011; Strohm et al., 2007), and formation of ferrous phosphate minerals (e.g., vivianite) under organic-enriched, anoxic conditions (Withers and Jarvie, 2008; House, 2003). The high ammonium concentrations may have been derived from decomposition of wetland vegetation, as observed in other natural wetlands (Garcia-Garcia et al., 2009). This biogeochemistry may have resulted in spatial variations of DOC and nutrients among the swamp waters.

Trace elements in the ARB can be controlled by complexation with DOC, redox reactions, and microbial re-mineralization among other processes. Although other workers have found correlations between dissolved Fe and DOC (Mora et al., 2010; Olivie-Lauquet et al., 2001; Pokrovsky and Schott, 2002; Kuchler et al., 1994; Viers et al., 1997, 2000), the DOC and Fe (both phases: colloidal (0.02-0.45 μm) and truly dissolved (< 0.02 μm)) were not correlated in the swamp or in the AR mainstem (Figure 23). However, pH and Fe are negatively correlated for both the colloidal (0.45-0.02 μm) and truly dissolved phases (< 0.02 μm) (Figure 24). This pH-Fe relationship has been observed in other fluvial environments (Ponter et al., 1990; Brick and Moore, 1996), and may indicate that Fe(II) predominates at a lower pH. For Mn, the correlations with DOC and

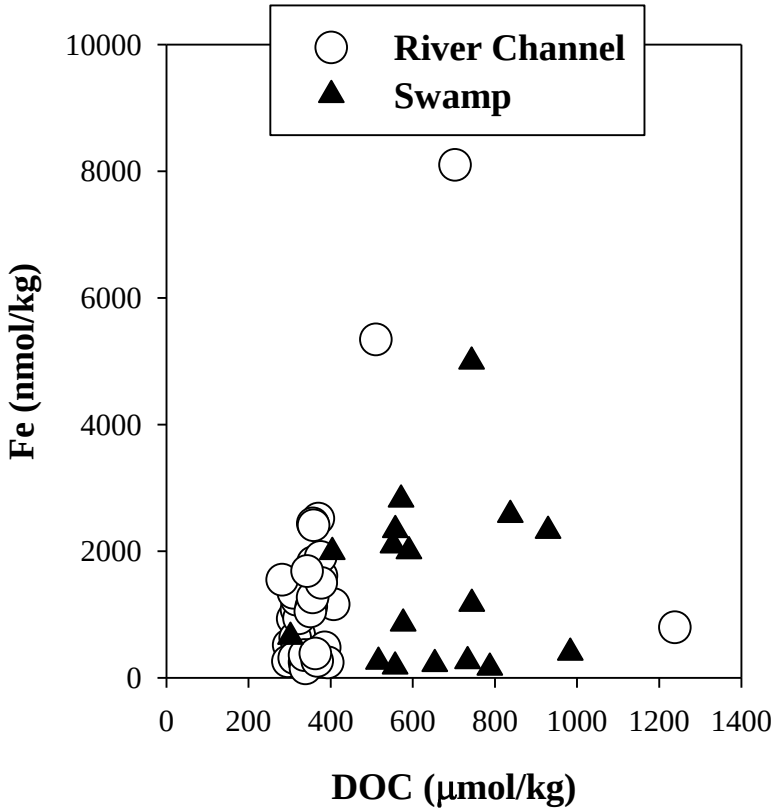

Figure 23. Fe distribution with DOC in the river channel (circle) and swamp (triangle) waters. We note that water samples from ARW1, ARE1 and ARE2 were treated as swamp type of water due to similar characteristics of pH and conductivity as well as dark brown color between these stations and swamps.

pH are not observed. However, the Mn concentrations in the swamp waters were much greater when compared to the AR main channel, probably due to reductive dissolution of Mn (Olivie-Lauquet et al., 2001). Nonetheless, Mn does not correlate with Fe, which may reflect the slow oxidation of Mn in comparison to Fe (Martin, 2005). That is, the reduced Fe rapidly forms Fe-hydroxide and re-precipitates, whereas the reduced Mn remains in solution, resulting in higher Mn concentrations than Fe in the swamp waters.

Fe/Mn-(oxy)hydroxide could also influence trace element distributions by either adsorbing upon reductive dissolution of these metal-oxides/oxyhydroxidesdepending on redox conditions. In the mainstem of the AR, positive correlations are observed between

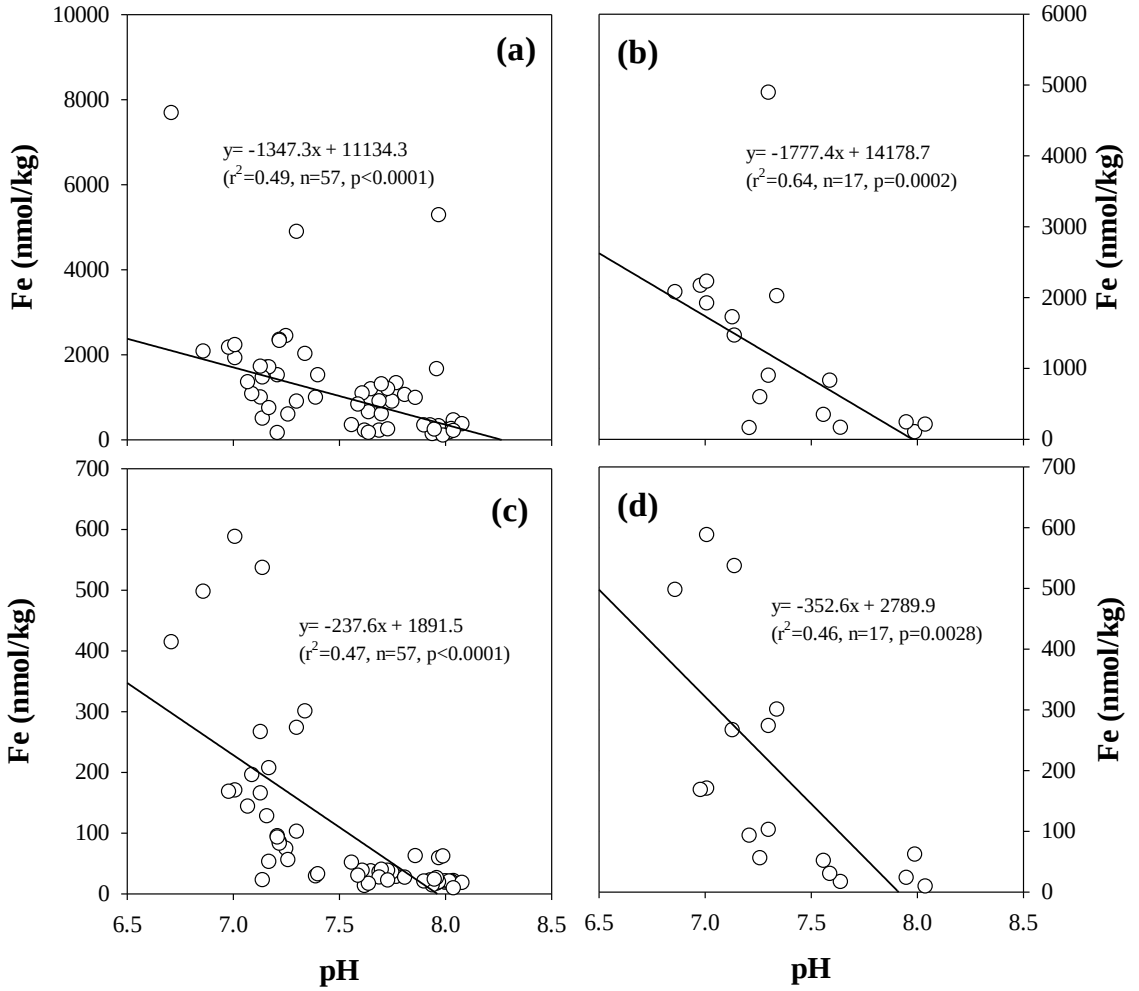

Figure 24. Plots of (a) colloidal Fe versus pH with all sites and (b) in the swamp waters, and (c) dissolved Fe with pH in all sites and (d) in swamp waters. All sites include results from river channel and swamp waters. For regression calculation, three data points (RR for April 2010 and June 2011, and ARW1 for November 2010) were eliminated due to unusually high concentrations. Water samples from ARW1, ARE1, and ARE2 were treated as swamp type of water due to similar characteristics of pH and conductivity as well as dark brown color between these stations and swamps.

colloidal Fe and colloid Cr, Cs, Pb, and Zn regardless of season (Figure 25). However, the truly dissolved Fe (< 0.02 μm) is not correlated with the truly dissolved Cr, Cs, Pb, and Zn. These observations suggest the removal of Cr, Cs, Pb, and Zn by adsorption onto the Fe/Mn-(oxy)hydroxide is important in the AR waters. Adsorption of Co, Cr, Zn, and Pb with Fe/Mn-(oxy)hydroxide is well-known (Zachara et al., 2001; Means et al., 1978; Johnson, 1992; Brick and Moore, 1996; Shiller, 1997; Pokrovsky and Schott, 2002). Due

to its particle reactive nature, Cs could also be adsorbed on Fe oxides (Gossuin et al., 2002). However, in swamp waters these relationships were only observed for Mn vs. Co, and no correlations were observed for the elements with Fe (both phases). The lack of correlation is probably due to a much higher Fe concentration than the other elements in the swamp waters, which makes it difficult to observe small the changes of these elements relative to much higher (at least 2-3 magnitudes) Fe concentration.

Redox-sensitive elements, Re, Mo, U, and V showed low concentrations at a lower pH, which may be related to removal of these elements by adsorption onto sediment surfaces under reducing conditions (Tribovillard et al., 2006; Elbaz-Poulichet et al., 1997).

Contribution of DOC, nutrients and trace elements from Red River and wetlands

As mentioned, AR is a major distributary of the MR, carrying 30% of the combined flow of the MR and the RR. That is, the MR chemical composition entering the ARB could be modified by the inputs from the RR and wetlands, and these inputs are perhaps most important for the chemical constituent fluxes through the AR onto the Louisiana Shelf.

Input from the Red River

The ARB input of DOC, nutrients, and trace elements from the RR relative to the MR is listed in Table 2. The contributions of DOC from RR account for over 20% of the DOC entering the ARB during April 2010 and June 2011 and 10% for November 2010, which are comparable to a recent study reporting ~ 11% (Shen et al., 2012). This distribution is probably due to the substantially higher DOC concentration in the RR than in the MR (Appendix). Similar to previous reports (Xu and Bryantmason, 2011;

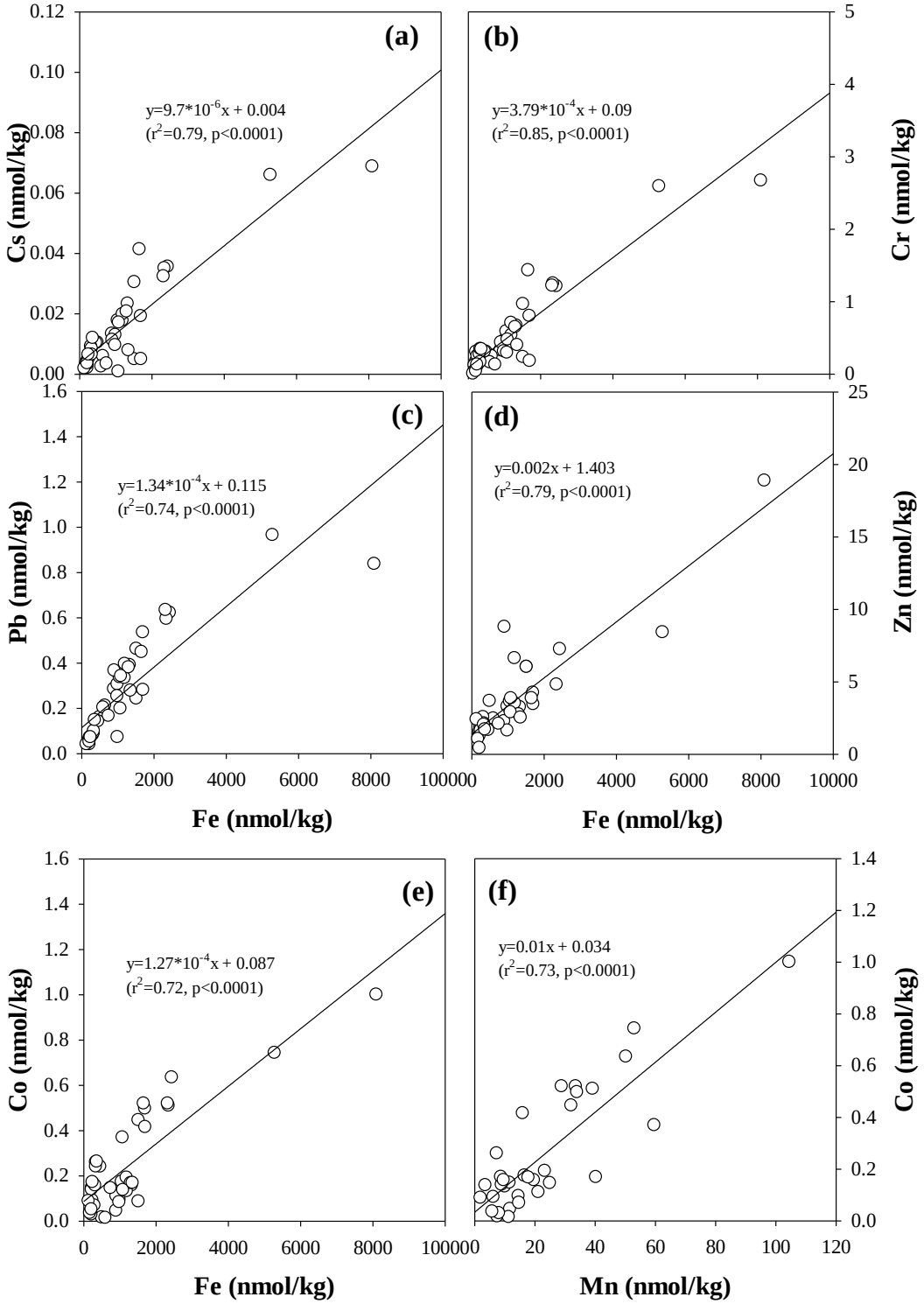

Figure 25. Graphs of colloidal fractions of Fe versus (a) Cs, (b) Cr, (c) Pb, (d) Zn (e) Co, and (f) colloidal fractions of Mn with Co in mainstem of AR (n=43). Samples from the stations such as ARW1, ARE1 and ARE2 were excluded in the linear regression due to their swamp type of water characteristics.

Turner et al., 2007), the contribution of the RR to nitrate in the ARB was less than1% due to the very low RR nitrate concentration. However, phosphate and silicate from the RR were responsible for up to 10% of the basin input due to comparable concentrations of phosphate and silicate in the RR and the MR.

The RR was a significant source of some trace elements to the AR (Table 8). For example, during April 2010 and June 2011, the RR contributed more than 20% of the ARB dissolved input of Co, Cr, Cs, Mn, Fe, Pb, Rb, and Zn due to the 5-10-fold higher RR concentrations of these elements as compared with the MR. During November 2010, the RR contributions of these elements were relatively low in comparison to the other two periods because of both the seasonally low RR concentrations and also the low RR hydrologic contribution to the AR. Manganese was the most extreme case in that its concentration was 45-fold higher in the RR than the MR in April 2010, and 5-10-fold greater during November 2010 and June 2011. This distribution indicates that about 87% of Mn loading into the ARB was derived from the RR during April 2010 and ~ 40% for the other two periods. These facts indicate that the RR can play an important role in the DOC, nutrient, and trace element input to the ARB, and also ultimately to the Louisiana Shelf.

In Table 8, the estimations of the initial composition of the ARB on conservative, discharge-weighted mixing of RR and MR concentrations with observed concentrations from AR1 were compared. Differences between the two numbers reflect both non-conservative mixing (e.g., adsorption/desorption due to differences in pH, DOC, and SPM) as well as additional inputs to the AR as it flows through the northern part of the floodplain. To account for both analytical error and possible short-term temporal variability in river concentrations as well as uncertainty in river mixing ratios, the

Table 8

Differences between field and estimated data at AR1

	Discharge	Contribution	DOC	NO_3	PO_4	SiO_3
	(m^3/day)	(%)		(µmol/L)		
April 15-16, 2010						
MR	7.51E+08	87	298	117.3	1.6	117
RR	1.10E+08	13	510	2.1	1.0	62
AR1	8.61E+08		325	113.6	1.3	109
Estimated			325	102.8	1.5	110
*Differences (%)			***0***	***-10***	***14***	***2***
RR contribution (%)			***20***	***0.3***	***8***	***7***
November 8-10, 2010						
MR	2.35E+08		296	101.8	1.1	222
RR	2.43E+07	91	332	4.3	0.7	153
AR1	2.59E+08	9	330	108.2	1.9	227
Estimate			299	92.9	1.1	216
*Differences (%)			***-9***	***-14***	***-42***	***-5***
RR contribution (%)			***10***	***0.4***	***6***	***6***
June 9-10, 2011						
MR	1.17E+09	88	282	94.3	2.0	145
RR	1.61E+08	12	703	7.0	2.1	112
AR1	1.33E+09		370	74.9	2.3	137
Estimate			333	83.7	2.0	141
*Differences (%)			***-10***	***12***	***-13***	***3***
RR contribution (%)			***26***	***1***	***13***	***10***

	Cd	Cs	Re	Pb	U	V	Cr	Mn	Fe
					(nmol/kg)				
April 15-16, 2010									
MR	0.12	0.02	0.09	0.18	4.3	24.7	1.6	31	518
RR	0.09	0.08	0.01	0.98	2.7	31.1	3.7	1375	5341
AR1	0.11	0.04	0.07	0.41	3.8	24.2	1.9	35	1359
Estimated	0.12	0.03	0.08	0.28	4.1	25.5	1.9	200	1125
*Differences (%)	***3***	***-18***	***3***	***-31***	***7***	***5***	***-3***	***468***	***-17***
RR contribution (%)	***9***	***34***	***2***	***44***	***8***	***15***	***25***	***87***	***60***
November 8-10, 2010									
MR	0.12	0.01	0.14	0.08	7.8	40.3	1.1	48	258
RR	0.06	0.02	0.02	0.05	1.4	31.0	0.4	442	228
AR1	0.17	0.01	0.14	0.07	9.6	45.7	1.1	30	232
Estimate	0.11	0.01	0.12	0.08	7.2	39.4	1.1	84	255
*Differences (%)	***-35***	***4***	***-12***	***10***	***-24***	***-14***	***-4***	***176***	***10***
RR contribution (%)	***5***	***12***	***1***	***5***	***2***	***7***	***4***	***48***	***8***

Table 8 (continued).

	Cd	Cs	Re	Pb	U	V	Cr	Mn	Fe
	(nmol/kg)								
June 9-10, 2011									
MR	0.11	0.04	0.08	0.48	2.9	28.9	1.8	68	1547
RR	0.07	0.12	0.01	0.86	0.3	36.8	4.5	289	8098
AR1	0.09	0.05	0.06	0.64	2.6	31.1	2.2	168	2514
Estimate	0.10	0.05	0.07	0.52	2.6	29.8	2.1	95	2340
*Differences (%)	***9***	***2***	***11***	***-18***	***2***	***-4***	***-3***	***-44***	***-7***
RR contribution (%)	***8***	***31***	***2***	***20***	***1***	***15***	***25***	***37***	***42***
	Co	Ni	Cu	Zn	Rb	Sr	Mo	Ba	As
	(nmol/kg)								
April 15-16, 2010									
MR	1.0	23.5	19.6	6.1	14.4	1887	8.1	447	14.8
RR	2.9	23.4	16.2	12.1	28.9	2635	5.4	481	11.6
AR1	1.1	23.0	17.8	6.1	16.0	1947	6.9	448	14.5
Estimated	1.3	23.5	19.2	6.8	16.2	1981	7.7	451	14.4
*Differences (%)	***14***	***2***	***8***	***12***	***1***	***2***	***13***	***1***	***-1***
RR contribution (%)	***29***	***13***	***11***	***22***	***22***	***17***	***9***	***13***	***10***
November 8-10, 2010									
MR	1.3	26.2	19.1	4.3	15.5	2540	19.0	546	25.5
RR	0.8	11.4	11.3	1.3	34.7	2866	12.7	583	26.2
AR1	1.2	27.8	20.1	7.1	18.3	3313	23.6	647	27.4
Estimated	1.2	24.9	18.4	4.0	17.2	2570	18.4	549	25.6
*Differences (%)	***-2***	***-11***	***-8***	***-43***	***-6***	***-22***	***-22***	***-15***	***-7***
RR contribution (%)	***6***	***4***	***6***	***3***	***18***	***10***	***6***	***10***	***9***
June 9-10, 2011									
MR	1.2	25.9	20.2	8.1	15.5	1757	10.4	456	20.7
RR	1.7	30.8	18.7	26.9	45.1	828	3.7	271	19.5
AR1	1.5	26.7	21.2	9.4	21.2	1589	8.1	425	20.9
Estimated	1.3	26.5	20.0	10.4	19.1	1645	9.6	434	20.6
*Differences (%)	***-12***	***-1***	***-5***	***10***	***-10***	***4***	***18***	***2***	***-2***
RR contribution (%)	***16***	***14***	***11***	***31***	***29***	***6***	***5***	***8***	***11***

*Differences (%) is calculated by ((Estimate – AR1)/AR1) x 100).

differences between estimated and observed concentrations lower than 20% (10% for DOC) were ignored. With that restriction, most constituents mixed approximately conservatively.

Among DOC and the nutrients, only phosphate during one sampling (November 2010) was observed to mix non-conservatively. Among the trace elements, As, Ba, Co,

Cs, Cr, Cu, Fe, Ni, Re, Rb, and V always mixed roughly conservatively. Only Mn was observed to behave non-conservatively during all three samplings, showing removal in April and November 2010 and addition during June 2011. During April 2010, Pb showed addition with only Mn showing removal. During November 2010, Cd, Mo, PO_4, Sr, U, and Zn showed addition with Mn again being the only element to show removal. During June 2011, Mn and Pb showed addition with no elements indicating removal. Note that overland flow of MR water due to the opening of the Morganza Spillway in May/June 2011 provided an input unaccounted for in our flow-weighted constituent estimate at that time. However, the extra ~4000 m^3/s flow through the spillway (Falicini et al., 2012) only changes the water mixing ratio slightly, even assuming that all of this flow reached AR1 (which it did not).

Because mixing experiments were not performed, it is difficult to ascribe causes to the apparent non-conservative behaviors. Because the upper AR is highly channelized, it seems more likely that observed increases in constituent concentrations are due to a process such as desorption rather than to an input from the surrounding floodplain. We also note that the least amount of non-conservative behavior was observed during the highest discharge (June 2011) and the greatest amount during the lowest discharge (November 2010). This behavior either indicates that at a low discharge additional sources (hyporheic or anthropogenic) are relatively more important or that increased velocity at a high discharge means there is less time for non-conservative desorptive input. That Mn is the only constituent to show removal may indicate that the Mississippi River is *seeding* the more Mn-rich Red River waters with Mn-removing microbial activity (e.g., Shiller and Stephens, 2005).

Interaction with wetlands in the ARB

Another important factor potentially altering the chemical constituents in the ARB is input from the wetlands. Though conservative behavior appears to characterize the mixing of most of the studed trace elements up to the AR sampling location, there were sudden increases concentrations of DOC, Co, Fe, Mn, and Zn, and decrease concentrations of NO_3, SiO_3, Cd, Cr, and Ni at mid-basin (AR4) during April and November 2010. With flow beyond AR4 (i.e., AR5) the concentrations of these elements became similar to these measured of AR2. Although these distributions were compatible with the input from the wetlands, this dramatic change was probably due to the incomplete mixing of waters from the wetlands and the river at AR4. Nonetheless, the element distributions in the mid-basin clearly indicated that there was an input (or interaction) from the surrounded wetlands or groundwater.

In Table 9, the input and output fluxes for the chemical constituents in the ARB by comparing them between AR1 and the combined AR outflows at the AR mouth (AR10) and Wax Lake delta (ARWL) were estimated. Again, the AR1 composition already accounts for the RR input and in-stream process (e.g., desorption) until that point. Thus, the differences between the upper (AR1) and lower the ARB (AR10+ARWL) portions of the AR likely reflect interaction with the wetlands, inputs from the eastern and western river flows, groundwater, and anthropogenic point sources. However, flux from the eastern and western sides of the ARB may be negligible due to a very low river inflow.

The DOC export fluxes differed less than 10% from the input during April and November 2010, which were within uncertainty restriction of 10%. During June 2011,

the DOC export was about 20%, probably due to the increase of inundation of the ARB at the time of additional input of MR water through Morganza spillway. For nutrients, the differences of export relative to input for nitrate and silica were within our uncertainty restriction of 20%. However, during June 2011, the ARB was a sink for nitrate. Phosphate was removed in the ARB during April 2010, whereas during the other two sampling compaigns, the basin was a source of phosphate to the river. For trace elements, the differences varied substantially among the elements as well as the seasons. During April 2010, the basin worked as a sink for Mn and Re by removing up to 40% (Mn), whereas the basin was a source for Pb. During November 2010, the basin removed Cd, Mn, and Mo up to 22% relative to input. During June 2011, Co, Mn and Pb were significantly higher in their export fluxes, whereas Cd, Cr, Cs and U were higher in their input fluxes.

Given our swamp water results, the input-output flux differences of the DOC, Cd, Cr, Cs, Mo, and U are compatible for the inputs from the wetlands. However, for Mn and Pb, the wetlands inputs may not fully explain the apparent removal of Mn in April and November 2010, and addition of Pb in April 2010 and June 2011 due to the fact that Mn and Pb concentrations were greatly higher and depleted, respectively, in the swamp waters than in the main river channel waters. Thus, the inputs from the wetlands should supposedly have an increased Mn or decreased Pb, which did not in our input-output estimation. This Mn and Pb distribution may be due to Mn oxidation in the hyporheic zone (Harvey and Fuller, 1998) or anthropogenic Pb input from the Mogan City. In June 2011, the high river flow may have increased the suspended particulate matter in the river, enhancing Mn desorption, or high river velocity may reduce hyporheic Mn oxidation, resulting in greater export than input at this time.

Table 9

Estimated input and export fluxes during April and November 2010, and June 2011

	Discharge*	DOC	NO_3	PO_4	SiO_3
	(m^3/day)		(10^3 kg/day)		
April 15-16, 2010					
Input	8.61E+08	3356	1239	40	2568
Export	8.72E+08	3278	1252	12	2420
MR	2.05E+09	7334	3365	101	6497
Export -Input (%)**		***-2***	***1***	***-224***	***-6***
AR/(AR+MR) (%)***		***31***	***27***	***11***	***27***
November 8-10, 2010					
Input	2.59E+08	932	337	9	1513
Export	2.48E+08	1027	358	15	1553
MR	6.00E+08	2132	855	21	3602
Export -Input (%)**		***9***	***6***	***42***	***3***
AR/(AR+MR) (%)***		***33***	***30***	***42***	***30***
June 9-10, 2011					
Input	1.33E+09	5322	1561	83	5062
Export	1.58E+09	6760	1144	113	6210
MR	3.01E+09	10186	3973	187	11754
Export -Input (%)**		***21***	***-36***	***26***	***18***
AR/(AR+MR) (%)***		***40***	***22***	***38***	***35***

	Cd	Cs	Re	Pb	U	V	Cr	Mn	Fe
	(kg/day)								
April 15-16, 2010									
Input	11.2	3.5	12.3	50.8	834	1120	83	9454	54232
Export	11.1	3.5	9.8	75.4	722	1109	77	6875	63006
MR	27.7	6.3	32.8	78.1	2085	2581	171	3445	59485
Export -Input (%)**	***0***	***0***	***-25***	***33***	***-16***	***-1***	***-8***	***-38***	***14***
AR/(AR+MR) (%)***	***29***	***36***	***23***	***49***	***26***	***30***	***31***	***67***	***51***
November 8-10, 2010									
Input	3.2	0.5	6.0	4.2	447	521	14	1192	3706
Export	2.7	0.5	6.0	4.2	400	583	14	973	3427
MR	7.9	1.1	15.2	10.1	1118	1232	35	1570	8666
Export -Input (%)**	***-22***	***-12***	***0***	***0***	***-12***	***11***	***-3***	***-22***	***-8***
AR/(AR+MR) (%)***	***25***	***29***	***28***	***29***	***26***	***32***	***28***	***38***	***28***
June 9-10, 2011									
Input	15.1	8.6	17.3	144.9	824	2026	147	6971	174581
Export	11.4	6.1	19.1	183.4	621	2158	121	42041	160969
MR	35.9	15.3	43.7	298.8	2086	4429	282	11326	260778
Export -Input (%)**	***-33***	***-43***	***10***	***21***	***-33***	***6***	***-22***	***83***	***-8***
AR/(AR+MR) (%)***	***24***	***29***	***30***	***38***	***23***	***33***	***30***	***79***	***38***

Table 9 (continued).

	Co	Ni	Cu	Zn	Rb	Sr	Mo	Ba	As
	(kg/day)								
April 15-16, 2010									
Input	64	1212	1041	388	1187	150123	632	53211	929
Export	64	1229	977	385	1292	160279	588	53230	878
MR	123	2885	2534	820	2507	340389	1570	125450	2271
Export -Input (%)**	***0***	***1***	***-7***	***-1***	***8***	***6***	***-7***	***0***	***-6***
AR/(AR+MR) (%)***	***34***	***30***	***28***	***32***	***34***	***32***	***27***	***30***	***28***
November 8-10, 2010									
Input	19	387	301	69	380	58647	454	19515	498
Export	20	387	323	85	368	61193	358	20962	494
MR	45	945	723	171	789	134118	1084	44873	1150
Export -Input (%)**	***9***	***0***	***7***	***19***	***-3***	***4***	***-27***	***7***	***-1***
AR/(AR+MR) (%)***	***31***	***29***	***31***	***33***	***32***	***31***	***25***	***32***	***30***
June 9-10, 2011									
Input	102	2120	1681	914	2161	192821	1214	79157	2056
Export	145	2312	1602	806	2680	217677	1148	98109	2789
MR	221	4683	3833	1612	3966	465468	2976	188080	4679
Export -Input (%)**	***30***	***8***	***-5***	***-13***	***19***	***11***	***-6***	***19***	***26***
AR/(AR+MR) (%)***	***40***	***33***	***29***	***33***	***40***	***32***	***28***	***34***	***37***

* River discharge at the Simmesport was used for input flux, and the combined discharges at the Morgan City and Wax Lake was used for output flux estimation. For the Mississippi River, the discharge record at the Tarbert Landing was used.

** The proportions were calculated by ((Export- Input) / Input) x 100

*** The contributions were calculated by (Output from the AR / (Output from the AR + MR)) x 100, and the MR output estimation employed assumptions that all the MR water enters the Louisiana Shelf.

AR contribution on the Louisiana Shelf

To investigate how much these ARB modifications could change the chemical fluxes to the Louisiana Shelf, the AR contribution of material to the Louisiana Shelf (~ 30% of total freshwater) was estimated (Table 3). If we assume all MR water enters the shelf, DOC via AR to the shelf was in the range of 31-40% of total fluvial DOC (combined DOC through the MR and AR), which was similar to previously reported long term (1996-2010) observation values (average 35%, Shen et al., 2012). The AR nitrate contribution to the shelf was about 22-30% of the N supply via rivers, and phosphate contributions were as high as 42% (range of 21-42%). For silicate, the contributions of

AR were in the range of 27-35% of the total fluvial silicate input to the shelf. These AR contributions of nutrients are comparable to a previous report (e.g., Turner et al., 2007).

The AR contributions of Ba, Cr, Cu, Ni, Sr, V, and Zn were found to account for around 30% of the total river drived elements, similar to the AR contribution to the total freshwater on the Louisiana Shelf (~ 30% of total freshwater). Among the studied elements, the AR contribution for Mn was the most extreme, accounting for up to ~ 80% of the total fluvial Mn on the shelf. Also, Fe from the AR was substantial accounting for up to 50% of the fluvial Fe loadings on the shelf. These Mn and Fe contributions greatly exceed the AR hydrologic contribution. Although there might have been different influences of the AR input to the shelf depending on seasonal changes of the AR plume direction (Dinnel and Wiseman, 1986), the AR contribution of trace elements to the shelf was surprisingly high in our study. If a significant fraction of the MR delta outflow flows to east or offshore (Dinnel and Wiseman, 1986; Zhang et al., 2012), the AR contributions of the material could be even higher than the above estimation.

Generally, during much of the year, the current in the Louisiana Shelf flows westward along the shore from the Mississippi River to Texas, however; during summer the flow reverses (Cochrane and Kelly, 1986). Based on surface $\delta^{18}O$ and $\delta^{2}H$, Strauss et al. (2012) suggested that Louisiana Shelf water was mainly influenced by the AR during July 2008. During June/July 2009, $\delta^{18}O$-salinity relationship of the shelf surface, middle, and bottom waters showed good agreement with the both AR and MR (Figure 26), suggestive of considerable AR freshwater source at that time. These findings indicate that the AR freshwater influence could be more (or equally) important in the shelf surface than in the MR during times of bottom water hypoxia. Thus, given our estimation

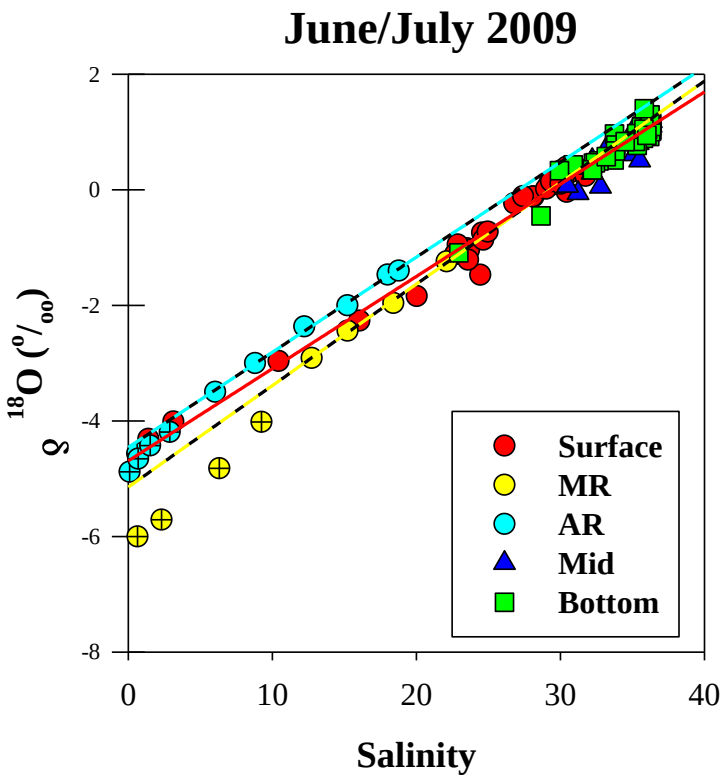

Figure 26. Distribution of δ ^{18}O versus salinity during June/July 2009. In regression, the low salinity δ ^{18}O in both MR and AR plumes were excluded. The rapid changes may reflect the changes of relative mixing ratio of major MR tributaries. Regression equations are y= 0.16x – 4.5 (r^2= 0.99, n=6, p< 0.0001), y= 0.18x – 5.1 (r^2= 0.99, n=4, p= 0.0012) and y= 0.16x – 4.7 (r^2=0.98, n=33, p< 0.0001) for the AR, MR, and surface waters, respectively.

as well as previous studies, the AR contribution of trace elements could be very important in the shelf water particularly during bottom water hypoxia, and for some elements (Fe, Mn), the AR contribution could be greater than the MR contribution, even though the AR makes up only 30% of freshwater outflow. Thus, the AR contribution needs to be adequately accounted in biogeochemical investigation and budget calculations for trace elements in Louisiana Shelf waters.

Conclusion

Temporal and spatial variations were observed for DOC, nutrients, and trace elements in the MR as well as the AR, probably due to seasonal changes of the mixing

ratio of major MR tributaries and stream redox processes. Contributions of DOC and nutrients from the RR to the AR were about 1-35%, which is similar to previous studies in this system. The RR contributed more than 20% of the ARB dissolved input of Co, Cr, Cs, Fe, Pb, Rb, and Zn due to the 5-10-fold higher RR concentrations of these elements as compared with the MR. For Mn, the RR contribution ranges between 40-87% of the Mn loading to ARB. Based on a comparison of the conservative, discharge-weighted mixing of RR and MR concentrations with observed concentrations from AR1, most of the elements mixed approximately conservatively in the upper system with the exception of Mn, which is possibly influenced by additional sources such as hyporheic fluxes or anthropogenic contamination.

To investigate the wetlands' influence on trace elements, nutrients, and DOC, river discharge weighted input-output fluxes were calculated. The computed DOC, nitrate, and silicate export fluxes are about 10-20%, which are within restriction of 20%. However, phosphate showed removal during April 2010 and addition during the other two times. For trace elements, the basin acted as a sink for Mn and Re, removing up to 40% (Mn), whereas the basin was a source for Pb. During November 2010, the basin removed Cd, Mn and Mo up to 22% relative to input. During June 2011, Co, Mn, and Pb were substantially higher in their export fluxes, whereas Cd, Cr, Cs, and U were higher in their input fluxes. Given our swamp water results, the input-output flux differences of the DOC, Cd, Cr, Cs, Mo, and U are compatible for the inputs from the wetlands as well as a possible anthropogenic source of Pb.

Assuming that the entire AR water reaches the Louisiana Shelf, the AR contribution of chemical constituents to the shelf relative to total fluvial inputs (MR + AR) was estimated.

The AR contributions of DOC and nutrients to the Louisiana Shelf are in the range of 31-40% and 22-42%, respectively, of the DOC and nutrient supply via all rivers, and these values are similar to previous studies in the ARB. Trace elements delievered via AR to the Louisiana Shelf were in the range of 30-79% of total fluvial element loadings. Among the studied elements, the AR contribution for Mn and Fe to the shelf was up to ~80 and ~50% of the total fluvial Mn and Fe, respectively, which greatly exceeded the AR hydraulic contribution to the shelf. Based on $\delta^{18}O$ and $\delta^{2}H$-salinity relationships, as well as current and wind conditions, the shelf freshwater source in summer (June/July 2009) was dominantly derived from the AR. Thus, the AR contribution of trace elements could be important in shelf water particularly during seasons of bottom water hypoxia. Overall, the ARB where the chemical constituents' modification are occurred plays a critical role in the chemical distributions on the Louisiana Shelf, and thus, the AR contribution should be adequately accounted for in biogeochemical studies of trace elements on the Louisiana Shelf.

APPENDIX A

Table

Results of April 2010. (Trace elements concentrations unit is in nmol/kg)

	Lat.	Lon.	Temp. (°C)	pH	DOC	NH_3	NO_2	NO_3	PO_4	SiO_3
					(µmol/kg)					
MR	31.072	91.583	18.6	7.14	298	0.3	1.8	117.3	1.6	117
RR	31.186	91.677	28.3	7.97	510	D.L.	0.1	2.1	1.0	62
AR1	30.568	91.758	19.9	7.77	325	0.2	1.6	113.6	1.3	109
AR2	30.368	91.637	18.3	7.75	308	0.2	1.5	113.9	1.2	106
AR3	30.346	91.721	17.5	7.39	327	D.L.	1.5	112.0	1.2	108
AR4	29.900	91.450	18.5	7.21	378	1.8	0.9	50.4	1.2	87
AR5	30.028	91.567	17	7.81	317	0.6	1.5	111.0	1.0	107
AR6	29.726	91.220	17.6	7.64	324	0.4	1.3	96.5	1.1	102
AR7	29.710	91.221	17.8	7.65	322	1.1	1.4	96.8	1.2	100
AR8	29.667	91.234	17.8	7.7	314	0.8	1.4	98.8	1.1	103
AR9	29.571	91.230	17.9	7.69	323	1.0	1.4	99.7	1.1	103
AR10	29.473	91.276	18.1	7.73	317	0.6	1.5	99.5	0.9	101
ARWL	29.370	91.385	17.6	7.7	310	0.7	1.4	105.3	1.1	104
ARL	29.546	91.431	20.7	7.13	407	0.9	0.3	13.6	2.1	73
ARE1	30.746	91.602	25.2	7.95	733	3.3	0.2	0.6	4.5	29
ARE2	30.398	91.512	19.2	7.01	552	0.8	0.9	35.0	2.5	78
ARE3	30.068	91.287	19.5	7.61	353	D.L.	1.4	95.5	1.1	96
ARE4	29.725	91.201	19.4	7.86	351	0.6	1.1	70.4	1.1	89
ARW1	29.729	91.205	21.8	6.98	557	0.8	0.0	0.3	1.1	10
ARW2	30.327	91.789	19.6	7.17	1238	0.9	1.4	80.4	0.8	91
ARS1	30.421	91.659	20.2	7.56	983	1.5	0.1	0.2	0.2	156
ARS2	30.423	91.687	21	7.34	929	5.6	1.7	4.3	4.4	144
ARS3	30.433	91.671	22	7.99	787	D.L.	D.L.	0.1	0.5	95

	As	Ba	Cd		Co		Cr		Cs		Cu	
	Dis.	Dis.	Col.	Dis.	Col.	Dis.	Col.	Dis.	Col.	Dis.	Col.	Dis.
MR	16.2	417.1	0.02	0.10	D.L.	1.00	0.32	1.29	0.011	0.012	0.08	19.54
RR	13.4	475.3	0.04	0.05	0.74	2.15	2.59	1.09	0.066	0.015	1.94	14.23
AR1	16.5	433.1	0.03	0.08	0.15	0.94	0.67	1.26	0.023	0.014	D.L.	18.03
AR2	15.3	437.1	0.02	0.08	0.04	0.96	0.33	1.28	0.013	0.012	D.L.	17.49
AR3	17.4	432.6	0.03	0.08	0.09	0.93	0.46	1.21	0.013	0.011	0.35	17.70
AR4	15.7	425.4	D.L.	0.07	0.08	1.89	0.23	0.71	0.005	0.011	0.79	11.21
AR5	14.5	422.6	0.02	0.09	0.17	0.87	0.59	1.11	0.018	0.011	0.92	16.95
AR6	15.7	432.1	D.L.	0.10	D.L.	1.06	0.25	1.00	0.006	0.012	0.74	15.49
AR7	15.0	445.0	0.02	0.09	0.19	1.18	0.71	0.93	0.018	0.012	1.25	16.31
AR8	13.0	448.8	0.02	0.08	D.L.	1.17	0.17	0.95	0.003	0.012	D.L.	16.11
AR9	15.9	453.9	0.02	0.09	0.11	1.35	0.44	0.97	0.011	0.010	1.96	15.40
AR10	15.2	464.0	0.02	0.09	0.13	1.13	0.54	1.11	0.020	0.009	0.29	17.04

Table (continued).

	As	Ba	Cd		Co		Cr		Cs		Cu	
	Dis.	Dis.	Col.	Dis.	Col.	Dis.	Col.	Dis.	Col.	Dis.	Col.	Dis.
ARWL	14.0	454.8	0.02	0.10	0.17	1.05	0.65	1.10	0.021	0.010	1.46	16.73
ARL	14.4	397.6	0.00	0.03	D.L.	0.91	D.L.	0.53	D.L.	0.011	D.L.	4.93
ARE1	66.5	243.4	0.03	0.03	D.L.	1.71	D.L.	0.38	D.L.	0.008	0.82	13.91
ARE2	20.1	403.6	D.L.	0.04	D.L.	1.74	D.L.	1.09	D.L.	0.010	D.L.	10.04
ARE3	14.8	421.2	0.03	0.09	0.14	1.23	0.48	1.15	0.017	0.012	D.L.	17.20
ARE4	14.6	433.3	0.02	0.07	0.08	1.29	0.32	0.78	0.010	0.014	0.16	13.87
ARW1	16.8	321.9	D.L.	0.03	D.L.	0.98	D.L.	0.88	D.L.	0.007	0.27	7.03
ARW2	14.6	435.8	0.03	0.07	0.14	1.64	0.13	0.85	0.004	0.013	1.33	12.79
ARS1	29.9	2835.1	0.02	0.04	0.14	6.88	D.L.	0.34	D.L.	0.018	0.47	0.89
ARS2	26.4	599.4	D.L.	0.06	0.13	3.34	D.L.	0.57	D.L.	0.017	0.23	2.13
ARS3	32.2	743.4	D.L.	0.03	D.L.	0.96	D.L.	0.37	D.L.	0.015	D.L.	4.39

	Fe		Mn		Mo	Ni		Pb	
	Col.	Dis.	Col.	Dis.	Dis.	Col.	Dis.	Col.	Dis.
MR	495.9	22.5	7.54	23.03	12.09	1.6	22.3	0.161	0.022
RR	5281.1	58.7	52.90	1322.10	6.19	3.6	20.3	0.966	0.016
AR1	1330.2	28.0	19.64	15.46	10.79	2.0	21.5	0.392	0.021
AR2	895.7	35.2	11.73	15.52	10.53	1.6	21.1	0.285	0.029
AR3	989.3	28.7	14.54	14.23	10.90	2.3	21.3	0.307	0.022
AR4	1516.3	94.7	D.L.	1748.44	9.12	0.6	20.9	0.243	0.017
AR5	1051.7	26.5	16.55	25.50	10.45	2.2	21.3	0.338	0.027
AR6	647.8	32.9	8.04	198.40	9.58	1.7	20.4	0.213	0.026
AR7	1185.3	37.0	23.28	279.34	10.14	3.1	20.9	0.335	0.022
AR8	597.1	33.5	11.26	248.26	9.40	1.6	21.0	0.204	0.030
AR9	902.7	35.3	21.13	321.03	10.39	2.4	21.1	0.367	0.022
AR10	1193.9	38.0	10.04	149.55	11.87	1.9	22.1	0.397	0.024
ARWL	1301.6	39.6	17.84	111.22	10.54	2.6	21.5	0.381	0.030
ARL	992.6	165.4	D.L.	1028.23	7.21	D.L.	23.5	0.074	0.020
ARE1	237.4	23.3	19.60	4.99	8.01	2.3	28.1	0.058	0.005
ARE2	1917.8	170.1	D.L.	1103.39	7.60	1.2	23.2	0.148	0.010
ARE3	1087.9	38.1	3.51	274.35	10.32	1.6	21.6	0.343	0.020
ARE4	985.2	62.2	D.L.	604.79	10.13	1.6	20.1	0.254	0.026
ARW1	2164.9	168.0	11.41	12.47	5.30	1.9	16.0	0.083	0.005
ARW2	742.9	52.6	24.82	1141.48	8.44	1.1	21.1	0.167	0.018
ARS1	342.9	51.4	D.L.	35713.67	6.36	1.2	15.7	0.005	0.003
ARS2	2017.6	300.2	165.42	4431.73	1.95	0.9	13.4	0.029	0.004
ARS3	99.1	61.6	5.94	11.56	2.79	1.3	15.3	0.005	0.003

	Rb	Re	Sr	U	V	Zn	
	Dis.	Dis.	Dis.	Dis.	Dis.	Col.	Dis.
MR	13.78	0.082	2023	4.57	24.7	3.8	2.2

Table (continued).

	Rb	Re	Sr	U	V	Zn	
	Dis.	Dis.	Dis.	Dis.	Dis.	Col.	Dis.
RR	28.19	0.014	2692	2.50	18.8	8.3	3.8
AR1	16.07	0.072	1977	4.40	23.2	3.1	2.9
AR2	15.82	0.073	1967	4.49	22.3	2.2	3.7
AR3	15.96	0.074	1965	4.44	22.8	3.2	3.1
AR4	17.74	0.056	1989	3.04	16.2	6.0	3.4
AR5	16.55	0.063	1936	4.04	21.0	3.6	2.7
AR6	16.85	0.059	2021	3.64	20.8	D.L.	13.3
AR7	17.25	0.059	2039	3.69	21.2	6.6	2.5
AR8	16.87	0.059	1965	3.58	21.6	2.5	2.5
AR9	16.67	0.060	2121	3.74	23.1	8.8	3.5
AR10	19.57	0.060	2285	3.75	23.0	3.5	2.3
ARWL	16.87	0.061	2238	4.12	20.3	2.8	4.7
ARL	16.37	0.042	2075	1.25	9.8	D.L.	2.7
ARE1	18.94	0.019	1533	2.17	35.6	4.1	1.6
ARE2	20.39	0.043	2134	1.73	14.6	3.1	3.6
ARE3	17.44	0.058	2082	3.63	21.9	3.9	3.5
ARE4	17.69	0.054	2083	2.93	18.3	1.7	4.8
ARW1	15.15	0.023	1359	0.72	6.7	2.5	0.9
ARW2	17.15	0.058	1971	3.00	18.1	2.0	2.7
ARS1	24.68	0.008	26091	3.82	2.2	0.4	1.0
ARS2	23.62	0.021	3131	3.45	5.7	D.L.	13.9
ARS3	19.64	0.019	4378	5.91	10.5	1.6	1.2

Abbreviation: Lat.: latitude, Lon.: Longitude, Temp.: Temperature, Cond.: conductivity, DOC: dissolved organic carbon, D.L.: detection limit, Dis.: dissolved (< 0.02 µm), Col.: colloid (0.02-0.45 µm), D.L.: detection limit.

Table

Results of November 2010. (Trace elements concentrations unit is in nmol/kg)

	Lat.	Lon.	Temp. (°C)	pH	Cond. (µm/s)	DOC	NH_3	NO_2	NO_3	PO_4	SiO_3
						(µmol/kg)					
MR	31.072	91.583	15.8	8.01	517	296.08	0.6	0.6	101.8	1.1	222
RR	31.186	91.677	20	7.62	432	332.29	2.7	0.8	4.3	0.7	153
AR1	30.568	91.758	17	8.00	576	330.46	0.5	0.2	108.2	1.9	227
AR2	30.368	91.637	16	7.96	540	311.46	0.5	0.2	105.0	1.8	219
AR3	30.346	91.721	17	8.00	541	336.63	0.7	0.3	103.2	1.6	225
AR4	29.900	91.450	17	8.04	524	385.63	0.5	0.0	70.9	1.2	187
AR5	30.028	91.567	17	8.03	544	347.88	0.5	0.0	112.0	2.1	237
AR6	29.726	91.220	18	8.03	546	346.21	0.5	D.L.	109.2	2.6	233
AR7	29.710	91.221	17	8.02	546	339.13	0.4	D.L.	113.3	1.4	230
AR8	29.667	91.234	18	7.97	556	350.54	0.5	0.0	98.2	1.8	223
AR9	29.571	91.230	18	7.96	574	342.79	2.0	0.0	100.5	1.8	224
AR10	29.473	91.276	18	7.93	556	351.88	1.2	0.0	99.2	1.6	228
ARWL	29.370	91.385	18	7.94	544	339.21	0.4	D.L.	106.5	2.3	236
ARL	29.546	91.431	19.3	7.69	490	393.25	0.4	0.0	49.2	1.2	195
ARE1	30.746	91.602	17	8.04	237	653.79	1.4	16.1	0.4	0.6	256
ARE2	30.398	91.512	16	7.59	379	576.79	1.5	0.1	3.2	1.6	249
ARE3	30.068	91.287	17	7.90	545	336.88	1.0	0.0	107.3	1.5	233
ARE4	29.725	91.201	17	7.73	541	367.38	0.7	0.0	83.8	1.7	220
ARW1	29.729	91.205	18.2	7.30	207	743.08	0.6	0.6	0.6	0.3	203
ARW2	30.327	91.789	18	8.08	538	362.63	1.2	0.2	104.2	1.8	228
ARS1	30.421	91.659	12	7.30	2659	743.54	20.2	0.5	2.7	0.1	306
ARS2	30.423	91.687	12	6.86	427	837.46	2.1	D.L.	1.2	4.3	241
ARS3	30.433	91.671	16	7.64	378	556.75	0.8	1.2	0.5	0.1	277

	As	Ba	Cd		Co		Cr		Cs		Cu	
	Dis.	Dis.	Col.	Dis.	Col.	Dis.	Col.	Dis.	Col.	Dis.	Col.	Dis.
MR	28.4	581.7	D.L.	0.13	0.09	1.17	0.11	1.02	0.005	0.010	D.L.	19.20
RR	27.7	557.5	0.03	0.03	D.L.	0.85	D.L.	0.43	D.L.	0.018	0.68	10.57
AR1	29.5	603.5	0.05	0.12	0.03	1.21	0.18	0.93	0.004	0.010	1.05	19.07
AR2	27.6	559.3	0.05	0.11	0.07	1.09	0.15	0.99	0.006	0.010	0.89	18.76
AR3	30.3	642.4	0.05	0.12	0.15	1.12	0.08	0.99	0.003	0.010	1.95	19.77
AR4	30.4	672.5	D.L.	0.10	0.24	1.74	0.32	0.93	0.010	0.009	1.20	20.00
AR5	28.4	610.3	0.01	0.11	0.14	1.04	0.31	0.93	0.004	0.010	0.84	19.91
AR6	28.7	617.8	D.L.	0.11	0.17	1.09	0.26	0.92	0.005	0.010	1.34	19.24
AR7	29.4	674.8	0.01	0.11	0.04	1.12	0.13	0.98	0.004	0.010	D.L.	20.34
AR8	26.9	670.9	D.L.	0.10	0.16	1.09	0.28	0.91	0.009	0.009	0.98	19.10
AR9	31.3	685.1	D.L.	0.10	0.52	2.05	1.44	0.87	0.041	0.009	1.56	17.49
AR10	27.4	588.7	D.L.	0.10	0.26	1.31	0.35	0.85	0.009	0.008	2.50	18.32
ARWL	28.0	654.1	0.00	0.11	0.09	1.14	D.L.	0.96	0.002	0.010	0.46	20.04
ARL	21.2	595.1	D.L.	0.08	0.05	1.24	0.05	0.66	0.004	0.011	0.50	13.59

Table (continued).

	As	Ba	Cd		Co		Cr		Cs		Cu	
	Dis.	Dis.	Col.	Dis.	Col.	Dis.	Col.	Dis.	Col.	Dis.	Col.	Dis.
ARE1	55.3	315.9	D.L.	0.05	0.36	1.95	D.L.	0.21	D.L.	0.005	0.51	2.82
ARE2	28.3	610.3	D.L.	0.05	0.28	1.28	0.52	0.37	0.015	0.006	0.30	9.89
ARE3	27.2	649.2	D.L.	0.12	0.24	1.49	0.17	0.91	0.007	0.009	1.22	19.95
ARE4	25.3	620.7	D.L.	0.09	0.17	1.57	0.14	0.75	0.007	0.009	0.64	17.12
ARW1	16.7	596.4	D.L.	0.06	0.07	2.10	0.05	1.06	D.L.	0.004	0.24	2.06
ARW2	31.0	631.8	D.L.	0.11	0.26	1.83	0.35	0.86	0.012	0.010	1.74	19.92
ARS1	19.7	3075.9	D.L.	0.08	0.12	3.71	0.12	0.30	D.L.	0.022	0.33	2.21
ARS2	20.2	602.7	D.L.	0.07	0.20	1.40	0.07	0.20	D.L.	0.011	D.L.	0.66
ARS3	26.9	899.4	D.L.	0.06	D.L.	0.58	D.L.	0.22	D.L.	0.009	0.17	1.13

	Fe		Mn		Mo	Ni		Pb	
	Col.	Dis.	Col.	Dis.	Dis.	Col.	Dis.	Col.	Dis.
MR	238.0	19.9	6.22	41.36	25.72	D.L.	26.1	0.066	0.015
RR	215.8	13.0	D.L.	445.47	14.35	0.3	11.4	0.043	0.004
AR1	214.5	18.3	8.10	22.20	23.60	3.2	25.2	0.058	0.013
AR2	295.3	16.7	14.76	13.02	25.26	3.1	25.0	0.082	0.013
AR3	225.0	20.6	11.57	108.01	24.91	3.7	26.8	0.072	0.013
AR4	455.4	20.9	D.L.	449.48	22.28	1.5	25.2	0.144	0.014
AR5	219.1	20.0	8.99	16.82	24.12	1.5	25.3	0.066	0.012
AR6	250.3	19.5	8.74	27.78	22.76	0.9	24.8	0.074	0.012
AR7	171.5	20.2	5.83	19.67	24.31	D.L.	26.2	0.052	0.013
AR8	316.3	19.0	9.60	37.13	22.80	1.1	24.4	0.085	0.014
AR9	1658.1	25.7	28.89	702.15	23.04	1.3	24.3	0.450	0.018
AR10	335.2	22.1	7.33	99.52	21.59	1.8	24.2	0.092	0.017
ARWL	132.6	13.9	1.95	37.22	24.00	1.1	24.9	0.042	0.014
ARL	213.4	26.9	D.L.	363.34	16.24	D.L.	19.9	0.054	0.016
ARE1	206.7	9.1	44.07	5.71	6.99	1.2	12.7	0.038	0.008
ARE2	826.2	29.8	11.43	129.94	8.35	0.5	22.5	0.156	0.006
ARE3	336.3	20.4	D.L.	365.90	24.08	2.4	25.9	0.101	0.015
ARE4	244.1	21.9	D.L.	382.07	20.61	D.L.	24.3	0.073	0.018
ARW1	4889.3	102.4	D.L.	1373.51	4.60	1.1	17.9	0.375	0.010
ARW2	365.1	17.9	D.L.	939.40	20.65	0.7	25.5	0.149	0.015
ARS1	895.0	273.3	D.L.	10913.16	6.45	D.L.	17.4	0.019	0.004
ARS2	2074.7	497.4	D.L.	5293.25	0.25	D.L.	4.1	D.L.	0.009
ARS3	162.0	16.5	5.45	6.21	3.49	D.L.	8.5	0.009	0.003

Table (continued).

	Rb	Re	Sr	U	V	Zn	
	Dis.	Dis.	Dis.	Dis.	Dis.	Col.	Dis.
MR	15.67	0.140	2729	10.66	41.0	2.0	2.3
RR	32.15	0.020	2867	1.50	30.8	D.L.	1.1
AR1	17.56	0.131	3041	10.35	45.7	1.4	5.7
AR2	16.12	0.130	2861	10.21	41.4	D.L.	2.4
AR3	17.32	0.137	2866	10.46	46.3	D.L.	4.0
AR4	16.26	0.121	2822	9.30	48.7	1.9	1.7
AR5	17.16	0.133	2825	10.32	46.7	1.9	1.9
AR6	17.21	0.130	2734	10.01	44.7	1.9	1.5
AR7	17.30	0.133	2979	10.28	46.4	1.3	2.3
AR8	18.02	0.122	3025	9.33	43.5	2.8	3.1
AR9	17.54	0.124	3196	9.78	53.1	4.1	3.1
AR10	16.79	0.124	2770	9.41	46.8	2.4	3.6
ARWL	16.44	0.137	2901	9.30	45.7	2.7	1.9
ARL	19.89	0.099	2447	6.86	32.1	D.L.	3.0
ARE1	20.47	0.016	1361	1.09	20.5	D.L.	2.6
ARE2	18.82	0.048	2048	3.91	27.4	2.8	0.6
ARE3	16.25	0.138	2834	10.77	46.2	2.2	1.7
ARE4	16.91	0.118	2834	8.92	42.7	D.L.	3.3
ARW1	9.55	0.014	1174	0.25	4.4	D.L.	8.5
ARW2	17.06	0.127	2861	8.91	48.0	2.0	1.8
ARS1	33.34	0.019	29908	8.49	3.7	D.L.	3.8
ARS2	37.51	0.008	2533	0.16	0.7	D.L.	4.0
ARS3	24.95	0.014	2554	3.77	7.5	D.L.	1.5

Abbreviation: Lat.: latitude, Lon.: Longitude, Temp.: Temperature, Cond.: conductivity, DOC: dissolved organic carbon, Dis.: dissolved (< 0.02 μm), Col.: colloid (0.02-0.45 μm), D.L.: detection limit.

Table

Results from June 2011. (Trace elements concentrations unit is in nmol/kg)

	Lot.	Lon.	Temp.	pH	Cond.	DOC	NH_3	NO_2	NO_3	PO_4	SiO_3
			(°C)		(µm/s)				(µmol/kg)		
MR	31.072	91.583	25.1	7.4	367.1	282	0.6	0.1	94.3	2.0	145
RR	31.186	91.677	29.3	6.71	127.2	703	3.6	0.2	7.0	2.1	112
AR1	30.568	91.758	27.2	7.25	328.5	370	1.5	0.2	74.9	2.3	137
AR2	30.368	91.637	25.4	7.22	329.3	357	1.2	0.2	78.6	2.0	137
AR3	30.346	91.721	26.2	7.22	328.7	359	1.3	0.3	67.6	1.9	123
AR6	30.028	91.567	26.1	7.16	324.9	357	2.0	0.5	51.9	2.3	146
ARE1	30.746	91.602	25.7	7.26	361.3	302	2.1	0.6	55.6	2.1	134
ARE2	30.398	91.512	27.6	7.13	355.8	404	7.9	2.1	22.3	6.4	152
ARE3	30.068	91.287	27.4	7.17	339.8	376	3.2	1.4	25.0	3.7	153
ARE4	29.725	91.201	27	7.09	327.7	356	5.2	1.0	25.9	3.1	165
ARW1	30.327	91.789	31.6	7.21	305	516	0.5	D.L.	0.6	0.7	105
ARW2	30.327	91.789	25.5	7.07	322	377	2.0	0.8	41.4	2.7	139
ARS1	30.433	91.671	27.2	7.01	334.9	571	7.7	0.0	1.1	10.5	180
ARS2	30.424	91.674	26.9	7.14	327.6	591	5.0	0.0	1.3	8.8	176

	As	Ba	Cd		Co	Cr		Cs		Cu		
	Dis.	Dis.	Col.	Dis.	Col.	Dis.	Col.	Dis.	Col.	Dis.	Col.	Dis.
MR	20.7	416.5	0.03	0.07	0.45	0.80	0.031	0.008	0.97	0.84	2.48	17.73
RR	18.4	261.0	0.04	0.03	1.00	0.68	0.069	0.056	2.67	1.80	4.90	13.82
AR1	21.1	403.6	0.03	0.06	0.64	0.85	0.036	0.012	1.21	0.99	3.86	17.29
AR2	19.7	415.1	0.02	0.06	0.51	0.89	0.035	0.012	1.25	0.87	2.33	17.96
AR3	21.7	406.6	0.03	0.07	0.52	1.18	0.032	0.010	1.22	0.86	3.37	17.17
AR6	24.2	434.4	0.02	0.04	0.50	1.06	0.019	0.010	0.80	0.67	2.05	14.08
ARE1	21.9	432.2	0.02	0.02	0.19	1.42	0.003	0.010	0.18	0.67	2.94	11.80
ARE2	35.3	465.2	0.03	0.08	0.28	1.76	0.007	0.017	0.39	0.54	2.13	10.80
ARE3	23.0	441.0	0.02	0.03	0.42	1.75	0.005	0.012	0.18	0.65	2.29	10.15
ARE4	26.9	442.0	0.02	0.01	0.37	1.94	D.L.	0.014	0.30	0.55	1.96	9.44
ARW1	19.9	411.0	D.L.	0.02	0.05	0.65	D.L.	0.010	D.L.	0.49	0.21	3.29
ARW2	21.5	428.6	0.02	0.03	0.17	1.07	0.008	0.012	0.40	0.63	0.59	13.44
ARS1	32.4	501.8	0.03	0.02	0.69	2.34	D.L.	0.017	0.25	0.61	3.46	3.23
ARS2	26.6	461.7	0.05	0.03	0.64	1.88	D.L.	0.016	0.24	0.64	3.71	4.06

	Fe		Mn		Mo	Ni		Pb	
	Col.	Dis.	Col.	Dis.	Dis.	Col.	Dis.	Col.	Dis.
MR	1514.9	32.2	32.09	36.33	13.21	4.5	21.5	0.463	0.014
RR	7684.3	414.1	104.49	184.69	4.12	5.4	25.4	0.838	0.017
AR1	2439.8	74.0	50.24	118.16	10.41	3.0	23.8	0.623	0.015
AR2	2348.4	85.1	39.22	78.61	11.62	3.9	22.7	0.596	0.016
AR3	2324.7	82.4	33.58	420.43	11.60	2.9	23.4	0.634	0.015
AR6	1696.1	127.7	34.01	450.99	10.96	3.2	21.2	0.536	0.024
ARE1	591.5	55.5	27.79	417.20	12.02	3.2	21.1	0.146	0.009
ARE2	1719.6	266.3	11.05	855.19	11.38	2.7	21.0	0.244	0.009

Table (continued).

	Fe		Mn		Mo	Ni		Pb	
	Col.	Dis.	Col.	Dis.	Dis.	Col.	Dis.	Col.	Dis.
ARE3	1700.4	206.8	15.96	1362.48	9.89	2.6	19.0	0.282	0.011
ARE4	1072.0	195.4	59.64	1778.12	9.80	3.3	18.3	0.200	0.011
ARW1	159.1	92.7	13.75	90.49	5.25	1.7	12.1	0.003	0.004
ARW2	1353.9	143.6	40.26	849.14	10.01	1.3	19.4	0.279	0.009
ARS1	2224.6	587.6	96.71	2394.13	7.12	2.5	15.7	0.157	0.023
ARS2	1463.5	536.5	200.77	1481.35	4.55	3.2	14.9	0.155	0.037

	Rb	Re	Sr	U	V	Zn	
	Dis.	Dis.	Dis.	Dis.	Dis.	Col.	Dis.
MR	14.02	0.075	1714	4.29	24.52	6.0	2.1
RR	44.84	0.008	848	0.20	20.67	18.9	8.0
AR1	19.47	0.062	1582	3.09	24.98	7.3	2.2
AR2	19.90	0.061	1619	3.35	24.79	4.8	4.1
AR3	19.64	0.060	1555	3.25	24.98	D.L.	9.7
AR6	18.25	0.057	1647	2.49	22.98	4.3	3.5
ARE1	14.67	0.069	1577	3.69	22.47	2.2	2.1
ARE2	21.56	0.067	1520	1.19	34.59	5.9	3.6
ARE3	19.02	0.063	1530	1.19	14.44	3.5	3.2
ARE4	19.26	0.060	1502	1.08	17.27	2.9	3.2
ARW1	17.29	0.042	1459	0.38	6.79	3.1	2.5
ARW2	17.70	0.056	1476	1.95	19.47	2.5	2.6
ARS1	28.25	0.057	1581	0.50	9.57	5.4	2.0
ARS2	29.06	0.053	1493	0.31	10.93	4.6	3.2

Abbreviation: Lat.: latitude, Lon.: Longitude, Temp.: Temperature, Cond.: conductivity, DOC: dissolved organic carbon, Dis.: dissolved (< 0.02 µm), Col.: colloid (0.02-0.45 µm), D.L.: detection limit.

REFERENCES

Baldwin, D.S., Mitchell, A.M. The effects of drying and re-flooding on the sediment and soil nutrient dynamics of lowland river-floodplain systems: A synthesis. *Regul. Rivers: Res. Mgmt.* **2000**, 16: 457-467.

Battle, J.M., Mihuc, T.B. Decomposition dynamics of aquatic macrophytes in the lower Atchafalaya, a large floodplain river. *Hydrobiologia* **2000**, 418: 123-136.

Bayley, P.B. Understanding large river-floodplain ecosystems. *BioScience* **1995**, 45(3): 153-158.

Bianchi, T.S., Filley, T., Dria, K., Hatcher, P.G. Temporal variability in sources of dissolved organic carbon in the lower Mississippi River. *Geochim. Cosmochim. Acta* **2004**, 68(5): 959-967.

Booth, M.S., Stark, J.M., Rastetter, E. Controls on nitrogen cycling in terrestrial ecosystems: A synthetic analysis of literature data. *Ecol. Monogr*. **2005**, 75(2): 139-157.

Brick, C.M., Moore, J.N. Diel variation of trace metals in the Upper Clark Fork River, Montana. *Environ. Sci. Technol*. **1996**, 30: 1953-1960.

Chow, A.T., Dai, J., Conner, W.H., Hitchcock, D.R., Wang, J.-J. Dissolved organic matter and nutrients dynamics of a coastal freshwater forested wetland in Winyah Bay, South Carolina. *Biogeochemistry* **2012**, DOI 10.1007/s10533-012-9750-z.

Christopher, S.F., Page, B.D., Campbell, J.L., Mitchell, M.J. Contrasting stream water NO_3^- and Ca^{2+} in two nearly adjacent catchments: the role of soil Ca and forest vegetation. *Glob. Change Biol.* **2006**, 12: 364-381.

Cochrane, J.D., Kelly, F.J. Low-frequency circulation on the Texas-Louisiana continental shelf. *J. Geophys. Res.-oceans.* **1986**, 91, 10645-10659.

Dinnel, A.P., Wiseman Jr, W.J. Fresh water on the Louisiana and Texas shelf. *Cont. Shelf Res*. **1986**, 6, 765-784.

Du Laing, G. Rinklebe, J., Vandecasteele, B., Meers, E., Tack, F.M.G. Trace metal behavior in estuarine and riverine floodplain soils and sediments: A review. *Sci. Total Environ*. **2009**, 407, 3972-3985.

Duan, S., Bianchi, T., Sampere, T.P. Temporal variability in the composition and abundance of terrestrially-derived dissolved organic matter in the lower Mississippi and Pearl Rivers. *Mar. Chem.* **2007**, 103, 172-184.

Duan, S.W., Bianchi, T.S. Seasonal changes in the abundance and composition of plant pigments in particulate organic carbon the lower Mississippi and Pearl Rivers (USA). *Estuar. Coast.* **2006**, 29, 427-442.

Elbaz-Poulichet, F, Nagy, A., Cserny, T. The distribution of redox sensitive elements (U, As, Sb, V and Mo) along a river-wetland-lake system (Balaton region, Hungary). *Aquat. Geochem.* **1997**, 3, 267-282.

Emmett, B.A., Hudson, J.A., Coward, P.A., Reynolds, B. The impact of a riparian wetland on stream water recently afforested upland catchment. *J. Hydrology* **1994**, 162, 337-353.

Fisher, J., Acreman, M.C. Wetland nutrient removal: a review of the evidence. *Hydrol. Earth Syst. Sci*. **2004**, 8(4), 673-685.

Fontenot, Q.C., Rutherford, D.A., Kelso, W.E. 2001. Effects of environmental hypoxia associated with the annual flood pulse on the distribution of larval sunfish and shad in the Atchafalaya River basin, Louisiana. *T. Am. Fish. Soc*. **130,** 107-116.

Ford, M., Nyman, J.A. Preface: an overview of the Atchafalaya River. *Hydrobiologia* **2011**, 658, 1-5.

Foster, I.D.L., Charlesworth, S.M. Heavy metals in the hydrological cycle: trends and explanation. *Hydrol. Process* **1996**, 10, 227-261.

Gadd, G.M. Microbial influence on metal mobility and application for bioremediation. *Geoderma*. **2004**, Dio:10.1016/j.geoderma.2004.01.002.

Garcia-Garcia, V., Gomez, R., Vidal-Abarca, M.R., Suarez, M.L. Nitrogen retention in natural Mediterranean wetland-streams affected by agricultural runoff. *Hydrol. Earth Syst. Sci*. **2009**, 13, 2359-2371.

Gossuin, Y., Colet, J.-M., Roch, A., Muller, R.N., Gillis, P. Cesium adsorption in hydrated iron oxide particles suspensions: An NMR study. *J. Magnetic Resonance* **2001**, 157, 132-136.

Guo, L., Santschi, P. H., Warnken, K. W. Dynamics of dissolved organic carbon in oceanic environments. *Limnol. Oceanogr.* **1995**, 40, 1392-1403.

Harvey, J.W., Fuller, C.C. Effect of enhanced manganese oxidation in the hyporheic zone on basin-scale geochemical mass balance. *Water Resour. Res*. **1998**, 34(4), 623-636.

House, W. Geochemical cycling of phosphrous in rivers. *Appl. Geochem.* **2003**, 18, 739-748.

Johnson, C.A., Sigg, L., Lindauer, U. The chromium cycles in a seasonally anoxic lake. *Limnol. Oceanogr.* **1992**, 37(2), 315-321.

Junk, W.J., Bayley, P.B., Sparks, R.E. The flood pulse concept in river-floodplain systems. In *Proceedings of the International Large River Symposium*. D.P. Dodge Eds. *Can. Spec. Publ. Fish, Aquat. Sci*. **1989**, pp 110-127.

Kerr, S.C., Shafer, M.M., Overdier, J., Armstrong, D.E. Hydrologic and biogeochemical controls on trace element export from northern Wisconsin wetlands. *Biogeochemistry* **2008**, 89, 273-294.

Khan, H., Brush, G.S. Nutrient and metal accumulation in a freshwater tidal marsh. *Estuaries* **1994**, 17(2), 345-360.

Kosolapov, D.B., Kuuchk, P., Vainshtein, M.B., Vatsourina, A.V. Microbial process of heavy metal removal from cabon-deficient effluents in constructed wetlands. *Eng. Life Sci.* **2004**, 2004 4(5), 403-411.

Kuchler, I.L., Miekeley, N., Forsberg, B.R. Molecular mass distributions of dissolved organic carbon and associated metals in waters from Ro Negro and Rio Solimoes. *Sci. Total Environ*. **1994**, 156(3), 207-216.

Lambou, V.W., Hern, S.C. Transport of organic carbon in the Atchafalaya Basin, Louisiana. *Hydrobiologia* **1983**, 98, 25-34.

Lane, R.R., Day, J.W., Marx, B., Reyes, E., Kemp, G.P. Seasonal and spatial water quality changes in the outflow plume of the Atchafalaya River, Louisiana, USA. *Estuaries* **2002**, 25(1), 30-42.

Lindau, C.W., Delaune, R.D., Scaroni, A.E., Nyman, J.A. Denitrification incypress swamp within the Atchafalaya River Basin, Louisiana. *Chemosphere* **2008**, 70, 886-894.

Martin, S.T. Precipitation and dissolution of iron and manganese oxides. In *Environmental Catalysis*. Eds.; Vicki H. Grassian, CRC Press **2005**, pp 61–82.

Mays, P.A., Edwards, G.S. Comparison of heavy metal accumulation in a natural wetland and constructed wetlands receiving acid mine drainage. *Ecol. Eng.* **2001**, 16, 487-500.

Means, J.L., Crerar, D.A., Borcsik, M.P., Duguid, J.O. Adsorption of Co and selected actinides by Mn and Fe oxides in soils and sediments. *Geochim. Comochim. Acta* 1978, 42(12), 1763-1773.

Mora, A., Baquero, J.C., Alfonso, J.A., Pisapia, D., Balza, L. The Apure River: geochemistry of major and selected trace elements in an Orinoco River tributary coming from the Andes, Venezuela. *Hydrol. Process*. **2010**, 24, 3798-3810.

Mulholland, P.J. Organic carbon flow in a swamp-stream ecosystem. *Ecol. Monogr.* **1981**, 51(3), 307-322.

Noe, G.B., Hupp, C.R. Seasonal variation in nutrients retention during inundation of a short-hydroperiod floodplain. *River Res. Applic*. **2007**, 23, 1088-1101.

Olivie-Lauquet, G., Gruau, G., Dia, A., Riou, C., Jaffrezic, A., Henin, O. Release of trace elements in wetlands: role of seasonal variability. *Wat. Res.* **2001**, 35(4), 943-952.

Ponter, C., Ingri, J., Burman, J.-O., Bostrom, K. Temporal variations in dissolved and suspended iron and manganese in the Kalix River, northern Sweden. *Chem. Geol*. **1990**, 81, 121-131.

Pokrovsky, O.S., Schott, J. Iron colloids/organic matter associated transport of major and trace elements in small boreal rivers and their estuaries (NW Russia). *Chem. Geol.* **2002**, 190, 141-179.

Rabalais, N.N., Diaz, R.J., Levin, L.A., Turner, R.E., Gilbert, D., Zhang, J. Dynamics and distribution of natural and human-caused hypoxia. *Biogeosciences* **2010**, 7, 585-619.

Rabalais, N.N., Turner, R.E., Justic, D., Dortch, Q., Wiseman Jr, W.J., Gupta, B.K.S. Nutrient changes in the Mississippi River and system responses on the adjacent continental shelf. *Estuaries* **1996**, 19(2B), 386-407.

Rucker, K., Schrautzer, J. Nutrient retention function of a stream wetland complex- A high-frequency monitoring approach. *Ecol. Eng.* **2010**, 36, 612-622.

Sabo, M.J., Bryan, C.F., Kelso, W.E., Rutherford, D.A. Hydrology and aquatic habitat characteristics of a riverine swamp: II. Hydrology and the occurrence of chronic hypoxia. *Regul. Rivers: Res. Mgmt*. **1999**, 15, 525-542.

Scaroni, A.E., Lindqu, C.W., Nyman, J.A. Spatial variability of sediment denitrification across the Atchafalaya River Basin, Louisiana, USA. *Wetlands* **2010**, 30, 949-955.

Scaroni, A.E., Nyman. J.A., Lindau, C.W. Comparison of denitrification characteristics amon therr habitat types of a large river floodplain: Atchafalaya River Basin, Louisiana. *Hydrobiologia* **2011**, 658, 17-25.

Seyler, P.T., Boaventura, G.R. Distribution and partition of trace metals in the Amazon basin. *Hydrol. Processes* **2003**, 17, 1345-1361.

Shen, Y., Fichot, C.G., Benner, R. Floodplain influence on dissolved organic matter composition and export from the Mississippi-Atchafalaya River system to the Gulf of Mexico. *Limnol. Oceangr*. **2012**, 57(4), 1149-1160.

Sheoran, A.S., Sheoran, V. Heavy metal removal mechanism of acid mine drainage in wetlands: A critical review. *Miner. Eng.* **2006**, 19, 105-116.

Shiller A.M., Stephens, T.H. Microbial manganese oxidation in the lower Mississippi River: Methods and evidence. *Geomicrobiol. J.* **2005**, 22, 117-125.

Shiller, A.M. Dissolved trace elements in the Mississippi River: Seasonal, interannual, and decadal variability. *Geochim. Cosmochim. Acta*, **1997**, 61(20), 4321-4330.

Shiller, A.M. Seasonality of dissolved rate earth elements in the lower Mississippi River. *Geochem. Geophy. Geosys.* **2002**, 3(11), 1068, doi:10.1029/2002GC000372.

Shiller, A.M. Syringe filtration methods for examining dissolved and colloidal trace element distributions in remote field locations. *Environ. Sci. Technol*. **2003**, 37(17), 3953-3957.

Strauss, J., Grossman, E.L., DiMarco, S.F. Stable isotope characterization of hypoxia-susceptible waters on the Louisiana Shelf: Tracing freshwater discharge and benthic respiration. *Cont. Shelf Res*. **2012**, 47, 7-15.

Strohm, T.O., Griffin, B., Zumft, W.G., Schink, B. Growth yields in bacterial denitrification and nitrate ammonification. *Appl. Environn. Microbio.* **2007**, 73(5), 1420-1424.

Tribovillard, N., Algeo, T.J., Lyons, T., Riboulleau, A. Trace metals as paleoredox and paleoproductivity proxies: An update. *Chem. Geol*. **2006**, 232(1-2): 12-32.

Turner, R.E., Rabalais, N.N. Changes in Mississippi River water quality this century. *BioScience* **1991**, 41(3), 140-147.

Turner, R.E., Rabalais, N.N., Alexander, R.B., McIsaac, G., Howarth, R.W. Characterization of nutrient, organic carbon, and sediment loads and concentrations from the Mississippi River into the northern Gulf of Mexico. *Estuar. Coast Shelf Sci.* **2007**, 30(5), 773-790.

Verhoeven, J.T.A., Arheimer, B., Yin, C., Hefting, M.M. Regional and global concerns over wetlands and water quality. *Trends Eco. Evol.* **2006**, doi:10.1016/j.tree.2005.11.015.

Viers, J., Barrous, G., Pinelli, M., Seyler, P., Oliva, P., Dupre, B., Boaventura, G.B. The influence of the Amazonian floodplain ecosystems on the trace element dynamics of the Amazon River mainstem (Brzzil). *Sci. Total Environ*. **2005**, 339, 219-232.

Viers, J., Dupre, B., Braun, J.-J., Deberdt, S., Angeletti, B., Ngoupayou, J.N., Michard, A. Major and trace element abundances, and strontium isotopes in the Nyong basin rivers (Cameroon): constraints on chemical weathering processes and elements transport mechanisms in humid tropical environments. *Chem. Geol.* **2000**, 211-241.

Viers, J., Dupre, E., Polve, M., Schott, J., Dandurand, J.-L., Braun, J.-J. Chemical weathering in the drainage basin of a tropical watershed (Nsimi-Zoetele site, Cameroon): comparison between organic-poor and organic-rich waters. *Chem. Geol*. **1997**, 140, 181-206.

Vymazal, J. Removal of nutrients in various types of constructed wetlands. *Sci. Total Environ.* **2007**, 380, 48-65.

Weis, J.S., Weis, P. Metal uptake, transport and release by wetland plants: implications for phytoremediation and restoration. *Environ. Int*. **2004**, 30, 685-700.

Withers, P.J.A., Jarvie, H.P. Delivery and cycling of phosphorus in rivers: A review. *Sci. Total Environ.* **2008**, 400, 379-395.

Xu, Y.J. Organic nitrogen retention in the Atchafalaya River swamp. *Hydrobiologia* **2006**a, 560, 133-143.

Xu, Y.J. Total nitrogen inflow and outflow from a large river swamp basin to the Gulf of Mexico. *Hydrol. Sci.* **2006**b, 51(3), 531-542.

Xu, Y.J., Bryantmason, A. Determining the nitrate contribution of the Red River to the Atchafalaya River in the northern Gulf of Mexico under changing climate. (conference paper) IAHS-AISH publication **2011**, 348, 95-100.

Zachara, J.M., Fredrickson, J.K., Smith, S.C., Gassman, P.L. Solubilization of Fe(III) oxide-bound trace metals by a dissimilatory Fe(III) reducing bacterium. *Geochim. Cosmochim. Acta* **2001**, 65(1), 75-93.

Zhang, X., Hetland, R.D., Marta-Almeida, M., DiMarco, S.F. A numerical investigation of the Mississippi and Atchafalaya freshwater transport, filling and flushing times on the Texas-Louisiana Shelf. *J. Geophy. Res.* **2012**, 117, C11009, doi:10.1029/2012JC008108.

CHAPTER V

TRACE ELEMENT DISTRIBUTIONS IN THE WATER COLUMN NEAR THE DEEPWATER HORIZON WELL BLOWOUT

Introduction

As a result of the April 2010 Deepwater Horizon oil rig explosion and blowout, an estimated 4.4 ± 0.8 million barrels (~ $5.0 \pm 1.0 \times 10^8$ L) of crude oil were released into the Gulf of Mexico (Crone and Tolstoy, 2010). Such a large oil release has the potential to seriously impact marine and coastal environments of the northern Gulf (Fowler et al., 1993; Bu-Olayan et al., 1998; Massoud et al., 1993). In addition to the crude oil, up to 1.25×10^{10} moles of methane were released to the deep water (Valentine et al., 2010), and nearly all the methane released was consumed by methanotrophic bacteria (Valentine et al., 2010, Kessler et al., 2011). The consumption of these hydrocarbons caused an estimated respiration of 2-4 $\times 10^{10}$ moles of oxygen at the same time (Kessler et al., 2011, Du and Kessler, 2012). About 6.8×10^6 liters of dispersant were used, 3.8×10^6 L for the surface and 3.0×10^6 L for the deep plume (Kujawinski et al., 2011). The dispersant used and the polycyclic aromatic hydrocarbons (PAHs) from the crude oil may have had a toxicological impact (Hicken et al., 2011; Linden et al., 1987).

Other work has shown that some trace metals can be highly enriched in crude oil, and the metal composition may vary with source (Ball et al., 1960; Bieber et al., 1960). However, there are few studies on trace element distributions in marine aquatic environments affected by spills. For example, Santos-Echeandia et al. (2008) and Prego

* This chapter of the dissertation has been published as: Joung, D.J. and Shiller, A.M. Trace element distributions in the water column near the Deepwater Horizon well blowout. Environ. Sci. Technol. 2013, 47, 2121-2168. It is used with permission of the American Chemical Society.

and Cobelo-Garcia (2003) observed significantly elevated dissolved Cu, Ni, and Zn in the water column above the Prestige fuel oil tanker wreckage off the coast of Spain. Fowler et al. (1993) found elevated concentrations of V, Ni, and Cr in Saudi Arabian sediments following the oil spill and fires from the 1991 Gulf War. Massoud et al. (1998) and Al-Abdali et al. (1996) likewise reported that the contamination of V and Ni in Arabian Gulf sediments was related to the wartime oil spill.

Despite these contamination reports, Portella et al. (2006) found that the complexation of metals with ligands in crude oil is very stable at pH 8. Based on an oil spill simulation in seawater, they concluded that metal ions stayed in the oil due to this strong ligand complexation. Cantu et al. (2000) reported that the partitioning rate of Ni and V complexed with deoxophyllorythroetioporphyrin (DPEP) from crude oil into the aqueous phase is very slow, so the contamination of drinking water by metals released from crude oil is small.

This paper reports the results of the selected dissolved metal concentrations in the water column near the Deepwater Horizon (also called the Macondo well or MC252) site after the blowout. Samples were collected during cruises to the area, two during the blowout and two after the well was capped, with the basic objective of understanding how and to what extent metal distributions were affected after the oil rig explosion.

Methods and Materials

Sample collection and measurement

Samples were collected from areas around the Deepwater Horizon accident site during four cruises in early and late May 2010, October 2010, and October 2011 (Appendix). The first and second samplings took place during the spill, and the last two cruises were carried out about 90 days and a year after the well was sealed.

For surface waters, grab sampling was performed from the bow of a small boat moving slowly forward by dipping an acid-cleaned polyethylene bottle into the water with gloved hands. Samples were taken 10-20 cm underneath the surface to avoid oil contamination at the interface. At several stations where a small boat was not available, a PVC pole (~5 m length) was used along with the acid-cleaned sampling bottle attached to collect water from the larger research vessel. Deeper water samples were collected from rosette-mounted, Teflon-coated Go-Flo or external spring Niskin bottles (General Oceanics) which were pre-cleaned using dilute acid (10% HCl), ultrapure water, an EDTA (10 mM) solution, and a final rinse with ultrapure water again. Sampling depths were determined through an examination of the in situ sensor profiles, paying particular attention to anomalies in dissolved oxygen (DO), light transmission, and CDOM fluorescence. Because of the short notice with which the first cruise was arranged, clean Go-Flo or Niskin bottles were not available. For that cruise, the ship's normal rosette-mounted Niskin bottles were used. For all cruises, unfiltered water samples were collected in acid-cleaned polyethylene bottles (from the Niskin and Go-Flo bottles or as surface grab samples) and subsequently cleanly filtered using acid-cleaned syringes attached to acid-washed 0.45 µm polyethylene filters (Whatman Puradisc) (Shiller, 2003). In a clean lab on shore, samples were acidified to pH < 2 using ultrapure HCl (Seastar Baseline). Trace element measurements were carried out using a sector-field inductively coupled plasma-mass spectrometry (SF-ICP-MS; Thermo-Fisher Element 2). An analysis of seawater was performed by either diluting the sample 20-fold with 0.3 M ultrapure HNO_3 for Ba and Mo or by using a magnesium hydroxide co-precipitation technique for Fe, Cu, Ni, Mn, Co, Cr, and V (e.g., Shiller and Bairamadgi, 2006; Shim et al., 2012). In

both cases, calibration was performed with isotope-dilution using enriched isotopic spikes obtained from Oak Ridge National Laboratory, excepting mono-isotopic Mn and Co that were calibrated using external standards (Shim et al., 2012). For river water samples, the analysis was carried out by diluting the samples 2-fold with 0.3 M ultrapure HNO_3 that contained In as an internal standard (Shiller, 2003). In order to verify the accuracy of the analysis, the certified seawater NASS-5 (NRC-Canada) was measured at the beginning and end of each analytical run (Appendix).

Polycyclic aromatic hydrocarbon (PAH) samples were also collected at the same depths as the trace elements. Soon after the collection, approx. 10 ml of dichloromethane was added to the samples in order to prevent degradation. Samples were then stored in the refrigerator. PAH analysis was performed at Texas A&M University using gas chromatography/mass spectrometry (Wade et al., 2011).

Oil and dispersant analysis

Samples of crude oil and dispersant were obtained from BP in the fall of 2010. These samples were decomposed using acid-based wet digestion in a closed vessel (Wondium et al., 2000; Duyck et al., 2007). To prepare crude oil and dispersant (Corexit 9500) samples for trace element analysis, approx. 0.1 g of oil or dispersant was first digested with 2 ml of ultrapure HCl in an acid-cleaned Teflon container. These tightly capped containers were heated 3-4 hours on a hot plate, and the solution was taken to near dryness. In order to fully digest the samples, 1 ml each of clean H_2O_2 and HNO_3 were next added to the samples. After heating and drying, ultrapure water was added to the solutions. This step was repeated three times, with the samples taken to near dryness each time. The solutions were then diluted with 5 ml of 0.16 M HNO_3, and.triplicate

samples were prepared. Finally, the solutions were measured using SF-ICP-MS similar to how the river water samples were analyzed.

Oil and dispersant leaching experiments

Oil-seawater mixing experiments were conducted with water from a station close to the wellhead (GIP 18; Appendix) during the October 2011 cruise. Surface and deep (1300 m) waters were collected and were treated with the addition of oil alone or oil and dispersant together. Also, in order to understand the effect of suspended particles on the oil distribution, surface water from the near shore (GIP 4, 20 km away from the Mississippi River) water was collected. Each experiment was conducted in triplicate using acid-cleaned 500-ml polyethylene bottles. Soon after collection, the 500 mL water samples were amended with 10 µl of oil alone or 10 µl each of the oil and dispersant. The oil and/or dispersant treated and non-treated samples were then vigorously mixed using a shaking plate for over 7 hours. All samples were then filtered using the same procedure as for the field samples (Shiller, 2003). The amount of oil addition was based on our observations of oil concentration in the subsurface oil plume during May 2010. In addition, river waters from the Mississippi and Pearl Rivers were also used for another mixing experiment. That experiment followed the same procedures as the seawater experiment, including the same added quantities of the oil and dispersant. An addition of the dispersant alone was also included in those river water experimental batches.

Results and Discussion

Metal concentrations in crude oil and dispersant

Metals in the Macondo well crude oil are low compared to many other crude oils (Ball et al., 1960) (Table 10). A previous analysis of the Macondo well crude oil by Liu

et al. (2012) found similar (e.g., Co, Ni, V) or significantly higher (Cr, Cu, Fe, Zn) metal concentrations compared with what is reported here. While it is uncertain as to the origin of the concentration discrepancies, oil concentrations of Cr and Fe of a level in Liu et al.'s (2012) should have been distinguishable in the observations report below. That is, our environmental and experimental results are compatible with our low concentrations of these elements in the Macondo crude. Possibly, their high values resulted from the filtration of samples through glass fiber filters, a sample preparation step avoided in this study. Nonetheless, even with lower values, the metal concentrations in the crude oil are generally much higher than the background levels of metal concentrations in the deep water (1000-1400 m; Table 10). For example, metal from the oil relative to water ([nmol/kg]/[nmol/kg]) varied from 0.5 to 120,000, with the lowest value for Mo and the highest value for Co. Thus, some metals in the crude oil could significantly alter the aqueous metal concentrations even with a high degree of dispersion of the oil in the water column. Trace elements in the dispersant were similar to or lower than the concentrations in the crude oil (Table 10). Thus, there is also the possibility of metal contamination from dispersant application, again depending on the degree of dilution. That said, it notes that samples collected in the deep submerged plumes had low concentrations of PAH's indicative of oil dilution factors greater than 10^4.

Filtration effects

In a river-influenced shelf environment such as the accident site, trace element samples need to be filtered because of the potentially large and variable contributions of particulate metals to unfiltered samples. However, filtration materials are also likely to adsorb dispersed crude oil. In a sense, that is desirable since the filtered concentrations

Table 10

Metal concentration in the crude oil from the Macondo well and dispersants used in this spill (in ppm)

	V	Cr	Mn	Fe	Co	Ref.
Crude oil	0.8	< 0.02	< 0.004	0.4	0.1	T
Dispersant	0.003	< 0.03	< 0.003	0.1	< 0.0004	T
Macondo well crude oil	0.2	9.4	ND	7.9	0.2	A
South Louisiana sweet crude oil	0.1					B
Previous studies (oil)	0.6-1200	0.04-1.2	0.05-0.15	0.05-6.6	< 0.03-0.6	C
Drilling Mud		15	205	6600	10	D
Average metal concentration depth from 1000 to 1350 m (October 2011)						
(nmol/kg)	31.0	3.1	2.7	0.9	0.014	
*Ratio (Oil/water)	484	134	25	7242	1.2×10^5	
**Expected metal concentration based on the highest PAHs concentration (120 µg/l)						
Increase by (nmol/kg)	0.18	0.01	0.001	0.08	0.02	
% relative to Oct. 2011	0.6	0.2	0.029	10.3	120	

	Ni	Cu	Zn	Mo	Ba	Ref.
Crude oil	1.9	0.02	< 0.09	0.01	< 0.02	T
Dispersant	0.02	0.01	0.11	0.01	< 0.03	T
Macondo well crude oil	1.5	0.5	18.0			A
South Louisiana sweet crude oil	0.9					B
Previous studies (oil)	0.1-96.5	0.02-3.58	0.1-2.5		~0.1	C
Drilling Mud	17	98			5.4×10^5	D
Average metal concentration depth from 1000 to 1350 m (October 2011)						
(nmol/kg)	4.7	1.3		112	61	
*Ratio (Oil/water)	7012	212		0.5	2.6	
**Expected metal concentration based on the highest PAHs concentration (120 µg/l)						
Increase by (nmol/kg)	0.40	0.003		0.001	0.002	
% relative to Oct. 2011	6.4	0.3		0.001	0.003	

*: Oil/water ratio is calculated from the concentrations in the crude oil and average deep seawater concentrations during October 2011, and is in nmol/kg:nmol/kg.

**: Expected metal concentration is estimated based on the highest PAHs concentration, 120 µg/l, in the subsurface oil plume during the late May.

ND: non detectable.

Ref.: Reference: A-Liu et al., 2012, B-Bieber et al., 1960, C-Ball et al., 1960; Bieber et al., 1960; Santos-Echeandia et al., 2008, Dunning et al., 1960; Stigter et al., 2000, Sugihara and Bean, 1962; All et al., 1983, Duyck et al., 2002, D-Pozebon et al., 2005, Crecelius et al., 2007, T- this study.

would thus be representative of the metal dissolved in the water rather than metal in water plus oil. To verify that crude oil was significantly removed during sample filtration, a simple mixing experiment was conducted. About 1 L of ultrapure water was mixed with 1 ml of the crude oil, and the mixture was vigorously shaken for 5 minutes. With such a high concentration of oil, it is likely that the oil remained as highly dispersed oil-droplets in the water. Three aliquots were then filtered and compared with three unfiltered aliquots. Filtration and measurement followed the same procedures as for other trace element samples. The UV-absorbance measurements at 254 nm were made. After filtration, the aliquots were visibly clearer than before, and the UV-absorbance was about two orders of magnitude higher in the un-filtered aliquots than in the filtered aliquots. Results of metal analysis also showed much higher concentrations in the un-filtered aliquots. For example, Co in the un-filtered fraction was about 20 times higher than in the filtered fraction. These facts indicate that the crude oil was effectively removed during filtration.

Leaching experiments of oil and dispersant with seawater and river water

The experimental results are summarized in Table 11. Although the results were scattered, metals such as Fe, Cu, and Ni increased ~10~100% in the oil plus dispersant treatment compared to the untreated seawater. For Co, it is clear that addition of oil alone showed an increase relative to the untreated seawater. Based on the concentration of Co in the Macondo crude, the addition of oil should have increased Co by 0.03 nmol/kg, which is close to the observed experimental increase (Tables 10, 11). Changes in Ba and Cr concentrations were within analytical error.

Since the observed degree of oil dilution in the submerged plumes was very high ($>10^4$), changes of metal concentration in the oil or oil plus dispersant mixtures were not

expected, except in the case of Co (Table 10). For example, Cu in the crude oil is 0.02 ppm, and the addition of 10 µl of oil and dispersant in 500 ml of seawater would lead to an increase of only 0.007 nmol/kg (i.e., < 1% of ambient), assuming 100% leaching efficiency. Nonetheless, the experiments show that for Cu, Fe, Ni, and Mn, the addition of oil plus dispersant to seawater did increase their concentrations (Table 11). These apparently unsupported increases were most pronounced in the mixtures with surface water from close to the Mississippi River delta while concentrations of metal in the deep water mixtures were within experimental error. This trend suggests that the metal increases that were not supported by metal in the oil/dispersant were due to the solubilization of metals from the suspended particles. This metal increase likely resulted from complexation of metals by sulfonate groups in the surfactant fraction of the dispersant. Based on the composition of Corexit 9500A (Kujawinski et al., 2011), the concentration of added sulfonate groups in this experiment was estimated to be ~2.4 µM. This concentration is 85-fold greater than the highest concentration reported in the deep submerged plumes (Kujawinski et al., 2011), which again showed considerable dilution. These preliminary results thus suggest that metal solubilization by dispersant complexation should have a minimal impact in the open ocean, but could well be significant in more particle-rich fluvial or nearshore environments as well as where dilution of the dispersant is minimal.

To further investigate the effect of the dispersant on the dissolved-particulate metal partitioning, mixing experiments with two local river waters were also conducted (Table 11). In these experiments, the unsupported increases of Cu were observed in the mixtures of dispersant alone and dispersant plus oil in both river waters. This observation

is consistent with the findings of the unsupported Cu from the seawater experiment (Table 2). Other metals (e.g., Fe, Zn, V, Mo, Ni) showed no significant variations among fractions, probably due to the much higher fluvial concentrations of these metals, which make it more difficult to observe any increase. Interestingly, Ba concentrations in the fluvial mixing experiments decreased 15-20% with the addition of the dispersant or the dispersant plus oil but not with the oil addition alone. Such a decrease was not observed in the seawater mixing experiments and this distribution suggests that the dispersant augments the partitioning of Ba to the suspended fluvial particles, which are known to have significant adsorbed Ba (Hanor and Chan, 1977). In addition, it has been reported that metals could be removed from the water by adsorption onto the oil particles (Liu et al., 2012). It has not observed such an effect in our experiments and speculate that the previous observation of metal uptake by weathered oil (Liu et al., 2012) may have been due to incorporation of particulate metals by oil aggregates.

Metal distributions in the water

In the surface waters, Ba, Cu, Ni, Fe, Mn, and Co were in similar ranges of 48 - 99, 1.0 - 3.7, 2.1 - 6.4, 0.1 - 3.0, 2.7 - 17.5 and 0.04 - 0.27 nmol/kg, respectively, over all four cruises (Appendix). The overall correlation with salinity suggests that the mixing of Mississippi River water with offshore waters is the dominant driver of the surface water concentration changes observed during these cruises. Although some scatter is observed in these trends, there is no correlation between this scatter and indicators of oil contamination such as PAH concentrations. This distribution suggests a minimal impact of the Macondo well oil or dispersants on surface water metal distributions. However, some caution is needed with respect to this conclusion, since the sampling ships necessarily had to avoid the most oil-contaminated surface waters.

Table 11

Mixing of oil and dispersant with seawater. Seawater was collected from stations GIP 4 and GIP 18, October 2011 (nmol/kg)

		V	Cr	Fe[§]	Ni	Cu
GIP4	No addition	34 ± 2	1.42 ± 0.03	3.8 ± 0.1	4 ± 1	5.1 ± 0.3
Surface	Oil	32.1 ± 0.4	1.6 ± 0.1	3.8 ± 0.6	5 ± 1	5.3 ± 0.3
	Oil+Dispersant	38 ± 1	1.56 ± 0.04	47 ± 9	8 ± 1	6.8 ± 0.2
GIP18	No addition	28.1 ± 0.8	2.4 ± 0.1	0.6 ± 0.2	1.2 ± 0.2	1.7 ± 0.1
Surface	Oil	29 ± 6	2.47 ± 0.02	0.5 ± 0.1	1.4 ± 0.6	1.7 ± 0.1
	Oil+Dispersant	31 ± 1	2.4 ± 0.1	1.1 ± 0.2	3.6 ± 0.8	2.2 ± 0.1
GIP18	No addition	24 ± 4	3.3 ± 0.1	0.8 ± 0.1	2.3 ± 0.7	1.1 ± 0.4
1300 m	Oil	26 ± 2	3.48 ± 0.05	0.76 ± 0.02	2.6 ± 0.5	0.83 ± 0.03
	Oil+Dispersant	29 ± 7	2.74 ± 0.03	1 ± 1	2.6 ± 0.5	1.2 ± 0.1
Mississippi	No addition	41.5 ± 0.8	3.3 ± 0.3	1.5 ± 0.2	21.3 ± 0.3	24.7 ± 0.1
River	Oil	42.2 ± 0.3	3.8 ± 0.3	1.8 ± 0.2	22.0 ± 0.1	25.2 ± 0.1
	Dispersant	41.6 ± 0.4	3.13 ± 0.07	1.4 ± 0.1	22.2 ± 0.2	27.5 ± 0.1
	Oil+Dispersant	41.9 ± 0.9	2.9 ± 0.3	1.2 ± 0.3	21.8 ± 0.3	27.7 ± 0.1
Pearl	No addition	31.5 ± 0.4	10.8 ± 0.3	18.4 ± 0.1	17.7 ± 0.3	14.9 ± 0.2
River	Oil	35 ± 5	11.4 ± 0.6	18.6 ± 0.4	18.1 ± 0.2	15.0 ± 0.3
	Dispersant	35.0 ± 0.4	12.2 ± 0.1	21.1 ± 0.2	18.8 ± 0.2	17.2 ± 0.2
	Oil+Dispersnat	34 ± 1	11.3 ± 0.8	20.9 ± 0.3	18.7 ± 0.2	18 ± 2
*Expected	Oil+Dispersant	0.25	0.017	0.14	0.56	0.007
Increase	Oil	0.25	0.007	0.01	0.55	0.005

		Zn	Mn	Co	Ba
GIP4	No addition	1.4 ± 0.2	8.9 ± 0.3	0.30 ± 0.01	177 ± 3
Surface	Oil	1.5 ± 0.1	9 ± 1	0.37 ± 0.04	175 ± 2
	Oil+Dispersant	2.2 ± 0.3	11.9 ± 0.7	0.38 ± 0.02	179 ± 4
GIP18	No addition	0.41 ± 0.04	4.2 ± 0.1	0.14 ± 0.01	76 ± 1
Surface	Oil	0.6 ± 0.1	4.2 ± 0.1	0.155 ± 0.002	75 ± 1
	Oil+Dispersant	0.4 ± 0.1	4.4 ± 0.1	0.17 ± 0.01	74 ± 1
GIP18	No addition	2.0 ± 0.4	6.1 ± 0.2	0.014 ± 0.003	63 ± 1
1300 m	Oil	1.9 ± 0.2	6.2 ± 0.2	0.03 ± 0.01	61 ± 2
	Oil+Dispersant	2.4 ± 0.7	6.0 ± 0.1	0.05 ± 0.01	63 ± 0
Mississippi	No addition	10.1 ± 0.9	39 ± 5	1.50 ± 0.09	441 ± 1
River	Oil	11.2 ± 0.2	45 ± 4	1.64 ± 0.06	439 ± 0
	Dispersant	10.6 ± 0.2	59 ± 5	1.59 ± 0.03	350 ± 2
	Oil+Dispersant	10 ± 1	50 ± 10	1.5 ± 0.1	348 ± 1
Pearl River	No addition	26.8 ± 0.3	2305 ± 9	6.21 ± 0.07	236 ± 2

Table 11 (continued).

		Zn	Mn	Co	Ba
Pearl River	Oil	28.0 ± 0.5	2280 ± 20	6.18 ± 0.09	237 ± 1
	Dispersant	31.2 ± 0.3	2280 ± 30	6.90 ± 0.05	201 ± 0
	Oil+Dispersnat	30 ± 1	2297 ± 4	6.8 ± 0.1	204 ± 2
*Expected	Oil+Dispersant	0.05	0.002	0.03	0.006
Increase	Oil	0.02	0.001	0.03	0.003

*: Expected increase was calculated based on the amount of crude oil and dispersant.

§: Unit is in μM only for Fe in the two river waters.

In the subsurface oil/gas plumes (1000 - 1300 m), no anomalies were observed in distributions of V, Ni, Mo, or Cr (Figure 27, Appendix). Given the low concentrations of these elements in the crude oil and the dispersant as well as the lack of effects in our mixing experiment with deep water, this distribution is not surprising. Note that no background trace element data exist for this region, though concentrations for the less reactive elements are similar to those reported for the Atlantic Ocean (Chan et al., 1977; Bergquist and Boule, 2006; Saito and Moffett, 2002; Bruland and Franks, 1983). Concentrations during the early May cruise do not appear to have been compromised by using the ship's Niskin bottles; nonetheless, in the following discussion the late May data (using cleaned sampling bottles) are more focused than the early May data.

For Co, the one element for which our experiments suggest the likelihood of a crude oil signal, there was a clear enrichment at depth during the blowout period in late May 2010 (Figure 27). The increase corresponded to the depth of the subsurface oil plume where the elevated in-situ CDOM, fluorescence, and beam attenuation as well as decreased DO were observed by author and by others (Joye et al., 2011; Diercks et al., 2010). Interestingly, the samples that were most enriched in PAHs had low dissolved Co, consistent with ambient background concentrations. Because our filtration experiments

showed oil removal by the filters, the Co enrichment is likely dissolved in the water rather than dispersed with oil. Thus, the trend of high Co with low PAH is not unreasonable. Furthermore, the Co-enriched samples tended to have PAH compositions that had low percentages of methylnaphthalenes (Figure 28). The methylnaphthalenes are the more soluble, lower molecular weight PAHs, and thus a lower percentages of these compounds suggests more exposure or weathering of the crude oil (Gonzalez et al., 2006; Boehm et al., 1997). Again, these findings are consistent with the idea that Co has been transferred from dispersed oil into the water.

Another element for which there was a clear enrichment in some late May 2010 deep plume samples was Ba (Figure 27). As noted above, Ba was not enriched in the crude oil or dispersant, and there was no Ba solubilization observed in our mixing experiments. Furthermore, the Ba enrichment did not correlate with the Co enrichment and peaked (during late May) in samples about 6 km away from the wellhead (Figure 28). However, the use of Ba salts in drilling muds is well-known (Neff, 2007; Trocine and Trefry, 1983). Despite the low solubility of barite in seawater (e.g., Neff, 2007, Church and Wolgemuth, 1972), evidence from corals in the Gulf of Mexico does suggest increased dissolved Ba resulting from use of Ba-containing drilling mud (Carriquiry and Horta-Puga, 2010; Deslarzes et al., 1995). Starting five days before our late May sampling, a *top kill* attempt to plug the leaking well resulted in the use of >105 bbl/d of heavy drilling mud for three days (National Commission). Given an average current speed of 1 - 3 cm/s at 900 m depth in this area (Diercks et al., 2010; Teague et al., 2006), the higher Ba within 10 km is well-matched to the sample collection time, May 30 and 31, confirming that the Ba anomaly was likely derived from top kill drilling mud usage.

Two elements that showed somewhat more complex distributions in the vicinity of the well were Mn and Fe (Figures 29, 30). For Mn, there is a clear trend of increasing concentrations for samples collected near the bottom (Figure 29), consistent with a flux of Mn from reducing hemipelagic sediments (Jones and Murray, 1985). However, a subset of the late May samples showed less variability with depth (Figure 27). This subset was also enriched in Ba, which correlated significantly with Mn in these samples (Figure 29), suggesting a slight Mn source from the top kill materials.

For Fe, the situation is less straightforward. Fe did show a vertical trend of increasing concentrations for near-bottom samples (Figure 30), as might be expected in a continental margin environment (e.g., Elrod et al., 2004; Cullen et al., 2009). However, there was also a lateral trend in these submerged plume samples with lower dissolved Fe closer to the wellhead during late May 2010 (Figure 30). While it is tempting to interpret this as a sign of biological Fe demand associated with methane and oil biodegradation, caution is needed in that regard because of the dynamics of the continental slope environment. The author notes, for example, that because the wellhead was in a depression surrounded by domes, the distance from the wellhead tended to be inversely correlated with depth for the late May samples (Appendix). Hence, Figures 30 is both probably reflective of the same topographic/benthic input control on Fe concentrations. Nonetheless, two distinct groups of samples are observed in both of these plots. It is noted that the two sample groups were not collected at different depths, or directions, or at different times. However, all of the higher Fe ("Group A") samples were from within 10 km of the wellhead. For the lower Fe sample group ("Group B") there was a correlation indicating lower methylnaphthalene percentage with greater Fe concentration

(Figure 30). As noted above, methylnaphthalenes are among the more soluble (Diercks et al., 2010; Gonzalez et al., 2006) and more readily weathered and biodegraded PAH components (Douglas et al., 1996); thus, this inverse correlation between percent methylnaphthalenes and Fe (as a proxy for distance from the wellhead) is reasonable. In contrast, the high Fe sample group ("Group A") had PAH compositions of 50-60%methylnaphthalenes (Figure 30), similar to the source oil PAH composition. This finding raises the intriguing possibility that the Group A samples had higher Fe because they had experienced less biodegradation and hence less biological removal of Fe.

Hazen et al. (2010) and Kessler et al. (2011) reported increased densities of microbial cells, including methanotrophs, in the subsurface oil/gas plume. Fe uptake by heterotrophic marine bacteria is well-established (Tortell et al., 1999; Pakulski et al., 1996), and methanotrophs are known to require Fe for enzymatic activity (Lieverman et al., 2004). Significant Fe uptake under these conditions is therefore likely. An important associated issue, therefore, is whether Fe availability might have been limiting to oil/gasbiodegradation. The microbial Fe demand is estimated during late May 2010 from bacterial C:N:Fe ratios (Tortell et al., 1999; Fagerbakke et al., 1996; Lee and Childress, 1994, Appendix) and observed nitrate depletions in the same plume samples that analyzed for metals (Shiller and Joung, 2012). The estimated Fe removal averaged 0.17 and 0.26 nmol/kg in Group A and B samples, respectively. This calculation is primitive and dependant on assumptions regarding elemental ratios in oil-degrading and methanotrophic bacteria (Appendix). Nonetheless, the Fe removal estimates represent a substantial though incomplete demand on the available Fe, which averaged 0.98 and 0.49 nmol/kg in the two sample groups (Appendix). Additionally, it is noted that the oxygen

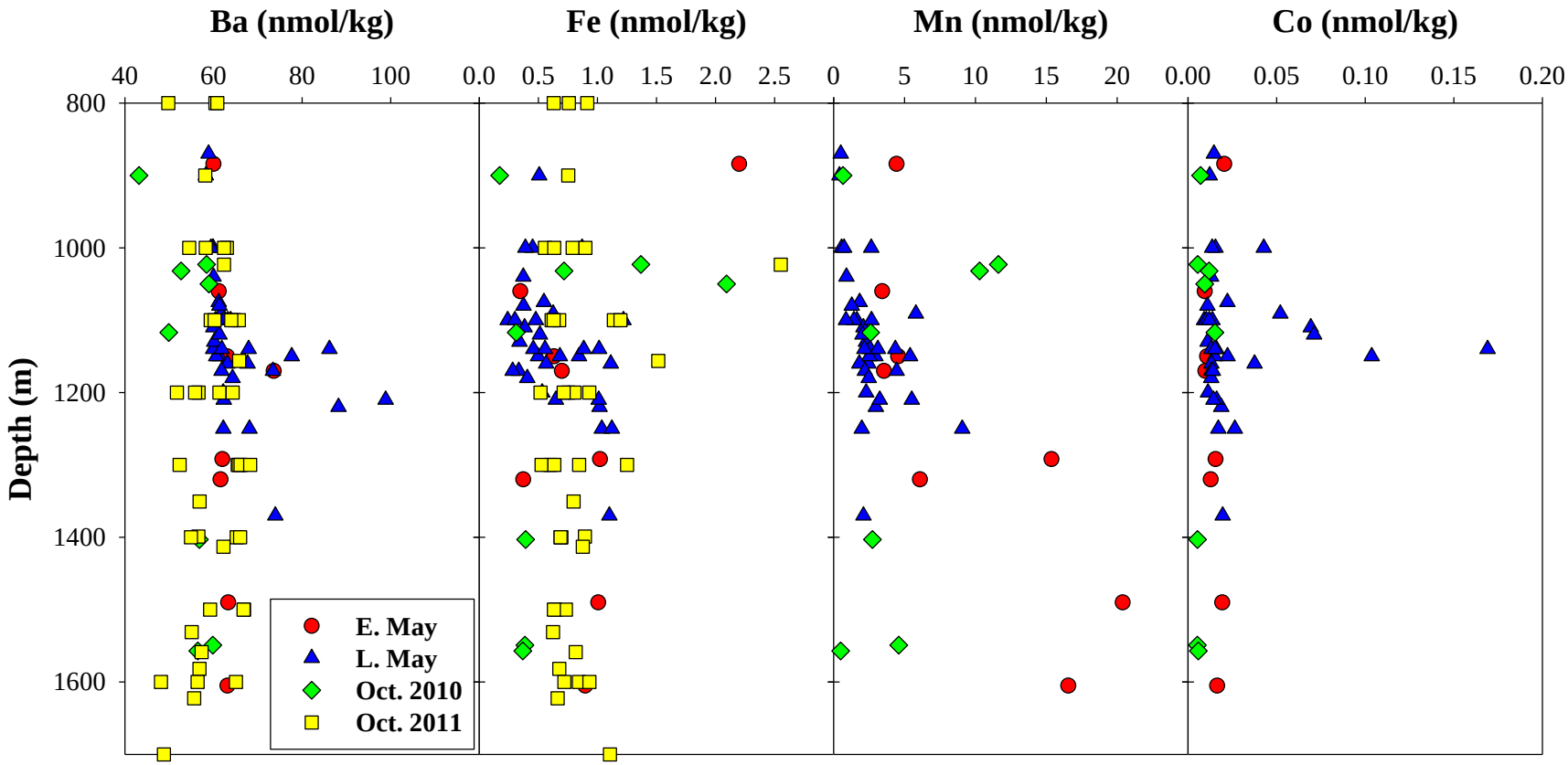

Figure 27. Vertical distributions of selected trace elements in early May, late May, October 2010, October 2011.

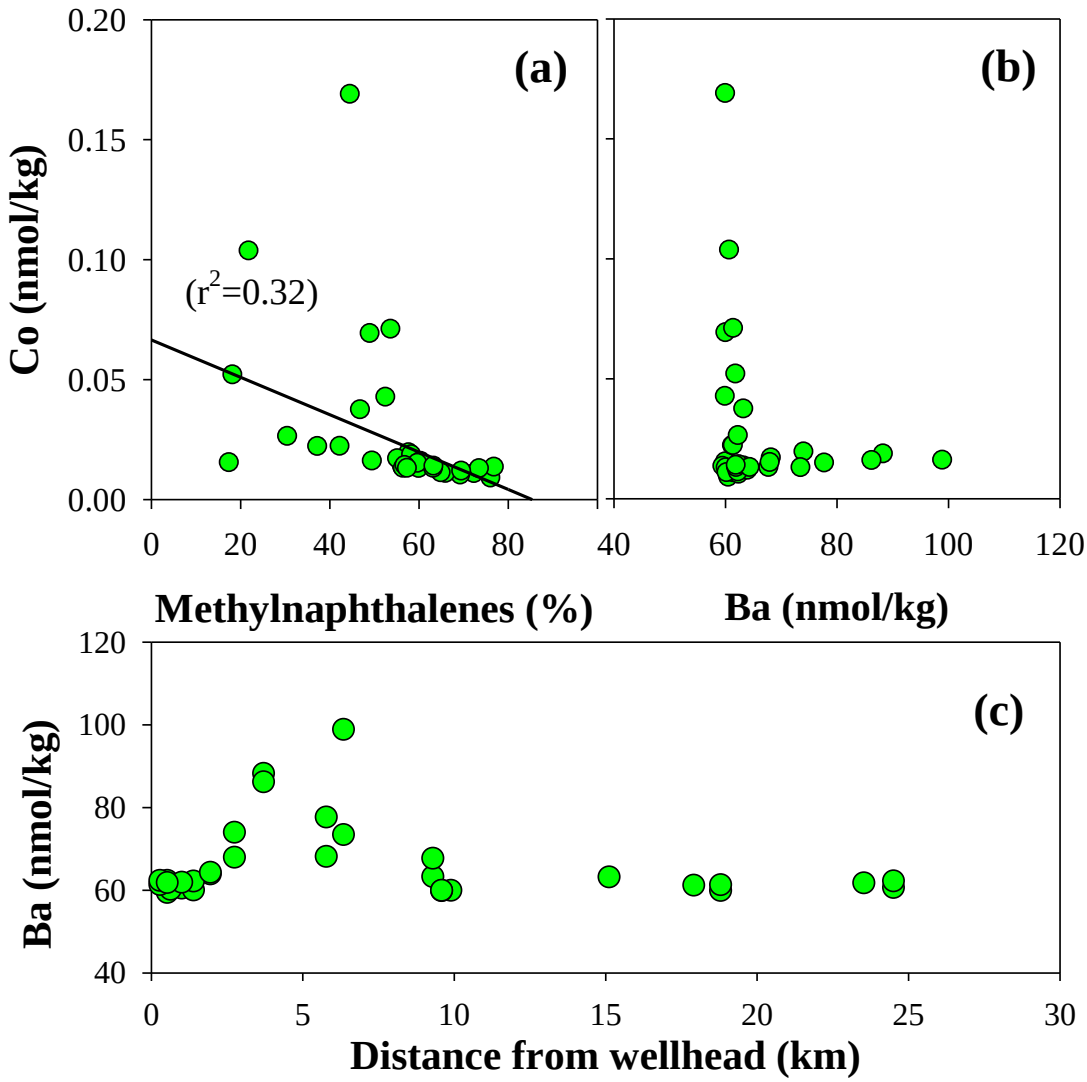

Figure 28. Plot of Co with (a) percent of total PAHs that were methylnaphthalenes, (b) Co versus Ba, and (c) spatial distribution of Ba in the submerged plumes (1000-1350 m). For the regression calculation, the highest value (0.17 nmol/kg) was excluded, and the equation was y= -0.00078x + 0.067 (n=32, p= 0.0008). With the highest value, the regression was y= -0.00096x + 0.080 with r^2=0.22 (n=33, p= 0.009). Only late May 2010 data were used.

removal data (Du and Kessler, 2012) suggests that the late May sampling occurred well before the most substantial growth phase of the microbial response to the oil/gas plume. The enhanced microbial growth during the later stages of the blowout could well have resulted in Fe depletion if cell densities were high enough and Fe recycling was minimal.

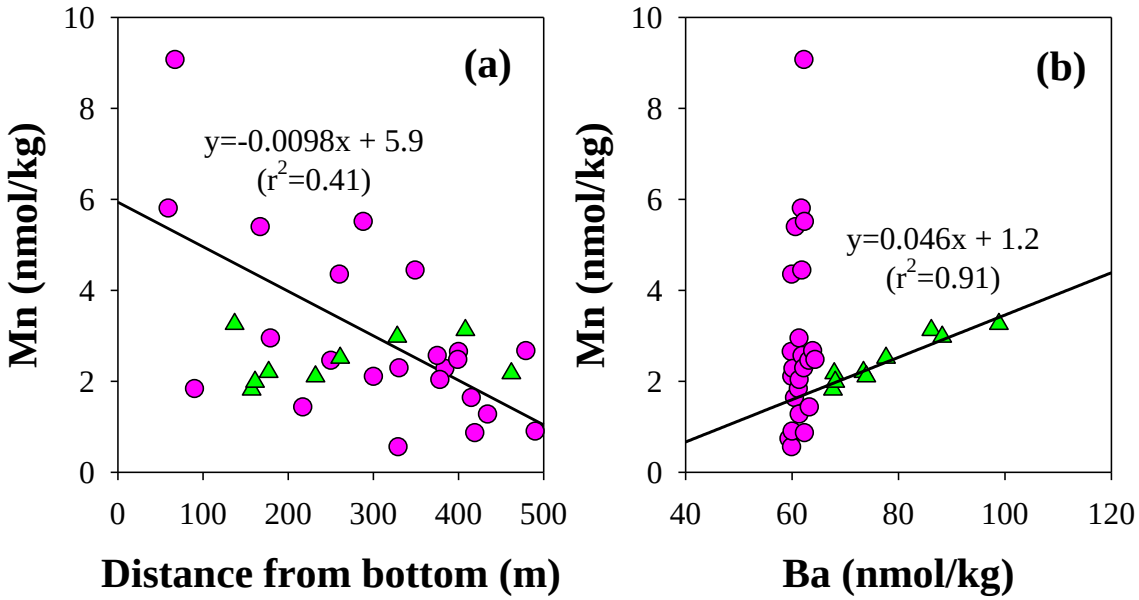

Figure 29. Mn distribution with (a) distance from the bottom (n= 24, p= 0.0007), and with (b) Ba in late May 2010. Samples with high Ba concentrations are plotted with triangles. For regression calculation in (a), the Ba-enriched samples (triangles) were excluded, for all data the regression was y = -0.0068x + 4.8, r^2 = 0.26, n=33, p= 0.0025). For graph (b) regression, only Ba-enriched samples (triangles, n= 9, p < 0.0001) were used.

Nonetheless, the enhanced growth in July 2010 appears to have been widely dispersed, as evidenced by the broader July spatial distribution of deep-water oxygen anomalies than in May and the fact that oxygen depletions were not observed to be greater than 25%, similar to what was observed in late May (Kessler et al., 2011; Du and Kessler, 2012). Thus, it is unlikely that the Fe concentrations were significantly more depleted during the later stages of the spill than what was observed in this study. Interestingly, Cu is also required by methanotrophs (Berson and Lidstrom, 1996), and its concentrations in the water were also low. However, the late May 2010 data showed no significant anomalies in its distribution (Appendix).

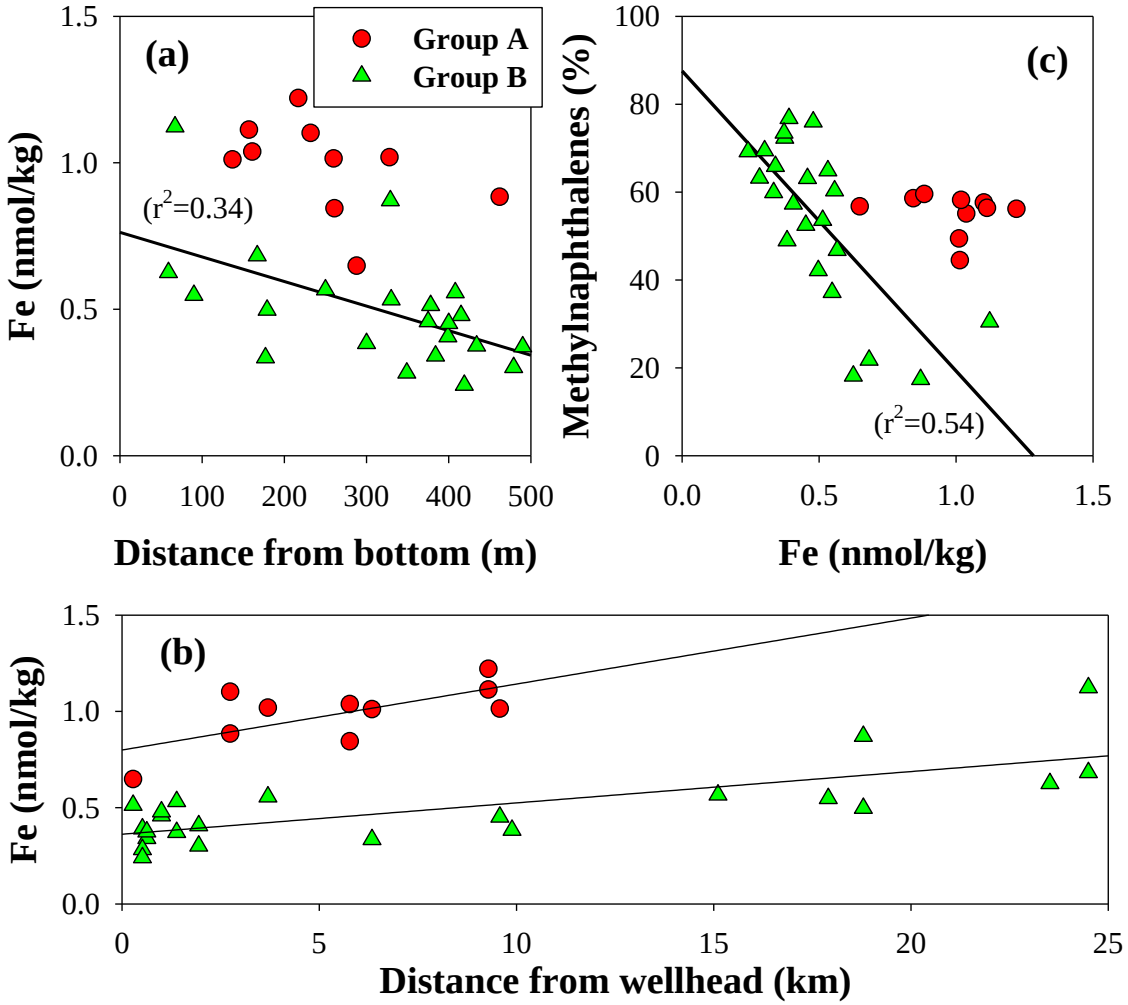

Figure 30. Plots of dissolved Fe with (a) distance from the bottom, (b) distance from the wellhead, and (c) percent methylnaphthalenes during late May 2010. Regressions for group A and B were y = 0.034x + 0.80 (r^2 = 0.46, n=10, p= 0.031) and y = 0.016x + 0.36 (r^2 = 0.55, n= 23, p< 0.0001), respectively. In graph (c), the regression was y = -68.2x + 87.5 (n=23, p< 0.0001).

Conclusion

Overall, the trace element concentrations determined in the crude oil released from the Deepwater Horizon blowout were low compared to some other crude oils including South Louisiana crude oil. Thus, anomalies in the dissolved trace elements measured in the water were generally insignificant. Even for Co, the one element with a

significant increase in the deep water oil/gas plume, increased concentrations were still low enough and confined to a small enough area to likely be of minimal consequence. Other minor increases in dissolved Ba and Mn appeared to be related to the drilling fluids and the top kill attempt on the well. Dissolved Fe concentrations in the depth range of the submerged oil/gas were low enough that enhanced microbial Fe demand could have affected its concentrations but probably not to the extent of Fe-limitation. The experiments in which oil and dispersant were added to various natural waters suggest that surfactants in the dispersant can solubilize metals from suspended particles, a factor which should be taken into account in future dispersant applications as well as in the development of new oil dispersing agents.

APPENDIX A

Determination of trace elements: The filtered samples were brought back to the clean lab on shore. The samples were acidified to pH < 2 by addition of 6 M ultrapure HCl (Seastar Baseline) to avoid adsorption onto container walls as well as biological activity. Elemental analyses were conducted using a sector-field inductively coupled plasma-mass spectrometry (Thermo-Fisher Element 2). For fresh water samples, analyses were performed as described in Shiller (2003). This analysis includes slight (30%) dilution of the samples with dilute (0.16 M) ultrapure nitric acid and calibration versus external standards. For seawater samples, it was utilized both the dilution and co-precipitation methods described in Shim et al. (2012). For Ba and Mo, the dilution method involves the dilution of the sample 20-fold with 0.3 M ultrapure HNO_3 (Seastar Baseline) and calibration by isotope dilution using spikes of enriched ^{135}Ba and ^{95}Mo. Other elements were determined by magnesium hydroxide co-precipitation with external standards calibration for Mn and Co and isotope dilution calibration for Fe, Cu, Ni, Cr, and V (Shim et al., 2012; Shiller and Bairamadgi, 2006).

Detection limits and recovery: In order to verify the accuracy of the analysis, certified seawater (NASS-5; NRC-Canada) was measured twice in a single analytical run. Detection limits were estimated based on 3x the standard deviation of our blank. Recovery and detection limit results are shown in Appendix table.

Anomaly estimation: Anomalies of dissolved oxygen (DO) and nutrients were estimated by differences of concentrations between May 2010 and October 2011. The October 2011 profiles of DO and nutrients in the 600 – 1600 m depth range from station GIP 18, the closest station to the wellhead, were fitted to 3rd order polynomials (Shiller and Joung, 2012). From these regressions, the background concentrations of DO and

nutrients were estimated, and the measured May 2010 concentrations were then subtracted from the estimated concentrations at the same depth. After nitrate anomaly calculation, carbon removal was estimated from C:N ratios of 12:1 and 5:1 for methanotrophs (Lee and Childress, 1994) and heterotrophic bacteria (Tortell et al., 1999), respectively. Iron removal was then estimated based on the heterotrophic bacteria ratio of 7.5 µmol-Fe/mol-C (Tortell et al., 1999). This ratio was also used for the Fe quota of methanotrophs.

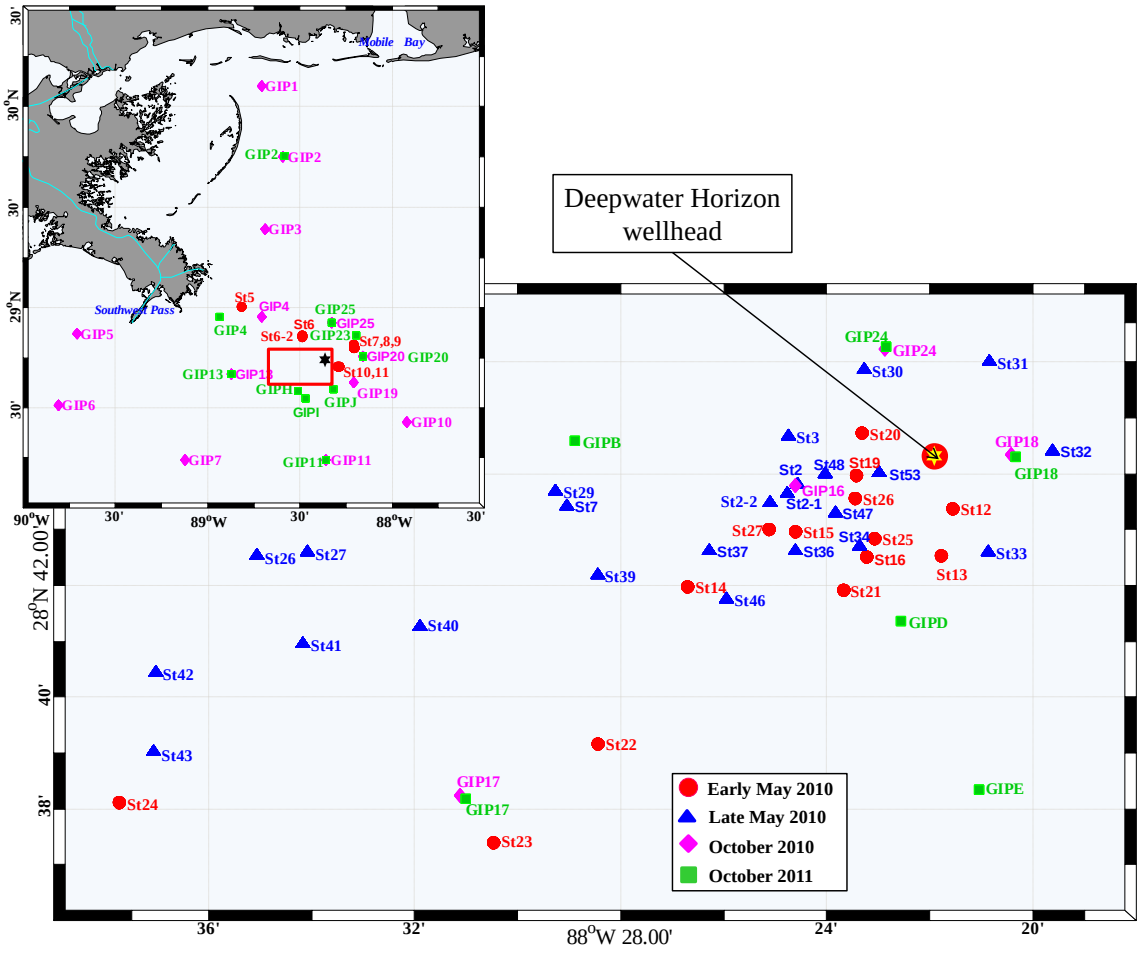

Figure: Map of sampling locations.

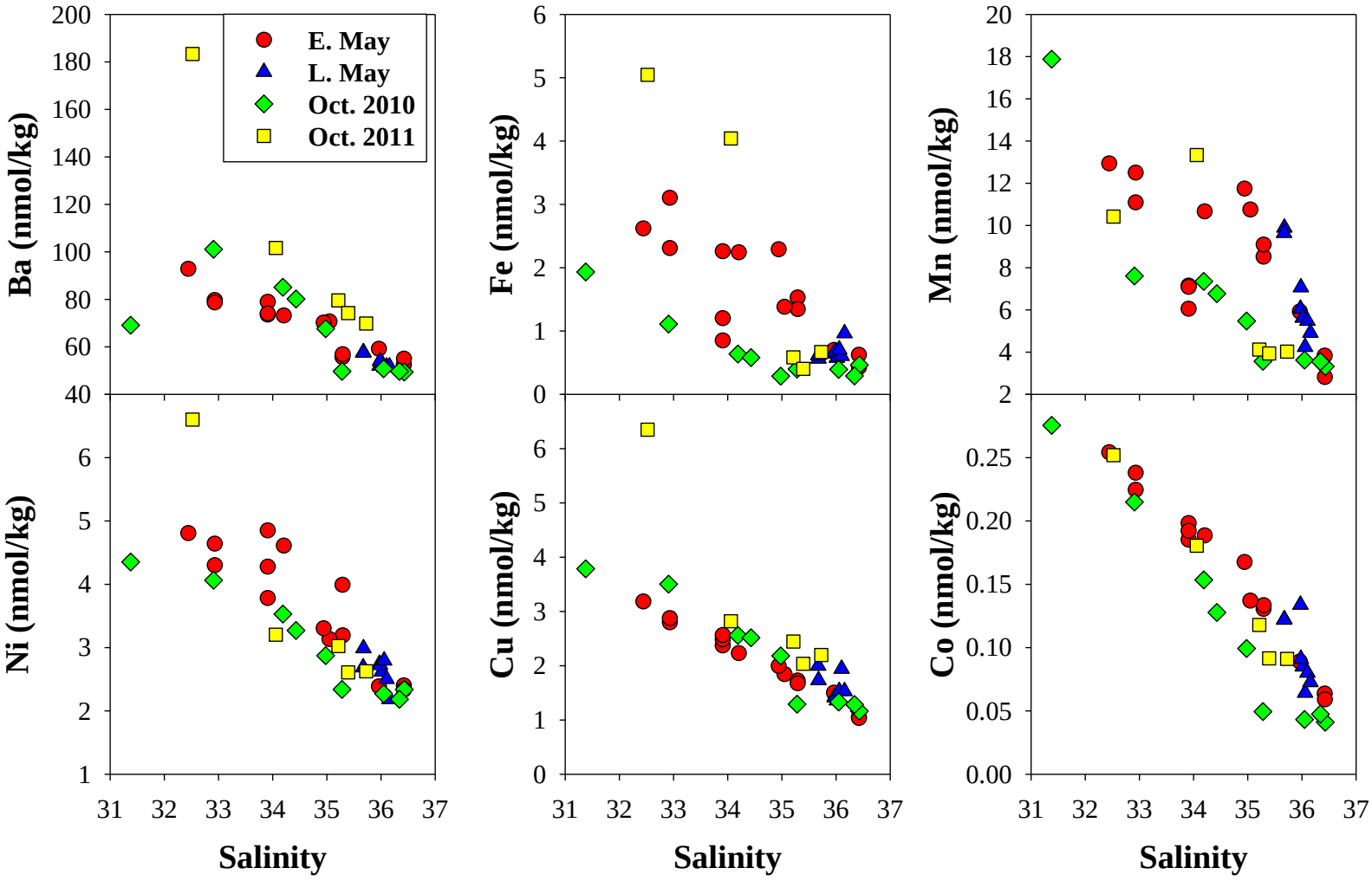

Figure. Metal distributions in surface waters. E. May and L. May are Early May 2010 and Late May 2010, respectively.

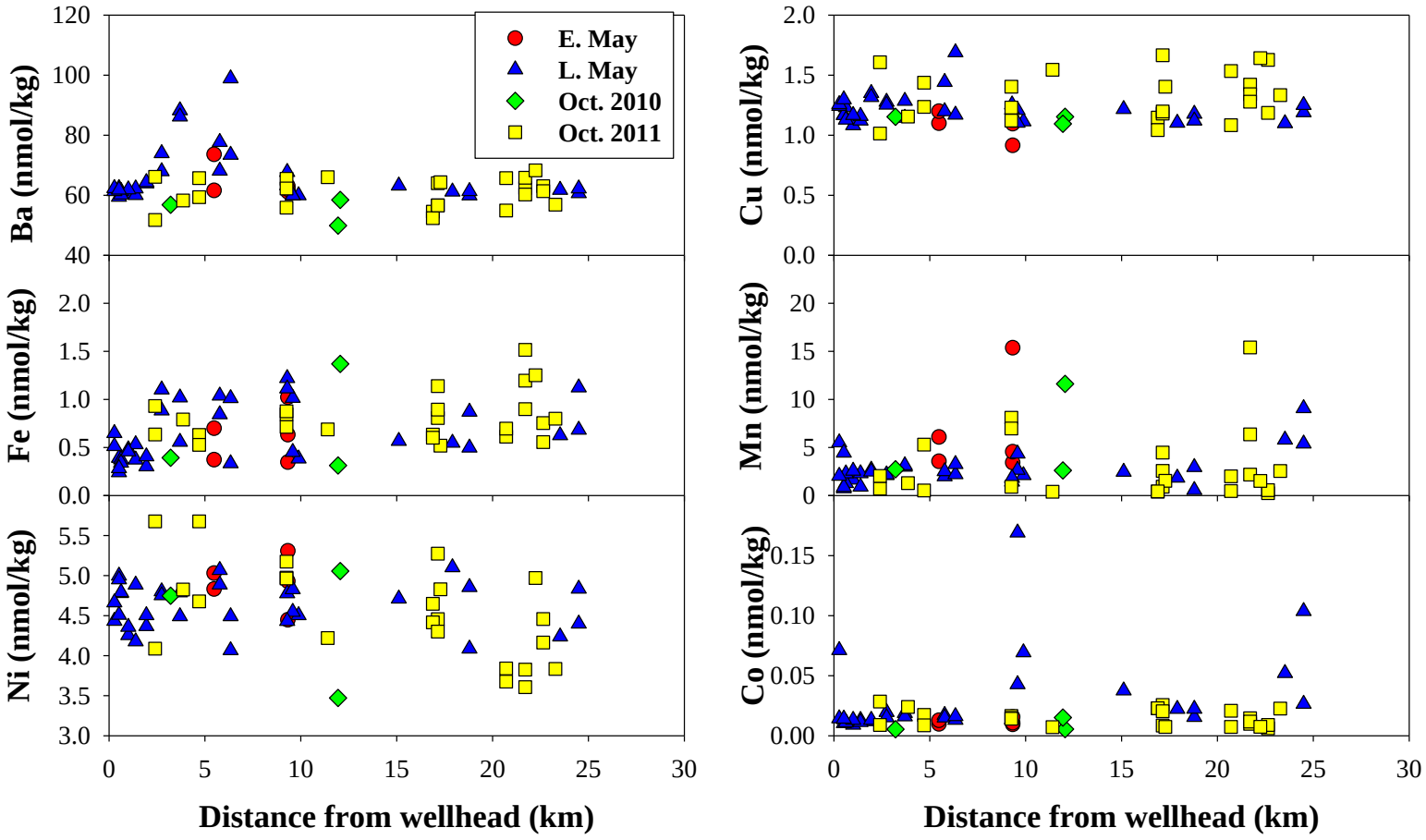

Figure. Spatial distributions of trace elements. Data are limited to the subsurface oil plume depth (1000 - 1350 m). Abbreviations same as the previous graph.

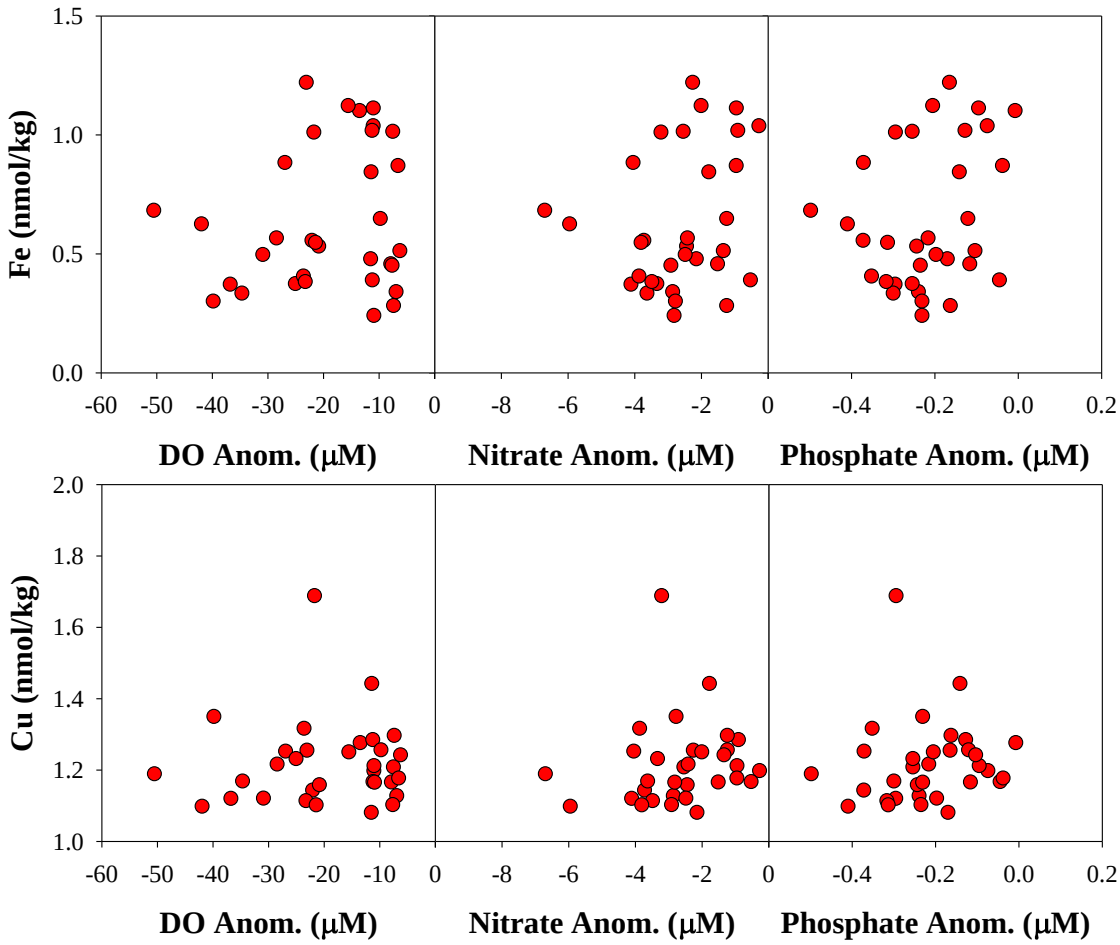

Figure. Fe and Cu distributions versus anomalies of dissolved oxygen (DO), nitrate, and phosphate at the depth of 1000-1350 m (Only late May data were used).

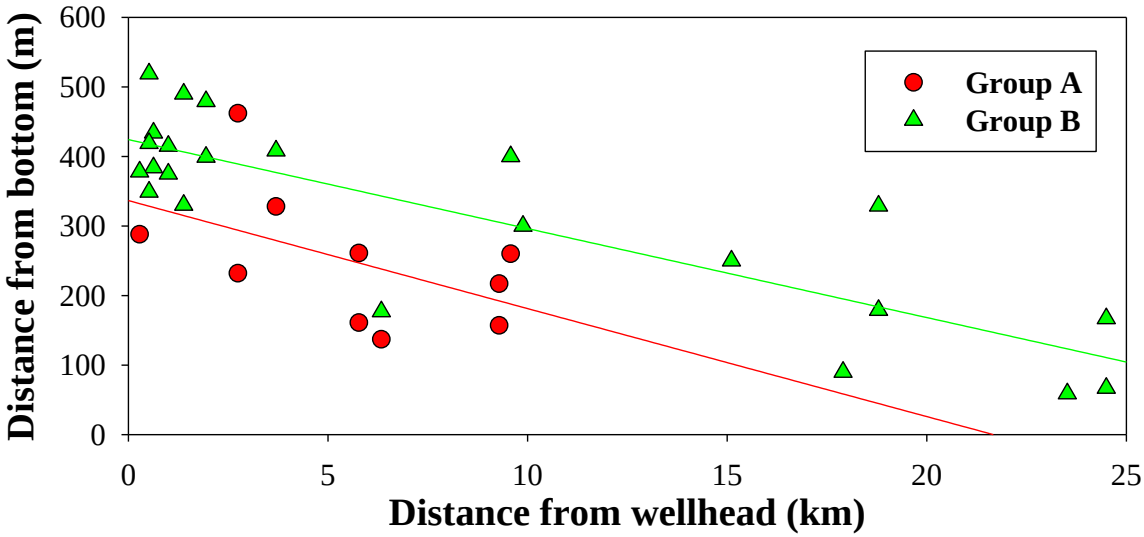

Figure. Distance from bottom versus distance from wellhead for sample groups A and B, and the regressions were y = -15.5x + 336 (r^2 = 0.27, n= 10, p=0.1274) and y = -12.8x + 424 (r^2 = 0.71, n= 23, p< 0.0001) for groups A and B, respectively.

Table

Detection limit and Recovery of NASS5 (n=20, and n=10 for Mo and Ba)

	V	Cr	Mn	Fe	Co	Ni	Cu	Mo	Ba
Detection Limit (nM)	0.4	0.06	0.1	0.3	0.003	0.3	0.5	0.9	1.5
NASS5 Accepted (nM)	23.6	2.12	16.7	3.7	0.190	4.3	4.7	100.1	37.4*
NASS5 Measured (nM)	23.1	2.14	16.7	3.6	0.189	4.3	5.0	98.1	38.1
Standard deviation (nM)	1.8	0.08	0.5	0.2	0.011	0.4	0.6	6.9	1.4
Recovery (%)	98	101	100	96	99	101	106	98	102

*NASS-5 concentrations were taken from Shim et al. (2012).

Table

Results from the Early May 2010 cruise

	Date	Lat.	Lon.	Dis.	Bot.	Sam.	Temp.	Sal.	DO	T.PAHs	Me.Na.
				(km)	(m)	(m)	(°C)		(µM)	(µg/L)	(%)
St 5	5/10	29.003	88.818	53.3	212	0	24.8	32.4	221		
						210	13.8	35.8	117		
St 6-1	5/10	28.854	88.485	17.5	894	0	24.8	32.9	218	2	63
						884	5.5	34.9	165	0.2	68
St 6-2	5/10	28.861	88.489	18.3		0	24.8	32.9	218		
St 7	5/11	28.815	88.206	17.2	1325	0	24.5	33.9	217	2830	29
St 8	5/11	28.798	88.210	16.1	1325	0	24.5	33.9	217	2725	18
St 9	5/11	28.801	88.202	16.9	1325	0	24.5	33.9	217	2355	14
St 10	5/11	28.708	88.295	7.3	1500	0	25.5	35.3	217	2117	12
St 11	5/11	28.708	88.287	8.1	1500	0	25.5	35.3	223	85	7
St 12	5/11	28.723	88.359	1.9	1615	0	24.9	36.4	213	4699	43
St 13	5/11	28.709	88.363	3.5	1615	0	24.9	36.4	213	918	16
						1605	4.3	35.0	213	0.2	56
St 14	5/12	28.700	88.445	9.3	1302	0	24.6	34.2	216	185	29
						1060	4.8	34.9	160		
						1150	4.6	35.0	161	7	72
						1292	4.4	35.0	207	1	57
St 15	5/12	28.716	88.410	5.5	1565	740	6.3	34.9	103	0.3	30
						1170	4.6	35.0	177	4	58
						1320	4.4	35.0	200	189	84
St 22	5/13	28.653	88.474	14.7	1494	0	24.2	35.0	212		
St 23	5/13	28.623	88.508	19.3	1640	0	23.8	34.9	212		
St 24	5/13	28.635	88.629	28.6	1322	0	24.5	36.0	215		

Abbreviation- Lat.: latitude, Lon.: longitude, Dis.: distance from the wellhead (N 28° 44.412', W 88° 21.676'), Sam. Depth: sampling depth, Temp.: temperature, Sal.: salinity, DO: dissolved oxygen, T. PAH: total polycyclic aromatic hydrocarbons, Me.Na.: methylnaphthalenes as a percentage of total PAHs.

Table (continued).

	Dis.	Bot.	Sam.	Mo	Ba	V	Cr	Fe	Ni	Cu	Mn	Co
	(km)	(m)	(m)					(nmol/kg)				
St 5	53.3	212	0	113	91	23	2.3	2.6	4.7	3.1	12.7	0.25
			210	120	45	34	3.1	13.1	4.2	1.0	195	0.08
St 6-1	17.5	894	0	114	78	17	2.2	3.0	4.5	2.7	12.2	0.23
			884	98	60	31	3.2	2.2	5.6	1.1	4.4	0.02
St 6-2	18.3		0	115	77	18	2.4	2.3	4.2	2.8	10.8	0.22
St 7	17.2	1325	0	122	77	25	2.4	0.8	3.7	2.3	5.9	0.18
St 8	16.1	1325	0	117	72	19	2.4	1.2	4.2	2.4	7.0	0.19
St 9	16.9	1325	0	118	72	24	2.4	2.2	4.7	2.5	6.9	0.19
St 10	7.3	1500	0	123	54	34	2.5	1.5	3.9	1.7	8.3	0.13
St 11	8.1	1500	0	123	56	31	2.5	1.3	3.1	1.6	8.9	0.13
St 12	1.9	1615	0	124	51	34	2.8	0.6	2.3	1.0	3.7	0.06
St 13	3.5	1615	0	132	54	35	2.8	0.4	2.3	1.0	2.7	0.06
			1605	121	63	31	3.1	0.9	4.4	1.2	16.6	0.02
St 14	9.3	1302	0	123	72	29	2.4	2.2	4.5	2.2	10.4	0.18
			1060	121	61	33	3.2	0.3	4.4	0.9	3.4	0.01
			1150	120	63	32	3.4	0.6	5.3	1.1	4.6	0.01
			1292	114	62	32	3.3	1.0	4.9	1.2	15.4	0.02
St 15	5.5	1565	740	120	57	33	3.3	2.2	6.4	0.8	1.4	0.04
			1170	125	74	31	3.3	0.7	4.8	1.1	3.6	0.01
			1320	122	62	32	3.2	0.4	5.0	1.2	6.1	0.01
St 22	14.7	1494	0	127	69	32	2.5	1.3	3.1	1.8	10.5	0.13
St 23	19.3	1640	0	125	69	32	2.5	2.2	3.2	1.9	11.5	0.16
St 24	28.6	1322	0	128	58	32	2.7	0.7	2.3	1.5	5.8	0.09

Abbreviation- Lat.: latitude, Lon.: longitude, Dis.: distance from the wellhead (N 28° 44.412', W 88° 21.676'), Sam. Depth: sampling depth, Temp.: temperature, Sal.: salinity, DO: dissolved oxygen, T. PAH: total polycyclic aromatic hydrocarbons, Me.Na.: methylnaphthalenes as a percentage of total PAHs.

Table

Results from late May 2010

	Date	Lat.	Lon.	Dis.	Bot. Depth	Sam. Depth	Temp.	Sal.	DO	T. PAHs	Me.Na.
				(km)	(m)	(m)	(°C)		(µM)	(µg/l)	(%)
St2-1	5/26	28.728	88.413	2.7	1524	0	27.5	35.7	199	6	4
St2-2	5/26	28.725	88.418	3.3	1524	0	27.5	35.7	199	6	44
St7	5/27	28.724	88.484	9.6	1400	900	5.4	34.9	161	1	43
						1000	5.0	34.9	173	20	52
						1140	4.6	34.9	189	5	45
St13	5/27	28.826	88.816	43.0	688	0	27.8	36.0	199	13	2
St26	5/28	28.709	88.584	19.5	1050	870	5.6	34.9	149	0.3	3
St27	5/28	28.710	88.568	17.9	1165	1075	4.7	34.9	168	2	37
St29	5/28	28.728	88.488	9.9	1410	1110	4.7	34.9	170	9	49
St30	5/30	28.764	88.388	3.1	1430	5.4	27.6	36.2	197	0.5	18
St31	5/30	28.767	88.347	5.1	1507	0	27.5	36.0	170	2	9
St32	5/30	28.740	88.327	5.9	1557	0	27.4	36.0	196	2	11
St33	5/30	28.710	88.348	4.9	1585	0	27.6	36.1	195	2	13
St34	5/30	28.712	88.390	2.8	1602	0	27.7	36.1	195	1	44
						1140	4.6	34.9	170	80	60
						1370	4.4	35.0	201	13	58
St36	5/30	28.710	88.410	3.7	1548	1140	4.6	34.9	175	445	60
						1220	4.5	35.0	193	71	58
St37	5/30	28.710	88.438	5.8	1411	1150	4.6	34.9	186	31	57
						1250	4.5	35.0	196	9	55
St39	5/30	28.703	88.438	9.3	1317	1100	4.8	34.9	169	10	56
						1160	4.6	34.9	188	18	56
St40	5/30	28.688	88.532	15.1	1410	1160	4.6	34.9	170	6	47
St41	5/30	28.683	88.570	18.8	1329	1000	5.0	34.9	175	0.3	17
						1150	4.6	35.0	167	1	42
St42	5/30	28.674	88.617	23.5	1150	1091	4.7	34.9	150	1	18
St43	5/31	28.650	88.618	24.5	1317	1150	4.6	35.0	147	1	22
						1250	4.4	35.0	191	2	30
St46	5/31	28.696	88.433	6.3	1347	1170	4.5	34.9	165	41	62
						1210	4.5	35.0	182	21	49
St47	5/31	28.722	88.397	1.9	1579	1100	4.8	34.9	153	29	69
						1180	4.5	34.9	177	117	57
St48	5/31	28.733	88.401	1.4	1530	1040	5.0	34.9	149	47	73
						1200	4.5	34.9	182	38	65
St53	6/01	28.734	88.383	0.5	1519	600	7.3	34.9	125	0.7	26
						1000	5.1	34.9	170	5	77
						1100	4.8	34.9	182	25	69
						1170	4.5	34.9	192	66	63

Table (continued).

	Date	Lat.	Lon.	Dis. (km)	Bot. (m)	Sam. (m)	Temp. (°C)	Sal.	DO (μM)	T.PAH (μg/l)	Me.Na. (%)
St57	6/01	28.737	88.393	0.6	1514	1080	4.8	34.9	165	35	72
						1130	4.6	34.9	189	52	66
St58	6/01	28.739	88.386	0.3	1498	1120	4.6	34.9	188	38	54
						1210	4.5	34.9	193	81	57
St59	6/01	28.742	88.379	1.0	1515	1100	4.7	34.9	181	26	76
						1140	4.6	34.9	189	30	63

	Dis.	Bot. Depth	Sam. Depth	Mo	Ba	V	Cr	Fe	Ni	Cu	Mn	Co
	(km)	(m)	(m)	(nmol/kg)								
St2-1	2.7	1524	0	117	56	33	2.7	0.5	2.9	1.7	9.7	0.12
St2-2	3.3	1524	0	119	56	33	2.8	0.6	2.6	2.0	9.4	0.12
St7	9.6	1400	900	117	58	34	3.3	0.5	4.3	1.1	0.4	0.01
			1000	117	60	32	3.3	0.5	4.8	1.1	2.7	0.04
			1140	115	60	32	3.3	1.0	4.5	1.2	4.4	0.17
St13	43.0	688	0	122	51	36	2.7	0.6	2.7	1.4	5.9	0.13
St26	19.5	1050	870	110	59	33					0.5	0.02
St27	17.9	1165	1075	116	61	33	3.3	0.5	5.1	1.1	1.8	0.02
St29	9.9	1410	1110	118	60	33	3.2	0.4	4.5	1.1	2.1	0.07
St30	3.1	1430	5.4	122	51	34	2.7	0.9	2.1	1.5	4.8	0.07
St31	5.1	1507	0	122	52	37	2.7	0.6	2.6	1.3	5.5	0.08
St32	5.9	1557	0	118	53	34	2.7	0.7	2.7	1.4	6.9	0.09
St33	4.9	1585	0	119	50	33	2.7	0.6	2.4	1.9	5.3	0.08
St34	2.8	1602	0	120	50	35	2.8	0.7	2.7	1.5	4.1	0.06
			1140	117	68	32	3.2	0.9	4.8	1.3	2.2	0.02
			1370	78	74	33	2.8	1.1	4.8	1.3	2.1	0.02
St36	3.7	1548	1140	120	86	32	3.3	0.6	4.5	1.1	3.1	0.02
			1220	115	88	32	3.1	1.0	4.8	1.3	3.0	0.02
St37	5.8	1411	1150	113	78	34	3.3	0.8	5.1	1.4	2.5	0.02
			1250	118	68	37	3.1	1.0	4.9	1.2	2.0	0.02
St39	9.3	1317	1100	117	63	33	3.3	1.2	4.8	1.3	1.4	0.01
			1160	112	68	34	3.4	1.1	4.4	1.2	1.8	0.01
St40	15.1	1410	1160	115	63	31	3.1	0.6	4.7	1.2	2.5	0.04
St41	18.8	1329	1000	116	60	32	3.3	0.9	4.1	1.2	0.6	0.02
			1150	115	61	33	3.3	0.5	4.9	1.1	2.9	0.02
St42	23.5	1150	1091	116	62	35	3.3	0.6	4.2	1.1	5.8	0.05
St43	24.5	1317	1150	119	61	33	3.2	0.7	4.8	1.2	5.4	0.10
			1250	116	62	35	3.2	1.1	4.4	1.3	9.1	0.03
St46	6.3	1347	1170	115	73	32	3.3	0.3	4.1	1.2	2.2	0.01
			1210	115	99	34	3.3	1.0	4.5	1.7	3.3	0.02

Table (continued).

	Dis.	Bot. Depth	Sam. Depth	Mo	Ba	V	Cr	Fe	Ni	Cu	Mn	Co
	(km)	(m)	(m)	(nmol/kg)								
St47	1.9	1579	1100	119	64	34	3.3	0.3	4.4	1.3	2.7	0.01
			1180	116	64	31	3.3	0.4	4.5	1.3	2.5	0.01
St48	1.4	1530	1040	115	60	36	3.2	0.4	4.9	1.1	0.9	0.01
			1200	115	62	32	3.2	0.5	4.2	1.2	2.3	0.01
St53	0.5	1519	600	117	52	31	3.2	0.7	4.6	0.9	0.4	0.03
			1000	115	59	32	3.2	0.4	5.0	1.2	0.7	0.01
			1100	117	62	33	3.2	0.2	5.0	1.2	0.9	0.01
			1170	113	62	33	3.2	0.3	4.5	1.3	4.4	0.01
St57	0.6	1514	1080	116	61	32	3.2	0.4	4.8	1.2	1.3	0.01
			1130	116	60	32	3.3	0.3	4.8	1.1	2.3	0.01
St58	0.3	1498	1120	115	61	34	3.1	0.5	4.4	1.2	2.0	0.07
			1210	118	62	35	3.2	0.6	4.7	1.3	5.5	0.01
St59	1.0	1515	1100	118	61	33	3.2	0.5	4.3	1.1	1.6	<0.01
			1140	115	62	34	3.3	0.5	4.4	1.2	2.6	0.01

Abbreviation- Dis.: distance from the wellhead (N 28° 44.412', W 88° 21.676'), Bot. Depth: bottom depth, Sam. Depth: sampling depth.

Table

Results from October 2010

	Date	Lat.	Lon.	Dis.	Bottom Depth	Sam. Depth	Temp.	Sal.	DO	Total PAH
				(km)	(m)	(m)	(°C)		(µM)	(µg/l)
GIP-1	10/11	30.101	88.703	151.4	16	0	24.2	31.4	170	<0.2
						12	24.9	32.6	209	<0.2
GIP-2	10/11	29.750	88.590	112.4	28	0	25.8	32.9	179	<0.2
						22.9	24.8	35.3	134	<0.2
GIP-3	10/11	29.387	88.686	72.2	53	50.35	20.3	36.5	130	0.8
GIP-5	10/12	28.868	89.703	27.6	72	53	20.8	36.4	92	<0.2
						67	19.4	36.4	141	<0.2
GIP-6	10/12	28.507	89.805	36.4	530	523	8.6	35.0	115	<0.2
GIP-7	10/12	28.237	89.119	57.5	1136	1050	4.9	34.9	177	
GIP-13	10/13	28.668	88.870	12.1	1025	1023	5.0	34.9	175	
GIP-4	10/13	29.953	88.703	24.4	126	125	17.5	36.3	135	<0.2
GIP-10	10/14	28.423	87.919	36.1	2315	2229	4.3	35.0	208	
GIP-11	10/15	28.235	88.355	56.1	1973	1032	4.9	34.9	180	
GIP-16	10/16	28.725	88.406	1.9	1560	0	25.6	34.2	176	
						1549	4.3	35.0	206	
GIP-18	10/16	28.737	88.337	0.6	1570	0	26.8	36.1	198	
						900	5.5	34.9	161	
						1557	4.3	35.0	206	
GIP-24	10/17	28.769	88.375	3.2	1418	0	25.6	35.3	193	
						1403	4.4	35.0	152	
GIP-17	10/17	28.636	88.518	11.9	1595	0	26.0	34.4	175	
						1117	4.8	34.9	204	
GIP-19	10/19	28.623	88.205	13.4	2010	0	27.0	36.4	195	
GIP-20	10/19	28.756	88.156	3.9	1760	0	26.8	36.3	223	<0.2
GIP-25	10/19	28.923	88.322	20.3	1160	0	25.9	35.0	228	

	Dis.	Bot. Depth	Sam. Depth	Mo	Ba	V	Cr	Fe	Ni	Cu	Mn	Co
	(km)	(m)	(m)	(nmol/kg)								
GIP-1	151.4	16	0	101	68	37	3.1	1.9	4.3	3.7	17.5	0.27
			12	109	121	31	2.9	4.7	4.5	3.2	87.0	0.36
GIP-2	112.4	28	0	103	99	25	3.2	1.1	4.0	3.4	7.4	0.21
			22.9	112	82	33	3.1	8.5	4.0	2.7	59.0	0.25
GIP-3	72.2	53	50.35	112	58	29	4.4	11.8	3.3	1.7	56.3	0.16
GIP-5	27.6	72	53	101	64	31	3.3	1.7	3.9	2.4	97.6	0.21
			67	113	54	33	3.9	6.1	3.0	1.6	121	0.13
GIP-6	36.4	530	523	111	48	25	5.3	2.1	4.9	0.8	53.7	0.01

Table (continued).

	Dis.	Bot. Depth	Sam. Depth	Mo	Ba	V	Cr	Fe	Ni	Cu	Mn	Co
	(km)	(m)	(m)	(nmol/kg)								
GIP-7	57.5	1136	1050	110	59	29	4.6	2.1	5.0	1.1	44.8	<0.01
GIP-13	12.1	1025	1023	114	58	33	5.2	1.4	5.1	1.2	11.6	<0.01
GIP-4	24.4	126	125	114	43	33	4.7	6.0	2.7	0.9	56.9	0.03
GIP-10	36.1	2315	2229	103	59	29	4.9	0.4	4.9	1.3	0.9	<0.01
GIP-11	56.1	1973	1032	101	53	32	6.1	0.7	3.8	1.1	10.3	0.01
GIP-16	1.9	1560	0	111	83	32	4.2	0.6	3.4	2.5	7.2	0.15
			1549	111	60	25	5.0	0.4	5.2	1.3	4.6	<0.01
GIP-18	0.6	1570	0	114	50	33	4.2	0.4	2.2	1.3	3.5	0.04
			900	112	43	30	4.3	0.2	3.2	0.8	0.7	<0.01
			1557	110	57	30	5.0	0.4	5.2	1.1	0.5	<0.01
GIP-24	3.2	1418	0	117	49	28	4.4	0.4	2.3	1.3	3.5	0.05
			1403	109	57	33	5.3	0.4	4.7	1.2	2.7	<0.01
GIP-17	11.9	1595	0	110	78	35	4.0	0.6	3.2	2.5	6.6	0.12
			1117	115	50	32	4.1	0.3	3.5	1.1	2.6	0.02
GIP-19	13.4	2010	0	116	48	32	3.7	0.5	2.3	1.1	3.2	0.04
GIP-20	3.9	1760	0	114	48	32	4.0	0.3	2.1	1.3	3.5	0.05
GIP-25	20.3	1160	0	112	66	34	4.6	0.3	2.8	2.1	5.3	0.10

Abbreviation- Lat.: latitude, Lon.: longitude, Dis.: distance from the wellhead (N 28° 44.412', W 88° 21.676'), Bot. Depth: bottom depth, Sam. Depth: sampling depth, Temp.: temperature, Sal.: salinity, DO: dissolved oxygen, Me.Na.: methylnaphthalenes as a percentage of total PAHs.

Table

Results from October 2011

	Date	Lat.	Lon.	Dis.	Bot. Depth	Sam. Depth	Temp.	Sal.	DO
				(km)	(m)	(m)	(°C)		(µM)
GIP-2	10/21	29.757	88.585	115.1	28	0	25.2	34.1	86
GIP-4	10/21	28.954	88.935	58.6	133	0	24.0	32.5	152
GIP-11	10/22	28.238	88.361	55.6	1973	0	26.2	35.4	132
						1100	4.7	34.9	186
						1400	4.3	35.0	203
						1971	4.3	35.0	207
GIP-I	10/22	28.546	88.469	22.6	1741	1000	5.2	34.9	170
						1200	4.6	34.9	191
						1739	4.3	35.0	207
GIP-H	10/22	28.586	88.512	20.7	1707	1100	4.9	34.9	179
						1400	4.4	35.0	201
						1600	4.3	35.0	205
						1704	4.3	35.0	205
GIP-17	10/23	28.636	88.517	16.9	1584	800	6.0	34.9	147
						1000	5.2	34.9	168
						1300	4.5	35.0	196
						1582	4.3	35.0	203
GIP-13	10/23	28.669	88.871	47.8	1026	0	26.0	35.7	189
						700	6.4	34.9	138
						800	5.9	34.9	148
						1023	5.4	34.9	163
GIP-G	10/23	28.685	88.553	17.1	1402	1100	4.9	34.9	180
						1200	4.7	34.9	187
						1399	4.4	35.0	200
GIP-B	10/24	28.743	88.482	9.3	1416	1200	4.6	34.9	192
						1300	4.4	35.0	198
						1413	4.3	35.0	205
GIP-24	10/25	28.771	88.381	3.9	1408	1000	5.1	34.9	173
GIP-18	10/25	28.738	88.339	4.7	1861	0	26.0	35.2	146
						1100	4.8	34.9	182
						1300	4.4	35.0	200
						1559	4.3	35.0	207
GIP-16	10/25	28.730	88.410	2.4	1534	1200	4.6	34.9	191
						1300	4.4	35.0	199
						1500	4.3	35.0	208
						1531	4.3	35.0	208
GIP-D	10/26	28.689	88.376	5.4	1625	1500	4.3	35.0	207
						1600	4.3	35.0	207
						1623	4.3	35.0	207

Table (continued).

	Date	Lat.	Lon.	Dis.	Bot. Depth	Sam. Depth	Temp.	Sal.	DO
				(km)	(m)	(m)	(°C)		(μM)
GIP-E	10/26	28.639	88.351	11.4	1715	1400	4.4	35.0	203
						1600	4.3	35.0	205
						1713	4.3	35.0	206
GIP-J	10/26	28.594	88.316	17.3	1854	1200	4.5	35.0	194
						1500	4.3	35.0	205
						1700	4.3	35.0	207
						1852	4.3	35.0	207
GIP-23	10/27	28.863	88.196	23.3	1353	1351	4.3	35.0	203
GIP-20	10/27	28.756	88.160	22.2	1759	900	5.5	34.9	160
						1300	4.4	35.0	199
GIP-25	10/28	28.925	88.326	21.7	1159	800	6.0	34.9	146
						1000	5.3	34.9	167
						1100	4.6	34.9	192
						1156	4.5	35.0	194

	Dis.	Bot. Depth	Sam. Depth	Mo	Ba	V	Cr	Fe	Ni	Cu	Mn	Co
	(km)	(m)	(m)	(nmol/kg)								
GIP-2	115.1	28	0	109	102	31	2.0	4.0	3.5	2.8	13.3	0.18
GIP-4	58.6	133	0	102	183	38	1.5	5.0	6.4	6.3	10.4	0.25
GIP-11	55.6	1973	0	110	74	26	2.4	0.4	2.4	2.0	3.9	0.09
			1100	108	65	32	3.2	0.7	4.7	1.4	0.2	<0.01
			1400	111	65	31	3.1	0.7	4.1	1.3	0.2	0.02
			1971	108	58	32	3.1	0.8	4.0	1.1	0.8	0.02
GIP-I	22.6	1741	1000	112	63	30	3.3	0.6	4.5	1.6	0.2	<0.01
			1200	108	61	33	3.1	0.8	4.2	1.2	0.6	<0.01
			1739	98	57	33	2.7	1.2	3.7	1.2	1.6	0.02
GIP-H	20.7	1707	1100	113	66	31	3.1	0.6	3.8	1.5	2.0	<0.01
			1400	113	55	31	3.0	0.7	3.7	1.1	0.5	0.02
			1600	110	65	30	3.0	0.7	4.5	1.3	11.5	<0.01
			1704	112	56	33	3.0	1.0	4.1	1.0	2.7	0.02
GIP-17	16.9	1584	800	114	60	27	3.2	0.8	5.3	1.6	0.2	0.02
			1000	112	55	29	3.0	0.6	4.6	1.1	0.4	0.02
			1300	108	52	33	2.9	0.6	4.4	1.0	0.4	0.02
			1582	113	57	33	3.1	0.7	3.9	1.2	4.7	0.02
GIP-13	47.8	1026	0	116	70	35	2.4	0.7	2.6	2.2	4.0	0.09
			700	112	60	34	2.7	1.0	2.6	1.9	2.9	0.05
			800	114	50	31	3.0	0.9	4.0	1.0	1.4	0.02
			1023	113	62	33	3.1	2.6	5.0	1.4	4.3	0.02
GIP-G	17.1	1402	1100	111	64	28	3.1	1.1	5.3	1.7	2.6	<0.01
			1200	114	57	31	3.0	0.8	4.5	1.2	0.9	0.02
			1399	110	57	30	3.0	0.9	4.3	1.2	4.5	0.02

Table (continued).

	Dis.	Bot. Depth	Sam. Depth	Mo	Ba	V	Cr	Fe	Ni	Cu	Mn	Co
	(km)	(m)	(m)	(nmol/kg)								
GIP-B	9.3	1416	1200	113	56	30	3.1	0.7	5.0	1.1	0.9	0.02
			1300	112	66	29	3.1	0.8	5.2	1.4	8.1	0.02
			1413	113	62	30	3.2	0.9	5.0	1.2	7.0	0.01
GIP-24	3.9	1408	1000	111	58	31	3.1	0.8	4.8	1.2	1.3	0.02
GIP-18	4.7	1861	0	113	80	35	2.2	0.6	3.1	2.4	4.1	0.12
			1100	109	59	32	3.1	0.6	5.7	1.2	0.5	0.02
			1300	111	66	27	3.1	0.5	4.7	1.4	5.3	<0.01
			1559	113	57	28	3.1	0.8	4.6	1.1	3.0	0.02
GIP-16	2.4	1534	1200	112	52	33	3.0	0.9	4.1	1.0	0.7	0.03
			1300	110	66	33	3.2	0.6	5.7	1.6	2.0	<0.01
			1500	116	59	33	3.1	0.6	4.6	1.4	1.6	0.02
			1531	114	55	33	2.9	0.6	3.9	1.1	1.1	0.03
GIP-D	5.4	1625	1500	113	67	30	3.1	0.7	5.6	1.5	1.6	0.01
			1600	113	56	31	3.1	0.8	4.3	1.2	1.4	0.02
			1623	115	56	33	2.9	0.7	4.1	1.2	1.1	0.02
GIP-E	11.4	1715	1400	113	66	30	3.2	0.7	4.2	1.5	0.4	<0.01
			1600	117	48	34	3.0	0.9	4.3	1.0	0.8	0.03
			1713	113	55	31	2.8	0.8	4.0	1.2	1.1	0.02
GIP-J	17.3	1854	1200	112	64	31	3.2	0.5	4.8	1.4	1.5	<0.01
			1500	114	67	29	3.1	0.6	4.1	1.6	3.8	<0.01
			1700	114	49	32	2.9	1.1	4.0	1.0	1.7	0.03
			1852	112	57	33	2.9	0.8	3.9	1.3	1.2	0.02
GIP-23	23.3	1353	1351	116	57	30	3.2	0.8	3.8	1.3	2.5	0.02
GIP-20	22.2	1759	900	113	58	33	3.4	0.8	5.5	1.3	0.5	0.02
			1300	115	68	31	3.3	1.3	5.0	1.6	1.5	<0.01
GIP-25	21.7	1159	800	110	61	30	3.4	0.6	5.5	1.2	0.2	0.01
			1000	113	62	32	3.3	0.9	6.3	1.4	2.2	0.01
			1100	113	60	33	3.1	1.2	3.6	1.3	6.4	0.02
			1156	110	66	32	3.3	1.5	3.8	1.3	15.4	0.01

Abbreviation- Dis.: distance from the wellhead (N 28° 44.412', W 88° 21.676'), Bot. Depth: bottom depth, Sam. Depth: sampling depth.

Table

Estimated anomalies in nutrients, dissolved oxygen (DO), carbon, and iron removal during late May 2010

	Dis.	Sam.	DO	DO*	NO_3	NO_3*	PO_4	PO_4*	C Rem.	Fe Rem.	Fe	Cu	T. PAH	Me. Na.
	(km)	(m)				(µM)					(nM)		(µg/l)	(%)
Group A														
St34	2.7	1370	201.0	-13.5	24.5	0.9	1.65	-0.01			1.10	1.28	12.7	58
St39	9.3	1100	169.3	-23.1	23.7	-2.3	1.61	-0.16	-27.1	-0.20	1.22	1.26	9.9	56
St37	5.8	1250	195.6	-11.0	24.2	-0.3	1.63	-0.07	-3.3	-0.02	1.04	1.20	8.6	55
St37	5.8	1150	186.1	-11.4	23.7	-1.8	1.61	-0.14	-21.3	-0.16	0.84		30.7	59
St39	9.3	1160	187.5	-11.0	24.4	-1.0	1.65	-0.10	-11.4	-0.09	1.11	1.21	18.0	56
St36	3.7	1220	192.9	-11.2	23.8	-0.9	1.59	-0.13	-10.9	-0.08	1.02	1.28	70.5	58
St46	6.3	1210	181.5	-21.7	21.6	-3.2	1.43	-0.29	-38.5	-0.29	1.01		21.4	49
St34	2.7	1140	169.6	-26.9	21.5	-4.0	1.38	-0.37	-48.6	-0.36	0.88	1.25	79.6	60
St7	9.6	1140	189.0	-7.5	23.0	-2.5	1.50	-0.25	-30.5	-0.23	1.01	1.21	4.7	45
St58	0.3	1210	193.4	-9.8	23.6	-1.2	1.60	-0.12	-14.9	-0.11	0.65	1.26	80.9	57
								average		-0.17	0.98			
Group B														
St36	3.7	1140	174.5	-22.1	21.8	-3.7	1.38	-0.37	-44.7	-0.34	0.56	1.14	44.3	60
St53	0.5	1000	169.9	-11.2	26.6	-0.5	1.77	-0.04	-6.3	-0.05	0.39	1.17	5.3	77
St57	0.6	1130	188.6	-6.9	22.8	-2.9	1.52	-0.24	-34.4	-0.26	0.34	1.13	52.0	66
St57	0.6	1080	165.2	-25.1	22.9	-3.3	1.52	-0.25	-40.0	-0.30	0.37	1.23	34.8	72
St48	1.4	1040	149.0	-36.8	22.5	-4.1	1.50	-0.30	-49.3	-0.37	0.37	1.12	47.1	73
St59	1.0	1140	188.7	-7.9	24.1	-1.5	1.64	-0.12	-18.2	-0.14	0.46	1.17	29.6	63
St59	1.0	1100	180.9	-11.5	23.8	-2.2	1.60	-0.17	-25.8	-0.19	0.48	1.08	25.7	76
St58	0.3	1120	188.3	-6.3	24.4	-1.3	1.66	-0.10	-16.1	-0.12	0.51	1.24	38.3	53
St48	1.4	1200	181.5	-20.8	22.5	-2.4	1.49	-0.24	-29.3	-0.22	0.53	1.16	37.6	65
St47	1.9	1180	176.9	-23.6	21.3	-3.9	1.39	-0.35	-46.5	-0.35	0.41	1.32	116.8	57
St47	1.9	1100	152.6	-39.8	23.2	-2.8	1.54	-0.23	-33.3	-0.25	0.30	1.35	29.2	69
St46	6.3	1170	164.8	-34.7	21.6	-3.6	1.44	-0.30	-43.6	-0.33	0.33	1.17	40.9	60
St53	0.5	1170	192.1	-7.4	24.0	-1.2	1.58	-0.16	-14.9	-0.11	0.28	1.30	66.2	63
St53	0.5	1100	181.5	-10.9	23.2	-2.8	1.54	-0.23	-33.8	-0.25	0.24	1.17	24.7	69
St7	9.6	1000	173.4	-7.7	24.2	-2.9	1.58	-0.23	-35.0	-0.26	0.45	1.10	19.7	52
St29	9.9	1110	170.2	-23.3	22.4	-3.5	1.45	-0.32	-41.8	-0.31	0.38	1.11	9.0	49
St40	15.1	1160	170.1	-28.4	22.9	-2.4	1.53	-0.22	-29.0	-0.22	0.57	1.22	5.5	47
St27	17.9	1075	168.3	-21.4	22.5	-3.8	1.47	-0.31	-45.7	-0.34	0.55	1.10	1.6	37
St41	18.8	1000	174.5	-6.6	26.1	-1.0	1.78	-0.04	-11.5	-0.09	0.87	1.18	0.3	17
St41	18.8	1150	166.7	-30.9	23.0	-2.5	1.55	-0.20	-29.8	-0.22	0.50	1.12	1.0	42
St42	23.5	1091	149.5	-41.9	20.1	-6.0	1.36	-0.41	-71.4	-0.54	0.63	1.10	0.6	18

Table (continued).

	Dis.	Sam.	DO	DO*	NO_3	NO_3*	PO_4	PO_4*	C Rem.	Fe Rem.	Fe	Cu	T. PAH	Me. Na.
	(km)	(m)				(µM)					(nM)		(µg/l)	(%)
Group B														
St42	23.5	1091	149.5	-41.9	20.1	-6.0	1.36	-0.41	-71.4	-0.54	0.63	1.10	0.6	18
St43	24.5	1150	147.0	-50.5	18.8	-6.7	1.25	-0.50	-80.4	-0.60	0.68	1.19	1.3	22
St43	24.5	1250	191.1	-15.5	22.5	-2.0	1.50	-0.21	-24.1	-0.18	1.12	1.25	1.8	30
								average		-0.26	0.49			

* Abbreviation- Dis.: distance from the wellhead (N 28° 44.412', W 88° 21.676'), Sam.: sampling depth, DO: dissolved oxygen, Anom.: anomaly, T.PAH: total polycyclic hydrocarbons, Rem.: removal, Me.Na.: methylnaphthalenes, DO*, NO_3 *and PO_4 *data and the anomaly calculation from Shiller and Joung (2012).

REFERENCES

Al-Abdali, F.; Massoud, M. S.; Al-Ghadban, A. N. Bottom sediments of the Arabian Gulf-III. Trace metal contents as indicators of pollution and implications for the effect and fate of the Kuwait oil slick. *Environ. Pollut.* **1996**, 93(3), 285-301.

All, M.F.; Bukharl, A.; Saleem, M. Trace metals in crude oils from Saudi Arabia. Ind. Eng. Chem. Prod. Res. Dev. **1983**, 22(4), 691-694.

Ball, J.S.; Wenger, W.J.; Hyden, H.J.; Horr, C.A.; Myers, A.T. Metal content of twenty-four petroleums. *J. Chem. Eng. Data*, **1960**, 5(4), 553-557.

Bergquist, B.A.; Boyle, E.A. Dissolved iron in the tropical and subtropical Atlantic Ocean. *Global Biogeochem. Cycles.* **2006**, 20, doi:10.1029/2005GB002505.

Berson, O.; Lidstrom, M. E. Study of copper accumulation by the type I methanotroph methylomicrobium albus BG8. *Environ. Sci. Technol.* **1996**, 30(3), 802-809.

Bieber, H.; Hartzband, H.M.; Kruse, E.C. Volatility of metal-porphyrin complexes in petroleum. *J. Chem. Eng. Data*, **1960**, 5(4), 540-546.

Boehm, P.D.; Douglas, G.S.; Burns, W.A.; Mankiewicz, P.J.; Page, D.S.; Bence, A.E. Application of petroleum hydrocarbon chemical fingerprinting and allocation techniques after the Exxon Valdez oil spill. *Mar. Pollut. Bull*. **1997**, 34(8), 599-613.

Bruland, K.W.; Franks, R.P. Mn, Ni, Cu, Zn, and Cd in the Western North Atlantic. Trace Metals in Seawater. Eds. Wong, C.S.; Bruland, K.W.; Boyle, E.; Burton, D.; Goldberg, E.D. NATO Conference Series IV; Marine Sciences, **1983**, 395-414.

Bu-Olayan, A.H.; Subrahmanyam, M.N.V.; Al-Sarawi, M.; Thomas, B.V. Effects of the Gulf War oil spill in relation to trace metals in water, particulate matter, and PAHs from the Kuwait coast. *Environ. Int.* **1998**, 24(7), 789-797.

Cantu, R.; Stencel, J.R.; Czernuszewicz, R.S.; Jaffe, P.R.; Lash, T.D. Surfactant-Enhanced partitioning of nickel and vanadyl deoxophylloerythroetioporphyrins from crude oil into water and their analysis using surface-enhanced Resonance Raman spectroscopy. *Environ. Sci. Technol.* **2000**, 34, 192-198.

Carriquiry, J.D.; Horta-Puga, G. The Ba/Ca record of corals from the Southern Gulf of Mexico: Contributions from land-use changes, fluvial discharge and oil-drilling muds. *Mar. Pollut. Bull.* **2010**, 60, 1625-1630.

Chan, L.H.; Drummond, D.; Edmond, J.M.; Grant, B. On the barium data from the Atlantic GEOSECS expedition. *Deep Sea Res.* **1977**, 24(7), 613-649.

Church, T. M.; Wolgemuth, K. Marine barite saturation. *Earth Planet. Sci. Lett.* **1972**, 15-35.

Crecelius, E., Trefry, J.; McKinley, J.; Lasorsa, B.; Trocine, R. Study of barite solubility and the release of trace components to the marine environment. U.S. Dept. of the Interior, Minerals Management Service, Gulf of Mexico OCS Region, New Orleans, LA. OC5 Study MMS, **2007**, 2007-061. pp. 36-37.

Crone, T. J.; Tolstoy, M. Magnitude of the 2010 Gulf of Mexico Oil Leak. *Science,* **2010**, 330, 634.

Cullen, J.; T., Chong, M.; Ianson, D. British Columbian continental shelf as a source of dissolved iron to the subarctic northeast Pacific Ocean, *Global Biogeochem. Cycles*, **2009**, 23, GB4012: DOI:10.1029/2008GB003326.

Deslarzes, K.J.P.; Boothe, P.N.; Presley, B.J.; Steinmetz, G.L. Historical incorporation of barium in the reef building coral Montastrea annularis at the Flower Garden Banks, north-west Gulf of Mexico. *Mar. Pollut. Bull.* **1995**, 30(11), 718-722.

Diercks, A.-R.; Highsmith, R.C.; Asper, V.L.; Joung, D.J.; Zhou, Z.; Guo, L.; Shiller, A.M.; Joye, S.B.; Teske, A.P.; Guinasso, N.; Wade, T.L.; Lohrenz, S.E. Characterization of subsurface polycyclic aromatic hydrocarbons at the Deepwater Horizon site. *Geophys. Res. Lett*. **2010**, 37, L20602; doi:10.1029/2010GL045046.

Douglas, G.S.; Bence, A,E.; Prince, R.C.; McMillen, A.J.; Butler, E.L. Environmental stability of selected petroleum hydrocarbon source and weathering ratios. *Environ. Sci. Technol.* **1996**, 30, 2332-2339.

Du, M; Kessler, J.D. Assessment of the spatial and temporal variability of bulk hydrocarbon respiration following the Deepwater Horizon oil spill. *Environ. Sci. Technol.* **2012**, 46(9) 10499-10507:doi 10.1021/es301363k.

Dunning, H.N.; Moore, J.W.; Bieber, H.; Williams, R.B. Porphyrin, nickel, vanadium, and nitrogen in petroleum. *J. Chem. Eng. Data*, **1960**, 5(4), 546-549.

Duyck, C.; Miekeley, N.; Porto da Silveira, C.L.; Qucelio, R.Q.; Campos, R.C.; Grinberg, P.; Brandao, G.P. The determination of trace elements in crude oil and its heavy fractions by atomic spectrometry. *Spectrochim. Acta B*, **2007**, 62, 939-951.

Duyck, C.; Miekeley, N.; Silveira, C.L.P.D.; Szatmari, P. Trace element determination in crude oil and its fractions by inductively coupled plasma mass spectrometry using ultrasonic nebulization of toluene solution. *Spectrochim. Acta B*, **2002**, 57, 1979-1990.

Elrod, V. A., Berelson, W.M.; Coale, K. H.; Johnson, K. S. The flux of iron from continental shelf sediments: A missing source for global budgets, *Geophys. Res. Lett*. **2004**, 31, L12307; DOI:10.1029/2004GL020216.

Fagerbakke, K.M.; Heldal, M.; Norland, S. Content of carbon, nitrogen, oxygen, surfur and phosphorus in native aquatic and cultured bacteria. *Aquat. Microb. Ecol.* **1996**. 10, 15-27.

Fowler, S.W.; Readman, J.W.; Oregioni, B.; Villeneuve, J.-P.; McKay, K. Petroleum hydrocarbons and trace metals in nearshore gulf sediments and biota before and after the 1991 war: An assessment of temporal and spatial trends. *Mar. Pollut. Bull.* **1993**, 27, 171-182.

Gonzalez, J.J.; Vinas, L.; Franco, M.A.; Fumega, J.; Soriano, J.A.; Grueiro, G.; Muniategui, S.; Lopez-Mahia, P.; Prada, D.; Bayona, J.M.; Alzga, R.; Albaiges, J. Spatial and temporal distribution of dissolved/dispersed aromatic hydrocarbons in seawater in the area affected by the Prestige oil spill. *Mar. Pollut. Bull*. **2006**, 53, 250-259.

Hanor, J. S.; Chan, L. H. Non-conservative behaviour of barium during mixing of Mississippi River and Gulf of Mexico waters. *Earth. Planet. Sc. Lett*. **1977**, 37, 242–250.

Hazen, T.; Dubinsky, E.A.; DeSantis, T.Z.; Andersen, G.L.; Piceno, Y.M.; Singh, N.; Jansson, J.K.; Probst, A.; Borglin, S.; Fortney, J.L.; Stringfellow, W.T.; Bill, M., Conrad, M.E., Tom, L.A.; Chavarria, K.L.; Alusi, T.R.; Lamendella, R.; Joyner, D.C.; Spier, C.; Baelum, J.; Auer, M.; Zemla, M.L.; Chakraborty, R.; Sonnenthal, E.L.; D'haeseleer, P.; Holman, H.-Y.N.; Osman, S.; Lu, Z.; Nostrand, J.D.V.; Deng, Y.; Zhou, J.; Mason, O.U. Deep-sea oil plume enriches indigenous oil-degrading bacteria. *Nature*, **2010**, 330, 204-208.

Hicken, C.E.; Linbo, T.L.; Baldwin, D.H.; Willis, M.L.; Myers, M.S.; Holland, L.; Larsen, M.; Stekoll, M.S.; Rice, S.D.; Collier, T.K.; Scholz, N.L.; Incardona, J.P. Sublethal exposure to crude oil during embryonic development alters cardiac morphology and reduces aerobic capacity in adult fish. *Proc. Natl Acad. Sci.* USA, **2011**, 108, 7086-7090 (doi:10.1073/pnas.1019031108).

Jones, C.J.; Murray, J.W. The geochemistry of manganese in the northeast Pacific Ocean off Washington. *Limnol. Oceanogr*. **1985**, 30(1), 81-92.

Joye, S.B.; MacDonald, I.R.; Leifer, I.; Asper, V. Magnitude and oxidation potential of hydrocarbon gases released from the BP oil well blowout. *Nature Geosci*. **2011**, 4, 160-164.

Kessler, J. D.; Valentine, D. L.; Redmond, M. C.; Du, M.; Chan, E. W.; Mendes, S. D.; Quiroz, E. W.; Villanueva, C. J.; Shusta, S. S.; Werra, L. M.; Yvon-Lewis, S.; Weber, T. C., A persistent oxygen anomaly reveals the fate of spilled methane in the deep Gulf of Mexico. *Science*, **2011**, 331, 312-315.

Kujawinski, E.B.; Kido Soule, M.C.; Valentine, D.L.; Boysen, A.K.; Longnecker, K.; Redmond, M.C. Fate of dispersant associated with the Deepwaer Horizon oil spill. *Environ. Sci. Technol.* **2011**, 45, 1298–306.

Lee, R.W.; Childress, J.J. Assimilation of inorganic nitrogen by marine invertebrates and their chemoautotrophic and methanotrophic symbioonts. *App. Environ. Microb*. **1994**, 60(6), 1852-1858.

Lieverman, R.L.; Rosenzweig, A.C. Biological methane oxidation: Regulation, biochemistry, and active site structure of particulate methane monooxygenase. *Crit. Rev. Biochem. Mol*. 2004, 39, 147-164.

Linden, O.; Rosemarin, A.; Lindskog, A.; Hoeglund, C.; Johansson, S. Effects of oil and oil dispersant on an enclosed marine ecosystem. *Environ. Sci. Technol.* **1987**, 21, 374-382.

Liu, Z.; Liu, J; Zhu, Q.; Wu, W. The weathering of oil after the Deepwater Horizon oil spill: insights from the chemical composition of the oil from the sea surface, salt marshes and sediments. *Environ. Res. Lett*. **2012**, 7 035302: doi:10.1088/1748-9326/7/3/035302.

Massoud, M.S.; Al-Abdali, F.; Al-Ghadban, A.N. The status of oil pollution in the Arabian Gulf by the end of 1993. *Environ. Int.* **1998**, 24(1/2), 11-22.

National Commission on the BP Deepwater Horizon Oil Spill and Offshore Drilling. Deep Water: The Gulf oil disasters and the future of offshore drilling. **2011**, p 150; www.oilspillcommission.gov/sites/default/files/documents/DEEPWATER_ReporttothePresident_FINAL.pdf.

Neff, J.M. Estimation of bioavailability of metals from drilling mud barite. *Intergr. Environ. Assess. Manag*. **2007**, 4(2), 184-193.

Pakulski, J.D.; Coffin, R.N.; Kelley, C.A.; Holder, S.L.; Downer, R.; Aas, P.; Lyons, M.M.; Jeffrey, W.H. Iron stimulation of Antarctic bacteria. *Nature*, **1996**, 383, 133-134.

Portella, C.M.M.A.; Tristao, M.L.B.; Felcman, J. Evaluation of the possibility of contamination of sea water by metal ions present in fuel oil. *Fuel*, **2006**, 85, 2162-2170.

Pozebon, D.; Lima, E.C.; Maia, S.M.; Fachel, J.M.G. Heavy metals contribution of non-aqueous fluids used in offshore oil drilling. *Fuel*, **2005**, 53-61.

Prego, R.; Cobelo-Garcia, A. Zinc concentrations in the water column influenced by the oil spill in the vicinity of the Prestige shipwreck. *Ciencias Marinas*, **2003**, 29(1), 103-108.

Saito, M.A.; Moffett, J.W. Temporal and spatial variability of cobalt in the Atlantic Ocean. *Geochim. Cosmochim. Acta* **2002**, 66 (11), 1943-1953.

Santos-Echeandia, J.; Prego, R.; Cobelo-Garcia, A. Influence of the heavy fuel spill from the Prestige tanker wreckage in the overlying seawater column levels of copper, nickel and vanadium (NE Atlantic ocean). *J. Mar. Sys*. **2008**, 72, 350-357.

Shiller, A.M. Syringe filtration methods for examining dissolved and colloidal trace element distributions in remote field locations. *Environ. Sci. Technol.* **2003**, 37(17), 3953 - 3957.

Shiller, A.M.; Bairamadgi, G.R. Dissolved gallium in the Northwest Pacific and the South and Central Atlantic Oceans: Implications for aeolian Fe input and a reconsideration of profiles. *Geochem. Geophy. Geosy.* **2006**, 7, Q08M09; DOI:10.1029/2005GC001118.

Shiller, A.M.; Joung, D.J. Nutrient depletion as a proxy for microbial growth in Deepwater Horizon subsurface oil/gas plumes. *Environ. Res. Lett.* **2012**, 7 045301 doi:10.1088/1748-9326/7/4/045301.

Shim, M.-J.; Swarzenski, P.W.; Shiller, A.M. Dissolved and colloidal trace elements in the Mississippi River delta outflow after hurricanes Katrina and Rita. *Cont. Shelf Res.* **2012**, doi:10.1016/j.csr.2012.03.007.

Stigter, J.B.; de Haan, H.P.M.; Guicherit, R.; Dekkers, C.P.A.; Daane, M.L. Determination of cadmium, zinc, copper, chromium and arsenic in crude oil cargoes. *Environ. Pollut.* **2000**, 107, 451-464.

Sugihara, J.M.; Bean, R.M. Direct determination of metallopophyrins in Boscan crude oil. *J. Chem. Eng. Data*, **1962**, 7(2), 269-271.

Teague, W.J.; Jarosz, E.; Carnes, M.R.; Mitchell, D.A.; Hogan, P.J. Low-frequency current variability observed at the shelfbreak in the northeastern Gulf of Mexico: May-October, 2004. *Cont. Shelf Res*. **2006**, 26, 2559-2582.

Tortell, P.D; Maldonado, M.T.; Granger, J.; Price, N.M. Marine bacteria and biogeochemical cycling of iron in the oceans. *FEMS Microbiol. Ecol.* **1999**, 29, 1-11.

Trocine, R.P.; Trefry, J.H. Particulate metal tracers of petroleum drilling mud dispersion in the marine environment. *Environ. Sci. Technol*. **1983**, 17 (9), 507-512.

Valentine, D. L.; Kessler, J. D.; Redmond, M. C.; Mendes, S. D.; Heintz, M. B.; Farwell, C.; Hu, L.; Kinnaman, F. S.; Yvon-Lewis, S.; Du, M.; Chan, E. W.; Garcia Tigreros, F.; Villanueva, C. J. Propane respiration jump-starts microbial response to a deep oil spill. *Science*, **2010**, 330, 208–211.

Wade, T.L.; Sweet, S. T.; Sericano, J.L.; Guinasso Jr, N.L.; Diercks, A.–R.; Highsmith, R.C.; Asper, V.L.; Joung, D.–J.; Shiller, A.M.; Lohernz, S.E.; Joye, S.B. Analyses of water samples from the Deepwater Horizon oil spill: Documentation of the subsurface plume. In Monitoring and Modeling the Deepwater Horizon Oil Spill: A Record-Breaking Enterprise, Geophys. *Monogr. Ser*, **2011**, doi:10.1029/2011GM001103.

Wondium, T.; Goessler, W.; Irgolic, K.J. Microwate digestion of "residual fuel oil" (NIST SRM 1634b) for the determination of trace elements by inductively coupled plasma-mass spectrometry. *Fresenius J. Anal. Chem*. **2000**, 367, 35-42.

CHAPTER VI

SUMMARY AND CONCLUSION

The large data set, gathered over the course of 10 field campaigns and covering different seasons and multiple depths, allowed for improving our understanding of the behavior of trace elements (TEs) in the Louisiana Shelf and open Gulf of Mexico waters. The seasonal variations of the chemical constituents at a low salinity reflect the seasonal changes in the river water endmembers that are associated with variation of mixing ratios of Mississippi River tributaries. Surface Mo, Cs, U, Ni, and Cu showed conservative behavior with minor scatter that coincided with high salinity and bottom waters. Based on the associated mixing experiments, nutrient and chlorophyll distributions, and surface-bottom concentration contrasts, the non-conservative behavior of TEs was variously related to colloidal flocculation (Fe, Cr), biological activities (Fe, Mn), desorption (Ba, Co, Mn), photochemical reaction (Cr), and benthic mobilization (Co, Cu, Ni, Mn). In June/July 2009 during strong water stratification the elevated Co, Fe, and Mn in some high salinity waters were observed, probably due to episodic vertical mixing associated with upwelling favorable summer winds.

During all study periods, the elevated bottom water Co, Mn, and Fe relative to surface and middle depths were observed, and these were negatively correlated with dissolved oxygen (DO), suggesting that the enrichment may be due to particulate or sedimentary dissolution and/or diffusion under reducing conditions. In contrast, the bottom water Cr and V showed removal at low DO, probably due to diffusion into sediment and/or adsorptive removal onto particles as result of reduction Cr.

Overall, this study suggests that during bottom water hypoxia, the Louisiana shelf acts as a significant sink or source for certain elements. Also, episodic vertical mixing with even a small scale could be an important advection mechanism for supplying/removing trace elements to/from surface waters. Thus, this vertical mixing should be accounted in studies of Louisiana Shelf biogeochemistry, particularly in relation to hypoxia.

Seasonal variation of Ba distribution in the Louisiana Shelf waters was found to be related to river endmember, desorption, vertical mixing, and removal associated with diatom blooms. This seasonal variation of the surface water Ba-salinity relationship could lead to a considerable uncertainty in salinity prediction when using Ba as a proxy for paleo-salinity changes. Thus, as is the case with nearly all paleoceanographic proxies, the planktonic foraminiferal Ba/Ca ratio should be used in conjunction with other constraining proxies (e.g., oxygen isotopes, Mg).

Temporal and spatial variations were observed for DOC, nutrients, and TEs in the AR water relative to these in the MR water, probably due to the seasonal changes of inputs from the Red River and wetlands. These inputs subsequently resulted in a considerable AR contribution of TEs relative to total fluvial element loadings, and the AR contribution was often higher than the AR hydrologic contribution. Thus, the AR contribution should be adequately accounted in the biogeochemical study or budget calculation of trace elements in the Louisiana Shelf.

Studies of TEs and nutrients in the water column affected by the Deepwater Horizon oil spill revealed that nitrate, phosphate, and dissolved oxygen (DO) were consumed by microbial activity during degradation of oil/gas in the subsurface plume.

Some TE concentrations were elevated in the subsurface oil plume in May 2010 relative to the October results. Examination of profiles, ancillary data sets (e.g., PAHs), and oil/dispersant leaching experiments suggest this increase is related to the inputs from crude oil (Co), drilling mud (Ba), and bottom sediment resuspension (Fe). Additionally, the biological removal of Fe during oil/gas degradation may have been a factor, too. Thus, studies of trace metals as well as other contaminants related to oil spills should consider all factors listed above.

Overall, the studies provide fundamental information about TEs such as the modification in the Atchafalaya River Basin, the influence of the modification in the Louisiana Shelf waters, and the impact of oil spills in aquatic environments. Thus, this research should be very useful for other studies dealing with trace element biogeochemistry in the Gulf of Mexico as well as the other estuarine environments.